Glucagon and Glucose Counterregulation: Pancreatic α-Cell Function and Dysfunction during Hypoglycaemia

A thesis submitted for the Degree of Doctor of Philosophy

at The University of Oxford

Alexander Hamilton

St. Edmund Hall

Hilary 2018



Diabetes UK Studentship

Oxford Centre for Diabetes, Endocrinology and Metabolism

Supervisors: Professor Patrik Rorsman and Doctor Andrei Tarasov

Glucagon and Glucose Counterregulation: Pancreatic α-Cell Function and Dysfunction during Hypoglycaemia

Degree of Doctor of Philosophy at The University of Oxford

Alexander Hamilton
St. Edmund Hall

Hilary 2018

Abstract

The glucagon-secreting α-cell is vital for the maintenance of glucose homeostasis and prevention of hypoglycaemia. Despite its importance many aspects of α-cell physiology are disputed. Thus, in this thesis, I aimed to elucidate several features of α-cell function – exploring how autonomic signals are integrated by the cell and how diabetes leads to its dysfunction.

The autonomic response to hypoglycaemia results in increased acetylcholine and adrenaline in the islet vicinity, which stimulate glucagon secretion. The mechanisms underlying these effects were investigated using live $[Ca^{2+}]_i$ imaging and patch-clamp electrophysiology. Adrenaline was found to target the α-cell via a β-adrenergic mechanism, inducing TPC2-mediated Ca^{2+} release from the (endo)lysosomal stores, which triggered calcium-induced calcium release from the endoplasmic reticulum (ER). Acetylcholine also induced ER Ca^{2+}-release via muscarinic G_q signalling. However, a component of the effect resulted from activation of a nicotinic pathway that evoked P/Q-type Ca^{2+} channel influx.

The glucagon response to hypoglycaemia is lost in diabetes. To investigate the effect of hyperglycaemia on α-cell function at low glucose, the Fh1βKO type 2 diabetic mouse model was used. In these mice, prolonged hyperglycaemia led to blunted glucagon secretion at low glucose. Using live pH imaging, it was shown that this was caused by

hyperglycaemia increasing flux through Na^+ coupled glucose transporters (SGLTs), disrupting Na^+-dependent acid extrusion and inducing cytoplasmic acidification. The resulting build-up of protons was speculated to compromise mitochondrial ATP production leading to the observed glucagon secretory defects. The effects of insulin-induced hypoglycaemia on δ-cell $[Ca^{2+}]_i$ activity were also investigated. Increased SGLT2 transport and low $[K^+]_o$, features of insulin-induced hypoglycaemia, were both shown to increase $[Ca^{2+}]_i$ activity in δ-cells, stimulating somatostatin secretion and consequently suppressing glucagon secretion. Together these data suggest that glucagon secretion at low glucose is lost due to the combined effects of hyperglycaemia-driven intrinsic dysfunction and insulin-induced somatostatin secretion.

Acknowledgements

I would like to thank both my supervisors for their guidance and support during my DPhil. Dr Andrei Tarasov for teaching me the ways of imaging, with great patience and understanding, and always being available to discuss any problems along the way. Prof Patrik Rorsman for providing me with the opportunity to work in his lab. His insight and enthusiasm were of great help.

I also wish to thank Dr Jakob Knudsen, for his contribution to many of the projects presented throughout this thesis, and Dr Quan Zhang and Dr Linford Briant for their help and patience in teaching me how to patch-clamp. And thank you to the rest of the Rorsman group for all their help.

I give special thanks to my parents for their encouragement and support throughout my time as a DPhil student, explaining my research to you was an invaluable exercise. As well as my twin brother Daniel, our 'telepathy' was crucial, and older brother Richard for his encouragement.

I'd like to thank my friend Scott Redpath for his continued support in the work-related arena, and Sean Hook for being the nicest man I know. As well as Harrison, Mike, Martin, Matt and Adam for the great weekends, festivals and holidays that kept me sane.

And finally, my girlfriend Vanessa for being there at 'the crunch'.

Statement of Authorship

All work presented in the main part of my thesis is my own. Data presented in Appendix 2, Appendix 3, Appendix 4 and Appendix 5 were collected by collaborators.

Electrophysiology recordings in Figure A2.1, Figure A2.3, Figure A5.1 l and Figure A.5.2 a, b, g were performed by Dr Quan Zhang.

Secretion experiments in Figure A2.2, Figure A3.1, Figure A5.1 a, b, c, d, e, f, h, i, j, k and Figure A5.2 e were performed by Dr Albert Salehi.

Secretion experiments in Figure A4.1 c, Figure A.4.3, Figure A.4.5 a, f, Figure A4.6 and Figure A4.8 a, b, a, d were performed by Dr Reshma Ramracheya.

Sodium and ATP measurements in Figure A4.5 b, c, d, e, Figure 4.7 a, b and Figure 5.2 c were performed by Dr Andrei Tarasov.

Insulin tolerance tests in Figure 5.1 g were performed by Dr. Elisa Vergari.

Glucose measurements in Figure A4.1 a, b, immunofluorescence staining in Figure A4.2 and qPCR in Figure A.4.4 were performed by Dr Julie Adam.

Pancreas perfusion experiments in Figure A3.2 and the enzyme activity assay in Figure 4.9 were performed by Dr Jakob Knudsen.

Table of Contents

Chapter 1: Introduction 19

1.1. Glucagon and glucose homeostasis 19

1.1.1. The α-cell 20

1.1.2. Hepatic effect of glucagon 20

1.2. Glucagon and diabetes 25

1.2.1. Glucagon secretory defects in diabetes 25

1.2.2. The glucagonocentric model of diabetes 26

1.3. Regulation of glucagon secretion 31

1.3.1 Control by glucose 31

1.3.2. Control by other nutrients 34

1.3.3. Paracrine regulation of glucagon secretion 38

1.3.4. Autocrine regulation of glucagon secretion 41

1.3.5. Autonomic regulation of glucagon secretion 41

1.3.6. Endocrine regulation of glucagon secretion 47

1.4. Impaired glucose counterregulation 50

1.4.1. The absent glucagon response to hypoglycaemia 50

1.4.2. Hypoglycaemia-associated autonomic failure (HAAF) 56

1.4.3. Non-HAAF related damage to the central nervous system 59

1.4.4. Damage to the peripheral nervous system in diabetes 60

1.5. Summary 62

1.6. Aims 63

Chapter 2: General Methods 64

2.1. Mouse Islet Isolation 64

2.2. Mouse Islet Culture 65

2.3. Human islet culture 65

2.4. Confocal $[Ca^{2+}]_i$ measurements 65

2.5. $[Ca^{2+}]_i$ imaging (hypo/hyperglycaemic culture) 70

2.7. Data analysis (Imaging) 73

2.8. Solutions 75

2.9. General Reagents 75

Chapter 3: Adrenergic Signalling in the Pancreatic α-Cell 76

3.1. Introduction 76

3.2. Methods 81

3.2.1. Mice 81

3.2.2. Imaging of PKA activity 81

3.2.3. $[Ca^{2+}]_i$ imaging (Fluo-4FF) 82

3.2.4. Reagents 83

3.3. Results 84

3.3.1. Effect of adrenaline on $[Ca^{2+}]_i$ in pancreatic α-cells within intact mouse and human islets 84

3.3.2. The role of adrenergic receptor subtypes in the adrenaline effect in pancreatic α-cells within intact mouse islets 88

3.3.3. The role of PKA and Epac2 in the adrenaline effect in pancreatic α-cells within intact mouse islets 90

3.3.4. Effect of Ca^{2+} channel blockers on the adrenaline effect in pancreatic α-cells within intact mouse islets 93
3.3.5. The role of intracellular Ca^{2+} in the adrenaline effect in pancreatic α-cells within intact mouse islets 95
3.3.6. Effect of insulin on the adrenaline response in pancreatic α-cells within intact mouse islets 102
3.3.7. Effect of hypo- and hyperglycaemic culture on adrenaline response in pancreatic α-cells within intact mouse islets 102
..... 103
3.3.8. Adrenaline effect in pancreatic β- and δ-cells within intact mouse islets 104
3.4. Discussion 106
3.4.1. Adrenaline increases $[Ca^{2+}]_i$ and glucagon secretion in pancreatic α-cells 106
3.4.2. Adrenaline acts via the β-adrenergic pathway 106
3.4.3. Noradrenaline likely dictates the sympathetic response to hypoglycaemia 107
3.4.4. The adrenaline effect on $[Ca^{2+}]_i$ in α-cells is conserved in human islets 108
3.4.5. PKA and Epac2 are crucial in increasing $[Ca^{2+}]_i$ upon adrenaline stimulation 109
3.4.6. The adrenaline effect results from (endo)lysosomal-ER Ca^{2+} release 110
3.4.7. L-type Ca^{2+} channels play a permissive role in adrenaline-induced glucagon secretion 112
3.4.8. α-cell 'adrenaline resistance' in impaired glucose counterregulation 115
3.4.9. Adrenaline inhibits $[Ca^{2+}]_i$ oscillations in β- and δ-cells 116
3.5. Conclusion 119

Chapter 4: Cholinergic Signalling in the Pancreatic α-Cell 120
4.1. Introduction 120
4.2. Methods 126
4.2.1. Mice 126
4.2.2. Electrophysiology 126
4.2.3. Islet dissociation (For $[DAG]_i$ Imaging) 127
4.2.4. $[DAG]_i$ imaging 128
4.2.5. Reagents 129
4.3. Results 130
4.3.1. Effect of acetylcholine on $[Ca^{2+}]_i$ in pancreatic α-cells within intact mouse and human islets 130
4.3.2. The role of muscarinic and nicotinic acetylcholine receptors in the acetylcholine effect in pancreatic α-cells within intact mouse and human islets 135
..... 140
4.3.3. Effect of acetylcholine on $[DAG]_i$ in dispersed mouse islets 141
4.3.4. The role of intracellular Ca^{2+} in the acetylcholine effect in pancreatic α-cells within intact mouse islets 143
4.3.5. The role of PKC in the acetylcholine effect in pancreatic α-cells within intact mouse islets 143
4.3.6. Effect of Ca^{2+} channel blockers on the acetylcholine effect in pancreatic α-cells within intact mouse islets 144
4.3.7. Effect of acetylcholine on pancreatic α-cells within intact mouse islets in the presence of EGTA 148
4.3.8. Effects of nicotine and acetylcholine on α-cell electrical activity in pancreatic α-cells within intact mouse islets 150
4.3.9. Effect of SSTR2 blockade on acetylcholine effect in pancreatic α-cells within intact mouse islets 152
4.3.10. Effect of hypo- and hyperglycaemic culture on the acetylcholine response in pancreatic α-cells within intact mouse islets 154

4.4. Discussion **157**
4.4.1. Acetylcholine increases $[Ca^{2+}]_i$ in pancreatic α-cells 157
4.4.2. The effect of acetylcholine on α-cell $[Ca^{2+}]_i$ is reliant predominantly on the muscarinic pathway 157
4.4.3. A nicotinic pathway is also present in α-cells 159
4.4.4. The role of the nicotinic pathway in ACh-induced glucagon secretion 160
4.4.5. Smoking-induced nicotine exposure and type 2 diabetes 162
4.4.6. Extracellular Ca^{2+} plays a permissive role in acetylcholine-induced glucagon secretion 162
4.4.7. Somatostatin signalling plays no role in the α-cell cholinergic response 164
4.4.8. The acetylcholine effect in β-cells 164
4.4.9. Hyperglycaemia does not decrease sensitivity to acetylcholine 165
4.4.10. Acetylcholine also stimulates human α-cells 166
4.5. Conclusion **169**

Chapter 5: Cytoplasmic Acidification Drives Glucagon Secretory Defects in Diabetes **170**
5.1. Introduction **170**
5.2. Methods **174**
5.2.1. Mice 174
5.2.2. Simultaneous $[Ca^{2+}]_i$ and pH_i measurements 174
5.2.3. Data analysis (simultaneous $[Ca^{2+}]_i$ and pH_i measurements) 177
5.2.4. Reagents 177
5.3. Results **178**
5.3.1. Effect of hyperglycaemia on cytoplasmic pH in pancreatic α-cells 178
5.3.2. Na^+-coupled glucose transport – a driver of α-cell dysfunction in diabetes? 184
5.4. Discussion **190**
5.4.1. Hyperglycaemia disrupts α-cell glucose sensing via cytoplasmic acidification 190
5.4.2. Acute effect of 20 mM glucose in α-cells is $[Ca^{2+}]_i$ independent 190
5.4.3. Acute effects of D-Glyceraldehyde and glucose in β-cells are dependent on $[Ca^{2+}]_i$ 193
5.4.4. Acidification of α-cells in Fh1βKO islets results from increased Na^+ influx via SGLT1 due to hyperglycaemia 194
5.4.5. Cytoplasmic acidification as a marker for β-cell dysfunction in diabetes 195
5.4.6. $[Ca^{2+}]_i$ dynamics in Fh1βKO α-cells 197
5.4.7. Reduced pH_i interferes with mitochondrial function 197
5.4.8. The pH-dependence of Fh1 results in increased succination in α-cells from Fh1βKO mice 202
5.4.9. An added benefit of SGLT-2 blockers? 202
5.5. Conclusion **206**

Chapter 6: Insulin-induced Hypoglycaemia Suppresses Glucagon Secretion by SGLT2-dependent Stimulation of Somatostatin Secretion from Pancreatic δ-Cells **207**
6.1. Introduction **207**
6.2. Methods **210**
6.2.1. Mice 210
6.2.2. Reagents 210
6.3. Results **211**
6.3.1. Effect of the non-metabolisable sugar methyl α-D-glucopyranoside (αMDG) on $[Ca^{2+}]_i$ activity in pancreatic δ-cells within intact mouse islets 211

6.3.2. Effect of lowering the extracellular K^+ concentration on $[Ca^{2+}]_i$ activity in pancreatic δ-cells within intact mouse islets 211
6.4. Discussion 214
6.4.1. Increasing flux through SGLT2 can activate the pancreatic δ-cell 214
6.4.2. Hypokalaemia causes dysregulation of somatostatin secretion, dampening the glucagon response in type 2 diabetes 215
6.4.3. Intrinsic α-cell dysfunction vs. Iatrogenic paracrine suppression 216
6.5. Conclusion 219

Chapter 7: General Discussion 220
7.1. Introduction 220
7.2. Key findings 220
7.3. Overall implications 223
7.4. Personal reflections 225
7.5. Future work 227

Appendix 1: Methods performed by collaborators 231
A1.1. Methods performed by collaborators throughout thesis 231
A1.1.1. Hormone secretion assays 231
A1.1.2. Human islet isolation 232
A1.2. Methods performed by collaborators specifically for Chapter 3 233
A1.2.1. Electrophysiology 233
A1.3. Methods performed by collaborators specifically for Chapter 4 234
A1.3.1. Pancreas perfusion 234
A1.4. Methods performed by collaborators specifically for Chapter 5 234
A1.4.1. Imaging of $[ATP/ADP]_i$ 234
A1.4.2. Immunofluorescence 234
A1.4.3. SGLT expression analysis 235
A1.4.4. Plasma glucose measurements 235
A1.4.5. Fumarate hydratase activity measurements 235
A1.5. Methods by collaborators specific for Chapter 6 236
A1.5.1. Electrophysiology 236
A1.5.2. Plasma glucose determinations and insulin tolerance tests 236

Appendix 2 - Data collected by collaborators in Chapter 3 237

Appendix 3: Data collected by collaborators in Chapter 4 240

Appendix 4: Data collected by collaborators in Chapter 5 242

Appendix 5: Data collected by collaborators in Chapter 6 251

References 254

List of Tables and Figures

Figure 1.1 - Gluconeogenesis and glycogenolysis pathways and glucagon.....24

Figure 1.2 - Roger Unger's glucagonocentric model 30

Figure 1.3 - K_{ATP} model of glucagon secretion 33

Figure 1.4 - Autonomic barriers to hypoglycaemia.....46

Figure 1.5 - Regulation of glucagon secretion 49

Figure 1.6 - Glucose dependence of islet hormone secretion in mouse and human islets ..54

Figure 2.1 - Mechanism of Fluo-4.....67

Figure 2.2 - 'Open' chamber used for confocal singular $[Ca^{2+}]_i$ recordings and simultaneous $[Ca^{2+}]_i$ and pH_i recordings 69

Figure 2.3 - 'Closed' Chamber used for PKA, $[DAG]_i$ and $[Ca^{2+}]_i$ hypo/hyperglycaemic culture imaging experiments 72

Figure 2.4 – Partial area under the curve calculation 74

Table 3.1 - Summary of adrenergic receptors 78

Figure 3.1 - Hypothesis 80

Figure 3.2 - The stimulatory effect of adrenaline on glucagon secretion is mediated by selective elevation of $[Ca^{2+}]_i$ in pancreatic α-cells 86

Figure 3.3 - Adrenaline functions via the β-adrenergic pathway in α-cells 89

Figure 3.4 - Adrenaline targets both PKA- and Epac2-dependent pathways.....92

Figure 3.5 - Adrenaline response is abolished in the presence of the L-type Ca^{2+}-channel blocker isradipine 94

Figure 3.6 - Adrenaline-induced glucagon secretion involves intracellular Ca^{2+} release ...99

Figure 3.7 - Adrenaline effect persists in absence of extracellular Ca^{2+} 101

Figure 3.8 - Effects of insulin and hypo/hyperglycaemic culture on the adrenaline-induced $[Ca^{2+}]_i$ increase.....103

Figure 3.9 - Effect of adrenaline on β-cells and δ-cells.....105

Figure 3.10 - Proposed model for role of extracellular Ca^{2+} 114

Figure 3.11 - Model.....118

Table 4.1 - Mammalian muscarinic acetylcholine receptors.....122

Table 4.2 - Mammalian nicotinic acetylcholine receptors 122

Figure 4.1 - Hypothesis 125

Figure 4.2 - The stimulatory effect of acetylcholine on glucagon secretion is mediated by elevation of $[Ca^{2+}]_i$ in pancreatic α-cells 131

Figure 4.3 - Acetylcholine increases $[Ca^{2+}]_i$ in a subset of α-cells in intact human islets 134

Figure 4.4 - Acetylcholine functions via muscarinic and nicotinic pathways.....137

Figure 4.5 – Oxotremorine and nicotine increase $[Ca^{2+}]_i$ in mouse and human α-cells 140

Figure 4.6 - Acetylcholine increases $[DAG]_i$ in majority of α-cells.....142

Figure 4.7 - Ca^{2+} dependence of the acetylcholine effect in α-cells.....146

Figure 4.8 - Removal of extracellular Ca^{2+} reduces acetylcholine effect in α- cells.....149

Figure 4.9 - Nicotine and acetylcholine do not stimulate electrical activity in mouse pancreatic α-cells.....151

Figure 4.10 - Somatostatin receptor antagonism has no effect on the acetylcholine response 153

Figure 4.11 - Hypo- and hyperglycaemic conditions do not affect ACh-induced $[Ca^{2+}]_i$ increase in pancreatic α-cells 155

Figure 4.12 - Cholinergic effect in β-cells.....156

Figure 4.13 - Model.....168

Figure 5.1 - SNARF-5F mechanism.....176

Figure 5.2 - Effect of glyceraldehyde on pH_i 179

Figure 5.3 - α-Cells in islets from Fh1βKO mice display cytoplasmic acidification 182

Figure 5.4 - β-Cells in islets from Fh1βKO mice display cytoplasmic acidification.....183

Figure 5.5 - Effect of $[Na^+]_o$ on cytoplasmic pH in α-cells.....185

Figure 5.6 - Effect of chronic high glucose culture on cytoplasmic pH in α-cells is alleviated by phlorizin 188

Figure 5.7 - Effect of chronic high glucose culture on cytoplasmic pH in β-cells with or without SGLT-blockers 189

Figure 5.8 - Representation of $[Ca^{2+}]_i$ and pH_i relationship in CTL α-cell 192

Figure 5.9 - K_{ATP} channel activity in α-cells and the effect of compromised ATP production 199

Figure 5.10 - Alternative Ca^{2+}-dependent mechanisms of mitochondrial acidification 201

Figure 5.11 - Model 205

Figure 6.1 - Effect of α-MDG and low $[K^+]_o$ on $[Ca^{2+}]_i$ in mouse pancreatic δ-cells 213

Figure 6.2 - Model 218

Figure A2.1 - Effect of adrenaline on electrical activity 237

Figure A2.2 - Adrenaline and glucagon secretion 238

Figure A2.3 - cAMP effect on exocytosis 239

Figure A3.1 - Cholinergic signalling and glucagon secretion 240

Figure A3.2 - Effect of nicotine and oxotremorine on glucagon and insulin secretion in pancreas perfusion experiments 241

Figure A4.1 - Fh1βKO glucose profiles and insulin secretion 242

Figure A4.2 - 2SC staining in tissues from non-diabetic and diabetic mouse models and human donors 243

Figure A4.3 - Glucagon secretion in Fh1βKO mice 244

Figure A4.4 - SGLT 1 and SGLT 2 expression in islet, heart and kidney 245

Figure A4.5 - Effect of phlorizin on glucagon secretion and $[ATP/ADP]_i$ 246

Figure A4.6 - Effect of chronic glyceraldehyde on insulin secretion 247

Figure A4.7 - Effect of high glucose on $[ATP/ADP]_i$ in islets from CTL, normoglycaemic Fh1βKO and hyperglycaemic Fh1βKO mice 248

Figure A4.8 - Restoration of glucose-stimulated insulin secretion by normoglycaemic culture and culture with the glucokinase inhibitor mannoheptulose 249

Figure A4.9 - pH dependence of fumarate hydratase activity 250

Figure A5.1 - Effects of insulin on somatostatin release in isolated mouse pancreatic islets. 252

Figure A5.2 - Effects of low $[K^+]_o$ and αMDG on electrical activity, somatostatin and glucagon secretion 253

Abbreviations

(myr)PKI	(myristoylated) Protein kinase inhibitor
$[Ca^{2+}]_i$	Cytoplasmic free Ca^{2+} concentration
$[DAG]_i$	Cytoplasmic DAG concentration
$[K^+]_o$	Extracellular K^+ concentration
$[Na^+]_i$	Cytoplasmic Na^+ concentration
$[Na^+]_o$	Extracellular Na^+ concentration
°C	Degrees Celsius
ACh	Acetylcholine
ADP	Adenosine 5'diphosphate
AMPK	5' adenosine monophosphate activated protein kinase
ANOVA	Analysis of variance
ATP	Adenosine 5'triphosphate
AUC	Area under the curve
BDNF	Brain-derived neurotropic factor
BIM	Bisindolylmaleimide I
BK channel	Big potassium channel
BSA	Bovine serum albumin
Ca^{2+}	Calcium
cADPR	Cyclic ADP ribose
cAMP	Cyclic adenosine-5'-monophosphate
CAMKII	Ca^{2+}/calmodulin-dependent protein kinase II
CBP	CREB binding protein

CD38	Cyclic ADP ribose hydrolase
CICR	Ca^{2+}-induced Ca^{2+} release
CNS	Central nervous system
CPA	Cyclopiazonic acid
CPT1	Carnitine palmitoyltransferase I
CREB	cAMP response element binding protein
CRTC2	CREB-regulated transcription coactivator 2
CTL	Control
DAG	Diacylglycerol
DMNV	Dorsal motor nucleus of the vagus nerve
DNA	Deoxyribonucleic acid
EGTA	Ethylene glycol-bis(β-aminoethyl ether)-N,N,N',N'-tetraacetic acid
Epac	Exchange factor directly activated by cAMP
ER	Endoplasmic Reticulum
ESI-05	4-Methylphenyl-2,4,6-trimethylphenylsulfone
eSIN	Early sympathetic islet neuropathy
F-6-P	Fructose-6-phosphate
F(1,6)P2	Fructose-1,6-biphosphate
F(2,6)P2	Fructose-2,6-biphosphate
FBPase-1	Fructose-1,6-bisphosphatase
FCS	Fetal calf serum
FFAR1	Free fatty acid receptor 1
G-1-P	Glucose-1-phosphate
G-6-P	Glucose-6-phosphate

G6Pase	Glucose-6-phosphatase
GABA	γ-aminobutyric acid
GADPH	Glyceraldehyde 3-phosphate dehydrogenase
GcgR	Glucagon receptor
GIP	Gastric inhibitory polypeptide
GIRK channel	G-protein-coupled inwardly-rectifying potassium channel
GK	Glucokinase
GLP-1	Glucagon-like peptide-1
GP	Glycogen phosphorylase
GPCR	G-protein coupled receptor
GRP	Gastrin releasing peptide
GS	Glycogen synthase
GSIS	Glucose-stimulated insulin secretion
h	Hour
H^+	Proton (Hydrogen ion)
HAAF	Hypoglycaemia-associated autonomic failure
HDAC	Histone deacetylase
IML	Intermediolateral cell column of the spinal cord
IP_3	Inotisol-1,4,5-triphosphate
IP_3R	Inotisol-1,4,5-triphosphate receptor
K^+	Potassium
K_{ATP} channel	ATP-sensitive potassium channel
KRB	Krebs-ringer buffer
l	Litre
M	Molar

mAChR	Muscarinic acetylcholine receptor
MCU	Mitochondrial Ca^{2+} uniporter
min	Minute
ml	Millilitre
mm	Millimetre
mM	Millimolar
mRNA	Messenger ribonucleic acid
Na^+	Sodium
NAADP	Nicotinic acid adenine dinucleotide phosphate
nAChR	Nicotinic acetylcholine receptor
NCLX	Mitochondrial Na^+/Ca^{2+} exchanger
NGF	Nerve growth factor
NHE	Na^+/H^+ antiporter
nm	Nanometre
nM	Nanomolar
NMJ	Neuromuscular junction
PACAP	Pituitary adenylate cyclase activating polypeptide
PEP	Phosphoenolpyruvate
PEPCK	Phosphoenolpyruvate carboxykinase
PFK-1	6-phosphofructo-1-kinase
PFK-2/FBPase-2	6-phosphofructo-2-kinase/fructose-2,6-bisphosphatase
pH_i	Cytoplasmic pH
PI3K	Phosphatidylinositide-3-kinase
PIP_2	Phosphatidylinositol-4,5-bisphosphate
PK	Pyruvate kinase

PKA	Protein Kinase A
PKC	Protein Kinase C
PNS	Peripheral nervous system
RFP	Red fluorescent protein
ROI	Region of interest
ROS	Reactive oxygen species
RPMI	Roswell Park Memorial Institute
RyR	Ryanodine receptor
s	Second
SEM	Standard error of mean
SERCA	Sarco-endoplasmic reticulum ATPase
SGLT	Na^+-coupled glucose transporter
SST	Somatostatin
SSTR	Somatostatin receptor
TCA cycle	Tricarboxylic acid cycle
TPC	Two-pore channel
TRPM channel	Transient receptor potential melastatin channel
VIP	Vasoactive intestinal peptide
VMH	Ventromedial hypothalamus
αMDG	Methyl-α-D-glucopyranoside
µg	Microgram
µl	Microlitre
µm	Micrometre
µM	Micromolar

Chapter 1: Introduction

1.1. Glucagon and glucose homeostasis

Glucagon, a 29-amino acid polypeptide synthesised and secreted by α-cells in the islets of Langerhans, is the body's principal hyperglycaemic hormone. Acting in opposition to insulin, glucagon is essential in maintaining normoglycaemia and preventing hypoglycaemia. When blood glucose levels fall, α-cells are stimulated and increase secretion of glucagon. Once secreted, glucagon's primary site of action is the liver, where it increases hepatic glucose output by stimulating liver glycogenolysis and gluconeogenesis, thereby increasing glycaemia (Jiang and Zhang, 2003). Due to these effects, glucagon plays an integral part in glucose counterregulation, the set of processes that protects against hypoglycaemia, encompassing both islet-specific changes and an autonomic response, which result in the upregulation of key counterregualtory factors (incl. glucagon, adrenaline, growth hormone and cortisol) that act to restore normoglycaemia (Gerich, 1988). Glucagon was originally labelled a contaminant after the successful isolation of insulin in 1921. As research into diabetes has advanced, the role of glucagon has gained prominence (Unger and Cherrington, 2012), with dysregulated glucagon secretion a feature of both type 1 and type 2 diabetes (Cryer, 2012). Understanding how glucagon secretion is regulated may therefore prove to be key in combatting the disease.

1.1.1. The α-cell

Glucagon-secreting α-cells are the second most abundant cell type in islets, accounting for 15-20% of total islet cells in rodents and ~40% in humans. They are found at the islet mantle in rodents but are evenly distributed throughout the human islet (Steiner et al., 2010). α-Cells receive various signals from paracrine, autocrine, endocrine, autonomic and metabolic sources, and it is the combined input of these signals which governs the secretion of glucagon. In the islet, they are inhibited by insulin (Cryer, 2012) and somatostatin (Hauge-Evans et al., 2009) secreted from neighbouring β- and δ-cells, respectively. However, they also possess intrinsic regulation in response to their metabolic environment (Bode et al., 1999, Liu et al., 2004, Leclerc et al., 2011, Zhang et al., 2013). Furthermore, α-cells receive signals from the periphery in the form of various hormones and neurotransmitters, which can either stimulate or suppress their activity. As a cell that operates predominantly under low energy conditions, regulation of the α-cell has been difficult to understand, especially compared with the neighbouring β-cell, and there remain numerous facets of α-cell physiology about which a consensus has not been reached (Gylfe and Gilon, 2014).

1.1.2. Hepatic effect of glucagon

After leaving the pancreas, glucagon travels to the liver via the hepatic portal vein (Davidson et al., 2016). Here, it binds to its receptor on hepatocytes, a 7-transmembrane domain GPCR[1] coupled predominantly with the G_s protein (Authier and Desbuquois,

[1] For all abbreviations, please refer to the abbreviations list at the start of the thesis

2008). The acute effect of glucagon on hepatic glucose output is almost entirely attributable to increased glycogenolysis (Cherrington, 1999), which is initiated when glucagon binds to its receptor, resulting in dissociation of the coupled G_s subunit into its constituent $G_{\alpha s}$ and $G_{\beta\delta s}$ subunits. The free $G_{\alpha s}$ subunit then stimulates adenylyl cyclase, increasing cytosolic levels of the secondary messenger cAMP. The rise in cAMP activates PKA, which phosphorylates glycogen phosphorylase kinase, enabling *it* to phosphorylate GP. GP can then catalyse the breakdown of glycogen into G-1-P, which is subsequently converted into G-6-P and finally glucose (Jiang and Zhang, 2003). Notably, glucagon has also been shown to inhibit glycogenesis (the reverse reaction) via suppression of GS activity by PKA and other kinases (Akatsuka et al., 1985, Roach, 1990) (Figure 1.1).

Upon glucagon administration glycogenolysis increases rapidly, peaking after 15 minutes and correlating with a rise in blood glucose. It is therefore central to the defence against hypoglycaemia, which requires rapid restoration of normoglycaemia to prevent against the damaging effects of hypoglycaemia (Cherrington, 1999). Contrastingly, the acute effect of glucagon on gluconeogenesis is minimal, despite its ability to increase gluconeogenic flux. Gluconeogenesis is dependent on the availability of glucogenic substrates such as amino acids and lactate from muscle, and glycerol from adipose tissue. These processes are largely independent of glucagon (Cherrington, 1999) with no evidence for expression of the glucagon receptor in muscle and only minimal levels in adipose tissue (Burcelin et al., 1995). This means that although increasing gluconeogenic flux, the effect of glucagon is transient due to low substrate availability (Cherrington, 1999). The role of gluconeogenesis in the response to acute hypoglycaemia is therefore minimal, however, under conditions of prolonged hypoglycaemia (Dobbins et al., 1991) and fasting (Rui, 2014), where gluconeogenic substrates are increased (due to the actions of other

counterregulatory hormones), the majority of hepatic glucose production occurs via gluconeogenesis.

The effect of glucagon on liver gluconeogenesis centres on activation of the gluconeogenic enzymes PEPCK (*catalyses* oxaloacetate → PEP), G6Pase (*catalyses* G-6-P → glucose), and FBPase-1 (*catalyses* F(1,6)P2 → F-6-P). While most enzymes involved in glycolysis and gluconeogenesis are shared, these enzymes are unique to gluconeogenesis and therefore determine its rate (Frayn, 2010). Similarly to glycogenolysis, the effect of glucagon on gluconeogenesis relies on increased cAMP/PKA signalling, with PKA-mediated activation of the transcription factors CREB and CRTC2, which form a complex with CBP, leading to upregulation of the PEPCK and G6Pase genes (Petersen et al., 2017) (Figure 1.1). Regulation of gene expression is typically a long-term effect, taking hours rather than minutes. Contrastingly, the stimulation of FBPase-1 occurs acutely due to removal of the allosteric inhibitor F(2,6)P2. F(2,6)P2 levels are determined by the bifunctional enzyme PFK-2/FBPase-2, a critical regulator of both glycolysis and gluconeogenesis (Frayn, 2010). The FBPase-2 domain catalyses the conversion of F(2,6)P2 into F-6-P with the PFK-2 domain catalysing the reverse reaction. Glucagon signalling results in PKA phosphorylation of PFK-2/FBPase-2, thereby favouring FBPase-2 activity and thus reducing cytosolic levels of F(2,6)P2. Crucially, F(2,6)P2 also allosterically stimulates the glycolytic enzyme PFK-1, which catalyses the reverse reaction of FBPase-1, its removal by FBPase-2 therefore also inhibits glycolysis (Rider et al., 2004) (Figure 1.1). Interestingly, the phosphorylation of PFK-2/FBPase-2 by PKA has also been shown to lead to dissociation of GK from PFK-2/FBPase-2 in the cytosol and its subsequent translocation to the nucleus, further reducing glycolysis and glycogenesis (Cullen et al., 2014). Glucagon is also reported to inhibit transcription of the GK gene

(Iynedjian et al., 1989) (Figure 1.1), and via PKA-dependent phosphorylation inhibit PK, which catalyses the conversion of PEP into pyruvate, the final step of glycolysis (Pilkis and Claus, 1991) (Figure 1.1). It is worth noting that as PFK-1, GK and PK are the three enzymes unique to glycolysis they largely determine glycolytic flux, catalysing the reverse reactions of FBPase-1, G6Pase and PEPCK(/Pyruvate carboxylase), respectively (Frayn, 2010).

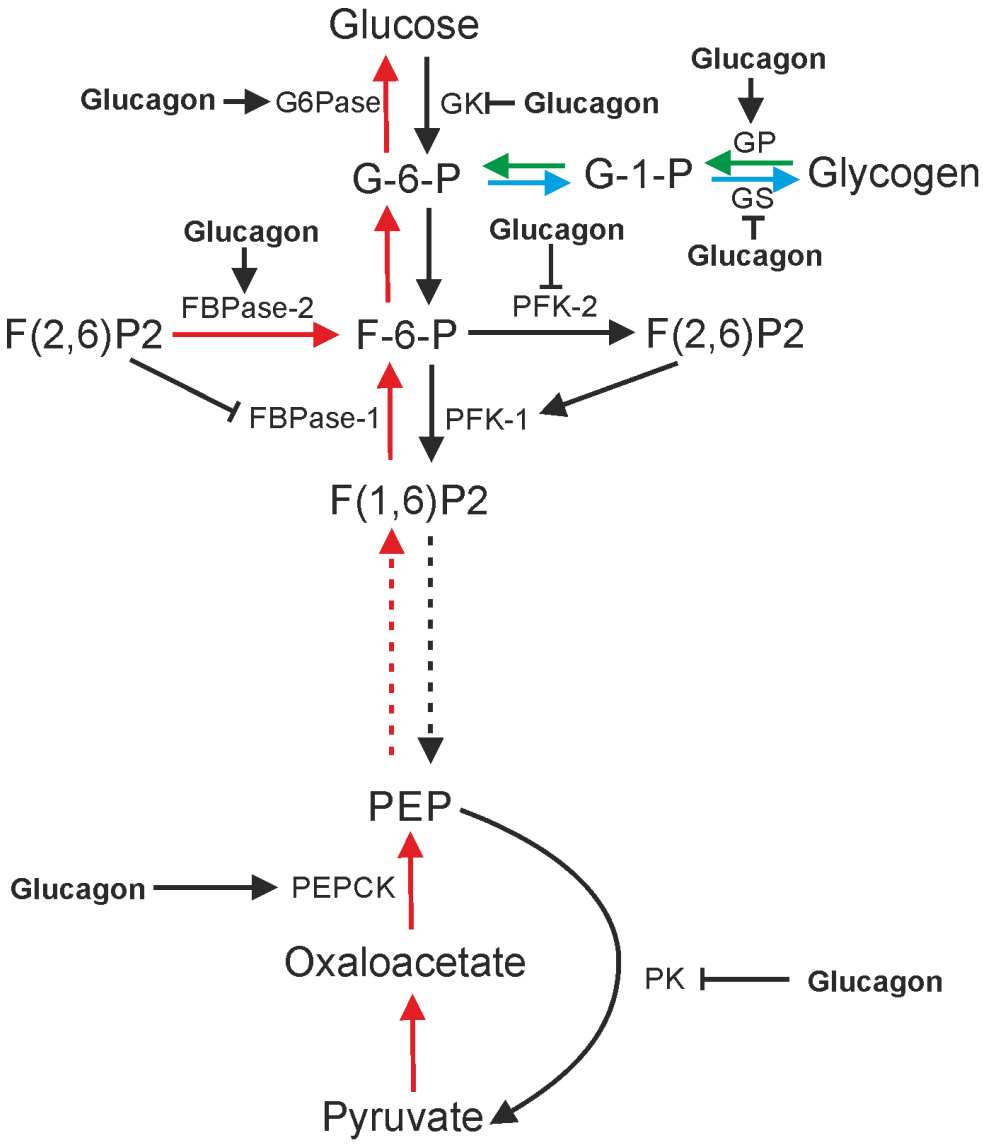


Figure 1.1 - Gluconeogenesis and glycogenolysis pathways and glucagon

Glucagon activates enzymes involved in gluconeogenesis and glycogenolysis whilst inhibiting enzymes involved in glycolysis and glycogenesis. Black arrows are steps in glycolysis; red arrows are steps in gluconeogenesis; green arrows are steps in glycogenolysis; blue arrows are steps in glycogenesis. Note, glycogen synthase actually catalyses conversion of UDP-glucose into glycogen after G-1-P conversion into UDP-glucose and that GK and G6Pase steps are also part of glycogenesis and glycogenolysis, respectively. ↓ - Stimulation ⊤ - Inhibition
Adapted from Jiang and Zhang (2003).

1.2. Glucagon and diabetes

1.2.1. Glucagon secretory defects in diabetes

The pathogenesis and pathology of diabetes have largely been attributed to the loss of GSIS. In type 1 diabetes, this is due to autoimmune destruction of the insulin-secreting β-cells. In type 2 diabetes, it occurs as a result of β-cell failure in the context of insulin resistance. This had led to the actions of glucagon and the other islet hormones often being overlooked. However, dysregulated glucagon secretion is a feature of all forms of diabetes (Lee et al., 2016b). While in healthy islets, glucagon secretion is low and relatively stable between ~5mM-20mM glucose, increasing progressively when glucose levels fall below ~5 mM glucose (Salehi et al., 2006, Vieira et al., 2007, Braun et al., 2010), this is not the case in diabetes. Firstly, inappropriately high plasma glucagon levels (hyperglucagonaemia) are reported in both type 1 and type 2 diabetes due a lack of suppression of glucagon secretion at high glucose. Moreover, it has been demonstrated hyperglucagonaemia compounds the effects of insufficient insulin secretion, contributing to both fasting (Gerich et al., 1975, Baron et al., 1987) and postprandial hyperglycaemia (Dinneen et al., 1995, Shah et al., 2000, Dunning and Gerich, 2007).

Insulin-dependent diabetic patients (type 1 and advanced type 2 diabetes) are also at risk of impaired glucose counterregulation, which heightens the risk of hypoglycaemia. This results from a combination of excessive insulin dosage and impaired glucagon responsiveness to hypoglycaemia, meaning when patients administer insulin blood glucose levels fall yet α-cells do not respond, leading to hypoglycaemia. Antecedent hypoglycaemia is then further deleterious to various autonomic pathways which also protect against hypoglycaemia, pushing the glycaemic thresholds of these responses

towards lower glucose concentrations (Cryer, 2002). This process is known as hypoglycaemia-associated autonomic failure (HAAF) and results in a further diminished glucose counterregulatory response but also hypoglycaemic unawareness, whereby cholinergic and adrenergic pathways (Towler et al., 1993) in the brain fail to engage, meaning the neurogenic symptoms associated with hypoglycaemia (e.g. shakiness, palpitations, anxiety, sweating, hunger, paraesthesia (Cryer, 1999)) are not triggered (Cryer, 2002). Impaired counterregulation remains the greatest barrier to effective glycaemic management in diabetes (Cryer, 2002), with hypoglycaemia potentially leading to seizure, coma and even death (Cryer, 2007).

How glucagon secretion becomes dysregulated in diabetes is unclear. There is evidence linking dysregulated glucagon secretion to changes in paracrine signalling caused by β-cell loss (Cryer, 2012) and heightened somatostatin secretion (Yue et al., 2012, Karimian et al., 2013), as well as intrinsic changes to the α-cell itself (Zhang et al., 2013). These mechanisms will be discussed in further detail later.

1.2.2. The glucagonocentric model of diabetes

After the isolation of insulin in 1921, the cause of all diabetic abnormalities was assigned to a lack of insulin (Unger and Cherrington, 2012). This 'insulinocentrism' persisted until 1975 when Unger and Orci (1975) proposed the bihormonal model, which stated that lack of insulin causes glucose underutilisation but it is glucagon that drives glucose overproduction through increased hepatic glucose output. It was largely based on the observation that relative or absolute hyperglucagonaemia was reported in all forms of

diabetes and that insufficient insulin secretion did not cause endogenous hyperglycaemia without glucagon.

More recently, as a result of studies in $GcgR^{-/-}$ mice, the role of glucagon has gained further prominence resulting in Unger proposing a glucagonocentric model of diabetes. This states that lack of insulin merely acts as a trigger which drives glucagon excess, and it is this excess that causes the diabetic phenotype (Unger and Cherrington, 2012). This model first came to fruition in studies in $GcgR^{-/-}$ mice who have had their β-cells destroyed by streptozotocin treatment, equivalent to type 1 diabetes. Interestingly, in these mice, despite a near complete loss of β-cells, diabetes does not manifest, suggesting glucagon plays a critical role in diabetes pathogenesis (Lee et al., 2011). In a follow-up study, the glucagon receptor was reintroduced to $GcgR^{-/-}$ mice and severe hyperglycaemia resulted, which reversed after 7 days once GcgR mRNA levels fell (reflecting turnover of GcgRs) (Lee et al., 2012). Crucially, the same was found in mouse models of type 2 diabetes, induced by high-fat diet and genetic ablation of the leptin receptor, which was avoided by knockout of the glucagon receptor (Lee et al., 2014).

Unger argues that either lack of insulin in type 1 diabetes or α-cell insulin resistance in type 2 diabetes, removes the tonic paracrine inhibition of insulin on glucagon secretion, leading to dysregulated glucagon secretion, which drives hyperglycaemia and the pathogenesis of diabetes (Figure 1.2). Note that glucagon excess in isolation cannot cause diabetes and when hyperglucagonaemia is induced in non-diabetic subjects without deficient insulin secretion blood glucose is unaffected, confirming that lack of insulin is essential for diabetes pathogenesis (Sherwin et al., 1976). In this respect, the glucagonocentric model does not disregard insulin but merely states that its principle

function is to suppress glucagon (Lee et al., 2011). Evidence for a critical role for glucagon in diabetes can also be extended to human studies, with suppression of glucagon secretion with somatostatin preventing hyperglycaemia and ketoacidosis in type 1 diabetes (Gerich et al., 1975, Raskin and Unger, 1978).

However, the glucagonocentric model is somewhat disputed. A common argument against the model is the presence of diabetes in patients who have undergone total pancreatectomy. This suggests that diabetes can manifest without the action of glucagon (Barnes and Bloom, 1976). Unger contests this assumption, arguing that extrapancreatic sources of glucagon are sufficient to drive diabetes pathogenesis after pancreatectomy (Lee et al., 2011), citing the observations that gastric and gut α-cells hypersecrete glucagon during insulin deficiency in depancreatized humans and animals (Mashiter et al., 1975, Matsuyama et al., 1979, Del Prato et al., 1980, Sudo et al., 1980, Bringer et al., 1981, Bajorunas et al., 1986, Tanjoh et al., 2003), with suppression of extrapancreatic glucagon preventing against hyperglycaemia in depancreatized dogs (Ross et al., 1978). The degree of β-cell ablation in the streptozotocin-treated mouse has also been questioned, Neumann et al. (2016) found if there was a complete lack of insulin by way of insulin gene knockout (Streptozotocin treatment caused 90% destruction of β-cell area in $GcgR^{-/-}$ mice (Lee et al., 2011)), glucagon receptor knockout was incapable of keeping mice alive, with only modest improvements in plasma glucose and ketone levels. This is not relevant for type 2 diabetes, where β-cell function and insulin action, although diminished, remain intact (particularly at the early stages of the disease before insulin-dependence develops). Whether insulin gene knockout truly reflects type 1 diabetes is also questionable. Keenan et al. (2010) reported residual insulin production in a cohort of 411 people who had had type 1 diabetes for at least 50 years. 67.4% had detectable C-peptide with a subset even

increasing C-peptide in response to a mixed meal, and post-mortem histology studies confirmed the presence of an insulin-positive β-cell mass, similar findings have also been reported in other studies (Meier et al., 2005, Keenan et al., 2007, Pipeleers et al., 2008, Liu et al., 2009, Rother et al., 2009, Gianani et al., 2010).

Whether we consider diabetes to be 'insulinocentric' or 'glucagonocentric' is a question of semantics; what is clear is that insulin lack or glucagon excess in isolation is not sufficient to cause diabetes, it is instead the imbalance of these two hormones which results in diabetes pathogenesis.

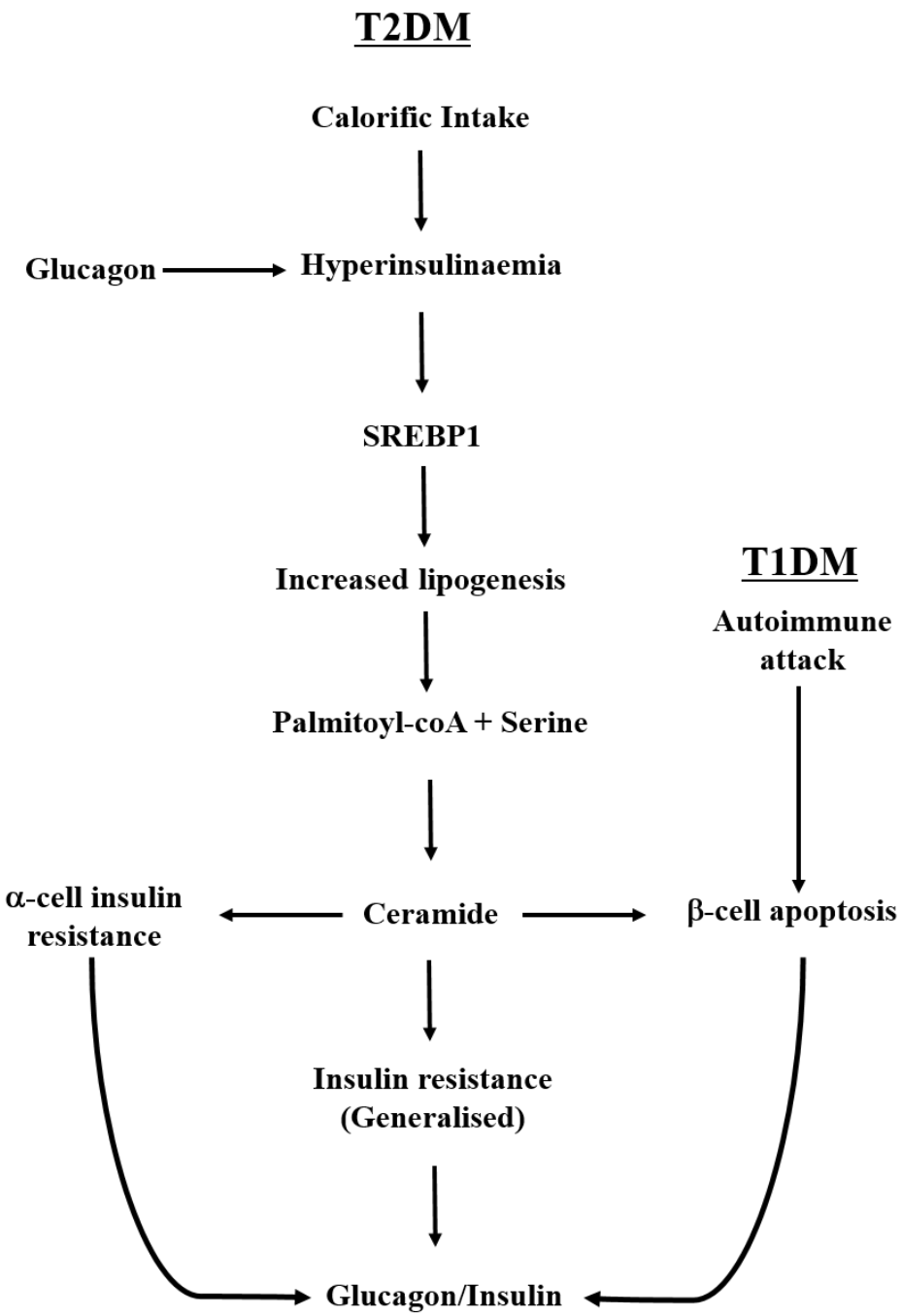


Figure 1.2 - Roger Unger's glucagonocentric model

Type 2 Diabetes Mellitus (T2DM): Calorific intake leads to hyperinsulinaemia, increased insulin activates the transcription factor SREBP1 leading to increased lipogenesis, production of palmitoyl-coA and serine, which leads to increased formation of ceramide. Ceramide has deleterious effects (via its effects on signalling pathways) on the islet cells, promoting α-cell insulin resistance and β-cell apoptosis. This creates an imbalance in glucagon and insulin which drives diabetes. **Type 1 Diabetes Mellitus (T1DM):** Autoimmune destruction of β-cells abolishes insulin secretion and therefore removes tonic inhibition from α-cells, increasing glucagon secretion. Leading to an imbalance in glucagon and insulin which drives diabetes. Adapted from Lee et al. (2014)

1.3. Regulation of glucagon secretion

Glucagon secretion is under the control of various metabolic, paracrine, autocrine, autonomic and endocrine factors, all of which can target the α-cell directly and diminish or enhance glucagon secretory output, often via a change in $[Ca^{2+}]_i$. In the following section, I will give a brief overview of the main types of regulation, focusing first on islet-specific regulation (metabolic, autocrine, paracrine) before moving on to discuss regulation from peripheral sources (autonomic, endocrine).

1.3.1 Control by glucose

Glucose is known to inhibit glucagon secretion. Yet a consensus on how this occurs has not been reached. Firstly, a model based largely on experiments performed on whole mouse islets proposes that, similarly to β-cells, α-cells detect glucose using the K_{ATP} channel. Crucially, unlike the β-cell, α-cell K_{ATP} channel activity is low even under hypoglycaemic conditions (for reasons that remain unresolved); this means even at low glucose the membrane is depolarized and α-cells are electrically active. Increasing glucose concentrations causes complete inhibition of the K_{ATP} channel, leading to stronger depolarization increasing action potential frequency but also (due to Na^+-channel inactivation) reducing action potential height. Importantly, glucagon secretion is tightly coupled with opening of P/Q-type Ca^{2+} channels, which are active at the peak of the action potential spike. Therefore, the reduction in spike height at high glucose means these channels do not open and glucagon secretion is inhibited (Zhang et al., 2013; Figure 1.3). An alternative model based on studies in single mouse α-cells identifies ER-Ca^{2+} release as a crucial trigger for glucagon secretion, which causes activation of store-operated channels

at the plasma membrane and subsequent opening of L-type Ca^{2+} channels, resulting in increased $[Ca^{2+}]_i$ and stimulation of glucagon secretion. Glucose, as a promoter of ER-Ca^{2+} sequestration via activation of the SERCA-ATPase, thereby inhibits glucagon secretion by preventing the activation of the store-operated current (Liu et al., 2004). Another model ascribes the inhibitory effects of glucose to it hyperpolarizing the cell membrane via activation of the Na^+/K^+-ATPase (Bode et al., 1999); a loss of AMPK action has also been attributed to the inhibitory effect of glucose on glucagon secretion (Leclerc et al., 2011). Both these latter studies were conducted in cell lines.

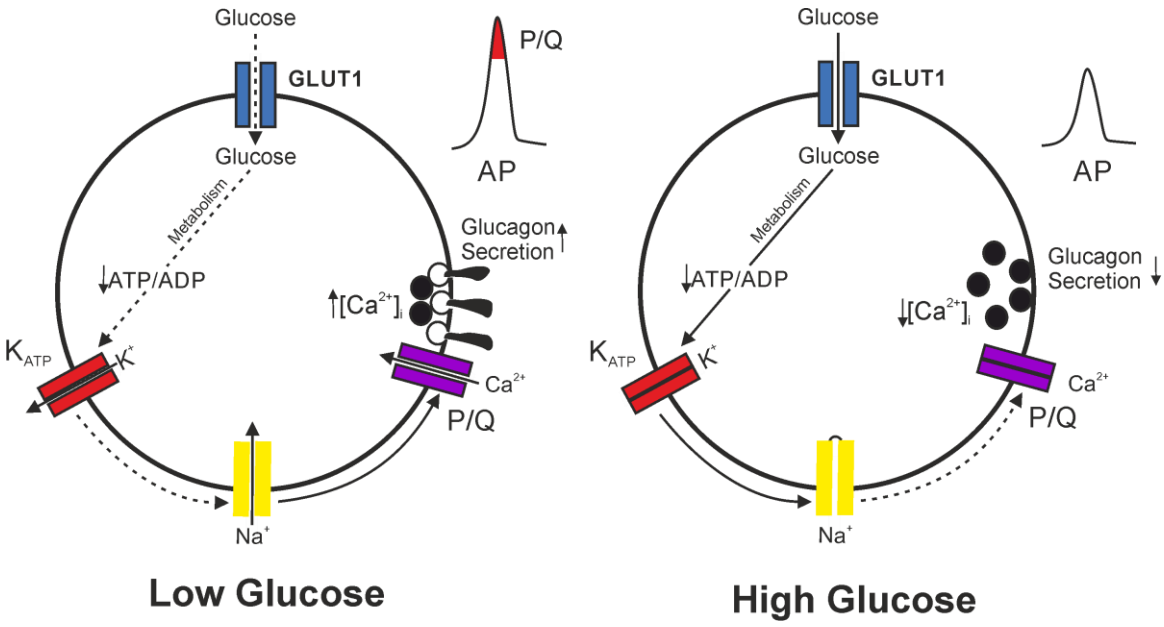


Figure 1.3 - K_{ATP} model of glucagon secretion

Even at low glucose, K_{ATP} channel activity is low. This result in membrane depolarization and action potential firing due to opening of voltage-gated Na^+ and Ca^{2+} channels at the plasma membrane. Most importantly, at the peak of the action potential (AP) P/Q-type Ca^{2+} channels open, stimulating glucagon secretion. At high glucose, the ATP/ADP ratio increases, closing remaining K_{ATP} channels, producing a stronger depolarization, which leads to Na^+ channel inactivation. This reduces the action potential height, meaning P/Q-type Ca^{2+} channels do not open and glucagon secretion is reduced. Adapted from Zhang et al. (2013).

1.3.2. Control by other nutrients

Conversely, despite also increasing ATP, other metabolites such as amino acids (Pipeleers et al., 1985, Kuhara et al., 1991, Dumonteil et al., 2000, Gannon and Nuttall, 2010) and fatty acids (Gremlich et al., 1997, Dumonteil et al., 2000, Bollheimer et al., 2004, Olofsson et al., 2004, Hong et al., 2005, Hong et al., 2007) actually stimulate glucagon secretion. From a physiological viewpoint, this is understandable. Firstly, glucagon is critical in maintaining amino acid homeostasis (Holst et al., 2017). Plasma amino acids are increased during prolonged fasting due to amino acid release from the muscle (Owen et al., 1979). Glucagon then promotes their uptake by the liver; glucogenic amino acids, particularly alanine and glutamine, can be used as precursors for gluconeogenesis, with glucagon shown to increase hepatic glutamine (Brockman and Bergman, 1975, Battezzati et al., 1998) and alanine uptake (Brockman and Bergman, 1975, Moule and McGivan, 1987), as well as increasing alanine transaminase activity (Begum and Datta, 1991), which catalyses the conversion of alanine into pyruvate. Glucagon also strongly promotes amino acid disposal through ureagenesis in the liver (Holst et al., 2017) and excretion in the kidney (Bankir et al., 2015).

However, amino acids are also increased in the postprandial state. Dietary protein increases both insulin and glucagon secretion, with insulin promoting protein synthesis in muscle. Notably, the effect of amino acids on insulin secretion in isolation is minimal compared to the effect on glucagon secretion, but is augmented in the presence of glucose (Gannon and Nuttall, 2010). The glucose dependence of the amino acid β-cell effects means insulin secretion is virtually unaffected by the high levels of plasma amino acids during fasting, allowing for optimal use in gluconeogenesis. However, after a mixed meal,

amino acids potentiate glucose-stimulated insulin secretion (GSIS) and are subsequently diverted towards the muscle for protein synthesis. Their stimulatory effect on glucagon secretion is overcome by glucose - whether this be via a direct metabolic effect or a paracrine effect potentiated by amino acids (Walker et al., 2011). Furthermore, if a meal is high in protein, the stimulation of glucagon secretion likely acts as a counterbalance reducing the glucose-lowering effects of insulin and preventing hypoglycaemia (Gromada et al., 2007).

When considering individual amino acids, most stimulate glucagon secretion with arginine, alanine and glycine consistently the most potent (Pipeleers et al., 1985, Kuhara et al., 1991, Gannon and Nuttall, 2010). Histidine is without effect (Kuhara et al., 1991, Gannon and Nuttall, 2010) and while there is some evidence for inhibition from amino acids such as leucine and isoleucine (Kuhara et al., 1991) these effects are minimal and in the case of leucine have been shown to only occur at non-physiological concentrations, with it acting as a stimulus at physiological levels (Leclercq-Meyer et al., 1985). Notably, Pipeleers et al. (1985) reported that a 'cocktail' of all 20 amino acids was a far more potent stimulant of glucagon secretion than any individual amino acid, suggesting they act synergistically to enhance glucagon secretion. One can assume due to the inhibitory effect of glucose that stimulation occurs via an ATP-independent mechanism. However, there have been very few studies into the mechanisms underpinning amino-acid induced glucagon secretion. Most have focused on arginine, arguably the most potent amino acid glucagon secretagogue, with its effect on glucagon secretion previously shown to be dependent on PKC signalling in rat islets (Bjaaland et al., 1988), and reduced by the mAChR antagonist atropine in humans (Czyzyk et al., 1981), indicating a potential secondary cholinergic effect. Notably, arginine is a precursor for nitric oxide, a key

signalling molecule. Using intact mouse islets, it was revealed that inhibiting nitric oxide synthesis significantly reduced arginine-induced glucagon secretion via a direct effect on the secretory machinery (Salehi et al., 1998). A study in human islets, which screened various amino acids demonstrated that glycine was actually the predominant amino acid responsible for stimulation of glucagon secretion. It achieved this by binding to its receptor and increasing $[Ca^{2+}]_i$, notably, its effect was reduced by increasing glucose (Li et al., 2013). It could also be the case, that amino acids simply maintain sufficient ATP levels in the absence of glucose, thereby ensuring proper cellular function and glucagon secretion, without dramatically increasing ATP such that it impacts on K_{ATP} channel activity.

Plasma free fatty acid concentration throughout the day follows an inverse relationship to glucose and insulin, with generally low post-prandial levels and high levels after an overnight fast, largely due to insulin inhibiting lipolysis (Frayn, 2010). At low glucose concentrations, free fatty acids are high. Their stimulatory effect on glucagon secretion is therefore expected. Of course, if a meal is high in fat, plasma free fatty acids will increase (Surina et al., 1993), which can potentiate insulin secretion in the presence of glucose (Parker et al., 2003). Note however that fats are absorbed into the bloodstream at a slower rate than carbohydrates and therefore plasma levels of glucose and free fatty acids do not peak at the same time (Thibodeau and Patton, 2003).

Notably, glucagon has been linked to regulation of lipid metabolism. It has been reported to increase fatty acid oxidation (Longuet et al., 2008) and ketogenesis (Pegorier et al., 1989, Vons et al., 1991) in hepatocytes. The hormone has also been shown to stimulate lipolysis in rat and human adipocytes (Heckemeyer et al., 1983, Perea et al., 1995), although this is disputed by a human *in* vivo study, which reported no change in lipolysis

after induction of hyperglucagonaemia in abdominal adipose tissue (Gravholt et al., 2001). Furthermore, as previously mentioned, the expression of glucagon receptors is low in adipose tissue (Burcelin et al., 1995). Moreover, if glucagon could stimulate lipolysis, one would expect a greater acute effect of glucagon on gluconeogenesis due to the liberation of the glucogenic substrate glycerol from triacylglyceride.

As with amino acids, fatty acids' stimulation of glucagon secretion likely occurs via an ATP-independent mechanism. Indeed, there have been several studies demonstrating that α-cells possess FFAR1, a GPCR that binds medium and long-chain fatty acids (Briscoe et al., 2003), causing an increase in $[Ca^{2+}]_i$ that stimulates glucagon secretion (Flodgren et al., 2007, Wang et al., 2011, Kristinsson et al., 2017). FFAR1 is specifically $G_{\alpha q/11}$-coupled (Briscoe et al., 2003) with its effects mediated via the IP_3/DAG pathway, demonstrated by inhibition of phospholipase C abolishing the effects of linoleic acid on α-cell $[Ca^{2+}]_i$ (Wang et al., 2011). Nevertheless, a stimulatory metabolic effect also appears to play a role with the long-term effect of the fatty acid palmitate not being reproduced entirely by FFAR1 agonists and the combined reduction in palmitate-induced glucagon secretion by FFAR1 antagonist and the CPT1 inhibitor etomoxir being larger than when either were used alone. It may therefore be the case that fatty acid metabolism is required to either provide substrate for the FFAR1 signalling pathway (e.g. DAG) (Kristinsson et al., 2017) or maintain ATP at a sufficient level for the α-cell to function. Additionally, in a study looking at α-cells within intact islets, application of the palmitate resulted in Ca^{2+} influx via L-type Ca^{2+} channels, coupled with a direct effect on glucagon granule exocytosis. It was speculated that this may be due to the fatty acid exerting a diazoxide-like effect on K_{ATP} channels, thereby reactivating channels closed by glucose and facilitating action potential generation. Electrogenic transport of the anionic palmitate counteracting the

depolarizing effects of glucose was also cited as a possible cause. Notably, palmitate also reduced somatostatin release by 50%, suggesting a secondary paracrine effect of the metabolite (Olofsson et al., 2004).

1.3.3. Paracrine regulation of glucagon secretion

The α-cell is under paracrine regulation from neighbouring β- and δ-cells, whose activity increases as glucose levels rise. β-cells secrete insulin and various other paracrine factors, which have also been shown to inhibit glucagon secretion. These include Zn^{2+} (Ishihara et al., 2003, Franklin et al., 2005, Zhou et al., 2007a), ATP (Tuduri et al., 2008), amylin (Gedulin et al., 1997, Gedulin et al., 2006) and serotonin (Almaca et al., 2016), which are co-secreted with insulin, and GABA (Wendt et al., 2004, Xu et al., 2006) and γ – hydroxybutyrate (GHB) (Li et al., 2013), which are released in distinct granules. GSIS begins at glucose concentrations as low as 3 mM in humans (Braun et al., 2010) and 6 mM in mice (Salehi et al., 2006, Vieira et al., 2007), increasing proportionally as glucose rises. Various mechanisms have been suggested for how insulin itself targets the α-cell. A study in dissociated rat islets indicated that insulin transiently increases α-cell K_{ATP} channel activity, leading to membrane hyperpolarization and a reduction in glucagon secretion. Notably, Zn^{2+} was also found to inhibit glucagon secretion by the same mechanism (Franklin et al., 2005). It has also been reported, in a study using both rat and human islets, that insulin promotes the translocation of $GABA_A$ receptors to the cell membrane in α-cells, the separately released GABA then binds causing membrane hyperpolarization due to Cl^- influx through the $GABA_A$ receptor, thus reducing glucagon secretion (Xu et al., 2006). Lastly, in a study using human and mouse islets it was shown that insulin signalling in the α-cell led to activation of phosphodiesterase 3B, which degrades cAMP resulting in

a reduction in glucagon secretion (Elliott et al., 2015). The mechanisms underlying the effects of other β-cell paracrine factors have also been revealed. Serotonin is found to bind to the G_i-coupled 5-HT_{1F} on α-cells, activating $G_{\alpha i}$ which subsequently inhibits adenylyl cyclase, reducing cAMP and suppressing glucagon secretion (Almaca et al., 2016). While ATP was found to bind to purinergic GPCRs, leading to silencing or reduced frequency of $[Ca^{2+}]_i$ oscillations in α-cells and a reduction in glucagon secretion (Tuduri et al., 2008). A study on human islets demonstrated that GHB, a downstream metabolite of GABA, is generated in β-cells during high glucose and secreted separately from insulin. It inhibits glucagon secretion by binding to its receptor on α-cells and reducing the stimulatory effects of glycine (discussed above) (Li et al., 2013). Note also that studies in mouse (Ravier and Rutter, 2005, MacDonald et al., 2007) and human islets (Ramracheya et al., 2010) dispute the inhibitory effect of Zn^{2+}.

Somatostatin secreted from pancreatic δ-cells is a potent inhibitor of both glucagon and insulin secretion (Hauge-Evans et al., 2009). Similarly to insulin, it is released in response to rising blood glucose, with the threshold for stimulation reported at 3mM glucose in humans (Braun et al., 2010) and 4 mM glucose in mice[2] (Salehi et al., 2006, Vieira et al., 2007). It continues to rise further as glucose is elevated to 20 mM. Once released it binds to the $G_{i/o}$-coupled somatostatin receptors (SSTRs) on neighbouring islet cells, with SSTR2 the main isoform in α-cells and SSTR5 the main isoform in β-cells (Strowski et al., 2000, Braun, 2014). Despite δ-cells only accounting for 5-10% of islet cells, SSTR2 blockade has illustrated the significant role of somatostatin in suppressing glucagon secretion both at low and high glucose (Vieira et al., 2007, de Heer et al., 2008, Li et al.,

[2] Note 3mM glucose not used in these experiments (0 mM → 1 mM → 4 mM etc.)

2015). The exact mechanism by which this occurs, however, is yet to be fully elucidated. $G_{\alpha i}$ signalling is commonly associated with a lowering of cAMP via inhibition of adenylyl cyclase; the cAMP lowering effects of somatostatin have indeed been demonstrated in mouse and human α-cells and correlate with a fall in glucagon secretion attributed to the resulting drop in cAMP/PKA signalling reducing granule exocytosis in a Ca^{2+}-independent manner (Elliott et al., 2015). However, this is not confirmed, when cAMP is clamped in single rat α-cells the inhibitory effect of somatostatin on exocytosis remains (Gromada et al., 2001a). Alternatively, the $G_{\alpha i}$ subunit has been reported to interact with the phosphatase calcineurin resulting in depriming of glucagon-containing granules close to L-type Ca^{2+} channels (Gromada et al., 2001a). Furthermore, somatostatin was shown to inhibit rat α-cell electrical activity via activation of a low-conductance K^+ channel dependent on $G_{\beta\gamma i}$ protein activation, thus inducing a hyperpolarizing current (Gromada et al., 2001b). More recently, it was demonstrated that, via gap junction connections between the two cell types, optogenic activation of β-cells could activate δ-cells, leading to somatostatin release and α-cell hyperpolarization, raising the interesting possibility that at least some part of the β-cell's inhibitory effect on glucagon secretion is actually due to a secondary effect on δ-cells (Briant et al., 2017).

It must also be noted that islet hormones can act in an endocrine as well as a paracrine manner. Studies have demonstrated that blood flow in mouse islets is predominantly directed from β- to α- to δ-cells (Jansson et al., 2016). This entails capillaries branching outward from the β-cell core, taking insulin to the non-β cell mantle, where α-cells then secrete glucagon into the bloodstream followed by δ-cells secreting somatostatin. It can, therefore, be assumed that somatostatin acts principally via paracrine signalling, while insulin likely targets the α-cell in a somewhat endocrine-dependent manner (in addition to

the effect mediated via gap junctions). As the morphology of the human islet is more heterogeneous, a pattern of blood flow between different cell types is unlikely (Cabrera et al., 2006). It is therefore likely that paracrine interaction between the islet cell types is of greater importance.

1.3.4. Autocrine regulation of glucagon secretion

Autocrine signalling has also been reported in α-cells. The amino acid and neurotransmitter glutamate is reported to be co-secreted with glucagon, and in a study utilising human, monkey and mouse islets was found to specifically stimulate α-cells by binding to AMPA ionotropic glutamate receptors. This was reported to result in membrane depolarization and subsequent opening of L-type Ca^{2+} channels, increasing $[Ca^{2+}]_i$ and thus stimulating glucagon secretion (Cabrera et al., 2008). There is also some evidence for glucagon itself acting upon the α-cell in an autocrine feedback loop, both in increasing exocytosis (Ma et al., 2005) and increasing its own expression (Leibiger et al., 2012).

1.3.5. Autonomic regulation of glucagon secretion

There are several barriers to prevent against hypoglycaemia, which activate sequentially as glucose falls. Firstly, there is a decrement in insulin secretion as β-cells are inhibited by low glucose (4.7-5.3 mM) (Taborsky and Mundinger, 2012); followed by an increment in glucagon secretion, resulting from both an intrinsic response to low glucose and a reduction in paracrine inhibition from β- and δ-cells. Accompanying these intraislet mechanisms is the autonomic defence against hypoglycaemia, which encompasses both parasympathetic and sympathetic branches and results in adrenaline release from the

adrenal medulla, release of noradrenaline from intraislet sympathetic nerve endings and release of ACh from intraislet parasympathetic nerve endings. Adrenaline (Schuit and Pipeleers, 1986, Johansson et al., 1989, Gromada et al., 1997, Liu et al., 2004, Vieira et al., 2004, De Marinis et al., 2010), noradrenaline (Hauge-Evans et al., 2010) and ACh (Iversen, 1973, Kimura et al., 1982, Patel, 1984, Berts et al., 1997) have all been shown to stimulate glucagon secretion, and together they are reported to account for 75-90% of the glucagon response to insulin-induced hypoglycaemia (Taborsky and Mundinger, 2012). The response is graded with intraislet parasympathetic nerve endings activating at mild hypoglycaemia (4.2-4.7 mM), adrenaline secretion at marked hypoglycaemia (3.6-3.9 mM) and the intraislet sympathetic nerve endings at severe hypoglycaemia (≤1.9 mM) (Taborsky and Mundinger, 2012) (Figure 1.4).

The autonomic response to hypoglycaemia begins in the CNS. Glucose counterregulation is a complex process that does not merely rely on one specific glucose sensing region. Instead several regions in the brainstem, hypothalamus and periphery (e.g. hepatic portal vein glucose sensors) appear to have intrinsic glucose sensing properties and are synaptically linked. It is therefore the integration of these signals which determines the counterregulatory response (Marty et al., 2007). Similarly to islets, glucose sensing in the brain is primarily dictated by the actions of two different cell types, glucose-inhibited (GI) neurones, which decrease firing in response to glucose, and glucose-excited (GE) neurones, which increase firing in response to glucose (Thorens, 2012). Different groups of GI neurones in the brainstem and hypothalamus form neurocircuits, which govern either the parasympathetic (Lamy et al., 2014, Verberne et al., 2014) or sympathetic response to hypoglycaemia (Verberne and Sartor, 2010, Garfield et al., 2014), activating sequentially as glucose falls. These send efferent projections to the dorsal motor nucleus of the vagus

nerve (DMNV), a part of the brainstem where parasympathetic output to the pancreas originates, or the intermediolateral cell column of the spinal cord (IML), where sympathetic efferent nerves to both the pancreas and adrenal medulla originate (Verberne et al., 2014, Steinbusch et al., 2015).

At mild hypoglycaemia (4.2 – 4.7 mM), efferent preganglionic parasympathetic nerves originating from the DMNV are activated, these converge at parasympathetic ganglia, secreting ACh into the synaptic cleft and via activation of nAChRs stimulate postganglionic parasympathetic nerves (Frayn, 2010). Parasympathetic nerve endings that innervate the islet then release ACh into the islet vicinity. Once released, ACh is reported to bind to M3 muscarinic receptors on α-cells, increasing $[Ca^{2+}]_i$ and stimulating glucagon secretion (Duttaroy et al., 2004, Verspohl et al., 1990, Karlsson and Ahren, 1993). The M3 muscarinic receptor is a G_q-coupled receptor meaning it likely acts via the phospholipase C pathway leading to IP_3-mediated Ca^{2+} release and PKC activation. However, intracellular characterisation of the mechanism of ACh-induced glucagon secretion has not been fully elucidated. ACh also stimulates insulin secretion (Malaisse et al., 1967, Iversen, 1973, Kimura et al., 1982), although at low glucose its effects are minimal (Gilon and Henquin, 2001).

If glucose continues to fall (3.6 mM – 3.9 mM) preganglionic sympathetic neurones originating from the IML are activated, these innervate the chromaffin cells of the adrenal medulla, releasing ACh, which binds to the nAChRs on chromaffin cells (Frayn, 2010), causing membrane depolarization and Ca^{2+} influx, inducing adrenaline secretion into the bloodstream (Zaika et al., 2004). Adrenaline is known to act directly on the liver, binding to β_2-adrenergic receptors to increase hepatic glucose output via enhanced glycogenolysis

and gluconeogenesis (Exton, 1987), similarly to glucagon itself. Notably, however, its stimulation of gluconeogenesis is principally due to its effects on peripheral tissues rather than a direct hepatic action. Adrenaline can liberate glucogenic substrates from muscle (amino acids, lactate) and adipose tissue (glycerol) (Sacca et al., 1983, Cherrington et al., 1984), a process glucagon has little control over. Thus, under conditions of prolonged hypoglycaemia, the two hormones likely act synergistically, with adrenaline principally delivering substrates to the liver where glucagon facilitates their uptake and conversion into glucose (Frizzell et al., 1988). In the islet, adrenaline stimulates glucagon secretion by increasing $[Ca^{2+}]_i$, yet a consensus has not been reached on exactly how this occurs. Firstly, it is disputed whether stimulation occurs solely via β-adrenergic receptors (Schuit and Pipeleers, 1986, Gromada et al., 1997, De Marinis et al., 2010) or also relies on α-1 adrenergic receptors (Vieira et al., 2004). And secondly, whether downstream signalling from these receptors results in intracellular Ca^{2+} release (Johansson et al., 1989), Ca^{2+} influx through L-type Ca^{2+} channels (Gromada et al., 1997, De Marinis et al., 2010) or a combination of both (Liu et al., 2004, Vieira et al., 2004). Adrenaline also suppresses insulin secretion (Nakaki et al., 1980, Schuit and Pipeleers, 1986, Langer, 1987).

Under severe hypoglycaemia (≤1.9 mM), preganglionic nerves originating from the IML are activated and reach sympathetic ganglia where they secrete ACh into the synaptic cleft, which binds to nAChRs activating the postganglionic sympathetic nerves (Frayn, 2010). Intraislet sympathetic nerve endings that innervate the islet then release noradrenaline into the islet vicinity (Taborsky and Mundinger, 2012), which targets α-cells and increases glucagon secretion (Hauge-Evans et al., 2010). One expects that noradrenaline stimulates glucagon secretion via the same mechanism as adrenaline due to the similarity of the two compounds (IUPHAR/BPS, 2015, IUPHAR/BPS, 2016). Notably, the suggestion that

sympathetic nerves activation follows sympathoadrenal activation is based on studies on pancreatic noradrenaline spillover which are only able to detect noradrenaline at glucose concentrations of ≤1.9 mM (Havel et al., 1996). It should be noted, however, this may be due to noradrenaline actions preceding its detection in spillover assays, as seen in the liver (Mundinger et al., 1997). This is reinforced by the crossover of neural pathways that control the chromaffin cells of the adrenal medulla and the sympathetic nerves that innervate the islet (Jansen et al., 1997). If this is the case, adrenaline and noradrenaline may act simultaneously to increase blood glucose.

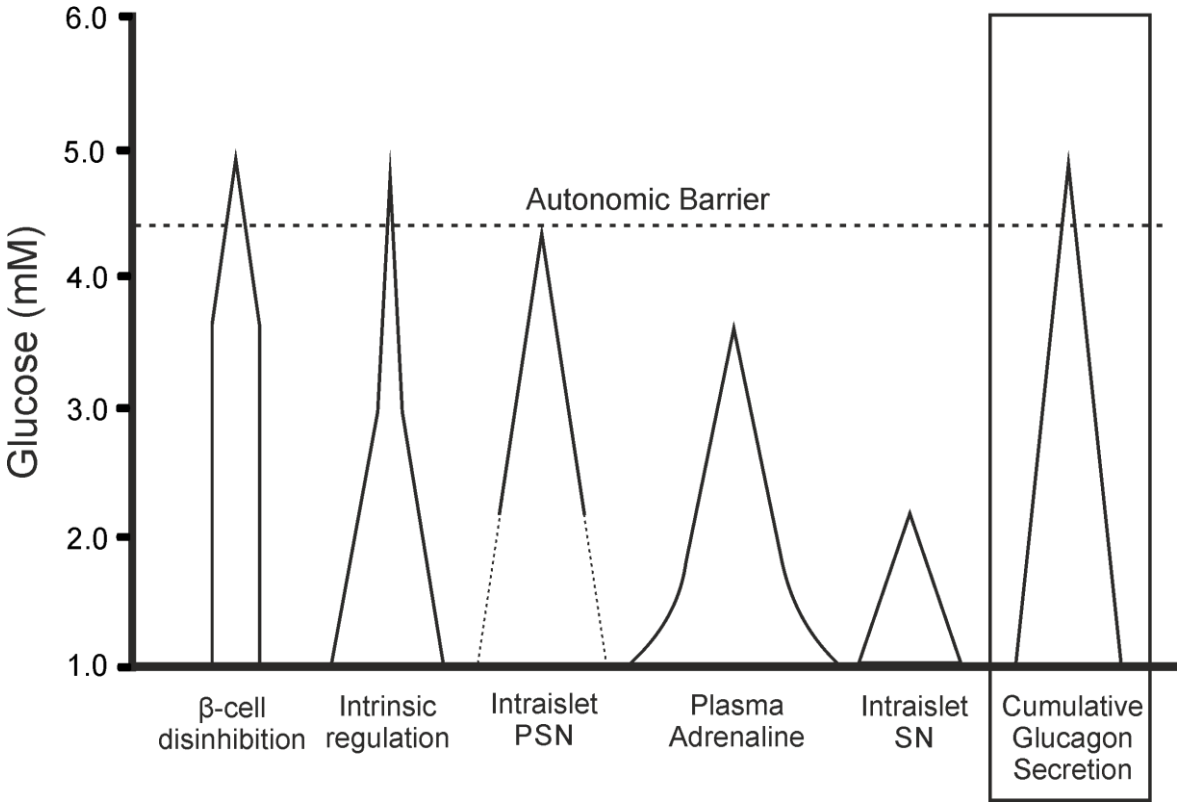


Figure 1.4 - Autonomic barriers to hypoglycaemia

From left to right At ~5.0 mM glucose, β-cells 'switch-off', this removes the tonic inhibitory effect of insulin on the α-cell (β-cell disinhibition), thereby increasing glucagon secretion. By ~3.8 mM β-cell disinhibition is complete with β-cell activity at a minimum. Coinciding with this, α-cell intrinsic glucose regulation stimulates glucagon secretion from the α-cell as glucose falls, dramatically increasing at glucose concentrations < 3 mM (based on Salehi et al., 2006). The first autonomic barrier to hypoglycaemia are the intraislet parasympathetic nerve endings (PSN), these are activated at 4.2 – 4.7 mM glucose and secrete ACh into the islet vicinity, stimulating glucagon secretion. Their activity increases proportionally as glucose falls, although their activity under severe hypoglycaemia has not been calculated. At 3.6 -3.9 mM, the sympathoadrenal system is activated resulting in increased adrenaline secretion from the adrenal medulla (increased plasma adrenaline). Adrenaline stimulates hepatic glucose output but also increases glucagon secretion. Its secretion increases proportionally until severe hypoglycaemia when it is stimulated further. Finally, under severe hypoglycaemia (≤1.9 mM), intraislet sympathetic nerve endings begin secreting noradrenaline into the islet vicinity, increasing glucagon secretion. Their activity increases proportionally as glucose falls. Together these processes result in a cumulative increase in glucagon secretion as glucose falls. Adapted from Taborsky and Mundinger (2012).

1.3.6. Endocrine regulation of glucagon secretion

There are numerous endocrine mediators of glucagon secretion. These include GLP-1, GIP, leptin and, as mentioned above, adrenaline[3]. The appetite suppressor leptin is a potent inhibitor of glucagon secretion. Released from adipocytes, the peptide hormone is a master regulator of body adiposity, primarily acting on the hypothalamus to inhibit food intake and increase energy expenditure, it can also lower blood glucose (D'Souza A et al., 2017). Some of its effects on glucagon secretion do indeed appear to be secondary to a change in hypothalamic signalling (Fujikawa et al., 2010, Denroche et al., 2016), however, a direct effect on the α-cell has also been demonstrated. Acute application of leptin to α-TC1-9 cells and α-cells in intact mouse and human islets induced membrane hyperpolarization, inhibited $[Ca^{2+}]_i$ dynamics and reduced glucagon secretion. These effects appeared to be driven by PI3K signalling, with the reduction of glucagon secretion and inhibition of $[Ca^{2+}]_i$ oscillations avoided in the presence of the PI3K inhibitor wortmannin (Tuduri et al., 2009).

The incretin hormone GLP-1, released by intestinal enteroendocrine L-cells in response to nutrients (Holst, 2007), has also been found to inhibit glucagon secretion. Firstly, in rat and mouse pancreas perfusion studies it has been demonstrated that GLP-1 inhibits glucagon secretion indirectly by increasing somatostatin secretion from δ-cells (de Heer et al., 2008, Orgaard and Holst, 2017). However, a direct effect on the α-cell has also been demonstrated. In mouse islets, GLP-1 via activation of PKA was reported to close N-type

[3] Adrenaline release in response to hypoglycaemia is clearly sympathetically-mediated yet as a hormone its action is endocrine.

Ca^{2+} channels (now believed to be P/Q-type channels, based on (Zhang et al., 2013)), reducing glucagon secretion (De Marinis et al., 2010). Interestingly, GIP released from neighbouring K-cells actually stimulates glucagon secretion (de Heer et al., 2008, Lund et al., 2011), via an increase in cAMP (Moens et al., 1996).

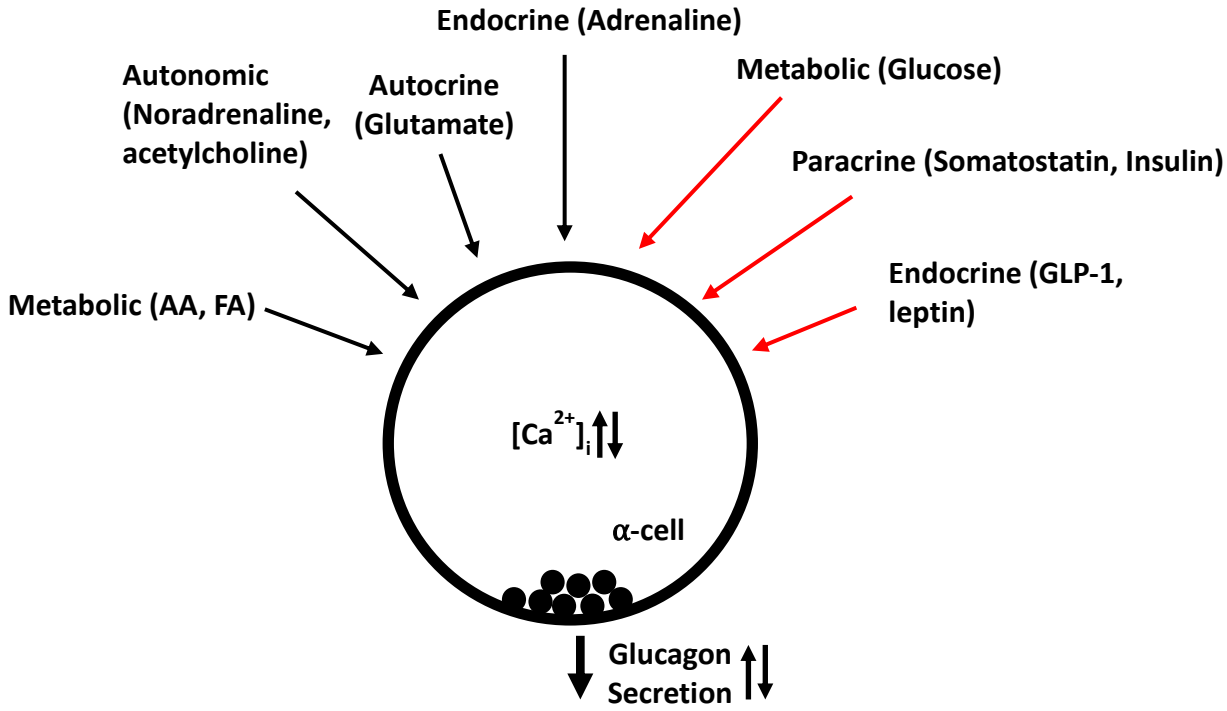


Figure 1.5 - Regulation of glucagon secretion

Glucagon secretion is regulated by various sources. Most of these act by increasing or decreasing $[Ca^{2+}]_i$, stimulating (black arrows) and inhibiting (red arrows) glucagon secretion, respectively. At any one time the α-cell is receiving numerous signals, these signals are integrated with $[Ca^{2+}]_i$ the output. Ca^{2+}-independent effects are also important yet are often accompanied by a change in $[Ca^{2+}]_i$.

1.4. Impaired glucose counterregulation

The importance of both intraislet and peripheral glucagon regulation is evidenced most strongly by impaired glucose counterregulation. Firstly, due to islet-specific changes, the glucagon response is lost exposing the individual to hypoglycaemia. The antecedent hypoglycaemia resulting from this then interferes with glucose sensing in the CNS, pushing the thresholds for autonomic activation to lower glucose concentrations (Cryer, 2002). Furthermore, there is also evidence for autonomic dysfunction prior to the occurrence of hypoglycaemia (Taborsky and Mundinger, 2012). The mechanisms underlying these changes will be discussed in this section.

1.4.1. The absent glucagon response to hypoglycaemia

What causes glucagon secretory defects in diabetes hinges on whether the α-cell is principally regulated by intrinsic glucose sensing or paracrine input from neighbouring β- and δ-cells. This is a central argument of α-cell physiology (Gromada et al., 2007). Of course, autonomic regulation is important but principally under marked hypoglycaemia when islet-specific mechanisms are impaired or insufficient (Sherck et al., 2001).

As diabetes is a condition characterised by impaired insulin secretion and with insulin being an established inhibitory signal for glucagon secretion, impaired glucose counterregulation and postprandial hyperglucagonaemia have both been attributed to the loss of insulin signalling in α-cells (Cryer, 2012). Regarding the latter, it is argued that when glucose is high, for example after a mixed meal, insulin is potently stimulated and its inhibitory effect on glucagon secretion supersedes any stimulatory effects of nutrients such

as fatty acids and amino acids. When the paracrine output is removed due to β-cell failure, glucagon secretion is thus elevated leading to postprandial hyperglucagonaemia (Kjems et al., 2001, Meier et al., 2006, Cooperberg and Cryer, 2010). Further support for this model comes from α-cell specific insulin receptor knockout mice, which are hyperglucagonaemic in the fed state (Kawamori et al., 2009), and type 1 diabetic patients, where oral and intravenous glucose tolerance tests fail to suppress glucagon secretion (Greenbaum et al., 2002). Furthermore, in isolated rat α-cells, glucose has been shown to stimulate electrical activity, increase $[Ca^{2+}]_i$ and stimulate glucagon secretion (Franklin et al., 2005, Olsen et al., 2005). Although these findings are disputed by other studies on single rodent α-cells (Pipeleers et al., 1985, Quoix et al., 2009). Of course, the actions of other β-cell secretory products and somatostatin cannot be ruled out.

These data strongly suggest the need for paracrine regulation for postprandial suppression of glucagon secretion, however, a role at low glucose (< 6 mM) and in glucose counterregulation appears more suspect. The inhibition of islet β-cells by falling blood glucose, and subsequent removal of insulin tonic inhibition from the α-cell, has been cited as a critical signal for the glucagon response to hypoglycaemia, in a model termed 'the switch-off hypothesis'. When insulin secretion is low or absent in diabetes, however, the lack of a decrement in insulin paracrine input as glucose falls means the α-cell is unresponsive and there is no increment in glucagon secretion (Hope et al., 2004, Zhou et al., 2004, Gosmanov et al., 2005, Israelian et al., 2005, Raju and Cryer, 2005, Zhou et al., 2007b, Cooperberg and Cryer, 2009). Studies on α-cell-specific insulin receptor knockout mice contest this assumption. In these animals, the β-cell signal is absent (as the α-cell is incapable of detecting any change in insulin) however, they still respond to insulin-induced hypoglycaemia with a 5-fold increase in glucagon secretion (Kawamori et al.,

2009). Also in type 1 diabetic patients, residual β-cell function does not correspond to a maintained glucagon response to hypoglycaemia (Sjoberg et al., 2002, Sherr et al., 2013). Furthermore, if paracrine control from the β-cell was solely responsible one would expect inhibition of glucagon secretion to share the same glucose-dependence as the stimulation of insulin; however, based on *in vitro* secretion assays this does not appear to be the case. Most notably, glucagon secretion is almost maximally-inhibited at ~3 mM glucose in both mouse and human islets, a concentration at which insulin secretion is low, it then increases dramatically as the glucose concentration approaches zero (Figure 1.6). It should also be noted that the large changes in glucagon secretion at low glucose may result in part from positive autocrine feedback from glutamate (Cabrera et al., 2008) and glucagon itself (Ma et al., 2005).

It has been argued that the small increases in somatostatin secretion at low glucose (~3 mM) are sufficient to inhibit the α-cell (Figure 1.6), based upon glucose being unable to suppress glucagon secretion in $SST^{-/-}$ mice[4] (Hauge-Evans et al., 2009). However, these findings are contested by the observation that glucose can still inhibit glucagon secretion when somatostatin signalling is specifically blocked in the α-cell by SSTR2 antagonists, in rodent (Vieira et al., 2007, de Heer et al., 2008, Li et al., 2015) and human islets (Ramracheya et al., 2010). Furthermore, another study in $SST^{-/-}$ mice refuted the findings of Hauge-Evans et al. (2009), showing that 7 mM glucose was still capable of inhibiting glucagon secretion (Cheng-Xue et al., 2013). Nevertheless, a role for abnormal somatostatin secretion in diabetes has been demonstrated. In diabetic rats, the glucagon response to hypoglycaemia was restored by inhibiting α-cell somatostatin signalling with an SSTR2 antagonist (Yue et al., 2012, Karimian et al., 2013). The actions of GABA and

[4] 0 mM, 2 mM, 5 mM and 20 mM glucose used

GHB, which are secreted separately from insulin at possibly lower glucose levels, should also be considered (Li et al., 2013). Although, notably, in mouse islets glucose is still capable of inhibiting glucagon secretion in the presence of $GABA_A$ receptor antagonist (MacDonald et al., 2007).

Notably, glucagon secretion reaches a nadir at ~5 mM glucose (Salehi et al., 2006, Braun et al., 2010) (Figure 1.6). Past this point, despite increased paracrine input, there is no extra inhibitory effect, in fact glucagon secretion increases. This is echoed by insulin not inhibiting glucagon secretion at glucose levels ≥6mM in mouse (Ravier and Rutter, 2005) and human islets (Ramracheya et al., 2010). This suggests intrinsic regulation brings glucagon secretion to a minimum. Therefore, rather than being responsible for glucose suppression of glucagon secretion, paracrine inhibition may be more likely to counteract the stimulatory effects of amino acids and fatty acids on glucagon secretion after a mixed meal, maintaining glucagon secretion at the level set by the intrinsic control of the α-cell (Walker et al., 2011).

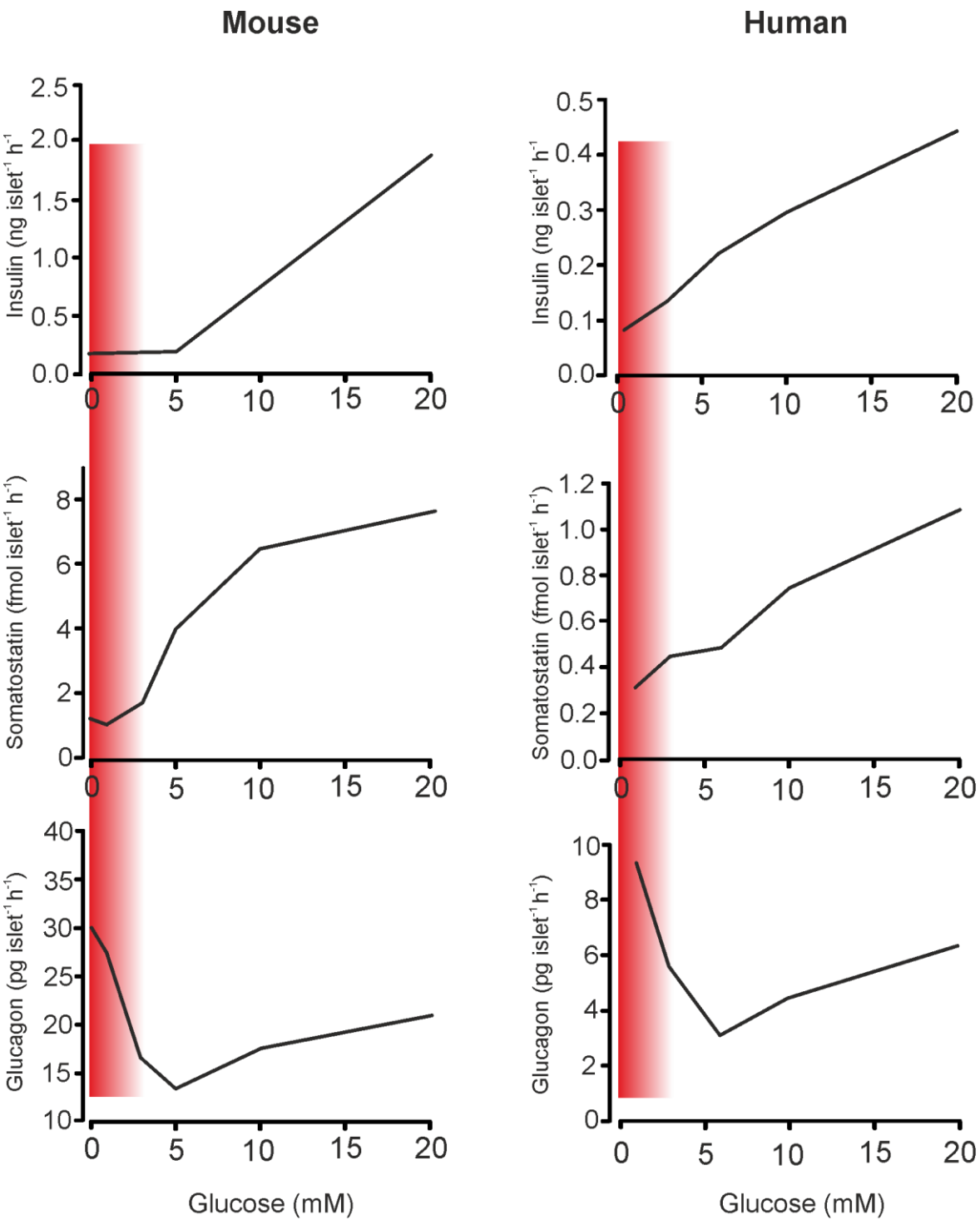


Figure 1.6 - Glucose dependence of islet hormone secretion in mouse and human islets

Glucose dependence of insulin, somatostatin and glucagon in mouse and human islets. The red shaded area represents glucose concentrations where insulin and somatostatin secretion are low. Adapted from Walker et al. (2011).

Evidence for intrinsic changes to the α-cell in diabetes have been illustrated by Zhang et al. (2013) in islets isolated from type 2 diabetic donors, which show a loss of glucose-induced suppression with lower glucagon secretion at 1 mM glucose and no further decrease at 6 mM glucose, in 50% of cases glucagon secretion was actually inverted with significantly higher secretion at 6 mM glucose compared to 1 mM glucose (Zhang et al., 2013). Interestingly, in non-diabetic donors this phenomenon could be replicated by application of the K_{ATP} channel activator diazoxide or the mitochondrial ATP synthase blocker oligomycin. Moreover, the effects of oligomycin on glucagon secretion could be reversed by applying the K_{ATP} channel blocker tolbutamide, with partial restoration of glucose-induced suppression when tolbutamide was applied to type 2 diabetic islets. This suggests glucagon secretory defects in type 2 diabetes involves increased K_{ATP} channel activity in α-cells, possibly reflecting decreased ATP production (Zhang et al., 2013).

Overall, it appears most likely that intrinsic control predominantly regulates the α-cell at low glucose (<6 mM), increasing glucagon secretion as glucose decreases; while at higher glucose concentrations, when β- and δ- cells are more active and the stimulatory effects of amino acids and fatty acids are unwanted, paracrine control takes hold, suppressing glucagon secretion (Gylfe and Gilon, 2014). By this logic, hyperglucagonaemia under hyperglycaemic conditions, results largely from a reduction in paracrine regulation, while absent glucagon responses involve aberrations in intrinsic glucose sensing. It should be stressed however that intrinsic and paracrine mechanisms are not mutually exclusive, with both likely to play a role, even if minimal at low and high glucose. Particularly if basal secretion of islet hormones is altered by diabetes (e.g. somatostatin).

1.4.2. Hypoglycaemia-associated autonomic failure (HAAF)

Impaired counterregulation is often accompanied by HAAF, greatly heightening the risk of hypoglycaemia. As discussed briefly earlier, HAAF results from repeated episodes of hypoglycaemia reducing the glycaemic thresholds that trigger glucose sensing in the brain (Cryer, 2013). Indeed, antecedent hypoglycaemia has consistently been shown to blunt adrenomedullary responses. The parasympathetic response, reflected by a drop in the cholinergically-regulated pancreatic polypeptide response to hypoglycaemia (Heller and Cryer, 1991, Davis et al., 1996), and sympathetic response, reflected by a reduction in hypoglycaemia-induced muscle sympathetic nerve activity (Davis et al., 1996), are also impaired (Taborsky and Mundinger, 2012). Interestingly, with 2-3 weeks of avoiding hypoglycaemia, HAAF can be alleviated whilst the glucagon response remains absent (Cryer, 2002).

Despite the potentially damaging effects of HAAF, the exact mechanism underlying the condition is unknown with several possible causes proposed. These include the 'systemic-mediator hypothesis', which posits that increased cortisol secretion after hypoglycaemia signals to the brain attenuating the autonomic responses (Davis et al., 1996, Davis et al., 1997). This is debatable, however, and may be due to the use of non-physiological doses. Indeed, increases in cortisol, similar to those produced by hypoglycaemia, have no effect on the sympathoadrenal response or neurogenic symptoms to hypoglycaemia (Raju et al., 2003, Goldberg et al., 2006), and inhibiting the cortisol response does not prevent HAAF (Goldberg et al., 2006). Interestingly, pancreatic polypeptide responses were blunted even when physiological doses were used (Raju et al., 2003), suggesting the parasympathetic response may specifically be attenuated by cortisol elevation.

A second theory is the ‘Brain-fuel hypothesis’. It argues that hypoglycaemia causes a fall in the rate of cerebral glucose metabolism, triggering autonomic responses. Thus, when normoglycaemia is restored there is an increase in brain glucose transport that reduces the fall in the rate of cerebral glucose metabolism when hypoglycaemia reoccurs, thereby attenuating autonomic responses. However, whether glucose uptake is actually increased after antecedent hypoglycaemia is doubtful, with studies using advanced brain imaging techniques suggesting that this is not the case (Cryer, 2013). Based on studies in rats, it has also been suggested that hypoglycaemia leads to an increase in the brain glycogen pool and that this extra source of glucose results in HAAF (Gruetter, 2003). However, this was not observed in humans, where brain glycogen was actually decreased in type 1 diabetic patients compared to controls (Oz et al., 2012). Alternatively, increased lactate transport may cause HAAF, with glucose depletion in the brain (due to recurrent hypoglycaemia) resulting in brain glucose metabolism being maintained by increased uptake of the metabolite (Herzog et al., 2013). Notably, infusion of lactate blunted autonomic responses to hypoglycaemia in non-diabetic and type 1 diabetic subjects (Maran et al., 2000).

A third model, named ‘the brain metabolism hypothesis’ posits that specific changes to glucose sensing neurones as a result of hypoglycaemia drive HAAF (Cryer, 2013). Evidence for this comes from changes to enzymes directly involved in brain glucose sensing after hypoglycaemia. For example, hypothalamic expression of GK increases after antecedent hypoglycaemia (Kang et al., 2008). Furthermore, pharmacologically increasing GK activity causes blunting of adrenaline, noradrenaline and glucagon responses to hypoglycaemia, while reducing GK expression results in an increased adrenaline response (Levin et al., 2008). This can be ascribed to increased glycolytic flux increasing ATP meaning low glucose concentrations are sensed as higher. AMPK is also associated with

glucose sensing in neurones; under hypoglycaemic conditions (high AMP:ATP ratio) its activity increases, stimulating neurotransmitter release from GI neurones and *vice versa* in GE neurones (Beall et al., 2012). Notably, its activity is reduced after recurrent hypoglycaemia (Alquier et al., 2007). Furthermore, pharmacological activation of AMPK in the hypothalamus has been shown to prevent the effects of recurrent hypoglycaemia on adrenaline and glucagon responses in a rodent model of type 1 diabetes (Fan et al., 2009), with AMPK suppression attenuating glucose counterregulatory responses (McCrimmon et al., 2008). The actions of insulin on hypothalamic neurones have also been studied, with neuron-specific knockout of the insulin receptor in mice resulting in a blunted sympathoadrenal response and reduced glucose responsiveness of GI neurones (Diggs-Andrews et al., 2010), similar observations were made in brain GLUT4 knockout mice (Reno et al., 2017). This suggests that insulin signalling, at least partly via promotion of GLUT4 translocation, is critical in priming glucose sensing neurones to a fall in blood glucose, with disruption to this signalling in diabetes potentially playing a role in HAAF development.

Lastly, the 'cerebral network hypothesis' suggests that increased synaptic activity (measured by increased blood flow) in specific brain regions after hypoglycaemia leads to suppression of hypothalamic activity, thereby attenuating the sympathoadrenal response (Cryer, 2013). One such region is the paraventricular nucleus of the thalamus, which after stress (e.g. hypoglycaemia) acts to suppress any subsequent episode of stress in a process known as habituation, and has been shown to directly affect the hypothalamus. Notably, after repeated episodes of hypoglycaemia synaptic activity in the paraventricular nucleus was increased in response to subsequent hypoglycaemia (Arbelaez et al., 2008). Furthermore, there is a decrease in glucose uptake (measured using [18 F]deoxyglucose

and reflective of reduced activity) in various brain regions including the hypothalamus and brainstem, associated strongly with glucose sensing, and the amygdala, associated with fear and anxiety (neurogenic symptoms), during hypoglycaemia in type 1 diabetic patients with hypoglycaemia unawareness compared to those without. Effects that are believed to be the result of 'habituation of higher behavioural responses' to hypoglycaemia (Dunn et al., 2007). Increased synaptic activity is also increased in the medial prefrontal cortex, a further region associated with habituation to stress (Teves et al., 2004).

1.4.3. Non-HAAF related damage to the central nervous system

Autonomic input is critical for the glucagon response to hypoglycaemia, accounting for 75%-90% of the glucagon response (Taborsky and Mundinger, 2012). Therefore, for the glucagon response to become absent in diabetes prior autonomic dysfunction independent of HAAF must presumably occur. Indeed, there are data that indicate hyperglycaemia can also have deleterious effects on CNS counterregulatory responses. In diabetic mouse models, ventromedial hypothalamic (VMH) extracellular basal levels of the inhibitory neurotransmitter GABA, an important regulator of the counterregulatory response (Chan et al., 2006), are elevated (Chan et al., 2011). Crucially, in these mice, glucagon and adrenaline responses were blunted. Moreover, while in non-diabetic animals GABA levels decreased in response to hypoglycaemia, in diabetic mice there was no change. Notably, restoration of normal GABA levels by enzyme knockdown normalised glucagon and adrenaline responses (Chan et al., 2011). In a follow up study, the elevated levels of VMH GABA were connected to excess glucose increasing production of the alternative fuel lactate, a precursor for GABA synthesis, which would also increase GABAergic GE neurone firing through ATP production and subsequent K_{ATP} channel closure (Chan et al.,

2013). Notably, VMH GABA levels were also increased after recurrent hypoglycaemia (Chan et al., 2008), a rise also associated with increased lactate (Chan et al., 2013) (likely caused by increased lactate uptake (Herzog et al., 2013)), suggesting a similar mechanism causes HAAF.

1.4.4. Damage to the peripheral nervous system in diabetes

Aberrations in the CNS may not fully explain the impaired autonomic response to hypoglycaemia. There is also evidence for damage to the PNS, disrupting autonomic islet input. Firstly, at mouse sympathetic ganglia, hyperglycaemia has been shown to increase the production of ROS, leading to oxidation of cysteine residues on the α3 subunit of ganglionic-type nAChRs, thereby inactivating them and depressing synaptic transmission. This mechanism was also demonstrated *in vivo* with diabetic mice shown to have 'depressed ganglionic transmission and reduced sympathetic reflexes', features which were absent in mice lacking the cysteine residues of the α3 subunit (Campanucci et al., 2010). More recently, these findings were extended to include parasympathetic and chromaffin cells of the adrenal medulla. It was found that sympathetic neurones and chromaffin cells were more prone to the effects of hyperglycaemia on synaptic transmission with clear differences between control and diabetic mice. Conversely, in parasympathetic neurones there was no effect of hyperglycaemia with no difference in synaptic transmission between control and diabetic mice. This was attributed to sympathetic neurones and chromaffin cells being more susceptible to hyperglycaemia-induced oxidative stress, with greater production of ROS compared to parasympathetic neurones (Rudchenko et al., 2014). Note that increased oxidation of nAChRs has not been

proven to disrupt islet sympathetic input but such an outcome is likely due to the location of these receptors (Taborsky and Mundinger, 2012).

A second defect of the PNS is islet denervation, which occurs early in type 1 diabetes (and immune animal models of diabetes) due to autoimmune destruction of sympathetic nerve terminals in a process known as early sympathetic islet neuropathy (eSIN). Interestingly, the immune mechanisms that target the sympathetic nerve terminals appear to be separate from those that cause β-cell destruction. Axonal degeneration occurs due to activation of p75 neurotropin receptors by the ligand BNDF, while activation of the tropomyosin receptor kinase A by NGF promotes axonal maintenance (Mundinger and Taborsky, 2016). Notably, knockout of p75 neurotropin receptors protects against eSIN in lymphocyte-induced diabetes (Taborsky et al., 2014), and it is believed that β-cells are the main source of islet NGF. Therefore, β-cell immune destruction may lead to a loss of NGF, causing an imbalance which promotes axonal degeneration via the p75 neurotropin receptor. Alternatively, increased ROS production due to autoimmune attack could activate the same pathway in a ligand-independent mechanism (Mundinger and Taborsky, 2016). Notably, eSIN has been demonstrated to cause a decrease in sympathetically-induced glucagon secretion in immune mouse models of diabetes (Mundinger et al., 2003, Taborsky et al., 2009), and is therefore a potential contributor to impaired conterregulation, particularly under severe hypoglycaemic conditions (Mundinger and Taborsky, 2016).

Notably, these mechanisms could precede intraislet dysfunction as unlike HAAF they are not the result of antecedent hypoglycaemia. Therefore, the loss of the glucagon response to

hypoglycaemia may be in part mediated by prior dysfunction of the PNS, leading to a drop in islet autonomic input.

1.5. Summary

My thesis' central theme is the regulation of glucagon secretion, specifically in relation to glucose counterregulation. The first two Results chapters will focus on autonomic mediation of glucagon secretion and the intracellular mechanisms that dictate this regulation. Chapter 3 specifically focusing on sympathoadrenal/sympathetic regulation of glucagon secretion, principally investigating the effect of adrenaline (and noradrenaline) on $[Ca^{2+}]_i$ dynamics in α-cells. Chapter 4 explores parasympathetic regulation of glucagon secretion, investigating the effect of ACh on $[Ca^{2+}]_i$ dynamics and membrane potential in α-cells. Defining the mechanism of ACh and adrenaline may provide ways to bypass the sympathetic and parasympathetic pathways, which are compromised in diabetes, to increase glucagon secretion. The next two Results chapters move away from autonomic regulation and instead focus on the dysfunction of the glucagon response to hypoglycaemia in diabetes. Chapter 5 deals with metabolic regulation, specifically how hyperglycaemia alters α-cell physiology and leads to the loss of the glucagon response to hypoglycaemia. To do this I used the Fh1βKO mouse, a mouse model of type 2 diabetes (Adam et al., 2017), to investigate changes in pH_i and $[Ca^{2+}]_i$ that result from hyperglycaemia. Chapter 6 focuses on paracrine regulation and its potential imbalance in diabetes as a result of insulin overdose. Specifically, investigating the mechanism underlying the effects of high concentrations of insulin on somatostatin secretion and, consequently, glucagon secretion at low glucose.

1.6. Aims

- Unveil the mechanism of how adrenaline stimulates the pancreatic α-cell
- Unveil the mechanism of how acetylcholine stimulates the pancreatic α-cell
- Learn how hyperglycaemia leads to defective glucagon secretion using the Fh1βKO mouse model
- Explore the mechanism underlying the effect of high concentrations of insulin on the pancreatic δ-cell

Chapter 2: General Methods

2.1. Mouse Islet Isolation

Mice were kept in a conventional vivarium at the Wellcome Trust Centre for Human Genetics (Oxford, UK) with a 12-hour-dark/12-hour-light cycle and *ad libitum* access to food and water. All mouse experiments were conducted in accordance with the United Kingdom Animals (Scientific Procedures) Act (1986) and the University of Oxford ethical guidelines. They were killed by cervical dislocation (Schedule 1). The abdomen was cut with surgical scissors exposing the gut. The bile duct was ligated at the *ampulla Vateri* (at the entrance to the duodenum) using surgical thread, this surgical thread was pulled downwards away from the head and clamped creating tension in the bile duct. Using a 2 ml syringe (BD, UK) and hypodermic needle (BD, UK), a solution containing 0.1 mg/ml liberase TL research grade (Roche, UK) was injected into the bile duct at the bifurcation of the duct beneath the liver. The inflated pancreas was excised and put into a 15 ml falcon tube (Sarstedt, UK). The pancreas was then incubated at 37 °C for 13 min in a water bath to facilitate collagenase digestion. The reaction was abruptly stopped by adding 12 ml of ice-cold hanks solution (Sigma, UK; Product code: H8264) containing 0.1% BSA (Sigma, UK). The tube containing the pancreas was shaken for 20 s and left on ice for 5 min, leading to formation of an islet-containing pellet and exocrine-containing supernatant. The supernatant was removed and islets were washed twice with hanks solution containing BSA to purify the sample further. Islets were then picked in a 35 mm suspension dish (Sarstedt, UK; Product code: 83.3900.500) using a p10 pipette into a 35 mm/60 mm suspension dish containing ice cold hanks solution with 0.1% BSA (Sigma, UK).

2.2. Mouse Islet Culture

Islets were then transferred then into a 35 mm/60 mm suspension dish (Sarstedt, UK; Product code: 83.3900.500/83.3901.500) containing 37 °C RPMI 1640 medium, supplemented with GlutaMax (Life Technologies, UK) and containing 11mM glucose (Sigma, UK), 10% FCS (Sigma, UK), 100 IU/mL penicillin and 100 μg/mL streptomycin (Life Technologies, UK). Islets were then cultured for 1h-24 h at 37 °C in an incubator (5% CO_2/95% Air) before starting experiments.

2.3. Human islet culture

Appendix 1 (A1.1.2) provides details of the human islet isolation. Human islets were picked using a p10 pipette from CMRL/UW into 37 °C RPMI 1640 medium, supplemented with L-glutamine (Life Technologies, UK; Product code: 11879-020) and containing 5mM glucose (Sigma, UK), 10% FCS (Life Technologies, UK), 100 IU/mL penicillin and 100 μg/mL streptomycin. Islets were cultured at 37 °C in an incubator (5% CO_2/95% Air) for between 1 h-24 h before starting experiments.

2.4. Confocal $[Ca^{2+}]_i$ measurements

Intact mouse and human islets were loaded in Fluo-4-AM (6 μM; Thermo Fisher, UK) dissolved in EC1 solution supplemented with 6 mM glucose. 1 μl of pluronic F-127 (0.03% solution; Thermo Fisher, UK) was added to aid with solubility of the Ca^{2+} dye. After 90 min (80 min for human islets) at room temperature and in the dark, islets were transferred to an open chamber (Figure 2.2; also used for simultaneous $[Ca^{2+}]_i$ and pH_i recordings, discussed in 5.2.2) before being imaged using a Zeiss AxioVert 200

microscope equipped with Zeiss 510-META laser confocal scanning system, using 40x/1.3 objective. The KRB bath solution was perifused at 200 μl/min (using a peristaltic pump) with various stimuli added, temperature of the bath solution was maintained at 34 °C[5] throughout each recording. A 488 nm argon laser (3% intensity) was used to excite Fluo-4[6] and emission was collected at 530 nm, using 512x512 frame scanning mode with a pixel dwell time of 6 μs and a bit depth of 8-bit. Images were acquired every 3.93 s (~0.25 Hz). The same settings were used for the gCAMP3 recordings in Chapter 3 (Figure 3.9) and Chapter 6 (Figure 6.1). In the former, RFP was excited by a 543 nm helium neon laser (2.8% intensity) with emission collected at 630 nm. Glucagon-secreting α-cells were identified by an increase in $[Ca^{2+}]_i$ in response to 1mM glutamate, with activation of AMPA ionotropic glutamate receptors, at low glucose, restricted to the α-cell subset of the islet (Cabrera et al, 2010).

[5] This temperature was used instead of the physiological 37 °C to minimise the damage of fluctuations in temperature. At 37 °C a change in temperature would have far greater deleterious effects on cell function than at 34 °C.

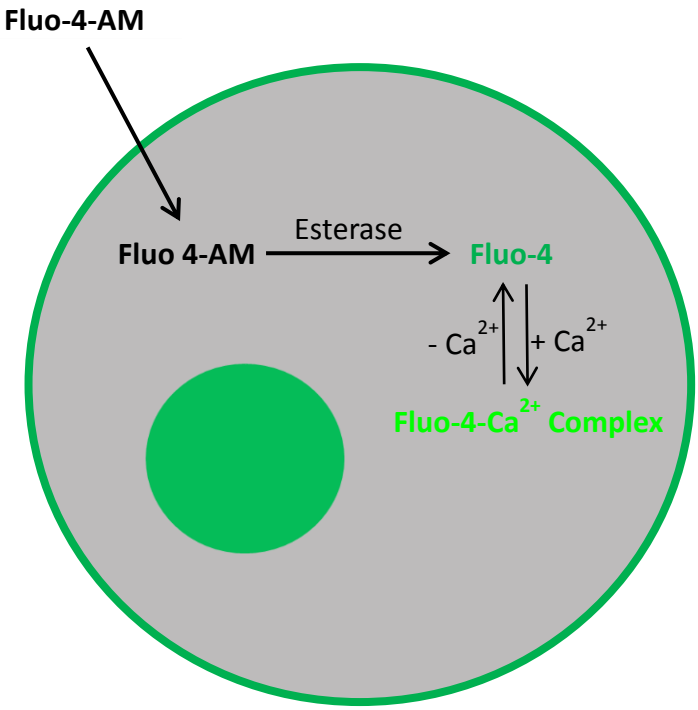
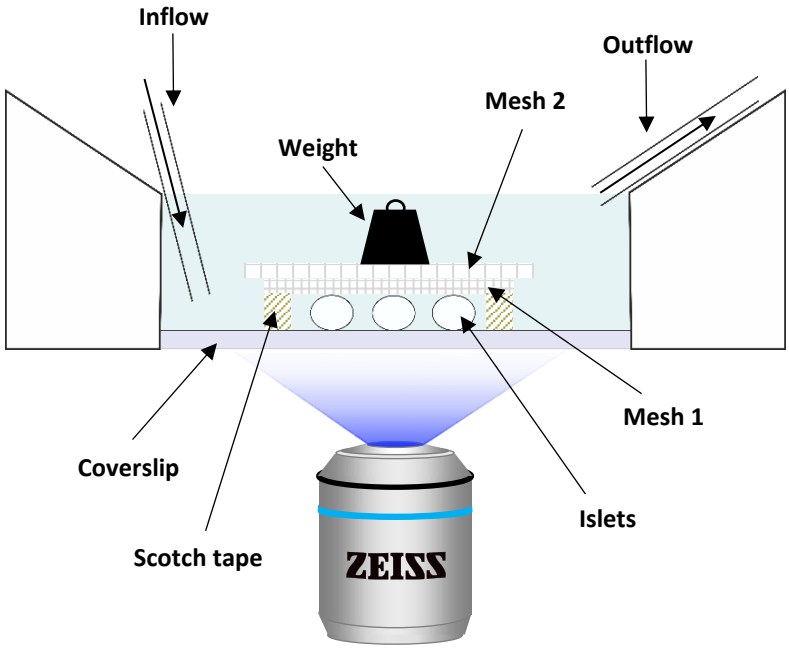


Figure 2.1 - Mechanism of Fluo-4

Fluo-4 in its esterified form (Fluo-4-AM) is able to cross the plasma membrane. Cellular esterases then break the ester bond. In its unesterified form Fluo-4 can bind Ca^{2+}, resulting in a change in conformation that increases the fluorescence intensity of the Fluo-4 probe. This allows $[Ca^{2+}]_i$ to be tracked, with Fluo-4 switching between the bound (Fluo-4-Ca^{2+} complex) and unbound state (Fluo-4) as $[Ca^{2+}]_i$ rises and falls, respectively.

a.


Inflow
Outflow
Mesh 2
Weight
Mesh 1
Coverslip
Islets
Scotch tape
ZEISS

b.

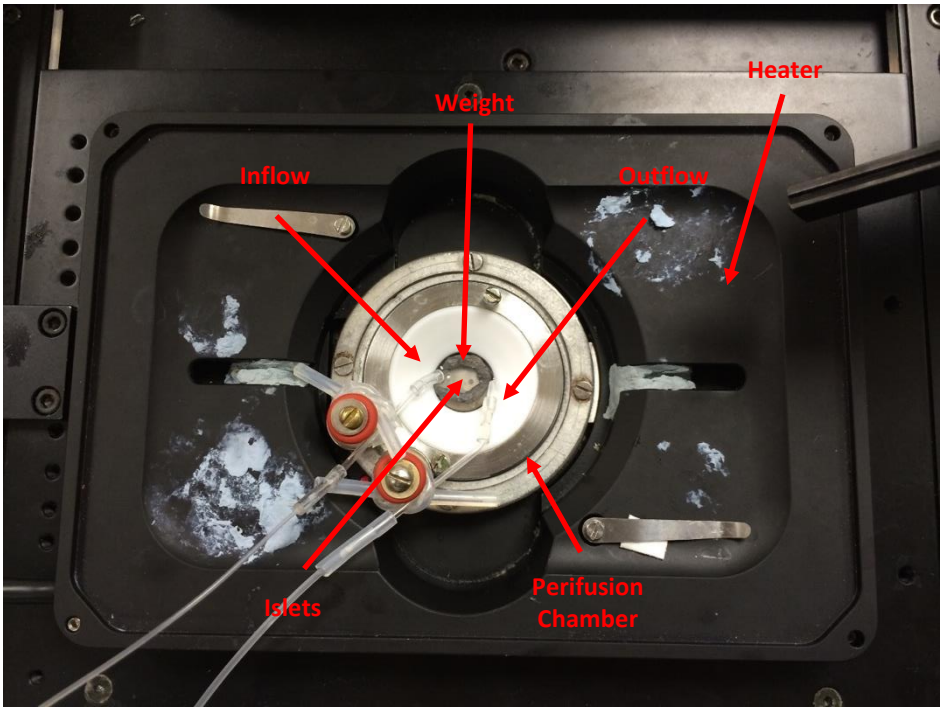
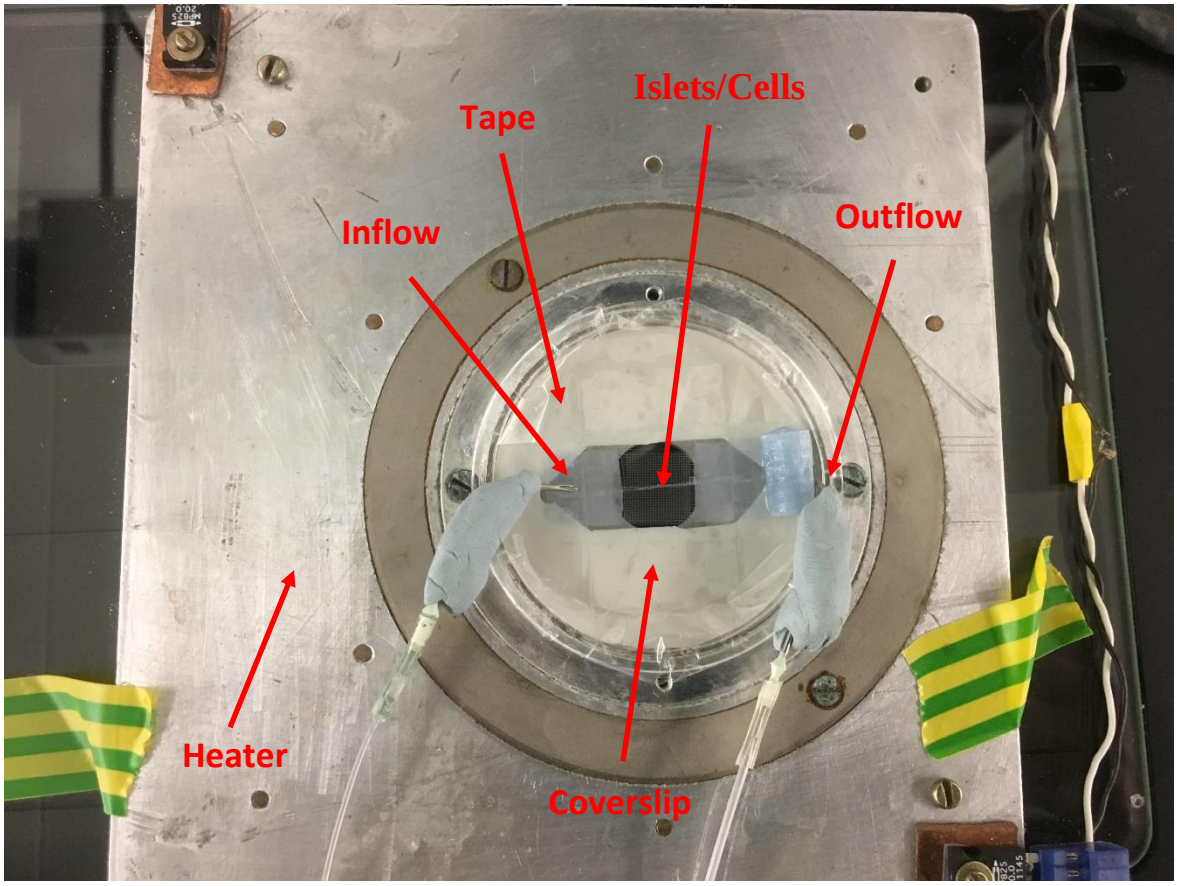

Heater
Weight
Inflow
Outflow
Islets
Perifusion
Chamber

Figure 2.2 - 'Open' chamber used for confocal singular $[Ca^{2+}]_i$ recordings and simultaneous $[Ca^{2+}]_i$ and pH_i recordings

(a) *Cross-sectional diagram of inverted confocal chamber* - The chamber is filled with EC1 solution, using a p10 pipette islets are then transferred to the centre of chamber. Using forceps, mesh 1 (60 µm thick, 60 µm opening; Plastok, UK) with sellotape attached is lowered onto the islets, sellotape side first. The sellotape means the mesh is elevated above islets thus preventing them from being squashed, mesh 1 provides adherence for the islets preventing movement. The second thicker mesh 2 (0.2 mM thick, 0.12 mm opening; Warner instruments, USA) is then place atop mesh 1, ensuring further stability. Finally, a ~0.8g metal weight is put on top securing everything in place. **(b)** *Image of chamber attached to microscope* - The chamber is fixed in place ready for imaging. It is surrounded by a heater set at 48 °C, ensuring the solution in the chamber is kept at 34 °C. Inflow and outflow are attached using magnets that adhere to the outside of the chamber. The inflow goes directly into the chamber, while the outflow sits on the surface of the bath solution, this prevents the chamber from drying out. Please note in the image, the objective lens is below the coverslip.

2.5. $[Ca^{2+}]_i$ imaging (hypo/hyperglycaemic culture)

For the experiments exploring the influence of chronic hypo/hyperglycaemic culture on the adrenaline effect, adenovirally-delivered GCamp6F Ca^{2+} sensor was used (Vector Biolabs, US; 10^5 units per islet – determined by infecting INS1 cells with serial dilutions of the virus). It was expressed for at least 6 h at 37 °C in an incubator (5% CO_2/95% Air) before starting experiments. For those looking at the effects of chronic hypo/hyperglycaemic culture on the ACh effect, Glu-gCAMP3 mice were used (Parker et al., 2012). These expressed the Ca^{2+} sensor gCAMP3 under the control of the glucagon promoter, meaning the sensor was specifically expressed in α-cells. In both cases, islets were placed in a 'closed' perifusion chamber (Figure 2.3; also used for PKA (Chapter 3) and $[DAG]_i$ (Chapter 4) imaging experiments), with 5mM, 11mM and 30mM islet groups partitioned separately, before being imaged on a Zeiss AxioZoom.V16 zoom microscope, using 2.3x/0.57 objective at a magnification of 10x - 12x. The probes were excited at 470 nm and emission collected at 535 nm, with images taken every 10s and an exposure time of 10 ms. The EC1 bath solution containing various stimuli was perifused continuously at 60 μl/min (using a peristaltic pump) and maintained at 34 °C. α-Cells were again identified based on an increase in $[Ca^{2+}]_i$ activity in response to glutamate (1 mM).


Tape
Islets/Cells
Inflow
Outflow
Heater
Coverslip

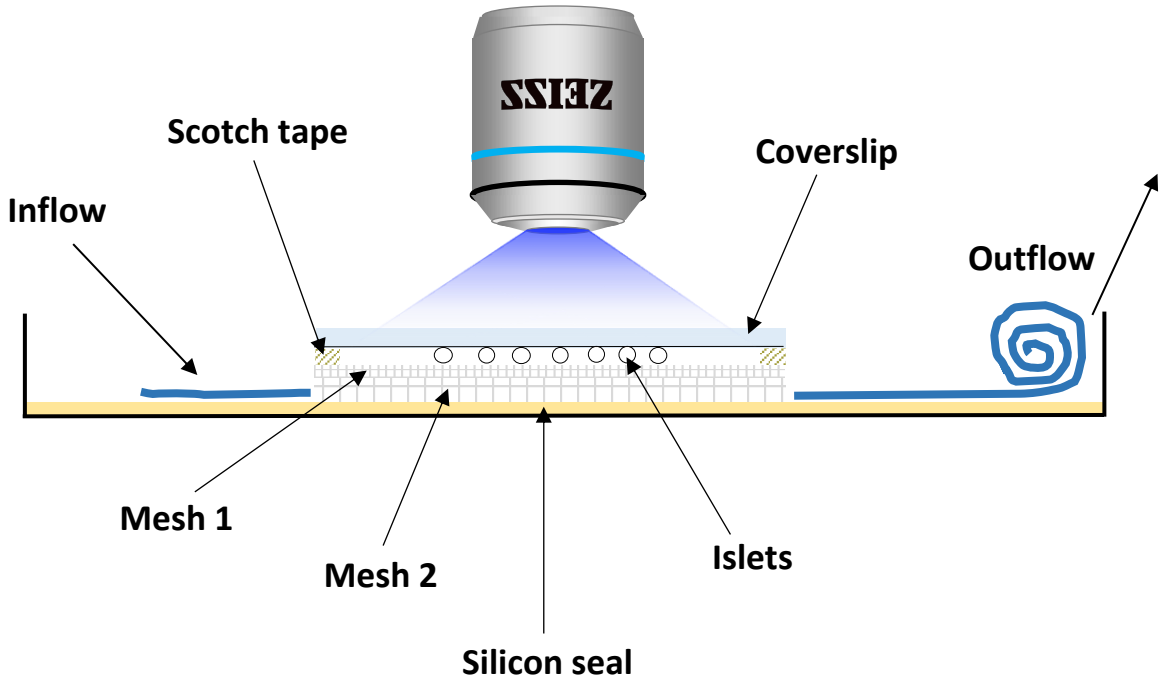

ZEISS
Scotch tape
Coverslip
Inflow
Outflow
Mesh 1
Mesh 2
Islets
Silicon seal

Figure 2.3 - 'Closed' Chamber used for PKA, $[DAG]_i$ and $[Ca^{2+}]_i$ hypo/hyperglycaemic culture imaging experiments

Picture of 'closed' chamber configuration used in experiments from above and cross-sectional diagram of 'closed' chamber - Any dust is removed from the chamber by applying and then removing sellotape. Dust is removed from the silicon seal using the same method, it is then placed down within the chamber ensuring no air pockets are present. The thick mesh (mesh 2; 0.2 mm thick, 0.12 mm opening; Warner instruments, USA) is soaked with EC1 solution and placed in the middle of the chamber, in the gap in the silicon seal. The inflow and outflow are cut from blue roll, wetted with EC1 solution and placed either side of gap in the silicon seal using forceps, as shown. For PKA and $[Ca^{2+}]_i$ imaging experiments, a second mesh (mesh 1) with sellotape attached (60 µm thick, 60 µm opening; Plastok, UK) is added atop of the thicker mesh and soaked. Mesh 1 plays the same role as it does in the 'open' chamber. Islets were pipetted centrally, in between the two bits of sellotape. The coverslip was then placed carefully down on top. For the $[DAG]_i$ experiments, single cells (positioned centrally) are attached to the coverslip so there is no need for mesh 1, the coverslip is placed cell-side down. The coverslip, in both cases, is secured in place using sellotape at both sides of the chamber, avoiding the opening where the islets/cells reside. The chamber is now ready for imaging, it is surrounded by a heater kept at 38 °C to maintain a bath solution temperature of 34 °C. Inflow and outflow tubing are attached using blue tack, there is a groove scratched into the chamber, which the inflow tube goes into, this ensures the bath solution does not spill over. The outflow tube is placed under the curled blue roll. The blue roll is long and curled, this means transfer from it is slow thus preventing the chamber becoming dry. The objective lens lies above the chamber.

2.7. Data analysis (Imaging)

For all recordings, image sequences were analysed using open-source FIJI software. Registration and background subtraction were performed to correct for movement and remove background fluorescence[7], respectively. Regions of interest (ROIs) were then selected based on specific cellular characteristics (e.g. stimulatory response to glutamate) with numerical data (ROI intensity vs. time) exported. For the singular $[Ca^{2+}]_i$ recordings (incl. Fluo-4, Fluo-4FF, gCAMP3 and gCAMP6f), the numerical data was analysed using IgorPro package (Wavemetrics), each trace was normalised (F/F_o) and baseline/bleach corrected with partial area under the curve (pAUC) then calculated by splitting each trace into 30 s intervals, the AUC was then computed for each interval using trapezoidal integration. pAUC points falling within a given region (e.g. 3 mM + 5 μM adrenaline) for each trace were averaged (Figure 2.4), the mean of these values across the α-cell population was then calculated to generate the final pAUC value (displayed in the column plot). Statistical analysis was performed using SPSS. Mann-Whitney U-test or Wilcoxon's paired test were used to compute the significance of difference between independent and dependent samples, respectively. Differences with $p < 0.05$ were considered significant.

[7] Not necessary for confocal recordings, where background fluorescence was negligible.

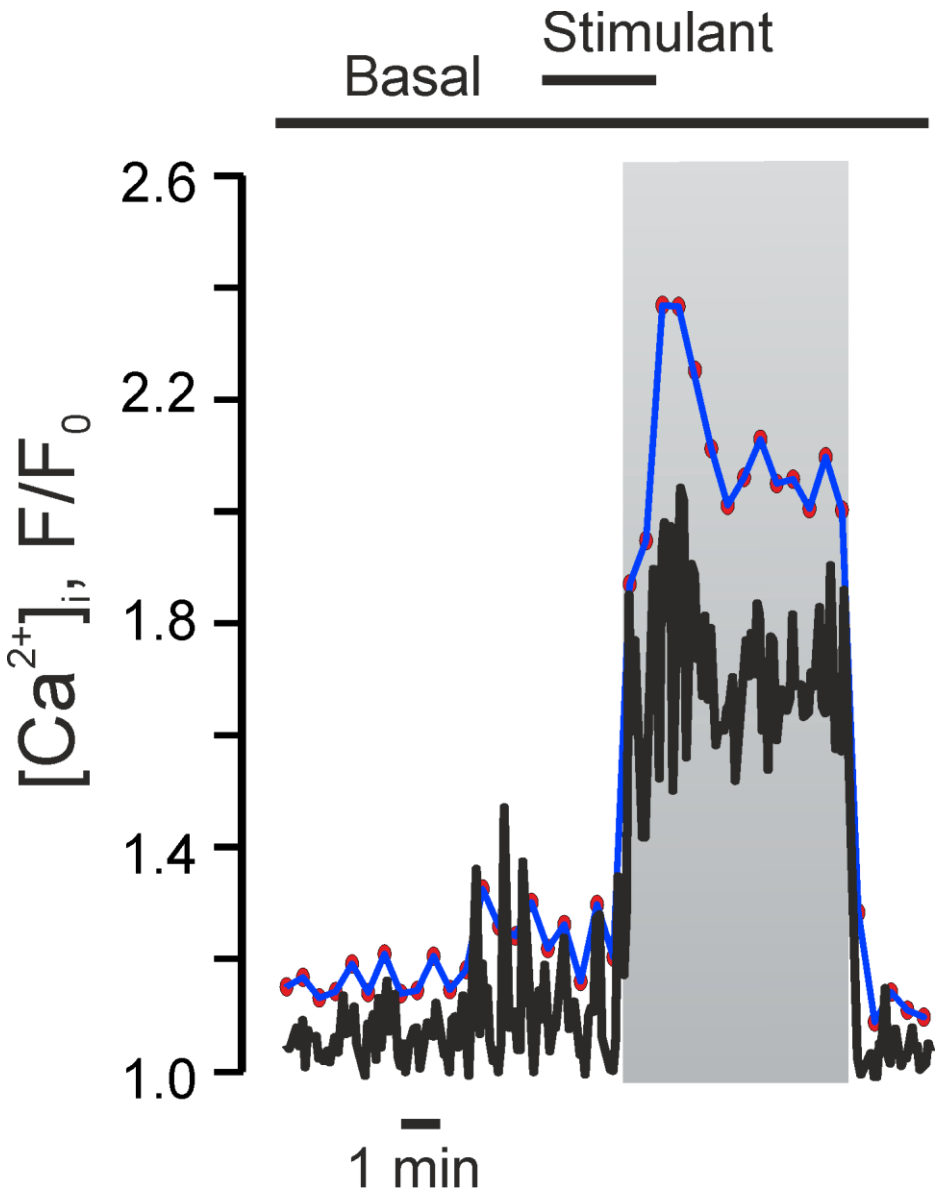


Figure 2.4 – Partial area under the curve calculation

pAUC trace (blue) for $[Ca^{2+}]_i$ trace (black) of a single cell. Each red point represent pAUC for given interval of the $[Ca^{2+}]_i$ trace. Points falling within the shaded region would be considered to represent the effect of the stimulant (e.g. adrenaline). These would be averaged to give the value of the effect for the given cell. Points falling before this point would be averaged to produce the basal value for the given cell.

The heatmaps used to present data for various cellular parameters (incl. $[Ca^{2+}]_i$, pH_i, $[DAG]_i$ and PKA) were produced by combining all ROI traces (1D waves) from a single recording into a single 2D wave using IgorPro. This wave could then be viewed as a heatmap, with minimum and maximum values (in terms of the colour scale) adjusted to reflect the strength of the effect (e.g. adrenaline or ACh) across the population. The standard deviation images were produced using the Z-Projection tool in FIJI, choosing the 'standard deviation' option and the time period related to each condition (e.g. Duration of application for 3 mM + 5 μM adrenaline).

2.8. Solutions

The extracellular solution (EC1) used for imaging and current-clamp electrophysiology experiments contained (mM)140 NaCl, 4.6 KCl, 2.6 $CaCl_2$, 1.2 $MgCl_2$, 1 NaH_2PO_4, 5 $NaHCO_3$ and 10 HEPES, (pH adjusted to 7.4, with NaOH).

2.9. General Reagents

D-Glucose, NaCl, KCl, $CaCl_2$, $MgCl_2$, NaH_2PO_4, $NaHCO_3$, HEPES, NaOH, EGTA and glutamate were all purchased from Sigma (UK). The L-type Ca^{2+} channel blocker isradipine and the P/Q Ca^{2+} channel blocker ω-agatoxin were purchased from Alomone Labs (Israel).

Chapter 3: Adrenergic Signalling in the Pancreatic α-Cell

3.1. Introduction

Adrenaline, the primary hormone in the 'flight-or-fight' response, acts as part of the sympathetic nervous system to initiate a wide-range of effects. This includes stimulation of glucagon secretion, which has been shown in mice (Schuit and Pipeleers, 1986, Johansson et al., 1989, Gromada et al., 1997, Liu et al., 2004, Vieira et al., 2004, De Marinis et al., 2010). The branch of the sympathetic nervous system associated with adrenaline secretion is known as the sympathoadrenal system; its activation is a critical feature of the body's response to hypoglycaemia, with impaired glucose counterregulation a feature of insulin-dependent diabetes (type 1 diabetes and advanced type 2 diabetes), and blunted adrenal responses a critical factor in its manifestation (Cryer, 2002).

The sympathoadrenal response is triggered by marked hypoglycaemia (3.6 – 3.9 mM) (Sprague and Arbelaez, 2011). This fall in blood glucose is sensed by neurones in the brain that signal via cholinergic pre-ganglionic sympathetic nerves to the chromaffin cells of the adrenal medulla leading to secretion of adrenaline (and noradrenaline[8]) (Verberne et al., 2016). Once released, adrenaline is known to act directly on the liver, binding to β_2-adrenergic receptors to increase hepatic glucose output via enhanced glycogenolysis and

[8] Noradrenaline accounts for 20% of total secretion from the adrenal medulla TREVINO, L. A. U., M.L.; LIEGEY DOUGALL, A.J. 2012. Adrenal Glands. *Encyclopedia of Human Behavior.* Second ed.. There is evidence that hypoglycaemia targets adrenergic chromaffin cells with noradrenergic chromaffin cells more associated with blood pressure VERBERNE, A. J., KORIM, W. S., SABETGHADAM, A. & LLEWELLYN-SMITH, I. J. 2016. Adrenaline: insights into its metabolic roles in hypoglycaemia and diabetes. *Br J Pharmacol,* 173**,** 1425-37.

gluconeogenesis (Exton, 1987), similarly to glucagon itself. Unlike glucagon, however, adrenaline can also suppress insulin secretion, stimulate lipolysis, reduce glucose utilisation (Bolli and Fanelli, 1999), stimulate amino acid and lactate release from muscle (Gromada et al., 2007), and, as mentioned, stimulate glucagon secretion (Schuit and Pipeleers, 1986, Johansson et al., 1989, Gromada et al., 1997, Liu et al., 2004, Vieira et al., 2004, De Marinis et al., 2010). Along with the sympathoadrenal system, the glucose counterregulatory response also encompasses the sympathetic nerves that innervate the pancreatic islet. The involvement of these sympathetic termini in the stimulation of glucagon secretion cannot be overlooked, as they release noradrenaline into the islet vicinity, which, crucially, has also been shown to stimulate glucagon secretion (Hauge-Evans et al., 2010).

In terms of adrenaline's direct effect on the α-cell, various mechanisms have been proposed. Adrenaline and noradrenaline can act via two types of GPCRs: α-adrenergic receptors, subdivided into α_1 and α_2, and β- adrenergic receptors, subdivided into and β_1-, β_2- and β_3 (Table 3.1). The two catecholamines bind to these receptors with almost identical affinity (IUPHAR/BPS, 2015, IUPHAR/BPS, 2016). Early work in single rat α-cells suggested a β-adrenergic mechanism resulting in increased cAMP and subsequent stimulation of glucagon secretion (Schuit and Pipeleers, 1986). This model was developed upon, again using single rat α-cells, with β-adrenergic signalling reported to initiate PKA-dependent L-type Ca^{2+} channel influx and accelerated granule mobilization (Gromada et al., 1997). A role for intracellular Ca^{2+} was first proposed by Johansson et al. (1989), working on single guinea pig α-cells, who suggested that Ca^{2+} pre-sequestered into the ER was released by adrenaline via a β-adrenergic mechanism. A later study (Liu et al., 2004), using single mouse α-cells, reconciled the two models above, proposing that adrenaline

initiates Ca^{2+}-mobilisation from the ER stores which induces a store-operated current at the plasma membrane, thereby causing depolarization, which in turn opens L-type Ca^{2+} channels. It was further argued that the store-operated current represented a mechanism whereby glucose inhibited α-cell excitability by promoting ER Ca^{2+}-sequestration (Liu et al., 2004). Further studies reported synergistic α_1 and β-adrenergic pathways. It was proposed that the α_1 pathway was responsible for the initial ER Ca^{2+} release while the 'late effect' was promoted by the β-pathway activating PKA-dependent L-type Ca^{2+} channel influx (Vieira et al., 2004). Most recently, in a study looking in whole mouse islets, De Marinis et al. (2010) highlighted the role of the low-affinity cAMP target Epac2, a guanine nucleotide exchange factor (GEF). They reported differential effects of GLP-1 (inhibitory) and adrenaline (stimulatory) on glucagon secretion, despite both agents increasing cAMP, which were ascribed to differences in key downstream targets. Specifically, adrenaline increasing cAMP more potently thereby activating Epac2 leading to opening of L-type Ca^{2+} channels and triggering of glucagon secretion (as opposed to Glp-1, which only activates PKA - see 1.3.6 for full mechanism) (De Marinis et al., 2010).

Receptor type	**β (β_1, β_2, β_3)**	**α_1**	**α_2**
G Protein	G_s	G_q	G_i
Second Messenger system	Adenylyl cyclase/cAMP	Phospholipase C/IP_3 + DAG	Inhibition of adenylyl cyclase

Table 3.1 - Summary of adrenergic receptors

Adapted from Frayn (2010)

While mouse studies have consistently shown adrenaline's stimulatory effect on glucagon secretion, a role in human islets has remained elusive. The importance of the human autonomic system in glucose counterregulation was demonstrated by ganglionic blockade

of nicotinic receptors that reduced glucagon secretion in response to insulin-induced hypoglycaemia by 75% (coupled with a 70% decrease in plasma adrenaline) (Havel and Ahren, 1997). However, blockade of adrenergic receptors, paradoxically, has no effect on the glucagon secretory response (Hilsted et al., 1991, Towler et al., 1993). Adrenaline also has no effect on glucagon secretion from human islets (Walker et al., 2011). This has led to speculation that neuropeptides, which are co-secreted with the classical neurotransmitters, are responsible for autonomic-controlled glucagon secretion in man (Taborsky and Mundinger, 2012).

A definitive model of adrenaline's effect on the α-cell is yet to be reached. Increased L-type Ca^{2+} channel influx is often ascribed a major role in increasing $[Ca^{2+}]_i$ with intracellular Ca^{2+} release, when shown, found to initiate L-type Ca^{2+} influx at the plasma membrane. A major discrepancy of the current models is the relatively weak effect of adrenaline on membrane potential (Figure A2.1) despite large effects on cytoplasmic $[Ca^{2+}]_i$ and glucagon secretion. This suggest that mobilisation of Ca^{2+} from intracellular (luminal) sources accounts for much of the adrenaline effect, with plasma membrane channels (e.g. L-type Ca^{2+} channels), if involved, likely to act as a trigger for CICR from the ER (Figure 3.1). It must also be noted that the majority of these studies were performed on single α-cells rather than intact islets, thus removing any cell-to-cell contacts and paracrine interactions that would undoubtedly affect α-cell behaviour and possibly the adrenaline response. In this study, I aimed to elucidate the mechanism of the adrenaline effect on the α-cell, focusing particularly on the role of intracellular Ca^{2+} stores, and whether the effect was conserved in human islets. I predominantly utilised confocal imaging of $[Ca^{2+}]_i$ in whole islets, which provides excellent spatial and temporal resolution for recording of α-cell signals.

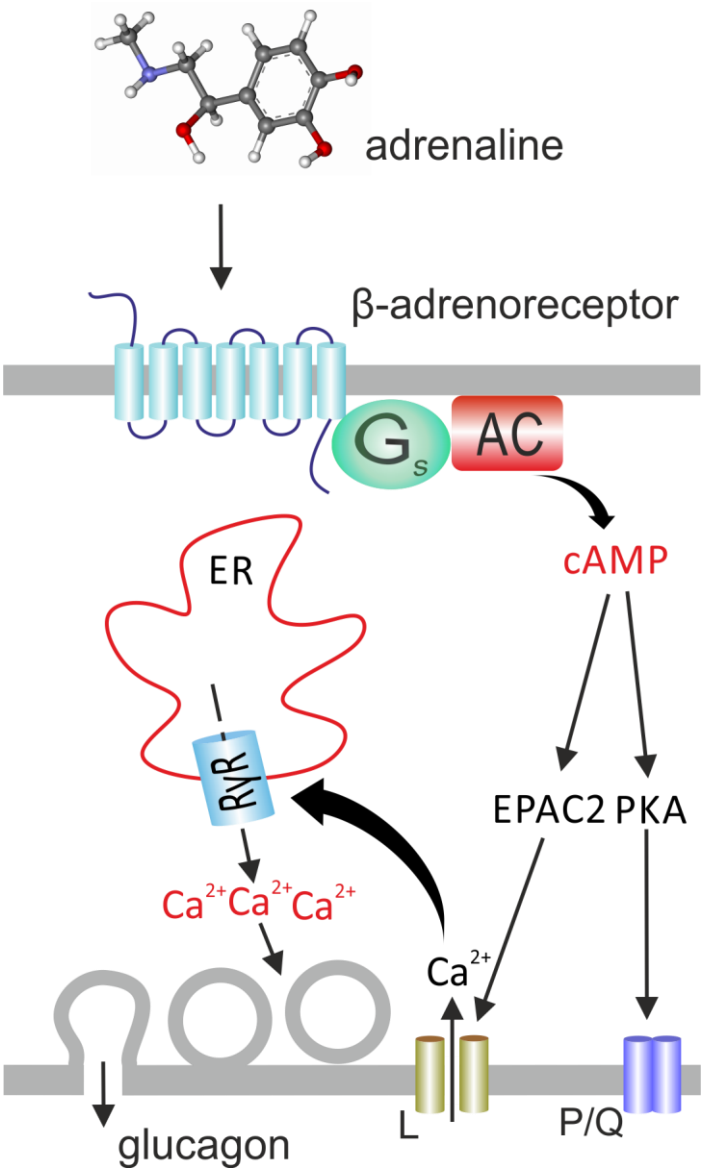


Figure 3.1 - Hypothesis

Adrenaline acts via the β-adrenergic receptor activating $G_{\alpha s}$, which signals to adenylyl cyclase (AC) leading to increased formation of the secondary messenger cAMP. This is proposed to activate the high-affinity cAMP target PKA, which closes P/Q-type Ca^{2+} channels, and the low-affinity cAMP target Epac2, which increases L-type Ca^{2+} channel influx. The Epac-2 dependent L-type Ca^{2+} channel influx overcomes the PKA-dependent P/Q-type Ca^{2+} channel closure resulting in increased $[Ca^{2+}]_i$, which triggers CICR from the ER, increasing $[Ca^{2+}]_i$ further and stimulating glucagon secretion.

3.2. Methods

For islet isolation, islet culture, confocal $[Ca^{2+}]_i$ imaging, data analysis, general reagents and solutions

Please refer to main methods section

3.2.1. Mice

Naval Medical Research Institute (NMRI) mice, an outbred strain of mice, were used throughout the study described in this chapter, except in the experiments using knockout mouse models. *Tpcn1*$^{-/-}$ and *Tpcn2*$^{-/-}$ mice were of a C57BL/6N background and were therefore compared to C57BL/6N control mice. The *CD38*$^{-/-}$ mice were of a C57BL/6J background and were therefore compared to C57BL/6J control mice. For the experiments looking at the effects of adrenaline on β- and δ-cells, SST-RFP mice were used, which were of a C57BL/6J background. A minimum of 2 mice were used for each condition, with *n* taken as number of cells.

3.2.2. Imaging of PKA activity

Real-time changes in PKA activity were reported in pancreatic islet cells using the recombinant FRET probe AKAR3 (Allen and Zhang, 2006), which was delivered into islets via an adenoviral infection (10^5 units per islet – determined by infecting INS1 cells with serial dilutions of the virus) and expressed for 36 h at 37 °C in an incubator (5% CO_2/95% Air). Islets were loaded into a 'closed' perifusion chamber (Figure 2.3) before being imaged with a Zeiss Axiozoom.V16 zoom microscope, using the 2.3x/0.57 objective

at a magnification of 4x-10x. AKAR3 was excited at 458 nm with emission collected at 485 nm and 515 nm. The bath solution containing various stimuli was perifused continuously at 60 µl/min (using a peristaltic pump) and maintained at 34 °C. Pancreatic α-cells were identified by an increase in PKA activity (AKAR3 FRET ratio) after application of adrenaline (5 µM). AKAR3 was a gift from Dr. Jin Zhang (Department of Pharmacology and Molecular Sciences, The Johns Hopkins University School of Medicine, Baltimore, USA).

3.2.3. $[Ca^{2+}]_i$ imaging (Fluo-4FF)

Intact mouse and human islets were loaded in Fluo-4FF (10 µM; Thermo Fisher, UK) dissolved in EC1 solution and supplemented with 6 mM glucose. 1 ul of pluronic F-127 (Thermo Fisher, UK) was added to aid with solubility of the Ca^{2+} dye. After 90 min at 37 °C in an incubator (5% CO_2/95% Air), islets were transferred to an open chamber (Figure 2.2) before being imaged using a Zeiss AxioVert 200 microscope equipped with Zeiss 510-META laser confocal scanning system, using 40x/1.3 objective. The EC1 bath solution was perifused at 200 µl/min (using a peristaltic pump) with various stimuli added, temperature of the bath solution was maintained at 34 °C throughout each recording. A 488 nm argon laser (3% intensity) was used to excite Fluo-4FF and emission was collected at 530 nm, using 512x512 frame scanning mode and recorded at 12-bit. Scan time was increased to 7.84s (including 5s interval to prevent bleaching), with a pixel dwell time of 13 µs.

3.2.4. Reagents

The membrane-permeable PKA inhibitor (myr-)PKI, the NAADP antagonist Ned-19, the inhibitor of vacuolar-H^+ ATPases Bafilomycin A1, SERCA-ATPase inhibitor thapsigargin and noradrenaline were obtained from Tocris Bioscience (UK). The Epac2 inhibitor ESI-05 was from BioLog (Germany). The α_1 adrenergic receptor antagonist prazosin was purchased from Abcam (UK). Adrenaline, propranolol, isoprenaline, ryanodine, insulin, diazoxide and forskolin were obtained from Sigma-Aldrich (UK).

3.3. Results

3.3.1. Effect of adrenaline on $[Ca^{2+}]_i$ in pancreatic α-cells within intact mouse and human islets

Adrenaline's effect on α-cell $[Ca^{2+}]_i$ dynamics was investigated using time-lapse confocal microscopy. Islets were perifused in a bath solution supplemented with 3 mM glucose, ensuring insulin and somatostatin secretion were low (Zhang et al., 2013; Figure 1.6) while also allowing adequate control of $[Ca^{2+}]_i$ by maintaining sufficient ATP levels for Ca^{2+}-ATPase pumps to function. α-Cells were identified by increased $[Ca^{2+}]_i$ in response to glutamate (1 mM), with mouse and human α-cells (but not β-cells) reported to possess ionotropic glutamate AMPA receptors (Cabrera et al., 2008). Most islet cells exhibited no evident $[Ca^{2+}]_i$ dynamics at 3 mM glucose; however, approximately 20% of cells displayed periodical $[Ca^{2+}]_i$ oscillations under basal conditions (Figure 3.2 a, d). Furthermore, over 70% of the cells active at low glucose responded to glutamate. Application of adrenaline (5 μM) initiated a rapid, potent and reversible increase in $[Ca^{2+}]_i$ ($p < 0.001$ vs. basal; $n = 29$; Figure 3.2 b, e) in glutamate-responsive cells but not among the remaining cell population (Figure 3.2 a, d)[9]. High (20 mM) glucose was added at the end of each recording to activate β-(and δ-) cells (approx. 80% of cells), further facilitating correct identification of islet cell subsets (Figure 3.2 d). The neurotransmitter noradrenaline also induced significant elevation of $[Ca^{2+}]_i$ in α-cells ($p < 0.001$ vs. basal; $n = 19$; Figure 3.2 f), albeit to a lesser extent than adrenaline ($p = 0.023$ vs. control). A response to adrenaline was also observed in human islets, with an effect of similar magnitude in terms of fold-

[9] There was also a subset of α-cells (2/29 - 7%) inactive at low glucose, which were responsive to glutamate and adrenaline.

change from basal ($p < 0.001$ vs. basal; $n = 55$, 3 donors; Figure 3.2 d, e). Adrenaline stimulated glucagon secretion in mouse islets by 3.8±0.8-fold (Figure A2.2 a).

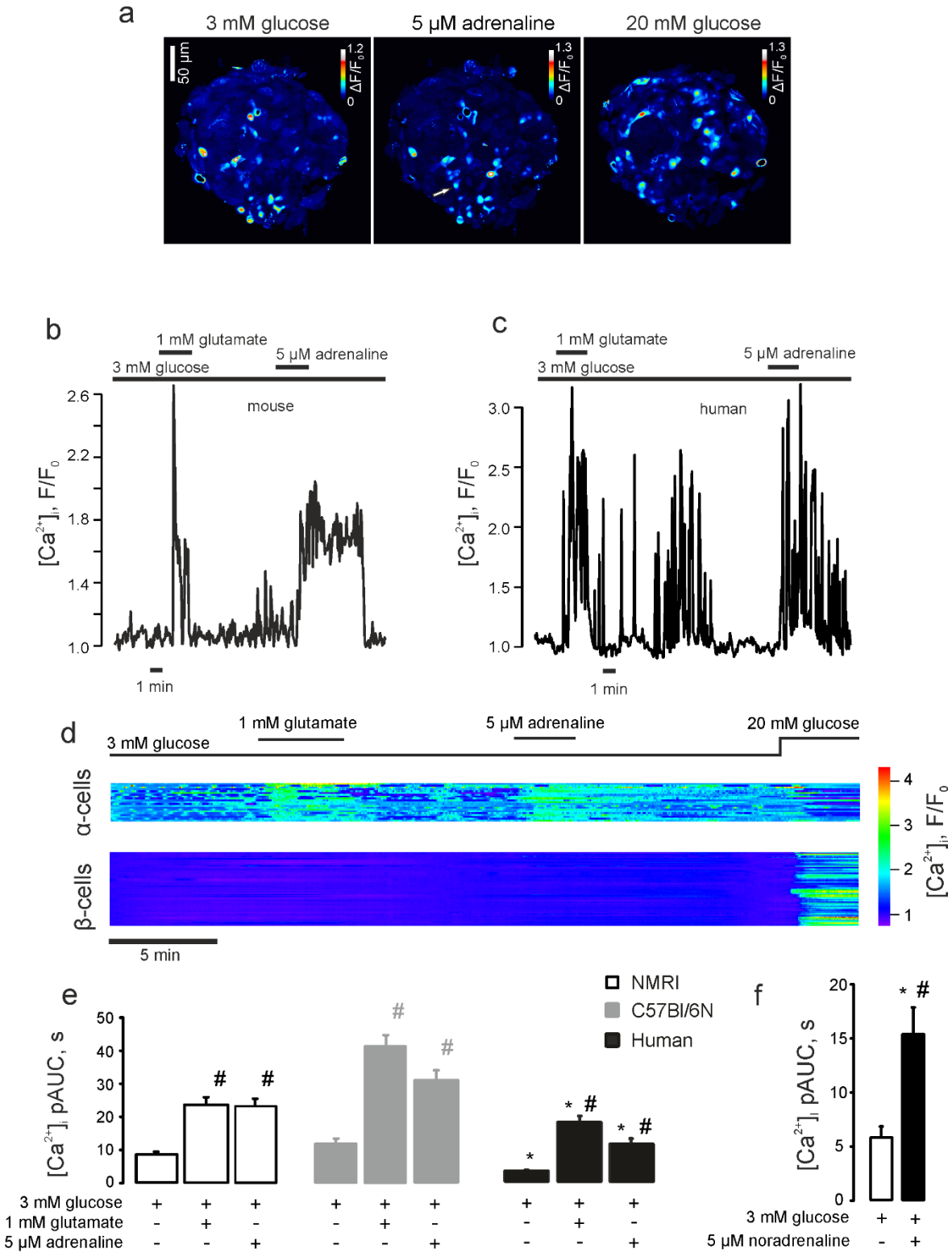


Figure 3.2 - The stimulatory effect of adrenaline on glucagon secretion is mediated by selective elevation of $[Ca^{2+}]_i$ in pancreatic α-cells

(a) Standard deviations of the Fluo-4 intensity imaged when the islet was perifused by the extracellular solution containing 3 mM glucose alone or with 5 µM adrenaline or 20 mM glucose, as indicated. The brighter cells are those with the higher difference between the minimal and maximal values (i.e. the cells in which $[Ca^{2+}]_i$ oscillates). The arrow indicates

a cell that was silent at 3 mM glucose but started spiking after adrenaline had been applied. **(b-c)** Typical single α-cell response to application of 1 mM glutamate and 5 μM adrenaline recorded in mouse (b) and human (c) islets, at 3 mM glucose. **(d)** Representative $[Ca^{2+}]_i$ heatmap of α- (*n* = 21; top) and non-α-cell (mostly, β-cells, *n* = 75; bottom) populations in NMRI mouse islets, each line represents a single ROI (cell). Populations differentiated based on response to glutamate. Note strong differences in the basal $[Ca^{2+}]_i$ dynamics as well as effects of adrenaline and high glucose between the two populations. **(e)** $[Ca^{2+}]_i$ changes in α-cells quantified as pAUC at 3 mM glucose alone and in the presence of glutamate or adrenaline in NMRI and C57BL/6N mouse islets and human islets. **(f)** $[Ca^{2+}]_i$ changes in α-cells quantified as pAUC at 3 mM glucose alone and in the presence of noradrenaline, in NMRI mouse islets. # Denotes significant ($p < 0.05$) vs. basal; * Denotes significant ($p < 0.05$) vs. NMRI control. Error bars represent ± SEM. Fluo-4 used throughout unless otherwise stated.

3.3.2. The role of adrenergic receptor subtypes in the adrenaline effect in pancreatic α-cells within intact mouse islets

To establish which adrenergic pathway(s) operate(s) in α-cells, the involvement of α_1- and β-adrenergic receptors (the inhibitory α_2-adrenergic receptor was ruled out) was tested pharmacologically. Firstly, the specific β-adrenergic agonist isoprenaline (5 μM) was applied in place of adrenaline, which generated a similarly potent $[Ca^{2+}]_i$ response (p = 0.155 vs. control; n = 27; Figure 3.3 a, d). Furthermore, the β-specific antagonist propranolol (4 μM), when applied acutely, completely blocked the adrenaline effect (p < 0.001 vs. control; n = 11; Figure 3.3 b, d). To investigate any role for the α_1-adrenergic receptor, the α_1-specific blocker prazosin (1 μM) was applied acutely; in this case, the adrenaline effect persisted in its presence (p = 0.525 vs. control; n = 49; Figure 3.3 c, d). These data suggest that the adrenaline effect in α-cells is mediated via β-adrenergic signalling.

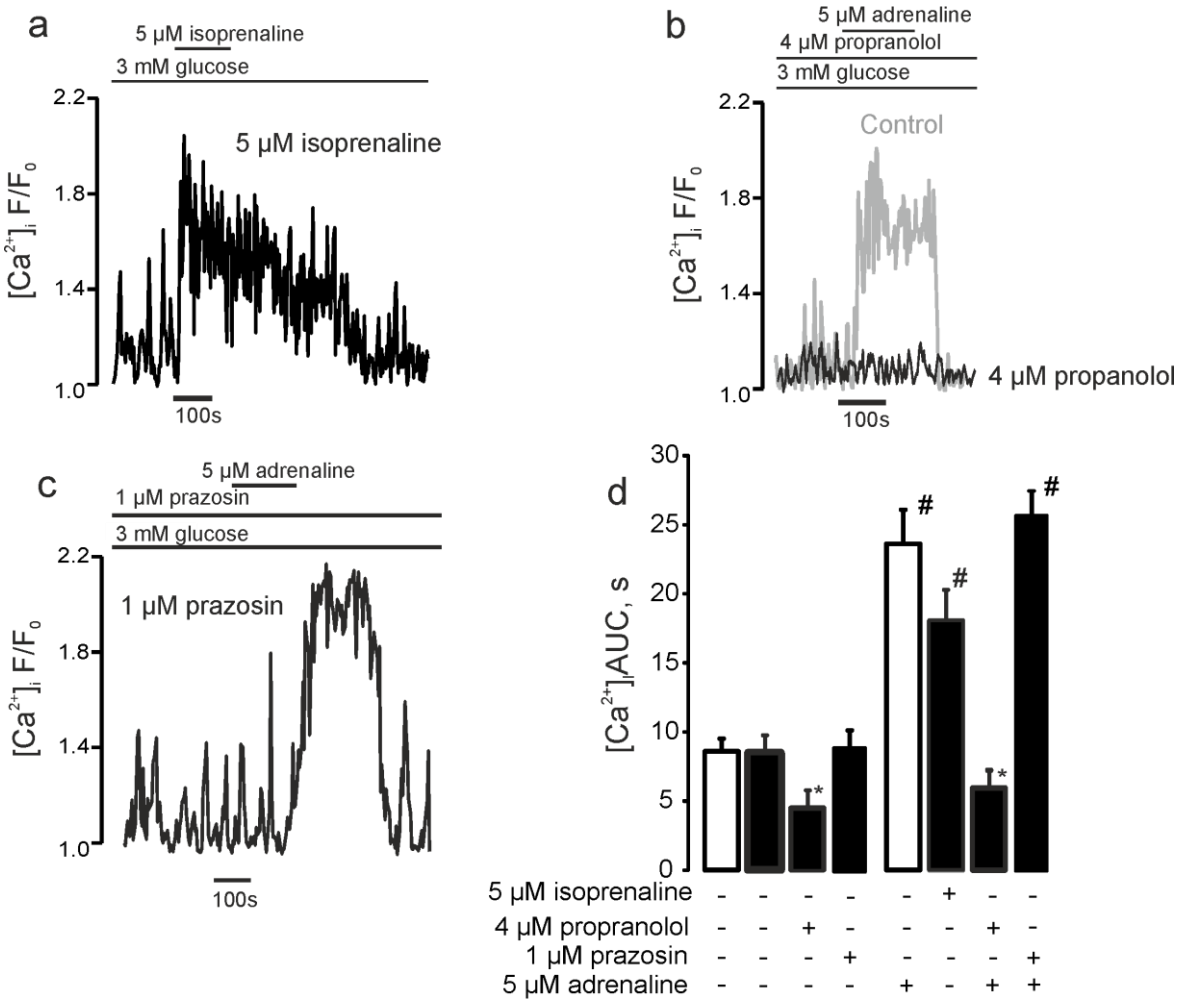


Figure 3.3 - Adrenaline functions via the β-adrenergic pathway in α-cells

(a) Representative recording of the effect of isoprenaline (5 µM) on $[Ca^{2+}]_i$ dynamics in α-cells. **(b)** Representative recording of the effect of adrenaline (5 µM) on α-cell $[Ca^{2+}]_i$ dynamics in the presence of propranolol (4 µM). The NMRI control trace (grey) is superimposed with the experimental trace. **(c)** Representative recording of the effect of adrenaline (5 µM) on α-cell $[Ca^{2+}]_i$ dynamics in the presence of prazosin (1 µM). **(d)** $[Ca^{2+}]_i$ in α-cells quantified as pAUC at 3 mM glucose and upon adrenaline stimulation (open columns), with isoprenaline or in the presence of propranolol or prazosin with corresponding basal values (black columns). # Denotes significant ($p < 0.05$) vs. basal; * Denotes significant ($p < 0.05$) vs. control. Error bars represent ± SEM. Fluo-4 used throughout unless otherwise stated.

3.3.3. The role of PKA and Epac2 in the adrenaline effect in pancreatic α-cells within intact mouse islets

Triggering of β-adrenergic signalling initiates a rapid increase in cAMP that can activate both PKA and Epac. To examine the contribution of the former, islets were pre-incubated in (myr-)PKI (1 μM), a PKA-specific inhibitor, for 1hr. The majority of α-cells (62.5% - 20/32 cells) in PKI-treated islets were unresponsive to adrenaline, reflected by a significant reduction in the magnitude of the adrenaline effect ($p < 0.001$ vs. control; $n = 32$; Figure 3.4 a, c). A significant increase in $[Ca^{2+}]_i$ from the basal state was still observed however, albeit minimal, due to a minority (37.5% - 12/32 cells) of responsive cells[10]. The involvement of Epac2 (expressed at much higher levels in α-cells than Epac1 (Adriaenssens et al., 2016)) was investigated by pre-incubating islets in ESI-05, an Epac2-specific inhibitor, for 1 hr. Most α-cells remained responsive in ESI-05-treated islets (83% - 10/12) yet often with weaker responses to adrenaline. Indeed, the magnitude of $[Ca^{2+}]_i$ increase was reduced significantly ($p = 0.004$ vs. control; $n = 12$; Figure 3.4 b, c), though less than in PKI-treated islets. Basal $[Ca^{2+}]_i$ dynamics were blunted in PKI- ($p = 0.042$ vs. control) and ESI-05-treated islets ($p = 0.003$ vs. control). Adrenaline's effect on glucagon secretion was also attenuated by both PKI and ESI-05 (Figure A2.2 b). Intriguingly, in ESI-05-treated islets this inhibition was more pronounced despite its relatively weaker effects on $[Ca^{2+}]_i$. This suggested Epac2 also acted in the 'late stages' of the effect, downstream from Ca^{2+}. Measurement of glucagon granule exocytosis (monitored as increases in membrane capacitance (ΔC_m) using standard whole-cell patch-clamp technique) confirmed this with cAMP-mediated exocytosis inhibited by ESI-05 but not PKI (Figure A2.3).

[10] Many of these 'responsive' cells had a diminished adrenaline response

To calibrate the relative cAMP levels associated with the adrenaline response, the adenylyl cyclase activator forskolin was applied in a dose-dependent manner (1 nM, 10 nM, 1 µM, 10 µM) with both $[Ca^{2+}]_i$ and PKA-activity measured separately. Interestingly, effects on $[Ca^{2+}]_i$ were only apparent at µM concentrations (1 µM forskolin: $p = 0.03$ vs. basal), with an 'adrenaline-like' effect only produced when 10 µM forskolin was applied ($p < 0.01$ vs. basal; $n = 20$; Figure 3.4 e) and a half maximal response reached at 5.3±1.5 µM forskolin (Figure 3.4 f); in contrast, PKA activity, measured with the FRET sensor AKAR3, increased proportionally from nM concentrations with a half-maximal response at 0.19±0.05 µM forskolin ($n = 98$; Figure 3.4 d, f). The disparity between $[Ca^{2+}]_i$ and PKA activity further highlights the requirement of Epac2 in the manifestation of the adrenaline effect. Notably, adrenaline (5 µM) produced an effect equivalent to 4.2±1.1 µM forskolin (Figure 3.4 f); supporting the notion that µM concentrations and hence high levels of cAMP are required to stimulate glucagon secretion (De Marinis et al., 2010).

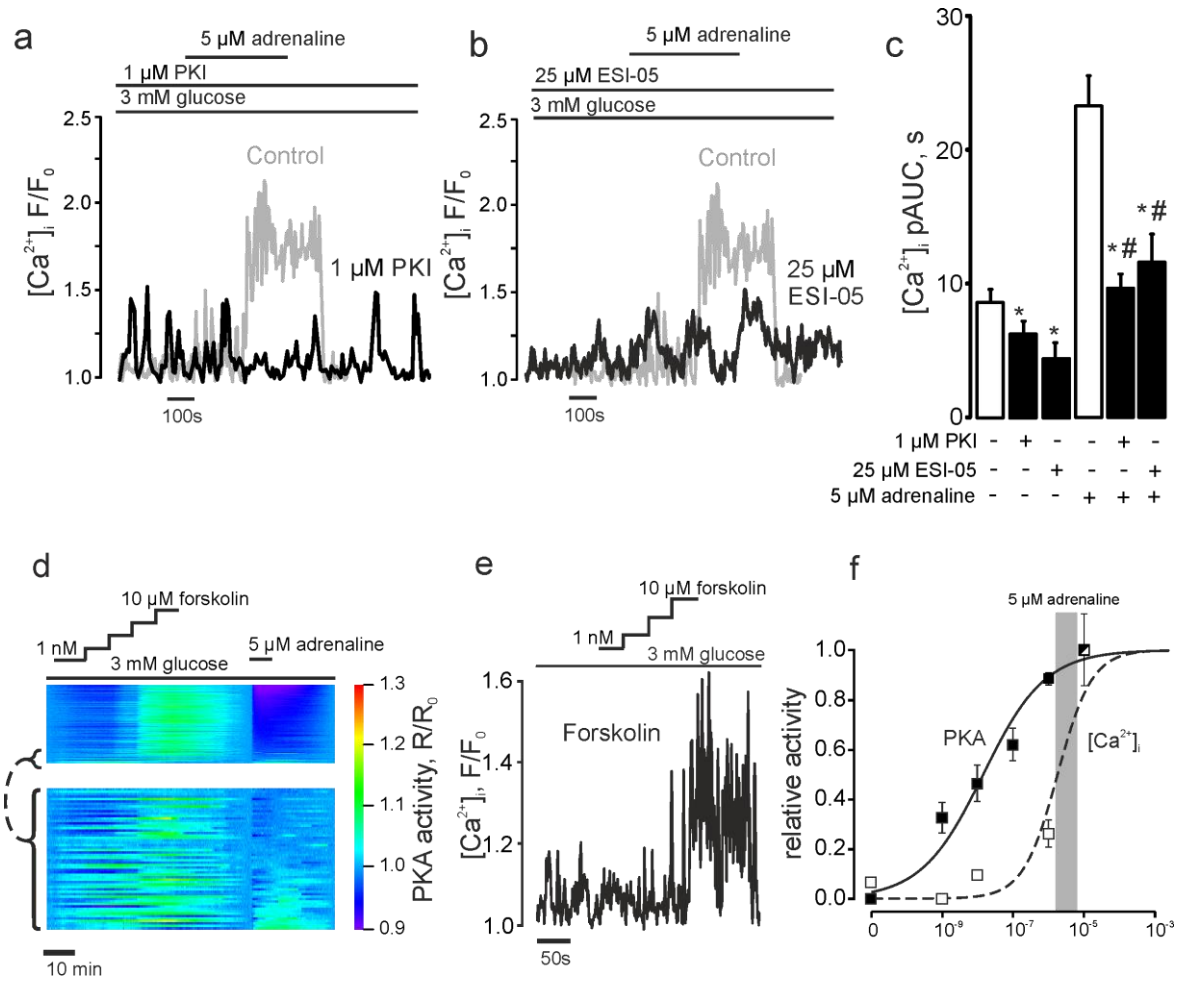


Figure 3.4 - Adrenaline targets both PKA- and Epac2-dependent pathways

(a) Representative recording of the effect of adrenaline (5 μM) on α-cell $[Ca^{2+}]_i$ dynamics in the presence of PKI (1 μM). The NMRI control trace (grey) is superimposed with the experimental trace. **(b)** Representative recording of the effect of adrenaline (5 μM) on α-cell $[Ca^{2+}]_i$ dynamics in the presence of ESI-05 (25 μM). The NMRI control trace (grey) is superimposed with the experimental trace. **(c)** $[Ca^{2+}]_i$ in α-cells quantified as pAUC at 3 mM glucose and upon adrenaline stimulation alone (open columns) or in the presence of PKI or ESI-05 (black columns). **(d)** Heatmap comparing the effects of adrenaline and forskolin (1 nM – 10 μM) on PKA activity, measured using AKAR3. Top panel shows all islet cells (n = 870) with bottom panel showing all α - cells (n = 62), identified by their stimulatory response to adrenaline. **(e)** Representative recording of effect of varying concentrations of forskolin on $[Ca^{2+}]_i$ dynamics. **(f)** Forskolin concentration-activation curves for PKA (solid line) and $[Ca^{2+}]_i$ (dashed line). The effect of 5 μM adrenaline on PKA measured from the same cells is mapped on to the curves as a shaded area (4.1±0.8 μM forskolin). # Denotes significant ($p < 0.05$) vs. basal; * Denotes significant ($p < 0.05$) vs. control. Error bars represent ± SEM. Fluo-4 used throughout unless otherwise stated.

3.3.4. Effect of Ca^{2+} channel blockers on the adrenaline effect in pancreatic α-cells within intact mouse islets

After confirming the involvement of PKA-dependent and PKA-independent pathways in the α-cell's response to adrenaline, the Ca^{2+} sources that could potentially be responsible for the effect were probed. The role of extracellular Ca^{2+} was examined by blocking P/Q-type- (approx. 20% of Ca^{2+} current (Zhang et al., 2013)) and L-type Ca^{2+}-channels (approx. 70% Ca^{2+} current (Gromada et al., 1997)) acutely. As expected, blocking P/Q-type Ca^{2+} channels with ω-agatoxin (200 nM) had no effect on the magnitude of the adrenaline-induced $[Ca^{2+}]_i$ response ($p = 0.257$ vs. control; $n = 13$; Figure 3.5 a, c) or glucagon secretion (Figure A2.2 c). While the L-type Ca^{2+} channel blocker isradipine (2 µM) blocked the adrenaline response, both in terms of $[Ca^{2+}]_i$ ($p < 0.001$ vs. control; $n = 17$; Figure 3.5 b, c), and glucagon secretion (Figure A2.2 c). Basal Ca^{2+} was also reduced in isradipine-treated α-cells ($p = 0.004$ vs. control; Figure 3.5 c). Notably, 2 out of 17 isradipine-treated α-cells did display a transient $[Ca^{2+}]_i$ response to adrenaline, as reported previously (Liu et al., 2004, De Marinis et al., 2010). All remaining cells were unresponsive meaning overall statistical significance was not reached ($p = 0.463$ vs. basal).

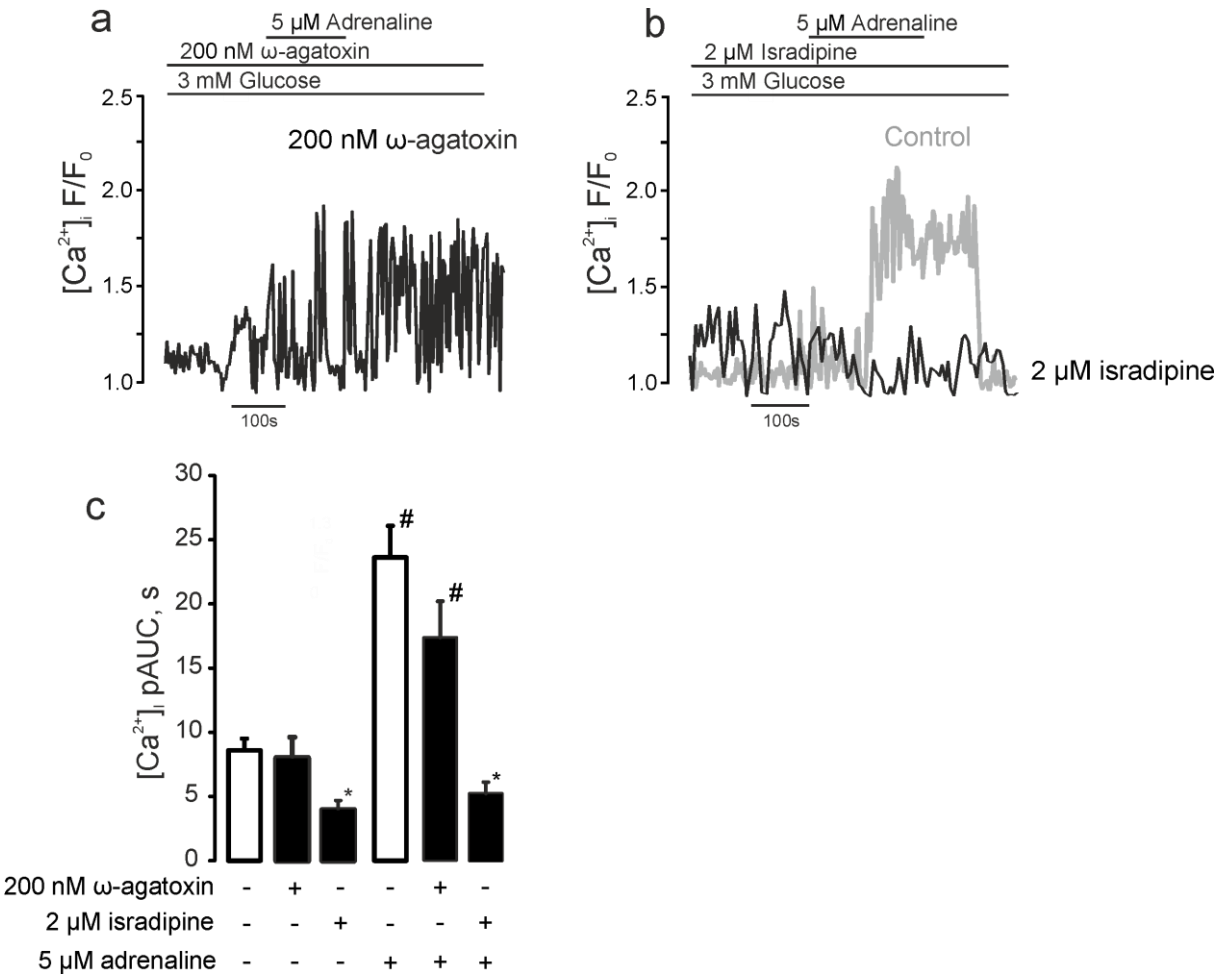


Figure 3.5 - Adrenaline response is abolished in the presence of the L-type Ca^{2+}-channel blocker isradipine

(a) Representative recording of the effect of adrenaline (5 µM) on α-cell $[Ca^{2+}]_i$ dynamics in the presence of ω-agatoxin (200 nM). **(b)** Representative recording of the effect of adrenaline (5 µM) on α-cell $[Ca^{2+}]_i$ dynamics in the presence of isradipine (2 µM). The NMRI control trace (grey) is superimposed with the experimental trace. **(c)** $[Ca^{2+}]_i$ in α-cells quantified as pAUC at 3 mM glucose and upon adrenaline stimulation alone (open columns) or in the presence of ω-agatoxin or isradipine (black columns). # Denotes significant ($p < 0.05$) vs. basal; * Denotes significant ($p < 0.05$) vs. control. Error bars represent ± SEM. Fluo-4 used throughout unless otherwise stated.

3.3.5. The role of intracellular Ca^{2+} in the adrenaline effect in pancreatic α-cells within intact mouse islets

Based on the electrophysiological data, it was presumed Ca^{2+}-entry via L-type channels merely triggers CICR from the ER and is not solely responsible for adrenaline-induced $[Ca^{2+}]_i$ increase in the α-cell. To examine whether this was the case, islets were pre-incubated in ryanodine (50 µM) for 1h, which acts antagonistically at this concentration (but agonistically at nM concentrations) (Meissner, 1986). Unexpectedly, in terms of $[Ca^{2+}]_i$, ryanodine-treated islets behaved similarly to control islets, with no significant difference in the magnitude of the adrenaline effect (p = 0.810 vs. control; n = 56; Fig. 3.6 a). In contrast, adrenaline-induced glucagon secretion was abolished (Figure A2.2 d). This paradox was also true in islets treated with SERCA Ca^{2+}-ATPase inhibitor thapsigargin (10 µM; p = 0.207 vs. control; n = 23; Figure 3.6 a). It was therefore postulated that adrenaline may function via multiple Ca^{2+}-release mechanisms, with both an ER component and a non-ER component acting in parallel. The $[Ca^{2+}]_i$ increase generated from the non-ER component would then be sufficient to saturate the high-affinity Fluo-4 dye (K_d = 300 nM). Indeed, when the same experiment was repeated using the low-affinity Fluo-4FF dye adrenaline's effect on $[Ca^{2+}]_i$ in ryanodine-treated islets was sharply diminished compared to control (p = 0.035 vs. control; n = 22; Figure 3.6 b, c).

The apparent existence of a non-ER Ca^{2+} source drew attention to the (endo)lysosomal (acidic) Ca^{2+} stores, which have been linked to β-adrenergic signalling in the heart (Lewis et al., 2012, Capel et al., 2015). To probe their involvement, the acidic stores were emptied by pre-incubation with bafilomycin, a specific inhibitor of vacuolar type-H^+ ATPases, for 20 min. Remarkably, this rendered 78% (28/36 cells) of α-cells completely unresponsive

to adrenaline ($p < 0.001$ vs. control; $n = 36$; Figure 3.6 h, i), with minimal responses in the remaining cells, and no significant elevation of $[Ca^{2+}]_i$ from basal ($p = 0.863$ vs. basal).

(Endo)lysosomes are equipped with two-pore channels (TPCs), NAADP-sensitive channels that can release Ca^{2+} into the cytosol (Calcraft et al., 2009). To pinpoint the mechanism underlying this release, mice lacking TPC isoforms, TPC1 (*Tpcn1*$^{-/-}$) and TPC2 (*Tpcn2*$^{-/-}$), were used. In the former, no significant differences were observed in the adrenaline response, $[Ca^{2+}]_i$ increases were almost identical ($p = 0.121$ vs. control; $n = 84$; Figure 3.6 d, f) and despite a marked decrease in glucagon secretion in response to adrenaline, this did not reach statistical significance (Figure A2.2 e). Interestingly, in the *Tpcn2*$^{-/-}$ islets, the effect on $[Ca^{2+}]_i$ was sharply reduced ($p < 0.001$ vs. control; $n = 27$; Figure 3.6 e, f) with adrenaline-induced glucagon secretion completely abolished (Figure A2.2 e). Notably, however, a minority (37% - 10/27 cells) of α-cells were still responsive in *Tpcn2*$^{-/-}$ mice, reflected by a small yet significant increase in $[Ca^{2+}]_i$ from basal glucose ($p < 0.001$ vs. basal).

The secondary messenger NAADP is integral for Ca^{2+}-release from the acidic stores, directly linked to the opening of TPCs (Calcraft et al., 2009). To establish NAADP's role in adrenaline-induced glucagon secretion, islets were pre-incubated in the NAADP-antagonist Ned-19 for 1 hr. This caused a slight yet significant reduction in the adrenaline-induced $[Ca^{2+}]_i$ response ($p = 0.048$ vs. control; $n = 28$; Figure 3.6 g, i) whilst eliminating any effect on glucagon secretion (Figure A2.2 e). Whole-body deletion of CD38, the main enzyme responsible for NAADP production, had a similar effect with a small yet significant reduction in the adrenaline effect on $[Ca^{2+}]_i$ compared to control ($p = 0.029$ vs.

control; n = 153; Figure 3.6 j, k) and abolished the effect of adrenaline on glucagon secretion (Figure A2.2 e).

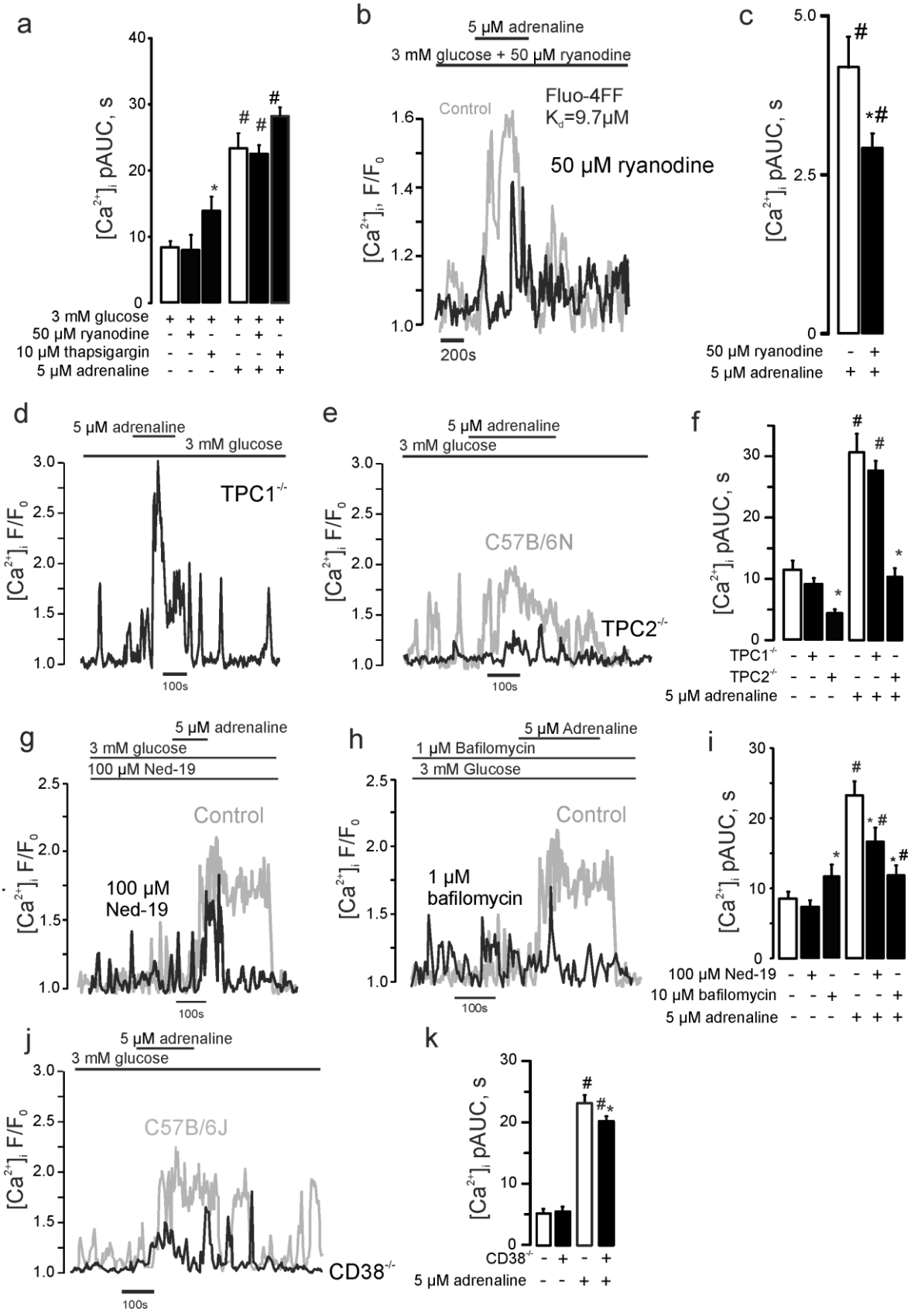

a
[Ca2+]i pAUC, s
3 mM glucose
50 μM ryanodine
10 μM thapsigargin
5 μM adrenaline
b
5 μM adrenaline
3 mM glucose + 50 μM ryanodine
Control
Fluo-4FF
Kd=9.7μM
50 μM ryanodine
[Ca2+]i, F/F0
200s
c
[Ca2+]i pAUC, s
50 μM ryanodine
5 μM adrenaline
d
5 μM adrenaline
3 mM glucose
TPC1-/-
[Ca2+]i F/F0
100s
e
5 μM adrenaline
3 mM glucose
C57B/6N
TPC2-/-
100s
f
[Ca2+]i pAUC, s
TPC1-/-
TPC2-/-
5 μM adrenaline
g
5 μM adrenaline
3 mM glucose
100 μM Ned-19
Control
100 μM Ned-19
[Ca2+]i F/F0
100s
h
5 μM Adrenaline
1 μM Bafilomycin
3 mM Glucose
Control
1 μM bafilomycin
[Ca2+]i F/F0
100s
i
[Ca2+]i pAUC, s
100 μM Ned-19
10 μM bafilomycin
5 μM adrenaline
j
5 μM adrenaline
3 mM glucose
C57B/6J
CD38-/-
[Ca2+]i F/F0
100s
k
[Ca2+]i pAUC, s
CD38-/-
5 μM adrenaline

Figure 3.6 - Adrenaline-induced glucagon secretion involves intracellular Ca^{2+} release

(**a**) $[Ca^{2+}]_i$ in α-cells quantified as pAUC upon adrenaline (5 μM) stimulation alone or in the presence of ryanodine (50 μM) or thapsigargin (10 μM). (**b**) Representative recording of the effect of adrenaline (5 μM) on α-cell $[Ca^{2+}]_i$ dynamics in the presence of ryanodine, visualized using the low-affinity probe Fluo-4FF (K_d = 9.7 μM). The NMRI control (grey) is superimposed with the experimental trace. (**c**) $[Ca^{2+}]_i$ in α-cells quantified as pAUC upon adrenaline stimulation alone or in the presence of ryanodine (n = 22), as measured using Fluo-4FF. **(d)** Representative recording of the effect of adrenaline (5 μM) on $[Ca^{2+}]_i$ dynamics in α-cells from *Tpcn1*$^{-/-}$ islets. **(e)** Representative recording of the effect of adrenaline (5 μM) on $[Ca^{2+}]_i$ dynamics in α-cells from *Tpcn2*$^{-/-}$ islets. The C57BL/6N control (grey) is superimposed with the experimental trace. **(f)** $[Ca^{2+}]_i$ in α-cells quantified as pAUC at 3 mM glucose and upon adrenaline stimulation in C57BL/6N control (*n* = 24; open columns), *Tpcn1*$^{-/-}$ and *Tpcn2*$^{-/-}$ mice (black columns). **(g)** Representative trace of the effect of adrenaline (5 μM) on $[Ca^{2+}]_i$ dynamics in α-cells from Ned-19-treated (100 μM) islets. The NMRI control (grey) is superimposed with the experimental trace. **(h)** Representative trace of the effect of adrenaline (5 μM) on $[Ca^{2+}]_i$ dynamics in α-cells from bafilomycin-treated (1 μM) islets. The NMRI control (grey) is superimposed with the experimental trace. **(i)** $[Ca^{2+}]_i$ in α-cells quantified as pAUC upon adrenaline stimulation alone or in the presence of Ned-19 or bafilomycin. **(j)** Representative trace of the effect of adrenaline (5 μM) on $[Ca^{2+}]_i$ dynamics in α-cells from *CD38*$^{-/-}$ islets. The C57BL/6J control (grey) is superimposed with the experimental trace. **(k)** $[Ca^{2+}]_i$ in α-cells quantified as pAUC at 3 mM glucose and upon adrenaline stimulation in C57BL/6J control (*n* = 64; open columns) and *CD38*$^{-/-}$ mice (black columns). # Denotes significant ($p < 0.05$) vs. basal; * Denotes significant ($p < 0.05$) vs. control. Error bars represent ± SEM. Fluo-4 used throughout unless otherwise stated.

The strong inhibition of the adrenaline response in bafilomycin-treated and *Tpcn2*$^{-/-}$ islets suggested the acidic stores were central to initiation of the adrenaline effect. (Endo)lysosomal Ca^{2+}-release has indeed been proposed as a trigger for CICR from the ER (Capel et al., 2015); raising the question that L-type Ca^{2+} influx may not be required for CICR to occur. To test this hypothesis, the K_{ATP} channel activator diazoxide (100 µM) was applied acutely. This hyperpolarizes the α-cell rendering voltage-gated ion channels (and hence extracellular Ca^{2+} influx) non-functional (Zhang et al., 2013). Basal $[Ca^{2+}]_i$ dynamics dissipated, as expected, yet the adrenaline response persisted ($p = 0.028$ vs. basal, $p < 0.001$ vs. basal (incl. Diazoxide); $n = 20$; Figure 3.7 b, c), with a transient increase in $[Ca^{2+}]_i$ in α-cells. This was further confirmed when free Ca^{2+} was removed from the extracellular solution using the Ca^{2+}-chelator EGTA (5 mM). Again, adrenaline induced a transient rise in $[Ca^{2+}]_i$, which could only have originated from inside the cell ($p = 0.001$ vs. basal, $p < 0.001$ vs. basal (incl. EGTA); $n = 84$; Figure 3.7 a, b, c).

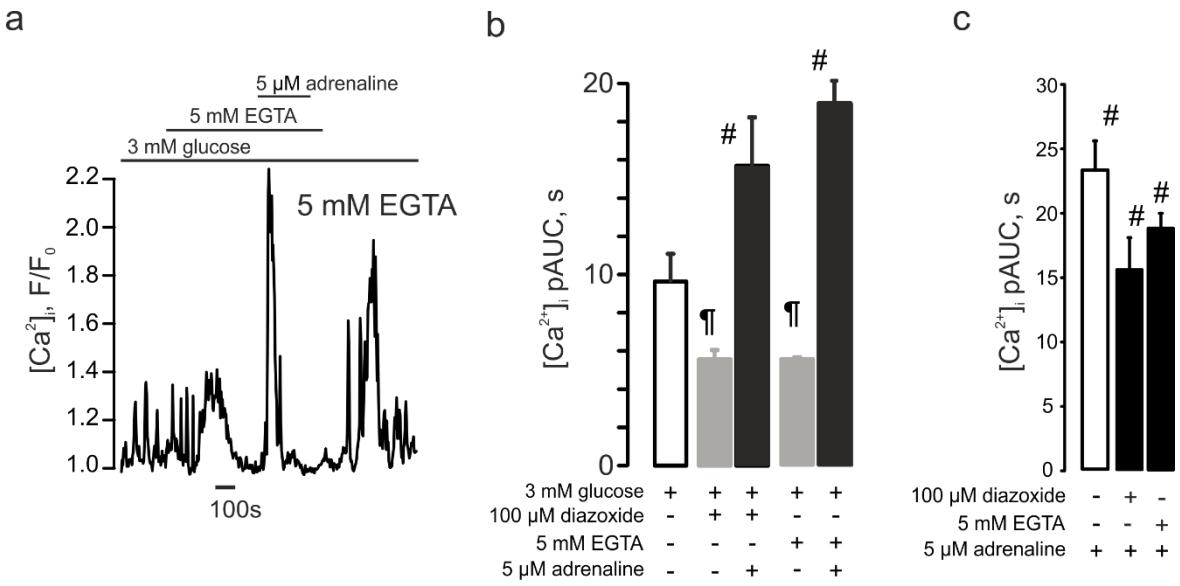


Figure 3.7 - Adrenaline effect persists in absence of extracellular Ca^{2+}

(a) Representative recording of the effect of adrenaline (5 µM) on α-cell $[Ca^{2+}]_i$ dynamics in the presence of EGTA (5 mM). Diazoxide-treated cells displayed an identical effect. **(b)** $[Ca^{2+}]_i$ in α-cells quantified as pAUC at basal glucose (open column) in presence of diazoxide/EGTA (grey columns respectively), effect of adrenaline in presence of diazoxide/EGTA (black columns respectively) **(c)** $[Ca^{2+}]_i$ in α-cells quantified as pAUC upon adrenaline stimulation alone (open columns), or in the presence of diazoxide or EGTA. # Denotes significant ($p < 0.05$) vs. basal; ¶ Denotes basal (diazoxide/EGTA) significantly ($p < 0.05$) different vs. basal. Error bars represent ± SEM. Fluo-4 used throughout unless otherwise stated.

3.3.6. Effect of insulin on the adrenaline response in pancreatic α-cells within intact mouse islets

Whole-body deletion of *Tpcn2* also disrupts β-cell $[Ca^{2+}]_i$ dynamics and insulin secretion, resulting in overall glucose intolerance (Arredouani et al., 2015). To determine whether the diminished adrenaline response in *Tpcn2*$^{-/-}$ mice was insulin-dependent, insulin was applied acutely to *wildtype* islets. This had no effect on the adrenaline-induced $[Ca^{2+}]_i$ response ($p = 0.776$ vs. control; $n = 20$), or basal $[Ca^{2+}]_i$ dynamics ($p = 0.476$; Figure 3.8 a), thus ruling out any potential influence of the β-cell phenotype on the adrenaline response in *Tpcn2*$^{-/-}$ mice.

3.3.7. Effect of hypo- and hyperglycaemic culture on adrenaline response in pancreatic α-cells within intact mouse islets

The absence of glucagon responses to hypoglycaemia is a hallmark of impaired glucose counterregulation in diabetes (Cryer, 2002). I sought to test whether part of this could be due to changes at the islet itself, specifically in relation to α-cell adrenaline sensitivity. Instead of using the trappable dye Fluo-4, mouse islets were transfected with the genetically encoded Ca^{2+}-sensor Gcamp6f to increase the signal-to-noise ratio of the imaging, pre-cultured at 5 mM, 11 mM and 30 mM glucose for 72 hr and assayed using Zeiss Axiozoom.V16 zoom microscope. Notably, basal $[Ca^{2+}]_i$ dynamics at the start of the recording were increased in the hyperglycaemic (30 mM; $n = 146$) group while adrenaline responses were blunted ($p < 0.001$ vs. 11 mM group) when compared to the normoglycaemic group (11 mM; $n = 102$); the opposite was true for the hypoglycaemic group (5 mM; $n = 65$) group ($p < 0.001$ vs. 11mM group) (Figure 3.8 b, c).

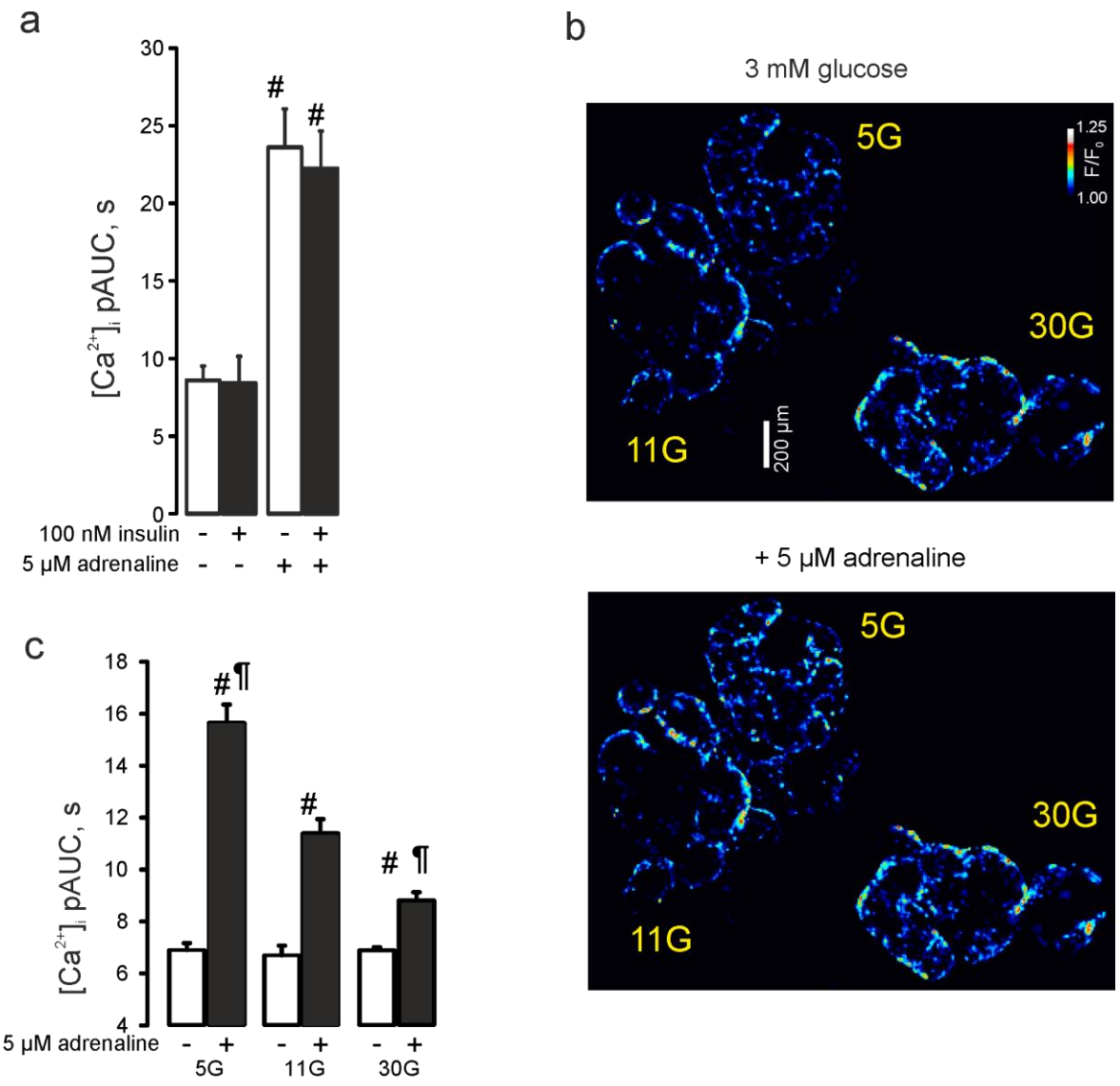


Figure 3.8 - Effects of insulin and hypo/hyperglycaemic culture on the adrenaline-induced $[Ca^{2+}]_i$ increase

(a) $[Ca^{2+}]_i$ in α-cells quantified as pAUC upon adrenaline (5 µM) stimulation alone or in the presence of insulin (100 nM), measured with Fluo-4. **(b)** Standard deviation of gCAMP6f intensity for different islet groups at basal glucose (Top panel) and with application of adrenaline (Bottom panel). **(c)** $[Ca^{2+}]_i$ in α-cells quantified as pAUC at varying glucose concentrations (5 mM, 11 mM and 30 mM), with basal glucose (open columns) and effect of adrenaline (black columns), measured with gCAMP6f. # Denotes significant ($p < 0.05$) vs. basal; * Denotes significant ($p < 0.05$) different vs. control. Error bars represent ± SEM.

3.3.8. Adrenaline effect in pancreatic β- and δ-cells within intact mouse islets

The effects of adrenaline on other islet cell types was briefly explored in a qualitative manner. SST-RFP mice were used which expressed the Ca^{2+}-sensor gCAMP3 throughout the whole body. δ-Cells were identified as any cell expressing RFP, while any cell without an RFP signal, which was silent at low (3 mM) and active at high glucose (20 mM) was regarded as a β-cell. Interestingly, adrenaline initiated rapid and almost synchronous silencing of β-cells at high (20 mM) glucose (n =173; Figure 3.9 a, c), active δ-cells (79% - 11/14) were also silenced (Figure 3.9 b). At low glucose, β-cells were inactive meaning any inhibitory effect of adrenaline was unapparent. While most δ-cells displayed minimal activity at low glucose (3 mM)[11], a remaining subset were active at low glucose with regular $[Ca^{2+}]_i$ oscillations (8/44 - 18%). $[Ca^{2+}]_i$ oscillations in these cells abruptly stopped after application of adrenaline (Figure 3.9 d).

[11] 24/44 (57%) showed low activity with sporadic $[Ca^{2+}]_i$ oscillations, 11/44 (25%) showed no activity

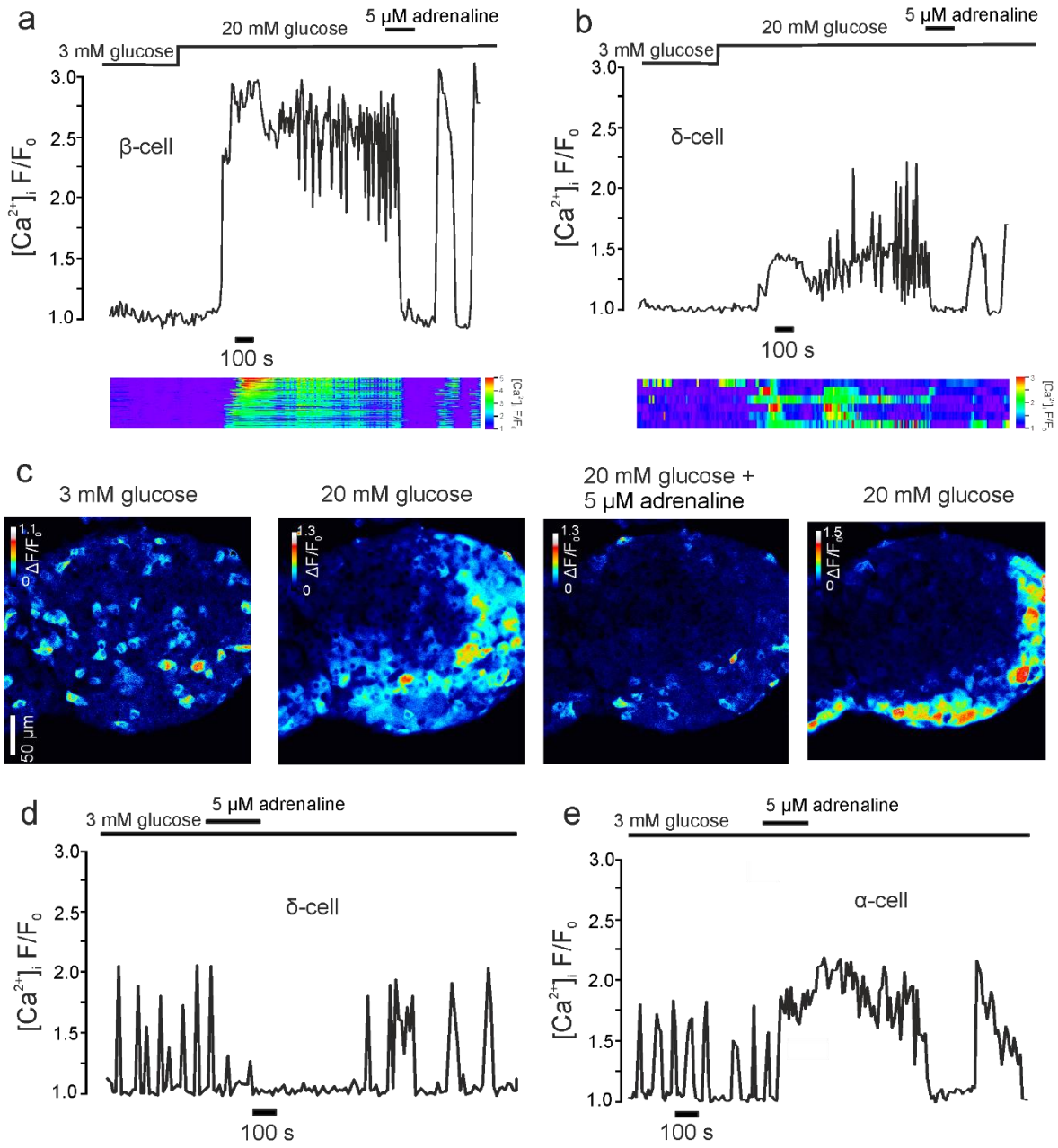


Figure 3.9 - Effect of adrenaline on β-cells and δ-cells

(a) Representative recording of effect of adrenaline (5 µM) on β-cells at high glucose and heatmap showing effect across β-cell population, each line represents a single β-cell. **(b)** Representative recording of effect of adrenaline (5 µM) on δ-cells at high glucose and heatmap showing effect across δ-cell population, each line represents a single δ-cell. **(c)** Images depicting standard deviation of gCAMP3 intensity at 3 mM glucose, 20 mM glucose, 20 mM glucose + 5 µM adrenaline and returning to 20 mM. **(d)** Representative recording of adrenaline (5 µM) on $[Ca^{2+}]_i$ dynamics in δ-cell active at low glucose. **(e)** Representative recording of adrenaline (5 µM) on $[Ca^{2+}]_i$ dynamics in α-cell active at low glucose. All measured with gCAMP3.

3.4. Discussion

3.4.1. Adrenaline increases $[Ca^{2+}]_i$ and glucagon secretion in pancreatic α-cells

These data cement a role for intracellular Ca^{2+} stores in the manifestation of adrenaline-induced glucagon secretion, resulting from a β-adrenergic mechanism that targets both PKA-dependent and Epac2-dependent pathways. The effect was conserved in human islets and mimicked by the neurotransmitter noradrenaline.

3.4.2. Adrenaline acts via the β-adrenergic pathway

The involvement of β-adrenergic receptors in adrenaline-induced glucagon secretion is widely accepted. Here, it has been further established with β-adrenergic stimulation mimicking and inhibition abolishing adrenaline's actions, both in terms of $[Ca^{2+}]_i$ and glucagon secretion. Interestingly, there was no indication of a role for α_1-adrenergic receptors, which have previously been linked to initiation of the adrenaline response facilitating proper execution of the β-adrenergic mechanism (Vieira et al., 2004). Notably, α_1 involvement was previously observed in single cells only and not in intact islets; with experiments in the perfused rat pancreas reproducing my results showing no inhibitory effect of prazosin on adrenaline-induced glucagon secretion (Filipponi et al., 1986). Islet dissociation is known to influence $[Ca^{2+}]_i$ dynamics in the α-cell (e.g. 93% of α-cells are silent at low glucose when dissociated (Liu et al., 2004)) and could also result in changes in gene expression, which may influence adrenergic receptor populations at the cell membrane thus accounting for the differential effects observed between islets and cells.

3.4.3. Noradrenaline likely dictates the sympathetic response to hypoglycaemia

The comparable effects of noradrenaline and adrenaline on $[Ca^{2+}]_i$ give an insight into the origin of sympathetically-mediated glucagon secretion. Adrenaline did produce a significantly larger increase in $[Ca^{2+}]_i$. This is likely as a result of its greater affinity at the β_2-adrenergic receptor (IUPHAR/BPS, 2015, IUPHAR/BPS, 2016), expressed alongside the β_1-adrenergic receptor in α-cells (De Marinis et al., 2010). Notably, plasma levels of adrenaline range between 10-100 nM (Laurent et al., 1998, Stich et al., 1999), i.e. the concentrations that have been shown to inhibit rather than stimulate glucagon secretion (De Marinis et al., 2010). The stimulatory micromolar levels of the agonist used are likely to occur only at nerve terminals (Ludwig et al., 1990), indicating that noradrenaline, not adrenaline, released from intraislet nerve endings is likely to direct the sympathetic glucagon response. This may explain why glucagon responses are impaired even when sympathoadrenal responses are normal in diabetic patients (Cryer, 2002).

It is worth noting however that mice who have undergone adrenalectomy (removal of the adrenal gland) do have a reduced glucagon response to hypoglycaemia, with chemical removal of sympathetic nerves terminals also attenuating the response[12]; suggesting both adrenaline, released from the adrenal medulla, and noradrenaline, released by the sympathetic nerve endings, are important in the glucagon response to hypoglycaemia (Karlsson and Ahren, 1991). It could be the case that plasma adrenaline does not directly control the α-cell but instead acts indirectly by controlling islet sympathetic input. Notably, in a study looking at exercise-induced adrenaline and noradrenaline release, adrenaline was found to act via presynaptic β_2-adrenergic receptors to increase

[12] Notably, the suppression of insulin was only lost in adrenalectomised mice.

noradrenaline release from sympathetic nerve endings (Scheurink et al., 1989). A similar permissive role of adrenaline may be at play during hypoglycaemia.

3.4.4. The adrenaline effect on $[Ca^{2+}]_i$ in α-cells is conserved in human islets

Adrenaline's stimulatory effect on α-cell $[Ca^{2+}]_i$ in human islets is contradictory to previous observations, which showed little evidence of adrenaline stimulating glucagon secretion. The reason for the absence of an effect in past experiments performed on humans may be to do with the methods involved. Firstly, in *in vivo* studies, patients were injected with adrenergic blockers along with insulin to lower blood glucose (Hilsted et al., 1991, Towler et al., 1993). This raises the possibility of off-target effects reducing the ability of the drugs to specifically inhibit α-cell adrenergic receptors. Secondly, the lack of effect on glucagon secretion from isolated human islets (Walker et al., 2011) may be explained by adrenaline inducing only a transient increase in glucagon, which is not detected during the 1 hour long incubation. Alternatively, the effects on $[Ca^{2+}]_i$ may not be reflected in terms of glucagon secretion due to the possibility of other islet cell types being activated by adrenaline and inhibiting the α-cell, overriding any stimulatory effect. Human β-cells, for instance, possess both stimulatory β-adrenergic receptors along with inhibitory α_2-adrenergic receptors (Lacey et al., 1993), compared to mouse β-cells which only possess the latter (Nakaki et al., 1980, Schuit and Pipeleers, 1986, Langer, 1987). Indeed, transient adrenaline-induced insulin secretion has been shown to occur in human islets (Lacey et al., 1993) (with resultant suppression of adrenaline-induced glucagon secretion possible). Nevertheless, activation of non α-cells by adrenaline at low glucose was not evident in my experiments with human islets. Further study will be required to fully

elucidate adrenergic signalling in the human islet but this finding suggests the human α-cell is targeted under hypoglycaemic conditions.

3.4.5. PKA and Epac2 are crucial in increasing $[Ca^{2+}]_i$ upon adrenaline stimulation

The data presented here indicate that a maximal adrenaline response relies on activation of PKA- and Epac2-dependent pathways with both PKI and ESI-05 significantly reducing the α-cell adrenaline response, both in terms of $[Ca^{2+}]_i$ and glucagon secretion. Notably, ESI-05 had greater effects on glucagon secretion despite more modest effects on $[Ca^{2+}]_i$. It can be inferred from this that PKA and Epac2 both shape the Ca^{2+} response with the latter also regulating the late stage of exocytosis, reinforced by the capacitance data (Figure A2.3). This is not dissimilar to the findings of De Marinis et al (2010), who highlighted Epac2 involvement in adrenaline-induced glucagon secretion through experiments conducted on Epac2-deficient mice. Notably, in islets from these mice a PKA-sensitive component of adrenaline-induced glucagon secretion persisted, with accompanying experiments in NMRI wildtype mice showing PKA-inhibition (with 8-Br-Rp-cAMPS) reducing but by no means abolishing the adrenaline effect, presumably due to an Epac2-sensitive component (De Marinis et al., 2010).

The forskolin dose-dependence data reinforce the requirement of Epac2 for proper execution of the adrenaline response, with a clear disparity between PKA activity and $[Ca^{2+}]_i$. It is clear from the data with PKI-treated islets that PKA is integral in mobilising Ca^{2+}, yet the observation that PKA activation is unable to generate any $[Ca^{2+}]_i$ response until cAMP concentrations synonymous with Epac2 are reached, raises the possibility of crosstalk between PKA- and Epac2-dependent pathways as opposed to them operating in

total isolation (e.g. Epac2 may act downstream from PKA). It must be noted, however, that the role of different PKA isoforms, PKA-RI and PKA-RII[13], may be shrouded by the non-specificity of the PKA sensor. PKA-RI and PKA-RII have different affinities for cAMP (Cummings et al., 1996). De Marinis et al. (2010) speculated that the PKA-sensitive component in Epac2-deficient mice was due to activation of the lower affinity PKA-RII while the inhibitory effect of GLP-1 was mediated via the high-affinity PKA-RI. Therefore, the disparity between PKA activity and Ca^{2+} mobilisation may not exclusively be due to Epac2 activation but, in part, be the result of late activation of PKA-RII.

3.4.6. The adrenaline effect results from (endo)lysosomal-ER Ca^{2+} release

The absence of an adrenaline-induced $[Ca^{2+}]_i$ increase in bafilomycin-treated islets demonstrates the central role the acidic Ca^{2+} stores play. It is proposed that Ca^{2+} release from these stores acts as a trigger for CICR from the larger ER, with little involvement of extracellular Ca^{2+} influx. This is supported by ryanodine having no additive inhibitory effects on glucagon secretion in *Tpcn2*$^{-/-}$ mice (Figure A2.2 e), demonstrating the hierarchal nature of adrenergic Ca^{2+} signalling, coupled with the adrenaline response persisting in the presence of EGTA/diazoxide, showing the effect is still present in the absence of extracellular Ca^{2+}, and the minimal effect of adrenaline on membrane potential, reflecting the negligible role of membrane channels in the α-cell response to adrenaline (Figure A2.1). The results in *Tpcn1*$^{-/-}$ and *Tpcn2*$^{-/-}$ mice show Ca^{2+} efflux from the acidic stores is via TPC2, the prominent isoform on late stage endosomes and lysosomes (Calcraft et al., 2009). This echoes Capel et al. (2015) findings in cardiomyocytes, where it was found that TPC2 is the target of β-adrenergic signalling, with Ca^{2+} release from TPC2

[13] This specifically refers to the two isoforms of the PKA regulatory subunit.

contributing to increased ER Ca^{2+} loading (via the SERCA-ATPase) as well as induction of CICR (via RyRs). The latter appears to be the likely outcome in α-cells with ryanodine blocking adrenaline-induced glucagon secretion, and significantly reducing the associated $[Ca^{2+}]_i$ increase in Fluo-4FF loaded islets (Figure 3.6 b, c).

The targeting of the acidic Ca^{2+} stores by β-adrenergic signalling is believed to be primarily accomplished via activation of ADP-ribosyl cyclases, which include CD38 and CD157. These enzymes convert NAD^+ into cADPR, an ER Ca^{2+}-mobilizing messenger; however, more pertinent to this study CD38 can also convert NADP to NAADP, the secondary messenger strongly linked to mediating acidic store Ca^{2+} release (Ferrero et al., 2014). High levels of cAMP are thought to underpin CD38 activity, specifically in relation to NAADP production (cADPR production is linked to cGMP) (Wilson and Galione, 1998), with Rah et al. (2010) demonstrating CD38 NAADP production relies on cAMP, PKA and notably Epac2 and its primary downstream target the GTPase Rap1. A recent study in *CD38*$^{-/-}$ mice underlined β-adrenergic targeting of CD38 in cardiomyocytes, revealing the enzyme's activity played a significant role in increasing $[Ca^{2+}]_i$ in response to isoprenaline (Lin et al., 2017).The contribution of CD38 and NAADP in sensitising TPC2 is also revealed in this study with islets from CD38KO$^{-/-}$ mice and Ned-19-treated islets both showing attenuated adrenaline responses. However, effects on $[Ca^{2+}]_i$, although significant, were modest, suggesting β-adrenergic signalling may also target the acidic stores via an NAADP-independent pathway. Notably, PKA can directly phosphorylate TPC2 at the s66 residue, increasing the open probability of the channel (Lee et al., 2016a).

3.4.7. L-type Ca^{2+} channels play a permissive role in adrenaline-induced glucagon secretion

The strong inhibitory effect of isradipine, both in terms of the adrenaline-induced $[Ca^{2+}]_i$ increase and glucagon secretion, is enigmatic given the lack of effect of adrenaline on electrical activity. There are a number of explanations for this apparent paradox. Firstly, there is evidence of shared pharmacology between L-type Ca^{2+} channels and TPCs; indeed, acidic stores can be targeted using high concentrations of L-type Ca^{2+} channel blockers (Genazzani et al., 1997). Therefore, the inhibitory effect seen here may result from blocking of TPC2 rather than L-type Ca^{2+} channels. Alternatively, isradipine's potency may reflect a depletion of the intracellular Ca^{2+} stores. Application of isradipine significantly reduced basal Ca^{2+}, unsurprising when one considers that L-type Ca^{2+} channels account for 70% of the inward Ca^{2+} current under hypoglycaemic conditions (Gromada et al., 1997). This may have rendered cytosolic Ca^{2+} insufficient to supply the ER (via the SERCA-ATPase) and/or the (endo)lysosome (via Ca^{2+}/H^+ exchange). Equally, a sufficiently high basal Ca^{2+} may be required for Ca^{2+}-dependent adenylyl cyclases to function, with ADCY3 and ADCY5 both expressed in α-cells (Adriaenssens et al., 2016, DiGruccio et al., 2016).

Previously, a transient $[Ca^{2+}]_i$ response has persisted in the presence of L-type blockade (Liu et al., 2004, De Marinis et al., 2010), this was seen in my experiments, albeit in a minority of cells (12% of cells), and was frequently observed with diazoxide and EGTA. This transient peak represents intracellular Ca^{2+} release, with the lack of a sustained effect previously put down to abolition of a late effect of adrenaline caused by L-type Ca^{2+} influx (Liu et al., 2004). Due to the minimal effects on membrane potential, it seems any effect of

adrenaline on L-type Ca^{2+} channels is negligible; the lack of a late effect may be better described by Ca^{2+} influx opposing the actions of the Na^{+}/Ca^{2+} antiporter (NCX) at the plasma membrane, which removes 1 Ca^{2+} ion from the cytosol in exchange for 3 Na^{+} ions, particularly when $[Ca^{2+}]_i$ is high (Carafoli et al., 2001). In the presence of diazoxide/EGTA, NCX would remove the store-released Ca^{2+} quickly and efficiently yet in control conditions with the additive extracellular Ca^{2+} influx this would take longer leading to the more sustained response seen in control conditions (Figure 3.10). The rarity of this effect in my experiments on isradipine-treated islets is likely due to the secondary effects described above (TPC2 inhibition, store depletion or compromised adenylyl cyclase function[14]), which may come to fruition with the relatively long application time (approx. 10 min).

The likely cause of the small depolarization observed in the patch clamp data is the secondary effect of store-operated Ca^{2+} release on channels at the plasma membrane. Indeed, in α-cells ER Ca^{2+} release can trigger opening of store-operated channels (SOCs) at the plasma membrane (Liu et al., 2004) and, in β-cells, Ca^{2+} release via TPC2 has been linked to increased membrane excitability via opening TRPM channels (Arredouani et al., 2015). This depolarization could feasibly then activate voltage-gated channels (e.g. L-type Ca^{2+} channels), but, even if this was the case, it appears unlikely that this would account significantly for the large increase in $[Ca^{2+}]_i$ as greater changes in membrane potential would be expected.

[14] TPC2 inhibition perhaps the most likely as EGTA and diazoxide greatly reduced basal $[Ca^{2+}]_i$ dynamics, so could feasibly also cause store depletion and compromise adenylyl cyclase function.

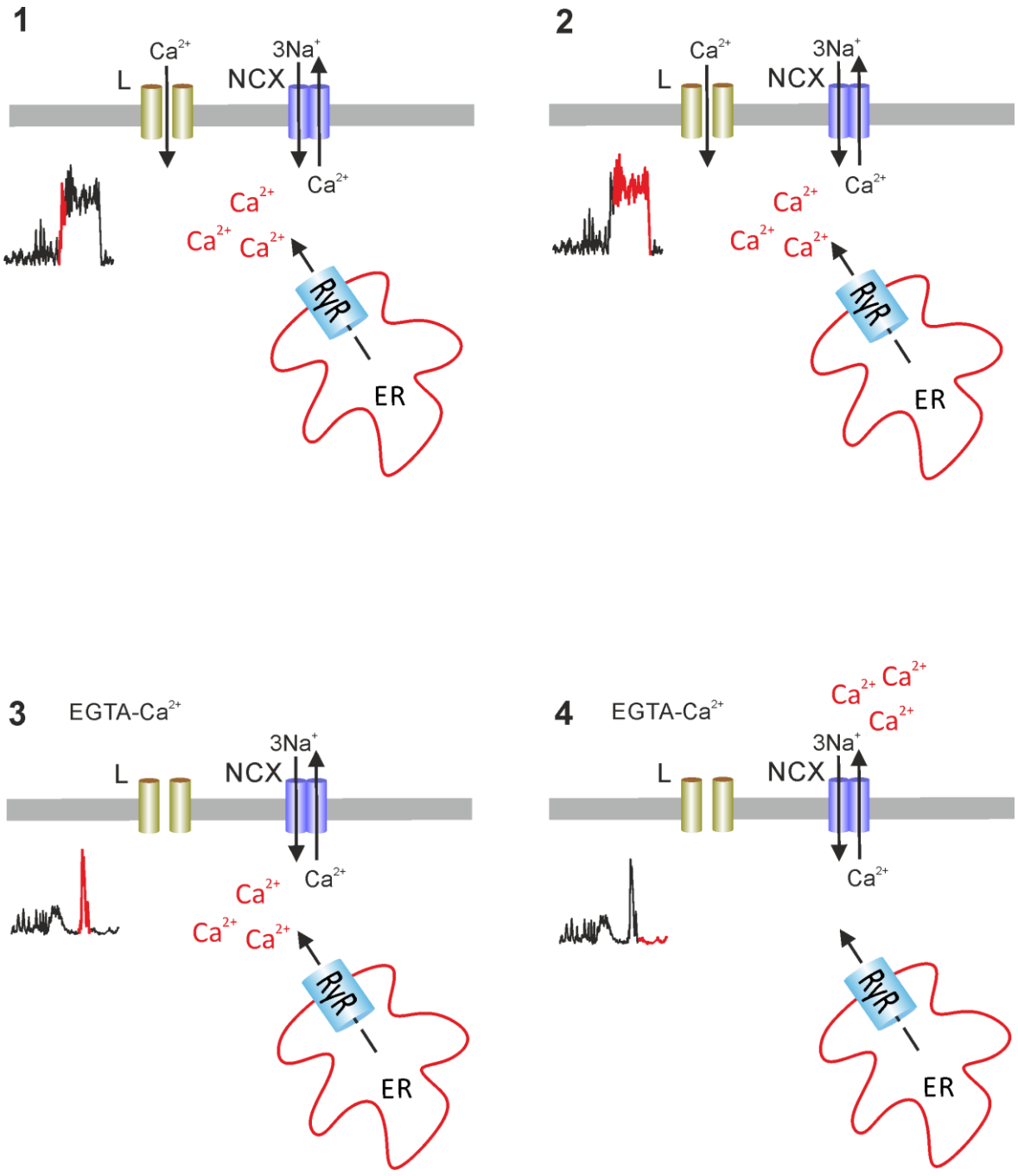


Figure 3.10 - Proposed model for role of extracellular Ca^{2+}

Control (top) – Adrenaline triggers CICR from the ER (1), the NCX removes Ca^{2+} ions but the influx of extracellular Ca^{2+}, primarily through the L-type Ca^{2+} channel, maintains $[Ca^{2+}]_i$ at a high level, resulting in a sustained response (2).
EGTA (bottom) – Adrenaline-induced CICR again results in a rapid increase in $[Ca^{2+}]_i$ (3), however, it is removed by the NCX and with no counteractive effect from Ca^{2+} influx, $[Ca^{2+}]_i$ is brought back to basal quickly, resulting in a transient effect (4). Diazoxide results in the same effect by hyperpolarizing membrane potential meaning voltage-gated Ca^{2+} channels are closed.

3.4.8. α-cell 'adrenaline resistance' in impaired glucose counterregulation

The finding that hyperglycaemic conditions reduce the α-cell's ability to mount a full adrenaline response could be key in understanding the development of impaired glucose counterregulation. Much of the reasoning behind the condition has centred on blunted countterregulatory responses due to the damaging effects of both hyper- and hypoglycaemia on the CNS and PNS (Taborsky and Mundinger, 2012). The apparent decreased sensitivity to adrenaline observed in islets exposed to hyperglycaemia suggests part of the impairment lies in the α-cell itself. This is supported by clinical studies on catecholamine sensitivity in type 1 diabetic and control subjects, in relation to hypoglycaemia unawareness. It was found that in control subjects, β-adrenergic sensitivity was increased following hypoglycaemia, while the opposite was true for type 1 diabetic subjects (Fritsche et al., 1998, Korytkowski et al., 1998). This supports my data, with a larger adrenaline response in islets cultured under hypoglycaemic conditions, similar to the control subjects, and attenuated in those exposed to hyperglycaemic conditions, similar to the type 1 diabetic subjects. The cause of these effects, however, is unknown. Hyperglycaemia may downregulate the expression of β-adrenergic receptors or components of the downstream intracellular machinery; it may also disrupt Ca^{2+} homeostasis in the α-cell by reducing the effectiveness of store-operated Ca^{2+}-release and function of calcium-dependent adenylyl cyclases. Indeed, $[Ca^{2+}]_i$ activity was increased at basal glucose, mirroring the fasting hyperglucagonaemia observed in some diabetic individuals (Baron et al., 1987), with the opposite being true for islets exposed to hypoglycaemia. High glucose also stimulates β- and δ-cells, leading to chronically high levels of insulin and somatostatin respectively. Crucially, these hormones can inhibit glucagon secretion by lowering cAMP (Elliott et al., 2015) potentially opposing the

actions of adrenaline. This inhibition would likely be removed once the islets were returned to basal glucose; however, the high glucose culture may have long-term effects on β- and δ-cells' activity. Indeed, plasma somatostatin levels have been shown to be increased in diabetes (Shi et al., 1996, Inouye et al., 2002), along with increases in content (Rastogi et al., 1990) and δ-cell number (Orci et al., 1976). Furthermore, in type 2 diabetic islets there is a 150% increase in basal somatostatin release (Vergari et al., In Press), which could counteract the ability of adrenaline to increase cAMP. Note, that basal insulin is unchanged in type 2 diabetic islets (Ashcroft and Rorsman, 2012). More work is required to underpin the exact mechanism which drives 'adrenaline-resistance' in the α-cell but these early findings present an intriguing avenue in fully understanding impaired glucose counterregulation.

3.4.9. Adrenaline inhibits $[Ca^{2+}]_i$ oscillations in β- and δ-cells

The findings in β- and δ-cells are unsurprising; it is firmly established that adrenaline inhibits insulin secretion via α_2-adrenergic receptors (Nakaki et al., 1980, Schuit and Pipeleers, 1986, Langer, 1987) with noradrenaline also reported to reduce somatostatin secretion (Hauge-Evans et al., 2010). Inhibitory α_2-adrenergic effects could either be mediated via a reduction in cAMP via inhibition of adenylyl cyclase or alternatively via activation of outward K^+ currents (Surprenant et al., 1992). The latter occurs due to $G_{\beta\gamma}$ signalling (rather than G_α signalling) opening GIRK channels at the plasma membrane, causing K^+ efflux (Luscher and Slesinger, 2010), which repolarises the cell membrane thereby inhibiting $[Ca^{2+}]_i$ influx and secretion. Due to the abrupt silencing nature of the effect in both cell types, a GIRK-channel mediated mechanism appears more likely and has notably been shown before in β-cells (Rorsman et al., 1991, Iwanir and Reuveny,

2008). Whether this inhibition contributes to adrenaline-induced glucagon secretion by removing the tonic inhibition of neighbouring β- and δ-cells appears unlikely; all β-cells and most δ-cells were inactive at low glucose meaning any paracrine inhibition of the α-cell at 3 mM glucose would be minimal. This is supported by noradrenaline's inhibition of δ-cells not influencing glucagon secretion at basal glucose alone (Hauge-Evans et al., 2010). However, under *in vivo* conditions when other metabolites would be present the effects of adrenaline on the other cell types may play a greater role in glucose counterregulation.

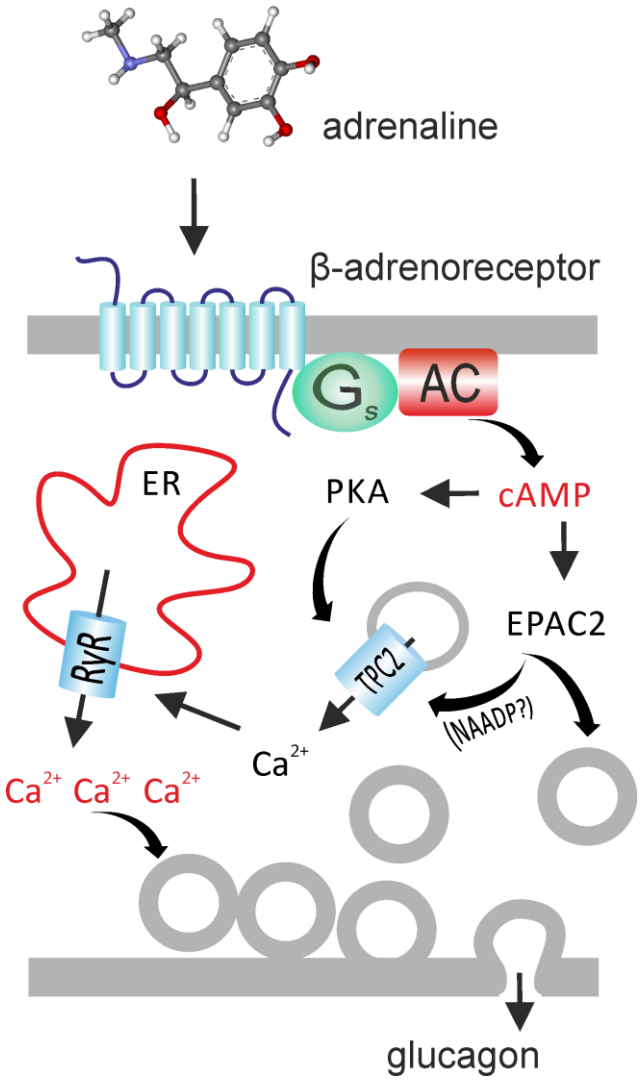


Figure 3.11 - Model

It is proposed that adrenaline binds to the β-adrenergic receptor, this leads to dissociation of the attached G_s subunit into $G_{\alpha s}$ and $G_{\beta\gamma s}$. The $G_{\alpha s}$ subunit activates adenylyl cyclase leading to rapid conversion of ATP into cAMP. The high levels of cAMP produced activate both PKA and Epac2, which act synergistically to increase $[Ca^{2+}]_i$ via initial triggering of (endo)lysosomal Ca^{2+} release. This occurs partly as a result of PKA/Epac2 activation of CD38, the principal enzyme responsible for NAADP production but an NAADP-independent mechanism may also exist (e.g. PKA phosphorylating TPC2 directly). Ca^{2+} is released from the lysosome into the cytosol via the NAADP-sensitive TPC2, where it can initiate CICR from the ER via sensitisation of RyRs. This could also occur indirectly via the (endo)lysosomal-released Ca^{2+} targeting CaMKII, which then sensitises RyRs (Capel et al., 2015). The role of extracellular Ca^{2+} entry appears to be permissive in that it provides Ca^{2+} for the cell but is not directly targeted by β-adrenergic signalling.

3.5. Conclusion

In this study, a prominent role for intracellular Ca^{2+} in adrenaline-induced glucagon secretion has been demonstrated; revealing a novel mechanism which highlights a crucial role for (endo)lysosomal Ca^{2+} stores in triggering CICR from the ER. This reconciles the large increases in $[Ca^{2+}]_i$ associated with the adrenaline effect with the relatively weak effects of the hormone on membrane potential.

It appears increasingly likely that adrenergic signalling is directed from the sympathetic nerves that innervate the islet rather than the adrenal medulla. This suggests impairment of the α-cell in diabetes likely results from aberrations such as islet denervation (Mei et al., 2002) rather than decreased adrenaline secretion from the adrenal medulla. Therefore, novel therapies against impaired glucose counterregulation should focus on specific amplifiers of glucagon secretion (e.g. activators of TPC2) that bypass sympathetic innervation.

Chapter 4: Cholinergic Signalling in the Pancreatic α-Cell

4.1. Introduction

The autonomic response to hypoglycaemia also encompasses the parasympathetic nervous system, whose activation precedes that of the sympathetic and sympathoadrenal responses, occurring during mild hypoglycaemia (4.2 – 4.7 mM). The effect is directed via parasympathetic nerve endings that innervate the islet. These secrete acetylcholine (ACh), which, like adrenaline, has been shown to stimulate glucagon secretion in animal models (Iversen, 1973, Kimura et al., 1982, Patel, 1984, Berts et al., 1997). Prior hypoglycaemia and subsequent HAAF also results in deterioration of the parasympathetic response, meaning islet cholinergic input is blunted in type 1 and advanced type 2 diabetes (Heller and Cryer, 1991, Davis et al., 1996, Taborsky and Mundinger, 2012).

The parasympathetic response to hypoglycaemia originates from neurones expressing Glut2 in the brainstem and hypothalamus that signal to the DMNV stimulating the vagus nerve in response to hypoglycaemia (Lamy et al., 2014, Verberne et al., 2014). With the pancreas receiving parasympathetic cholinergic fibres that originate in the DMNV, ACh is subsequently released from islet parasympathetic nerve terminals. As opposed to adrenaline and noradrenaline, which only feature once hypoglycaemia is pronounced, parasympathetic activity is believed to be sensitive to small, physiological changes in glucose (Lamy et al., 2014).

ACh binds to two types of receptors, the metabotropic, G-protein coupled muscarinic ACh receptors (mAChRs) and the ionotropic nicotinic ACh receptors (nAChRs). The mAChRs

are further separated into 5 different subtypes (Table 4.1), while the nAChRs are oligomers composed of 5 subunits, which vary in composition (Table 4.2).

Receptor type	M1	M2	M3	M4	M5
G Protein	G_q	G_i	G_q	G_i	G_q
Second Messenger system	Phospholipase C/IP_3 + DAG	Inhibition of adenylyl cyclase	Phospholipase C/IP_3 + DAG	Inhibition of adenylyl cyclase	Phospholipase C/IP_3 + DAG

Table 4.1 - Mammalian muscarinic acetylcholine receptors

mAChRs are GPCRs formed of 7 transmembrane domains. They are abundantly expressed in the CNS but also found in peripheral tissues where they mediate the response to ACh secreted from postganglionic fibers of the parasympathetic nervous system. They are coupled to either stimulatory G_q or inhibitory G_i proteins (Wess et al., 2007).

Type	Neuronal		Muscle
Subtype	Homomeric	Heteromeric	Heteromeric
Ligand binding subunits	α7 α9	α2 α3 α4 α6 β2 β4	α1 δ ε γ
Structural subunits	N/A	α5 β3	β1
Receptor examples	$(\alpha7)_5$ $(\alpha9)_5$	$(\alpha3)_2(\beta4)_3$ $(\alpha3)_3(\beta4)_2$ $(\alpha4)_2(\beta2)_3$ $\alpha4\alpha6(\beta2)_2\beta3$	$(\alpha1)_2\beta1\delta\gamma$ (Embryonic) $(\alpha1)_2\beta1\delta\varepsilon$ (Adult)

Table 4.2 - Mammalian nicotinic acetylcholine receptors

The nAChRs are ionotropic receptors, which open in response to ACh. They are non-selective cation channels, permeable to Na^+, K^+ and Ca^{2+} (Colquhoun et al., 2003), and can be divided into neuronal-type, expressed primarily in the CNS and PNS, and muscle-type, expressed at the neuromuscular junction (NMJ). They are pentamers, formed either of identical subunits (homomeric) or different subunits (heteromeric) (Papke, 2014). The composition of subunits confers certain characteristics, with differences in Ca2+ permeability, desensitisation and agonist sensitivity (Colquhoun et al., 2003). The ligand-binding subunits form dimers, which are binding sites for agonists; single structural subunits can sometimes complete the pentamer (Papke, 2014). These can elicit changes in the receptor's behaviour (e.g. α5 incorporation increases Ca^{2+} permeability (Gerzanich et al., 1998)). While heteromeric muscle-type forms only 2 types of receptor, the neuronal heteromeric are diverse due to multiple binding dimers being able to be formed between α2-α6 and β2-β4 subunits, with added diversity from incorporation of structural subunits (Millar and Gotti, 2009). Note that homomeric subunits have been found to form heteromeric receptors too, with α7 forming with β2 subunits (Thomsen et al., 2015) and α9 with the α10 subunit (not shown) (Boffi et al., 2017). Adapted from (Papke, 2014).

In animal models, cholinergic stimulation has been shown to induce glucagon secretion, with several studies indicating this is primarily via the muscarinic pathway (Iversen, 1973, Kimura et al., 1982, Patel, 1984, Berts et al., 1997). Studies using antagonists that favour specific muscarinic subtypes have demonstrated that the effect is primarily directed via the G_q-coupled M3 subtype (Verspohl et al., 1990, Karlsson and Ahren, 1993). This was confirmed in M3 receptor knockout mice where the glucagon response to the muscarinic agonist oxotremorine M was 'virtually abolished' (Duttaroy et al., 2004). Despite its role in glucose counterregulation, the parasympathetic nervous system is generally associated with 'rest and digest' processes. This is reflected by ACh also stimulating insulin secretion (Malaisse et al., 1967, Iversen, 1973, Kimura et al., 1982), again via the M3 mAChR (Verspohl et al., 1990, Karlsson and Ahren, 1993, Duttaroy et al., 2004), with important roles in maintaining glucose homeostasis and proper insulin secretion (Gautam et al., 2006).

In humans, the picture is less clear. *In vivo* studies consistently show that hypoglycaemia induces islet parasympathetic activity (reflected by an increase in pancreatic polypeptide secretion, whose secretion is under tight cholinergic control (Schwartz et al., 1978)) with proper transmission of autonomic signals being integral to the glucagon response (Schwartz et al., 1978, Havel and Ahren, 1997). Yet blockade of mAChRs has often been shown to have little effect on glucagon secretion (Hilsted et al., 1991, Towler et al., 1993). Therefore, (as with adrenaline) it has been suggested that neuropeptides co-secreted with ACh may play a more prominent role in human glucose counterregulation (Taborsky and Mundinger, 2012). Recent studies on isolated human islets, paint a different picture, finding parasympathetic innervation to be less prevalent in human islets, with α-cells actually secreting ACh at low glucose, stimulating β-cells and thus priming them for a rise

in blood glucose by ‘sensitising them to subsequent stimuli’ (Rodriguez-Diaz et al., 2011). A follow-up paper further showed ACh to have no significant effect on glucagon secretion *in vitro* (Molina et al., 2014). Nevertheless, there is some evidence for a direct role of ACh. The glucagon response to hypoglycaemia induced by 2-Deoxy-D-Glucose (2-DG) was attenuated by atropine in humans (Hedo et al., 1978). Additionally, although unrelated to hypoglycaemia, stimulation of both insulin and glucagon secretion by intravenous L-arginine infusion, was also reduced by atropine, with cholinergic stimulation using prostigmin having the opposite effect, indicating a role for islet cholinergic input in nutrient utilisation (Czyzyk et al., 1981).

While previous studies have highlighted the stimulatory effect of ACh on glucagon secretion, there has been no confirmation of the intracellular mechanism behind this effect. From previous data highlighting the importance of the M3 mAChR, a G_q-mediated mechanism appears likely. With ER-mediated Ca^{2+} increase and PKC activation the likely downstream targets (Figure 4.1). This project aimed to confirm this and any effect in human islets, using confocal $[Ca^{2+}]_i$ imaging and patch clamp electrophysiology.

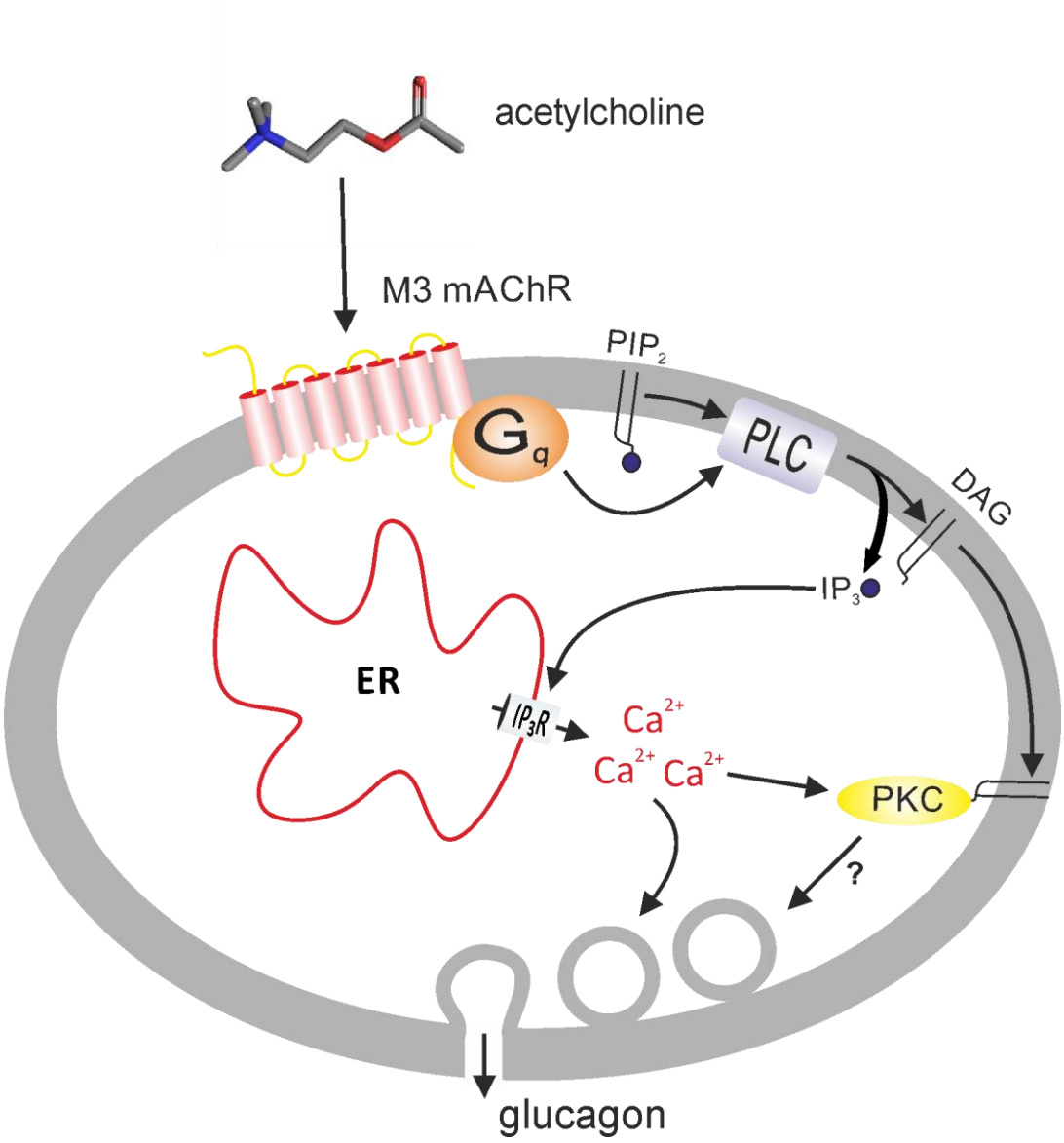


Figure 4.1 - Hypothesis

It is proposed that ACh binds to the M3 mAChR causing dissociation of G_q into $G_{\alpha q}$ and $G_{\beta\gamma q}$ subunits, $G_{\alpha q}$ subsequently signals to phospholipase C (PLC) leading to conversion of the membrane-bound PIP_2 into the secondary messengers DAG and IP_3. The free, cytosolic IP_3 binds to the IP_3 receptor (IP_3R) on the ER, which opens leading to ER-Ca^{2+} release. The increase in $[Ca^{2+}]_i$ stimulates glucagon secretion. Meanwhile, the combined increase in $[DAG]_i$ and $[Ca^{2+}]_i$ activates PKC, which in turn may stimulate glucagon secretion via Ca^{2+}-dependent and/or Ca^{2+}-independent mechanisms.

4.2. Methods

For islet isolation, islet culture, confocal $[Ca^{2+}]_i$ imaging, data analysis, general reagents and solutions

Please refer to main methods section

4.2.1. Mice

C57BL/6J mice were used throughout the study. A minimum of 2 mice were used for each condition, with *n* taken as number of cells. For the experiments looking into the effects of hypo/hyperglycaemic culture on α-cell cholinergic signalling, mice expressing the genetically-encoded Ca^{2+}-indicator gCAMP under the control of the glucagon promoter (Glu-gCAMP3) were used. They were of a C57BL/6J background.

4.2.2. Electrophysiology

Electrophysiological measurements were performed on α-cells within intact islets (from C57BL/6 mice), using an EPC-10 patch-clamp amplifier (HEKA Electronics, Germany) and Pulse software. The holding pipette and electrodes were pulled from borosilicate glass (Harvard apparatus, UK; Product code: 30-0055 – holding pipette; World precision instruments, UK; Product code: 1B150-6 - electrodes) using a HEKA PIP6 temperature controlled pipette puller (HEKA Electronics, Germany), and fire-polished using a heating filament. Islets were then visualised using a Zeiss axioskop 2 FS mot microscope. To measure membrane potential, the perforated patch configuration was chosen. A pipette solution (IC1) containing (mM) 76 K_2SO_4, 10 NaCl, 10 KCl, 1 $MgCl_2$, 5 HEPES (pH 7.35 with KOH), and the EC1 bath solution were used. Amphotericin B (0.16 mg/mL; Sigma, UK) was added to the pipette solution, thereby providing the membrane perforation

necessary to gain electrical access to the cytosol. The holding pipette was moved using a manual micromanipulator (Scientifica, UK) and used to secure the islet in place. The electrode was dipped in IC1 solution excl. amphotericin for ~1s, to ensure perforation did not occur too quickly and prevent against damage to the cell, before being backfilled with IC1 solution incl. amphotericin. An electronic micromanipulator (Scientifica, UK) was used to move the electrode (tip resistance = 4-7 MΩ) towards the islet. Once cell contact had been made, using light and consistent suction a gigaseal was formed. Allowing for sufficient time for membrane perforation (5-10 min), membrane potential was recorded in current-clamp mode, without current injection. α-Cells were identified as those displaying spontaneous electrical activity at low (1 mM) glucose. The EC1 bath solution was perifused at 200 µl/min (using a peristaltic pump) with various stimuli added, temperature of the bath solution was maintained at 34 °C throughout each recording (the optimal temperature for gigaseal formation).

4.2.3. Islet dissociation (For $[DAG]_i$ Imaging)

Intact mouse islets (10-100) were added to 5ml RPMI 1640 medium, GlutaMax supplemented (Life Technologies, UK) - containing 11 mM glucose (Sigma, UK), 10% FCS (Sigma, UK), 100 IU/mL penicillin and 100 µg/mL streptomycin (Life Technologies, UK) in a 15ml falcon tube (Sarstedt, UK). Ensuring islets were at the bottom of the tube, the RPMI medium was removed leaving approx. 100 µl Trypsin (2.5 ml; 37 °C; Life Technologies, UK) was then added and the islets were incubated at 37 °C in a water bath for 75 s. Islets were then spun down at 90 g for 60 s. Trypsin was removed (leaving 100 µl) and 5 ml RPMI added. Ensuring islets were at the bottom, RPMI was removed again leaving approximately 100 µl. Using a p200 pipette islets were dispersed by gently aspirating until islet number had decreased and turbidity had increased (indicating islet

dissociation). The resulting solution was dispensed in three droplets onto coverslips (Thermo Fisher, UK) placed into 60 mm dishes (Sarstedt, UK; Product code: 83.1801.002). The number of coverslips varied depending on the amount of solution. Up to three dishes (each containing 1 coverslip) were added to a larger 150 mm dish (Sarstedt, UK; Product code: 82.1184.500) lined with wetted tissue paper, to maintain humidity, before being transferred an incubator (37 °C; 5% CO_2/95% Air), where they were left for at least 1 h to allow cells to adhere to the coverslip.

4.2.4. $[DAG]_i$ imaging

The dispersed islet cells were transfected with baculovirally delivered Red DAG downward probe (Montana Molecular, USA) and Green cADDis cAMP upward probe (Montana Molecular, USA). 12.5 µl of each probe, dissolved in RPMI (3 mM glucose), was added to 25 µl RPMI (17 mM glucose) with 1 µl of the HDAC inhibitor sodium butyrate (500 mM; Montana molecular, USA) added to improve probe expression. After ensuring cell attachment had occurred, each cell-containing droplet was aspirated and replaced with a droplet containing the probe mixture. Transfection took 24 h - 48 h at 37 °C in a tissue culture incubator. The coverslip with attached cells was then loaded into a 'closed' perifusion chamber (Figure 2.3) before being imaged on Zeiss AxioZoom V16 zoom microscope, using magnifications between 10x and 14x. The EC1 bath solution was perifused at 60 µl/min (using a peristaltic pump) and maintained at 34 °C throughout. The DAG probe was excited at 470 nm with emission collected at 535 nm, while the cAMP probe was excited at 440 nm with emission collected at 485 nm. Images were taken every 30s with an exposure time of 100 ms at several locations throughout the coverslip simultaneously. α- and β-cells were distinguished by their response to 5 µM adrenaline, with adrenaline known to increase cAMP in α-cells via β-adrenergic receptors (De Marinis

et al, 2010) and decrease it in β-cells via α_2 adrenergic receptors (Nakaki et al., 1980, Schuit and Pipeleers, 1986, Langer, 1987), δ-cells are inhibited by noradrenaline so would be unlikely to increase cAMP in response to the hormone (Hauge-Evans et al., 2010).

4.2.5. Reagents

Acetylcholine, atropine, glutamate, CPA, K_2SO_4, KOH and nicotine were purchased from Sigma-Aldrich (UK). Oxotremorine M from Insight Biotechnology Ltd (UK). The nicotinic antagonist tubocurarine, SSTR2 antagonist CYN 154806 and PKC inhibitor BIM were purchased from Tocris Bioscience (UK).

4.3. Results

4.3.1. Effect of acetylcholine on $[Ca^{2+}]_i$ in pancreatic α-cells within intact mouse and human islets

ACh (10μM) was found to stimulate $[Ca^{2+}]_i$ dynamics in mouse α-cells at low glucose ($p < 0.001$ vs. basal; $n = 95$; Figure 4.2 a, b, c, d), with 90% of glutamate-responsive cells responding to the neurotransmitter with a rapid, potent and reversible increase in $[Ca^{2+}]_i$. This was replicated in secretion experiments using carbachol (non-specific cholinergic agonist), which induced a 3.3-fold increase in glucagon secretion (Figure A3.1 a). ACh also stimulated mouse β-cells, inducing a transient increase in $[Ca^{2+}]_i$ in 75% of cells (121/162 cells; Figure 4.2 a, d).

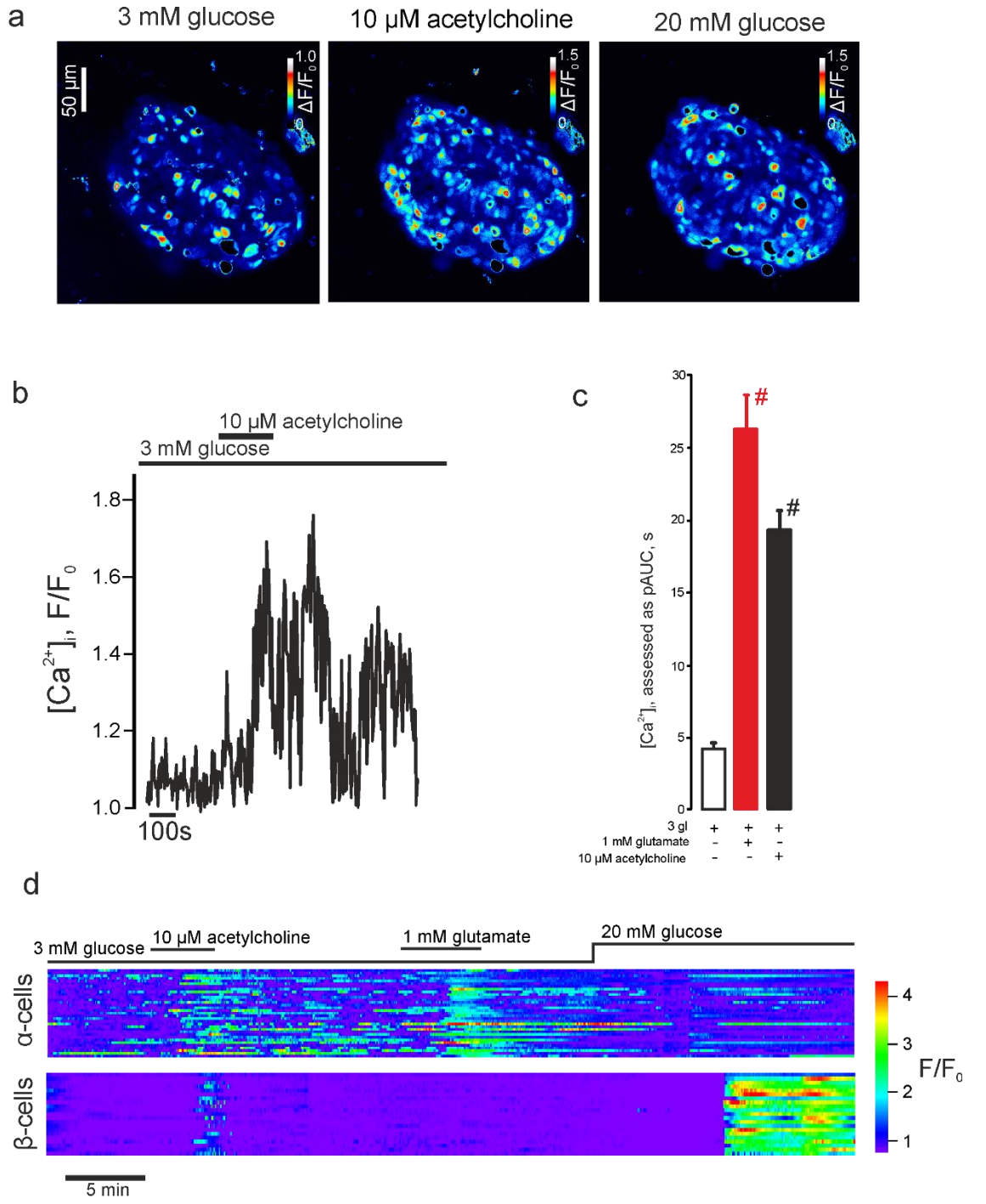


Figure 4.2 - The stimulatory effect of acetylcholine on glucagon secretion is mediated by elevation of $[Ca^{2+}]_i$ in pancreatic α-cells

(a) Standard deviations of the Fluo-4 intensity imaged when the islet was perifused by EC1 solution containing 3 mM glucose alone or with 10 µM ACh (n.b. the activation of both α- and β-cells) or 20 mM glucose, as indicated. **(b)** Representative recording of single α-cell response to application of 10 µM ACh at 3 mM glucose. **(c)** $[Ca^{2+}]_i$ changes in α-cells quantified as pAUC at 3 mM glucose alone (open column) and in the presence of glutamate (red column) or ACh (black column) **(d)** Representative $[Ca^{2+}]_i$ heatmap of α- (*n* = 33; top) and non-α-cell (mostly, β-cells, *n* = 21; bottom) populations, each line

represents a single ROI (cell). Populations differentiated based on response to glutamate. # Denotes significant ($p < 0.05$) vs. basal. Error bars represent ± SEM. Fluo-4 used throughout unless otherwise stated.

In human islets, the effects were more modest. ACh did initiate a significant increase in $[Ca^{2+}]_i$ ($p < 0.001$ vs. basal; $n = 70$, 5 donors; Figure 4.3 a, b) although this was seen in only 54% of α-cells with differential responses to the neurotransmitter across different islets (Figure 4.3 c). Its effect in β-cells was also limited, affecting only 38% (17/45) of cells (Figure 4.3 d).

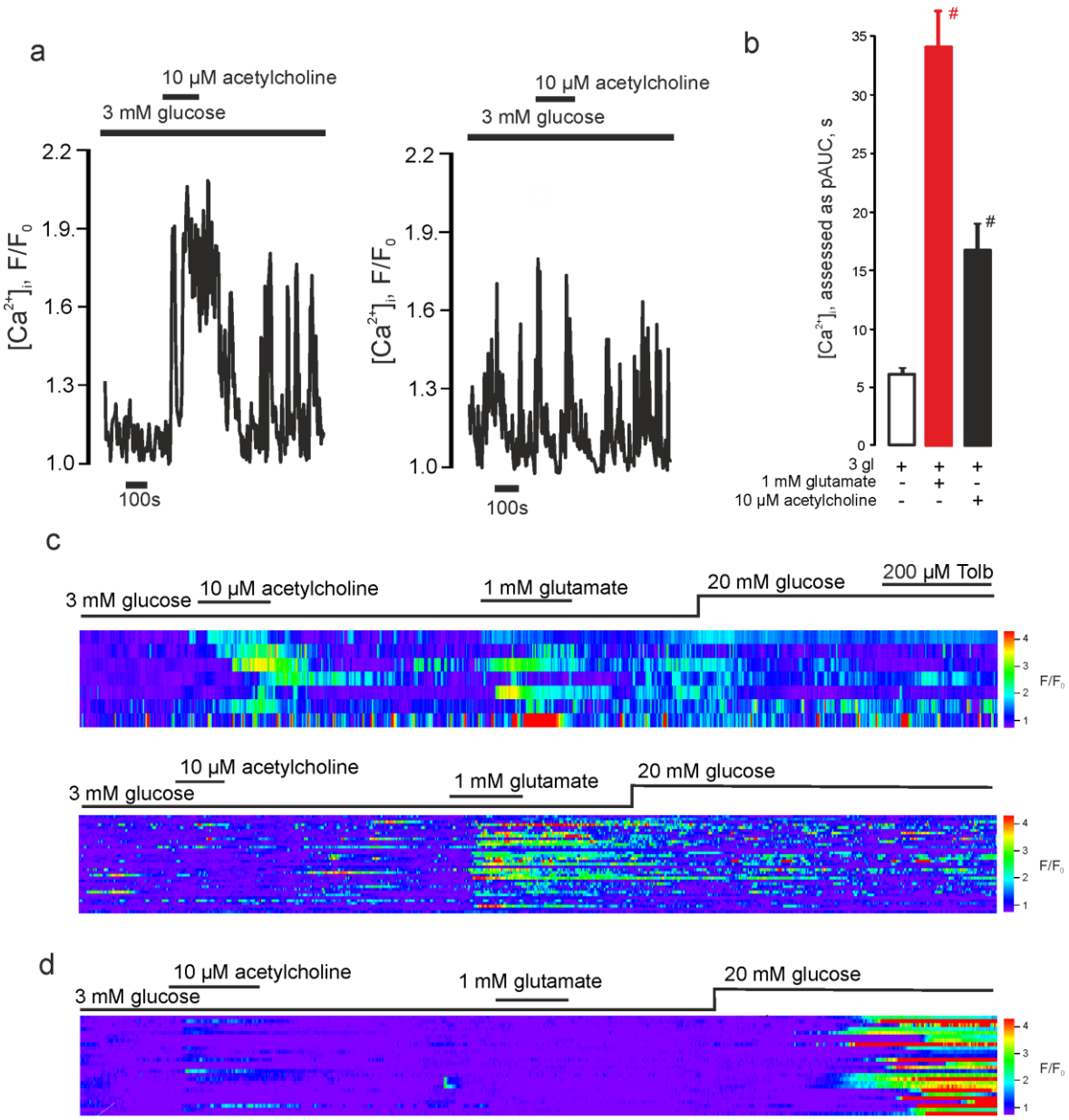


Figure 4.3 - Acetylcholine increases $[Ca^{2+}]_i$ in a subset of α-cells in intact human islets

(a) Representative recording of the two types of responses to ACh (10 μM) on $[Ca^{2+}]_i$ dynamics in pancreatic α-cells from human islets. Left panel shows responsive cells, right panel shows unresponsive cells **(b)** $[Ca^{2+}]_i$ quantified as pAUC at 3 mM glucose (open column), in the presence of glutamate (red column) and ACh (black column) in α-cells from human islets. **(c)** Representative heatmaps from different human donors, showing heterogeneity of the effect. N.b. clear ACh effect in top panel and lack of effect in bottom panel. Each line represents a single ROI. **(d)** Representative heatmap of ACh effect in human β-cells. # Denotes significant ($p < 0.05$) vs. basal. Error bars represent ± SEM. Fluo-4 used throughout unless otherwise stated.

4.3.2. The role of muscarinic and nicotinic acetylcholine receptors in the acetylcholine effect in pancreatic α-cells within intact mouse and human islets

After confirming the effect of ACh on $[Ca^{2+}]_i$ in the α-cell, I aimed to clarify whether the response was mediated via activation of mAChRs or nAChRs. To test the muscarinic pathway, the competitive mAChR antagonist atropine (10μM) was applied at the same time as ACh (10μM). The short application time of atropine was used to minimise its non-muscarinic effects on $[Ca^{2+}]_i$ (see Hedlund et al., 1985). Atropine significantly reduced the ACh effect in α-cells ($p < 0.001$ vs. control; $n = 30$; Figure 4.4 a, d), rendering 50% of cells (15/30) completely unresponsive with the majority of remaining cells displaying attenuated responses. A significant increase from basal did remain however ($p < 0.001$ vs. basal). In β-cells, the ACh effect was completely abolished (Figure 4.12 b). Unsurprisingly, atropine greatly reduced cholinergically-induced glucagon secretion (Figure A3.1 c).

The atropine-resistant component may suggest the presence of a nicotinic component in the α-cell cholinergic response. To investigate this further, the non-specific, competitive nAChR antagonist tubocurarine (10 μM) was applied simultaneously with ACh. This led to a significant reduction in the ACh $[Ca^{2+}]_i$ effect ($p = 0.018$ vs. control; $n = 44$; Figure 4.4 b, d). Interestingly, the reduction appeared to result largely due to a diminished response in a subset of α-cells rather than an attenuation across the whole α-cell population (Figure 4.4 b), with a large increase in $[Ca^{2+}]_i$ persisting ($p < 0.001$ vs. basal). Notably, tubocurarine had a negligible effect on cholinergically-induced glucagon secretion (Figure A3.1 c). The ACh response in β-cells also remained (Figure 4.12 c). Combined application of atropine and tubocurarine resulted in complete abolition of the

ACh response with no increase in $[Ca^{2+}]_i$ over the basal value ($p = 0.739$ vs. basal; $n = 31$; Figure 4.4 c, d). The effect in β-cells was also absent (Figure 4.12 d).

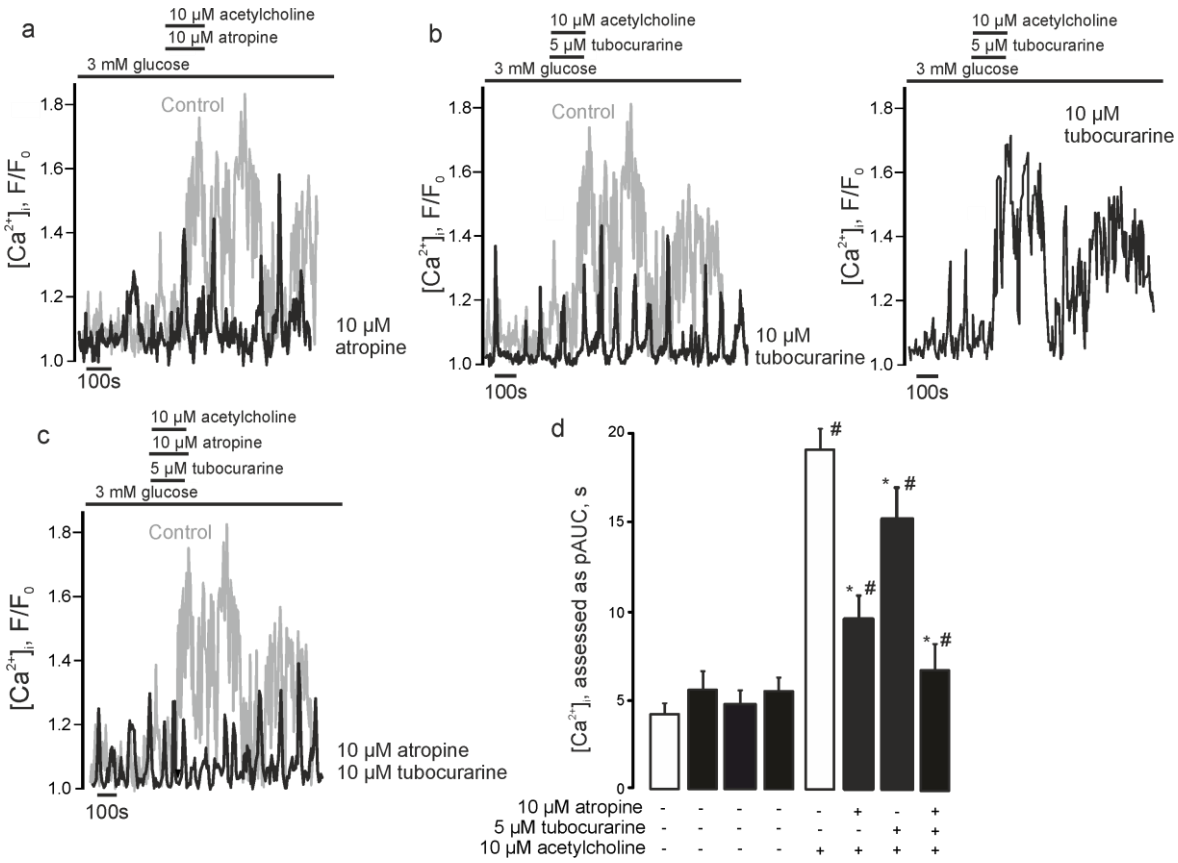


Figure 4.4 - Acetylcholine functions via muscarinic and nicotinic pathways

(a) Representative recording of the effect of ACh (10 μM) on α-cell $[Ca^{2+}]_i$ dynamics in the presence of atropine (10 μM). The C57BL/6J control trace (grey) is superimposed with the experimental trace. **(b)** Representative recordings of the effect of ACh (10 μM) on α-cell $[Ca^{2+}]_i$ dynamics in the presence of tubocurarine (5 μM). First panel shows α-cell with attenuated response (25% - 11/44 cells), the C57BL/6J control trace (grey) is superimposed with the experimental trace. 2nd panel shows fully responsive α-cell (75% - 33/44 cells). **(c)** Representative recording of the effect of ACh (10 μM) on α-cell $[Ca^{2+}]_i$ dynamics in the presence of atropine (10 μM) and tubocurarine (5 μM). The C57BL/6J control trace (grey) is superimposed with the experimental trace. **(d)** $[Ca^{2+}]_i$ in α-cells quantified as pAUC at 3 mM glucose and ACh alone (open columns); or ACh in the presence of atropine, tubocurarine or atropine and tubocurarine with corresponding basal values (black columns). # Denotes significant ($p < 0.05$) vs. basal; * Denotes significant ($p < 0.05$) vs. control. Error bars represent ± SEM. Fluo-4 used throughout unless otherwise stated.

To further assess the contribution of the muscarinic and nicotinic pathways specific agonists were applied in place of ACh. Firstly, to examine the muscarinic pathway, the mAChR agonist oxotremorine M was used. It significantly elevated $[Ca^{2+}]_i$ in all sampled α-cells ($p < 0.0015$ vs. basal, $n = 21$; Figure 4.5 a, c), with an effect of similar magnitude to ACh ($p = 0.424$ vs. control); β-cells were also responsive (Figure 4.12 e). This was replicated in terms of glucagon secretion, with a large increase in response to oxotremorine M in both static secretion assays (Figure A3.1 b) and pancreas perfusion experiments (Figure A3.2 a). In human islets, oxotremorine M initiated significant elevation of $[Ca^{2+}]_i$ in 63% of α-cells ($p = 0.004$ vs. basal; $n = 19$, 3 donors; Figure 4.5 f), with no difference in the magnitude of the effect compared to ACh ($p = 0.342$ vs. ACh). Oxotremorine M also increased $[Ca^{2+}]_i$ in 25% (5/20) of β-cells (data not shown).

To further probe the nicotinic component of the cholinergic response, nicotine (10 μM) was applied in place of ACh. It induced a significant increase in $[Ca^{2+}]_i$ ($p < 0.001$ vs. basal; $n = 64$; Figure 4.5 b, c). The effect was limited to a subset of α-cells (71% - 46/64 cells), in which nicotine generally caused smaller, more transient increases in $[Ca^{2+}]_i$ compared to ACh ($p = 0.021$ vs. ACh) and oxotremorine M ($p = 0.024$ vs. oxotremorine M). Additionally, application of nicotine had no effect in β-cells (Figure 4.12 f). To ensure the nicotinic component was not originating from the intraislet sympathetic nerve terminals, which can remain attached to isolated islets (Karlsson et al., 1997), propranolol was applied acutely. The nicotinic response was marginally reduced in its presence ($p = 0.042$ vs. control; $n = 37$; Figure 4.5 d) but a clear elevation from basal remained ($p < 0.001$ vs. basal). Furthermore, in islets cultured overnight, in which most nerve endings would be degraded (Karlsson et al., 1997, Cabrera et al., 2008), there was no difference in the magnitude of the effect compared to acutely isolated islets ($p = 0.0118$; Figure 4.5 e).

Notably, nicotine also induced an increase in glucagon secretion, both in static secretion assays (Figure A3.1 b) and in pancreas perfusion experiments (Figure A3.2 a). In human islets, nicotine caused a significant elevation of $[Ca^{2+}]_i$ ($p = 0.02$ vs. basal; $n = 41$, 2 donors; Figure 4.5 f), although the effect was smaller than that of ACh ($p = 0.025$ vs. ACh), only affecting 37% (15/41) of α-cells. No β-cells responded (data not shown).

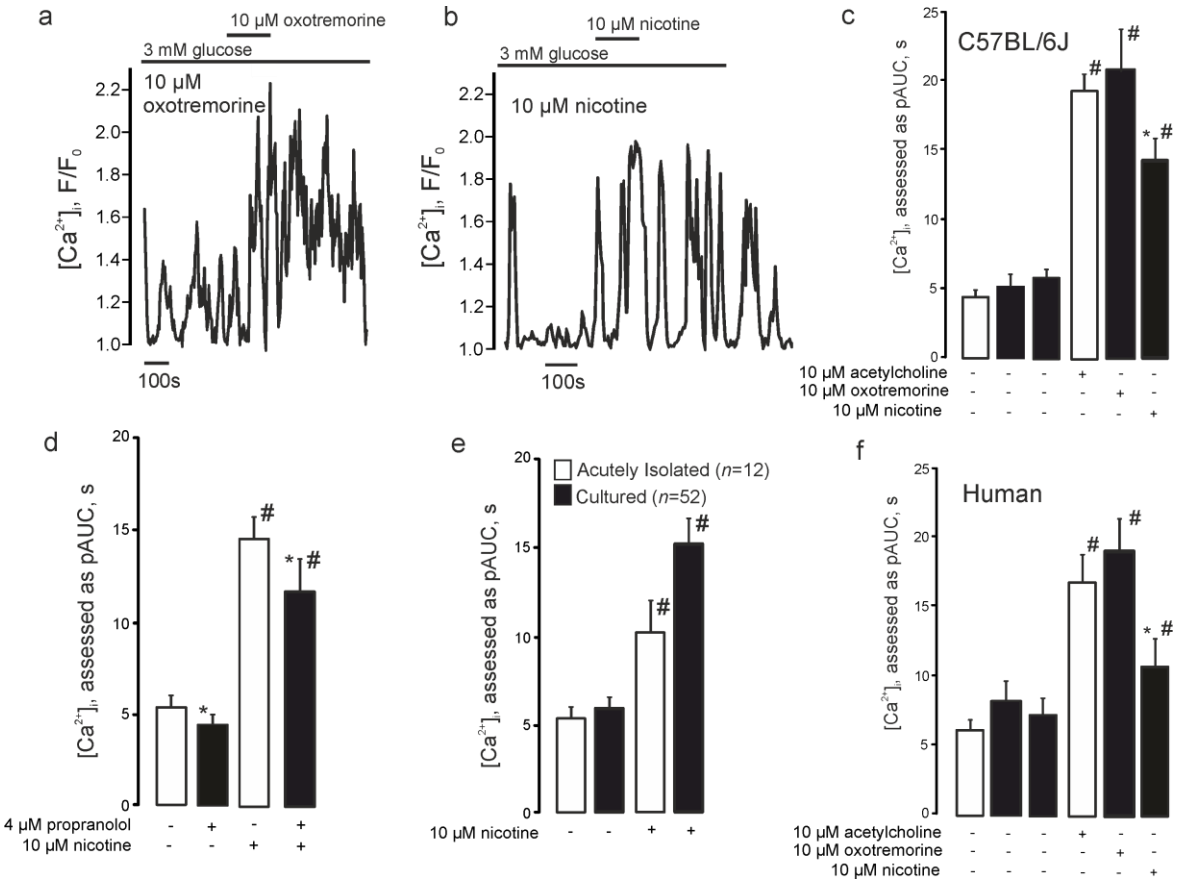


Figure 4.5 – Oxotremorine and nicotine increase $[Ca^{2+}]_i$ in mouse and human α-cells

(a) Representative recording of the effect of oxotremorine M (10 μM) on α-cell $[Ca^{2+}]_i$ dynamics. **(b)** Representative recordings of the effect of nicotine (10 μM) on α-cell $[Ca^{2+}]_i$ dynamics. **(c)** $[Ca^{2+}]_i$ in α-cells quantified as pAUC at 3 mM glucose and ACh (open columns) or oxotremorine M or nicotine with corresponding basal values (black columns) in C57BL/6J mice **(d)** $[Ca^{2+}]_i$ in α-cells quantified as pAUC at 3 mM glucose and nicotine alone (open columns) or in the presence of propranolol (black columns). **(e)** $[Ca^{2+}]_i$ in α-cells quantified as pAUC at 3 mM glucose and nicotine in acutely isolated (open columns) and cultured islets (black columns). **(f)** $[Ca^{2+}]_i$ in α-cells quantified as pAUC at 3 mM glucose and acetylcholine (open columns) or oxotremorine M or nicotine with corresponding basal values in human islets # Denotes significant ($p < 0.05$) vs. basal; * Denotes significant ($p < 0.05$) vs. control. Error bars represent ± SEM. Fluo-4 used throughout unless otherwise stated.

4.3.3. Effect of acetylcholine on $[DAG]_i$ in dispersed mouse islets

To confirm ACh stimulation results in activation of the G_q pathway (associated with the M3 mAChR) and compare its relative contribution in α- and β-cells, the downstream secondary messenger DAG was imaged in dispersed islets using a baculovirally delivered probe. In α-cells, ACh resulted in an increase in $[DAG]_i$ in a majority of cells (69% - 35/51 cells), with a subset not responding to the neurotransmitter (31 % - 16/51 cells; Figure 4.6). In non- α-cells, ACh increased $[DAG]_i$ in 94% (312/332) of cells and the magnitude of the effect was also much larger compared to responsive α-cells (Figure 4.6). δ-cells account for approximately <10% of islet cells in rodents (Steiner et al., 2010) and have been shown to be inhibited by the neurotransmitter in rodents so would be unlikely to increase $[DAG]_i$ in response to ACh (Vonen et al., 1989, Hauge-Evans et al., 2009). Therefore, it can be assumed that the remaining unresponsive non-α-cells are δ-cells.

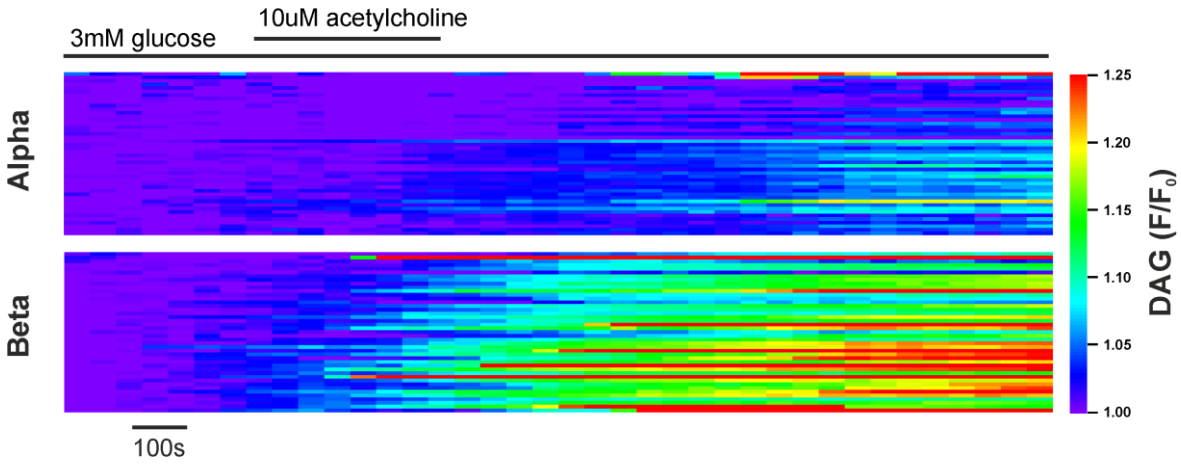


Figure 4.6 - Acetylcholine increases $[DAG]_i$ in majority of α-cells

Heatmap depicting change in $[DAG]_i$ upon ACh (10 μM) application, using baculoviral-delivered Red DAG downward probe. α-cells (n = 51) top panel, β-cells (n = 57) bottom panel, each line represents single ROI (cell). N.b. relatively lower % of responsive α-cells and difference in magnitude between the two cell types.

4.3.4. The role of intracellular Ca^{2+} in the acetylcholine effect in pancreatic α-cells within intact mouse islets

The production of DAG from PIP_2 is accompanied by the production of the Ca^{2+}-mobilising secondary messenger IP_3, which can initiate ER Ca^{2+} release via IP_3Rs. To investigate whether ACh was inducing ER Ca^{2+} release in α-cells, the ER Ca^{2+} stores were depleted by pre-incubating islets in the SERCA-Ca^{2+} ATPase inhibitor CPA (10μM) for 20 min. This dramatically reduced the ACh effect in α-cells ($p < 0.001$ vs. control; $n = 48$; Figure 4.7 a, c), with 69% (33/48) of cells unresponsive to the neurotransmitter; despite this, across the population significant elevation of $[Ca^{2+}]_i$ from basal remained due to a small number of responsive cells ($p < 0.001$ vs. basal). In β-cells, ACh had minimal effect after CPA-treatment (Figure 4.12 g).

Notably, CPA also attenuated the stimulatory effect of oxotremorine M, reflected by a significant reduction in the $[Ca^{2+}]_i$ response compared to oxotremorine M alone ($p = 0.022$ vs. oxotremorine M; $n = 20$; see Figure 4.7 g). Unlike oxotremorine M, nicotine was still able to initiate a full response in the presence of CPA, with no difference in the magnitude of the effect compared to nicotine applied alone ($p = 0.539$ vs. nicotine; $n = 17$; Figure 4.7 h).

4.3.5. The role of PKC in the acetylcholine effect in pancreatic α-cells within intact mouse islets

Upon activation of the muscarinic pathway, the combined increase in DAG and Ca^{2+} can result in the downstream activation of PKC (Gilon and Henquin, 2001). To test whether PKC was contributing to increased $[Ca^{2+}]_i$ in the α-cell, islets were pre-incubated with the

PKC-inhibitor BIM for 1 hr. The ACh effect remained the same in the presence of BIM (p = 0.799 vs. control; n = 23; Figure 4.7 b, c), indicating that the increase in $[Ca^{2+}]_i$ is not PKC-dependent. Contrastingly, the ACh effect in β-cells appeared to be attenuated slightly (Figure 4.12 h).

4.3.6. Effect of Ca^{2+} channel blockers on the acetylcholine effect in pancreatic α-cells within intact mouse islets

After identifying a critical role for intracellular Ca^{2+} in the α-cell ACh response, specifically in relation to the muscarinic pathway, the role of extracellular Ca^{2+} was investigated. Isradipine was again used to block L-type Ca^{2+} channels. It had negligible effect on the magnitude of the ACh $[Ca^{2+}]_i$ response[15] (p = 0.123 vs. control; n = 13; Figure 4.7 d, f), with a transient effect observed in 9 out of 13 cells, as reported previously in single mouse α-cells using carbachol (Liu et al., 2004), and more sustained responses in the remaining 4 cells. Conversely, glucagon secretion in response to carbachol was greatly reduced by isradipine (Figure A3.1 d). Application of the P/Q-type Ca^{2+} channel blocker ω-agatoxin (200 nM) resulted in a slight yet significant reduction in the ACh $[Ca^{2+}]_i$ response (p = 0.043 vs. control; n = 32; see Fig. 4.7 e, f). It also decreased cholinergically-induced glucagon secretion (Figure A3.1 d). Notably, β-cells were still responsive to ACh in the presence of both isradipine and ω-agatoxin (Figure 4.12 i, j).

As the effect of nicotine was resistant to CPA and direct Ca^{2+} entry through the nAChR is minimal (Colquhoun et al., 2003), a secondary effect on voltage-gated Ca^{2+} channels

[15] Note that the glutamate effect, although diminished, was not absent after isradipine treatment meaning α-cells were identifiable.

appeared likely. Indeed, ω-agatoxin application significantly reduced the α-cell nicotinic response ($p = 0.001$ vs. nicotine alone; $n = 52$; Figure 4.7 h), although an increase in $[Ca^{2+}]_i$ from basal glucose persisted ($p < 0.001$ vs. basal). Isradipine was without a statistically significant effect on the nicotinic response ($p = 0.074$ vs. nicotine alone; $n = 44$; Figure 4.7 h), with a clear increase from the basal state ($p < 0.001$ vs. basal).

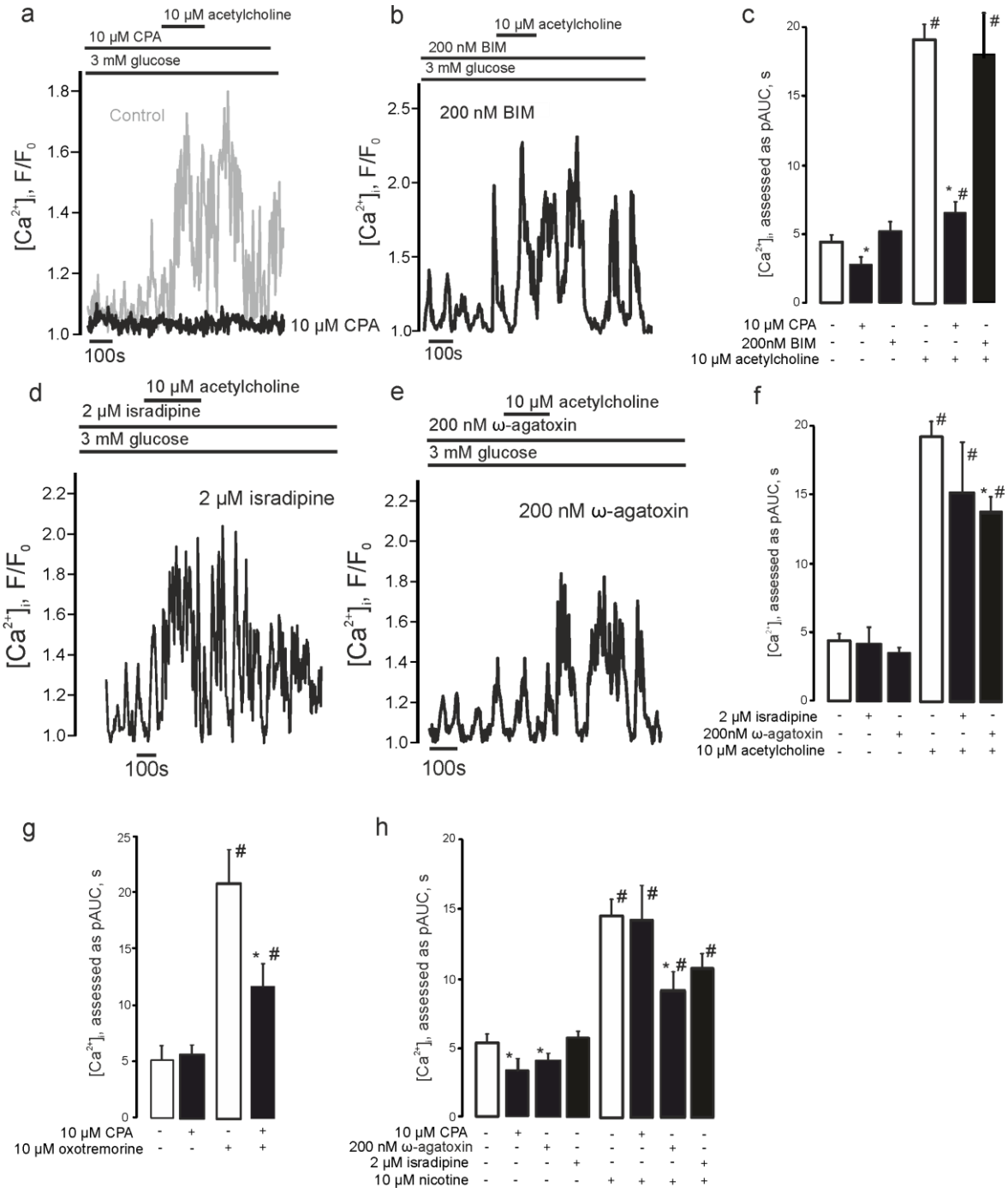


Figure 4.7 - Ca^{2+} dependence of the acetylcholine effect in α-cells

(a) Representative recording of the effect of ACh (10 µM) on α-cell $[Ca^{2+}]_i$ dynamics in the presence of CPA (10 µM). The C57BL/6J control trace (grey) is superimposed with the experimental trace. **(b)** Representative recordings of the effect of ACh (10 µM) on α-cell $[Ca^{2+}]_i$ dynamics in the presence of BIM (200 nM). **(c)** $[Ca^{2+}]_i$ in α-cells quantified as pAUC at 3 mM glucose and ACh alone (open columns) or in the presence of CPA or BIM (black columns). **(d)** Representative recording of the effect of ACh (10 µM) on α-cell $[Ca^{2+}]_i$ dynamics in the presence of isradipine (2 µM). **(e)** Representative recordings of the effect of ACh (10 µM) on α-cell $[Ca^{2+}]_i$ dynamics in the presence of ω-agatoxin (200 nM). **(f)** $[Ca^{2+}]_i$ in α-cells quantified as pAUC at 3 mM glucose and ACh alone (open columns) or in

the presence of isradipine or ω-agatoxin (black columns). **(g)** $[Ca^{2+}]_i$ in α-cells quantified as pAUC at 3 mM glucose and oxotremorine M alone (open columns) or in presence of CPA (black columns). **(h)** $[Ca^{2+}]_i$ in α-cells quantified as pAUC at 3 mM glucose and nicotine alone (open columns) or in the presence of CPA, ω-agatoxin and isradipine (black columns). # Denotes significant ($p < 0.05$) vs. basal; * Denotes significant ($p < 0.05$) vs. control. Error bars represent ± SEM. Fluo-4 used throughout unless otherwise stated.

4.3.7. Effect of acetylcholine on pancreatic α-cells within intact mouse islets in the presence of EGTA

To further investigate the relative contribution of extracellular and intracellular Ca^{2+} to the ACh effect, the Ca^{2+} chelator EGTA (5 mM) was applied to 'remove' Ca^{2+} from the extracellular solution. Similarly to adrenaline, a transient effect persisted in its presence ($p < 0.001$ vs. basal (incl. EGTA); $n = 22$; Figure 4.8 a, b). However, this was only seen in 64% of cells (14/22 cells) and was often diminished. In the remaining 8 cells, no effect was apparent (36%) (Figure 4.8 a). In β-cells, the transient effect persisted in a majority of cells (Figure 4.12 k).

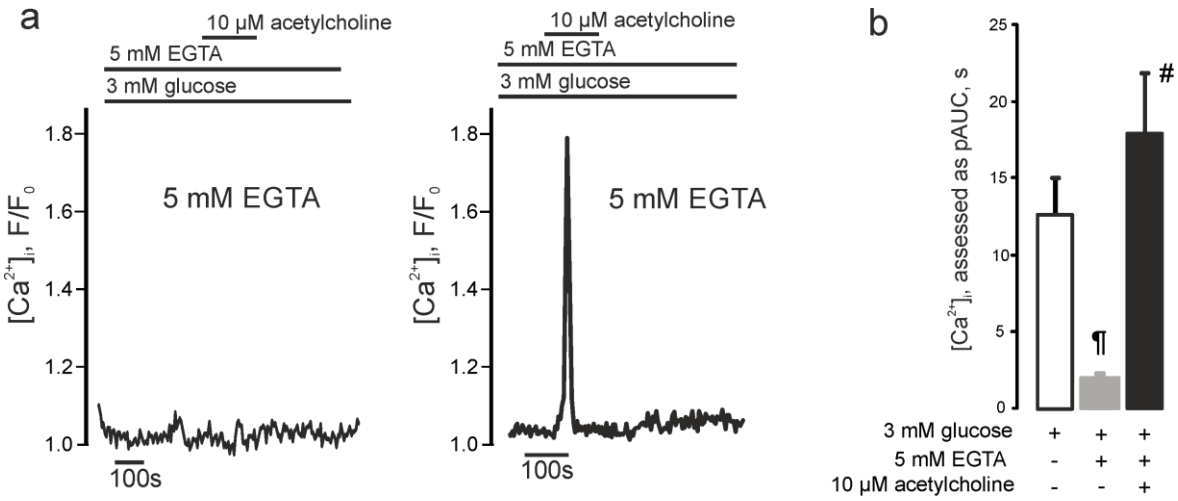


Figure 4.8 - Removal of extracellular Ca^{2+} reduces acetylcholine effect in α- cells

(a) Representative recordings of the effect of ACh (10 µM) on α-cell $[Ca^{2+}]_i$ dynamics in the presence of EGTA (5 mM). Left panel shows an unresponsive α- cell, right panel a responsive α-cell. Cells ranged between these two types of response. **(b)** $[Ca^{2+}]_i$ in α-cells quantified as pAUC at basal glucose (open column), after EGTA application (grey column) and after ACh application (black column). # Denotes significant ($p < 0.05$) vs. basal (EGTA); ¶ Denotes basal (incl. EGTA) significantly ($p < 0.05$) different vs. basal. * Denotes significant ($p < 0.05$) vs. control. Error bars represent ± SEM. Fluo-4 used throughout unless otherwise stated.

4.3.8. Effects of nicotine and acetylcholine on α-cell electrical activity in pancreatic α-cells within intact mouse islets

To further investigate the effects of nicotine and ACh and the role of membrane potential in α-cell cholinergic signalling, whole-cell perforated patch clamp was performed on α-cells within intact islets. Overall, nicotine had no major effect on action potential frequency with negligible change in most cells (75% - 9/12). In the remaining cells, nicotine actually reduced action potential frequency (25% - 3/12; Figure 4.10 a). The effects of ACh were also heterogeneous. In 50% (2/4) of α-cells ACh induced membrane hyperpolarization (Figure 4.10 b). While other recordings showed minimal change in electrical activity when ACh was applied (50% - 2/4 cells).

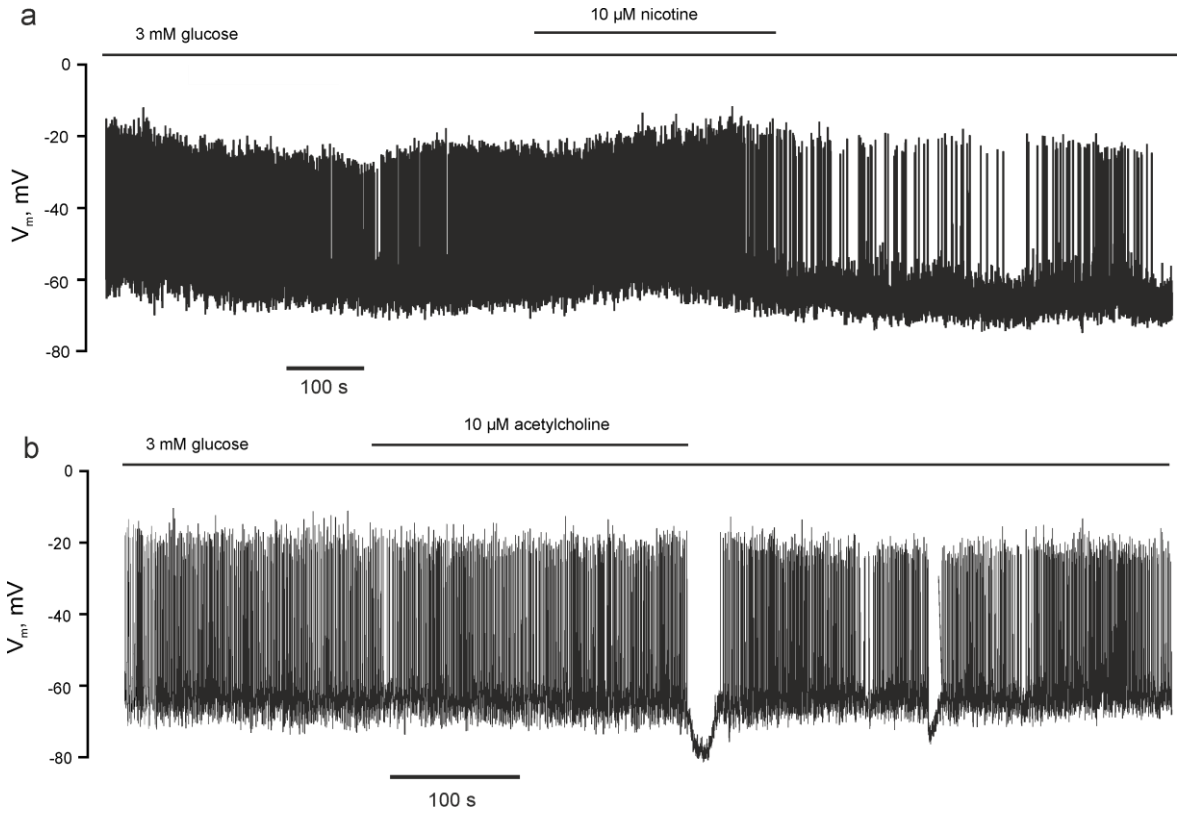


Figure 4.9 - Nicotine and acetylcholine do not stimulate electrical activity in mouse pancreatic α-cells

(a) Representative recording of the inhibitory effect of nicotine (10 μM) on membrane potential in α-cells. **(b)** Representative recording of the inhibitory effect of ACh (10 μM) on membrane potential in α-cells.

4.3.9. Effect of SSTR2 blockade on acetylcholine effect in pancreatic α-cells within intact mouse islets

As alluded to earlier, cholinergic signalling has been found to inhibit somatostatin secretion in rodents (Samols et al., 1978, Vonen et al., 1989, Hauge-Evans et al., 2009). Crucially, however, this inhibition has only been observed at high glucose when somatostatin secretion is high. Nevertheless, small amounts of somatostatin are secreted at low and intermediate glucose (Vieira et al., 2007, Vergari et al., In Press), which might affect α-cell cAMP levels and $[Ca^{2+}]_i$ dynamics. Thus, the effect of ACh on α-cells may, in theory, be affected by cholinergic signalling in δ-cells. To test whether changes in δ-cell input as a result of ACh could have any effect on glucagon secretion at low glucose, α-cell somatostatin signalling was blocked by applying 100 nM of the SSTR2 antagonist CYN 154806. At this concentration, the drug selectively inhibits somatostatin mediated effects in α-cells (Strowski et al., 2000, Braun, 2014). Interestingly, the application of CYN 154806 increased α-cell basal $[Ca^{2+}]_i$ dynamics in 58% of α-cells (15/26 cells) ($p = 0.002$ vs. basal; $n = 26$; Figure 4.9 a, b), yet ACh was still able to further increase $[Ca^{2+}]_i$ substantially ($p < 0.001$ vs. basal (incl. CYN 154806)). Notably, the ACh effect was not significantly different in magnitude when compared to the CYN 154806-free control ($p = 0.098$ vs. control; Figure 4.9 b), even when preceding basal values were subtracted ($p = 0.116$ vs. control; Figure 4.9 c). β-Cells remained responsive to ACh in the presence of CYN 154806 (Figure 4.12 l).

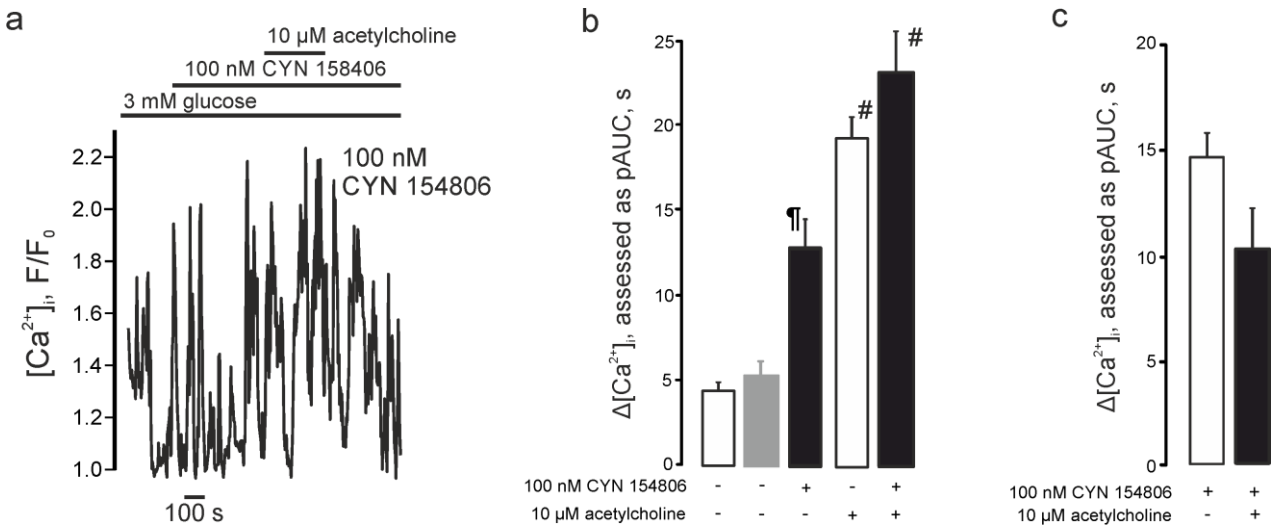


Figure 4.10 - Somatostatin receptor antagonism has no effect on the acetylcholine response

(a) Representative recording of the effect of ACh (10 µM) on α-cell $[Ca^{2+}]_i$ dynamics in the presence of CYN 154806 (100 nM). The C57BL/6J control trace (grey) is superimposed with the experimental trace. **(b)** $[Ca^{2+}]_i$ in α-cells quantified as pAUC at 3 mM glucose and ACh alone (open columns) in control experiments. At basal (3 mM glucose) before CYN 154806 application (grey column), and at basal and ACh in the presence of CYN 154806 (black columns). **(c)** $\Delta[Ca^{2+}]_i$ change in response to ACh in control (difference between open columns from b) and CYN 154806-treated α-cells (difference between black columns from b). ¶Difference vs. basal condition is significant ($p < 0.05$); # Difference vs. basal+CYN 154806 is significant ($p < 0.05$). Error bars represent ± SEM. Fluo-4 used throughout unless otherwise stated.

4.3.10. Effect of hypo- and hyperglycaemic culture on the acetylcholine response in pancreatic α-cells within intact mouse islets

The effects of hypo- and hyperglycaemia on the ACh response were also investigated in Glu-gCAMP3 mice. In islets cultured for 72 h under hypoglycaemic conditions (5 mM glucose) there was no significant differences in responsiveness to ACh compared to the normoglycaemic (11 mM glucose) group ($p = 0.200$ vs. 11 mM group). However, in the group cultured under hyperglycaemic conditions (30 mM glucose), the effect of ACh on $[Ca^{2+}]_i$ increased ($p < 0.001$ vs. 11 mM group; $n = 347$). Basal $[Ca^{2+}]_i$ dynamics were also increased in the hyperglycaemic group (Figure 4.11).

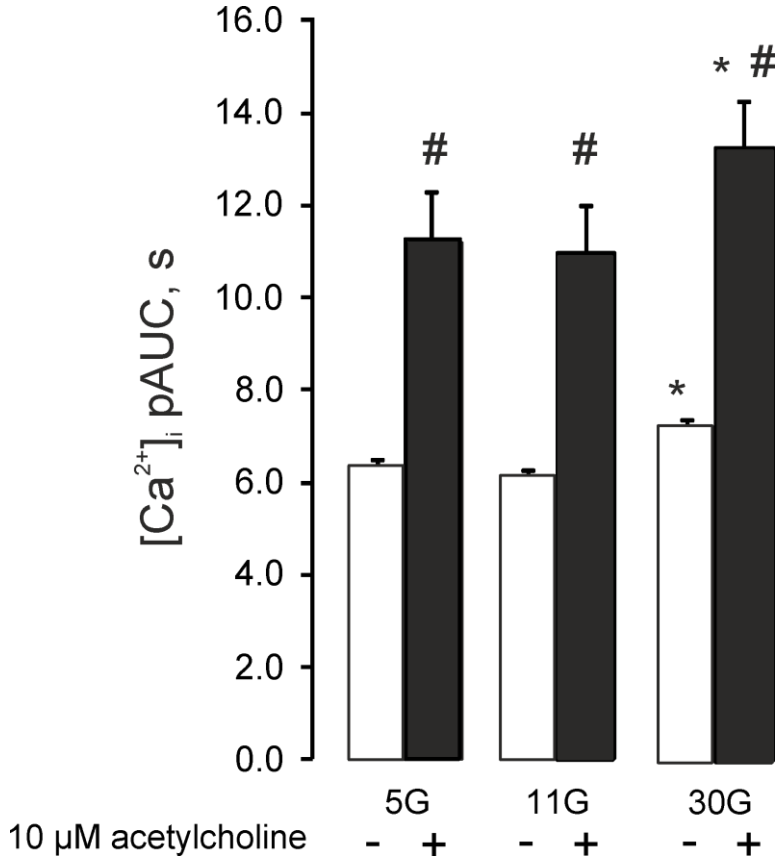


Figure 4.11 - Hypo- and hyperglycaemic conditions do not affect ACh-induced $[Ca^{2+}]_i$ increase in pancreatic α-cells

$[Ca^{2+}]_i$ quantified as pAUC at 3 mM glucose (open columns) and after ACh (10 µM) application (black columns) in islets cultured at 5 mM glucose, 11 mM glucose and 30 mM glucose. # Denotes significant ($p < 0.05$) vs. basal; * Denotes significant ($p < 0.05$) vs. 11 mM glucose group. Error bars represent ± SEM.

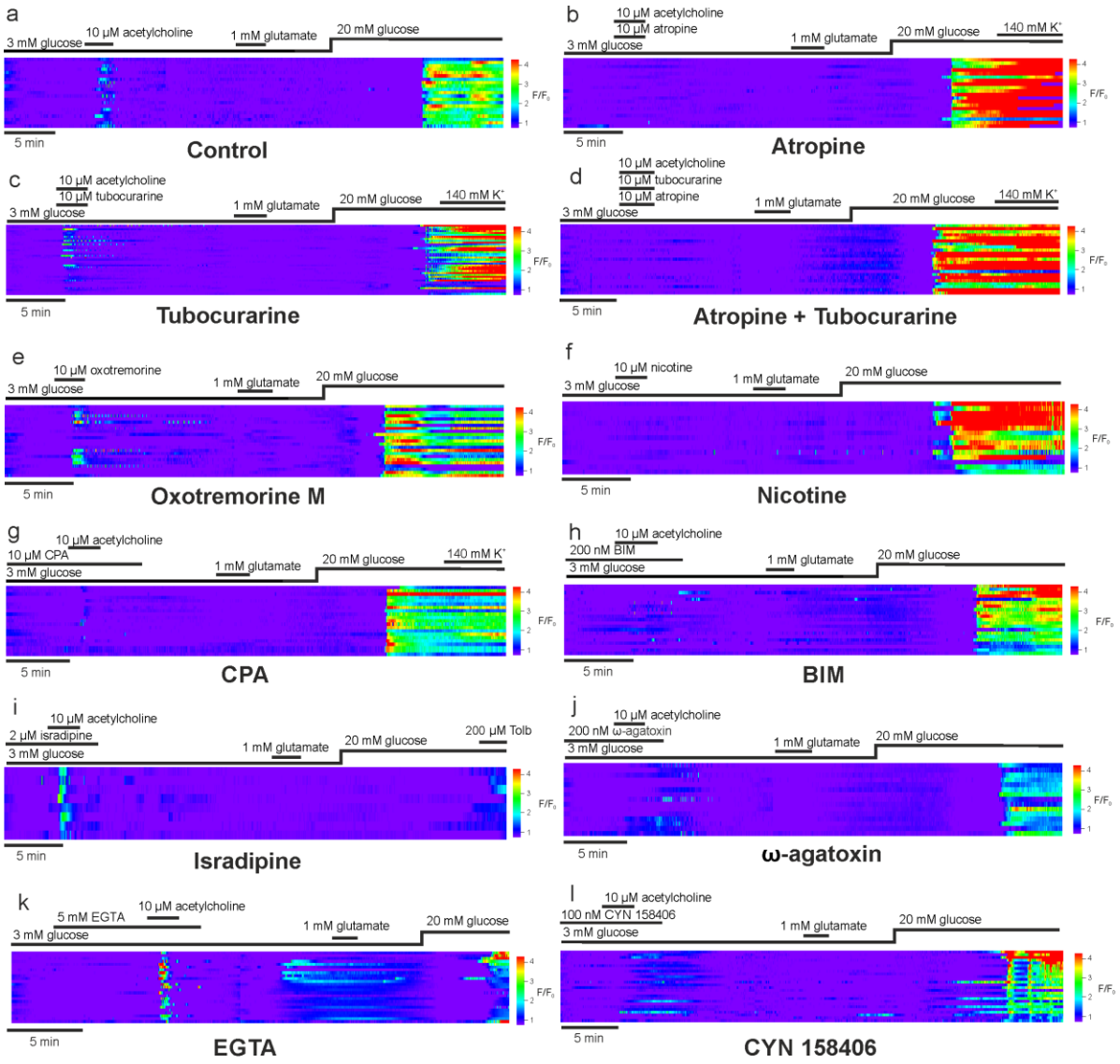


Figure 4.12 - Cholinergic effect in β-cells

Representative heatmaps of effects in β-cells, each line represents a single β-cell.
(a) Control **(b)** Atropine **(c)** Tubocurarine **(d)** Atropine + Tubocurarine **(e)** Oxotremorine **(f)** Nicotine **(g)** CPA **(h)** BIM **(i)** Isradipine **(j)** ω-agatoxin **(k)** EGTA **(l)** CYN 154806

4.4. Discussion

4.4.1. Acetylcholine increases $[Ca^{2+}]_i$ in pancreatic α-cells

These data elucidate how ACh stimulates glucagon secretion, revealing a muscarinic pathway that targets the ER Ca^{2+} stores yet also a nicotinic component that appears to influence P/Q-type Ca^{2+} channel influx. There are clear differences in the response between α- and β-cells, with the latter appearing to rely exclusively on the muscarinic pathway. The effect is somewhat conserved in human islets with evidence of muscarinic and nicotinic involvement, but limited to a subset of α-cells.

4.4.2. The effect of acetylcholine on α-cell $[Ca^{2+}]_i$ is reliant predominantly on the muscarinic pathway

The muscarinic pathway was confirmed to play a critical role in ACh-induced glucagon secretion. Antagonism of the mAChRs with atropine sharply reduced the potency of ACh to increase $[Ca^{2+}]_i$ in the α-cell; while the mAChR agonist oxotremorine M initiated a rapid, potent and reversible response, mimicking ACh. With previous studies reporting α-cell cholinergic signalling to be mediated via M3 mAChR subtype (Verspohl et al., 1990, Karlsson and Ahren, 1993, Duttaroy et al., 2004), the effects of atropine and oxotremorine M were expected.

Activation of the M3 receptor is associated with activation of the G_q pathway, resulting in IP_3-mediated Ca^{2+} release from the ER and activation of PKC, both of which have been linked to an increase in islet hormone secretion (Gilon and Henquin, 2001). Activation of this pathway was confirmed with ACh application inducing an increase in $[DAG]_i$ in a

majority of α-cells. The experiments with CPA did indeed illustrate that ER Ca^{2+} release was a downstream target of muscarinic stimulation (presumably via IP_3-mediated Ca^{2+} release), with both ACh and oxotremorine M considerably less potent when CPA was present. Blocking PKC function with BIM, however, had little effect on the ACh-induced $[Ca^{2+}]_i$ response. The kinase is instead likely to increase hormone secretion by sensitising the secretory machinery to Ca^{2+}, as seen in β-cells (Jones et al., 1985, Tamagawa et al., 1985, Arkhammar et al., 1986b, Bozem et al., 1987, Hughes et al., 1987, Ammala et al., 1994).

Regarding the effect of ACh on α-cell membrane potential, the hyperpolarization seen in 50% of cells could be due to cholinergic activation of neighbouring δ- or β-cells. Notably, both somatostatin (Gromada et al., 2001b) and β-cell-derived GABA (possibly in conjunction with insulin translocation of $GABA_A$ receptors to the plasma membrane) have been reported to induce hyperpolarization in α-cells by stimulating K^+ efflux (Rorsman et al., 1989, Xu et al., 2006). It should be noted however that the experiments with CYN 154806 dispute a stimulatory effect of ACh on δ-cells. Alternatively, the effect may be caused by the ER-mediated $[Ca^{2+}]_i$ increase opening Ca^{2+}-sensitive K^+ channels at the plasma membrane (e.g. BK channels), resulting in K^+ efflux. This may function to desensitise the α-cell, preventing against excessive cholinergic stimulation and Ca^{2+} toxicity. Notably, there is evidence of expression of these channels in mouse α-cells (Benner et al., 2014, Adriaenssens et al., 2016). As the number of recordings was limited, more work is required to ascertain the precise effect of ACh on α-cell membrane potential.

4.4.3. A nicotinic pathway is also present in α-cells

Alongside the muscarinic response in α-cells, a nicotinic pathway was also revealed; antagonism of nAChRs with tubocurarine caused a subtle decrease in the ACh $[Ca^{2+}]_i$ response. While the agonist nicotine increased $[Ca^{2+}]_i$ in 71% of the α-cells. nAChRs are non-selective cation channels, generally associated with Na^+ influx but also permeable to Ca^{2+} (Colquhoun et al., 2003), meaning direct Ca^{2+} entry through the receptor can occur. It is demonstrated that activation of the nAChR results in depolarization triggering Ca^{2+} entry via P/Q-type Ca^{2+} channels, which are fundamental to glucagon secretion under hypoglycaemic conditions (Zhang et al., 2013). As there was an ω-agatoxin-resistant component, a proportion of the Ca^{2+} influx likely occurs via the nAChR itself. Application of propranolol reduced the magnitude of the ACh response but only very slightly. Importantly, a clear elevation of $[Ca^{2+}]_i$ from the basal state remained. This indicates that the effect is real and not purely a consequence of nicotine stimulating sympathetic nerve endings and initiating intraislet noradrenaline release. This was further backed up by the similarity in response between acutely isolated and cultured islets. It should be noted that the effects of nicotine on membrane potential contest what is observed in the $[Ca^{2+}]_i$ imaging experiments. While it appeared to reduce action potential frequency in a subset of α-cells, based on the $[Ca^{2+}]_i$ imaging data one would expect the opposite to occur. More work is therefore required to ascertain the exact mechanism by which nicotine increases $[Ca^{2+}]_i$ in α-cells.

The nicotinic effect appeared to be limited to a specific subset of α-cells with many cells resistant to tubocurarine and nicotine. The $[DAG]_i$ imaging data emphasises this, suggesting there is a population that does not increase $[DAG]_i$ in response to the neurotransmitter, indicating that they may favour the nicotinic pathway. This observation

conflicts somewhat with the oxotremorine M $[Ca^{2+}]_i$ data, which shows that the muscarinic response is ubiquitous to all α-cells. This discrepancy may be due to differences between intact and dispersed islets as well as the sensitivity of the DAG probe, which may be insufficient to detect any changes in these cells. Either way, there is clear heterogeneity in the α-cell $[DAG]_i$ response, which likely originates from variable activation of both pathways across the α-cell population. Furthermore, the smaller magnitude of the $[DAG]_i$ response compared to β-cells supports the notion of a prominent nicotinic pathway in α-cells.

4.4.4. The role of the nicotinic pathway in ACh-induced glucagon secretion

nAChRs are typically associated with synaptic transmission in the CNS, PNS and NMJ (Albuquerque et al., 2009). However, there is evidence for expression and function in non-neuronal tissues. This includes islets, with a recent study by Ganic et al. (2016) confirming a critical role for nAChRs in ACh-stimulated insulin secretion[16]. They proposed that initial opening of the fast-acting nAChRs acted to 'prime' the β-cell preparing it for muscarinic activation; with the dual application of oxotremorine M and nicotine mirroring the effect of ACh on insulin secretion, and dwarfing the effect of oxotremorine M alone. Based on previous studies and my own data, it is clear that muscarinic stimulation predominates over any nicotinic effect in α-cells. Identifying a precise role of the nicotinic pathway in ACh-induced glucagon secretion is therefore difficult. It may, as seen in β-cells, act to

[16] Notably, in this study they used 10 mM glucose and only looked at insulin secretion. The absence of a β-cell nicotinic effect in my experiments is likely due to any change in $[Ca^{2+}]_i$ it initiates being undetectable by Fluo-4. β-cells would be hyperpolarized at 3 mM glucose, meaning any effect of nicotine would be unlikely to stimulate electrical activity and Ca^{2+} influx.

facilitate the muscarinic response, providing the optimal environment for muscarinic activity to trigger glucagon secretion. This could feasibly involve Ca^{2+} influx, resulting from nicotinic depolarization, supplementing the ER Ca^{2+} stores (via the SERCA-ATPase), which the muscarinic pathway targets. This is supported by the EGTA data, with the removal of extracellular Ca^{2+}, which is targeted by the nicotinic pathway, reducing the potency of the ACh response in a number of cells. It must be noted, however, that phospholipase C activity is Ca^{2+}-dependent (Gilon and Henquin, 2001); indeed, application of another Ca^{2+}-chelator BAPTA significantly reduced inositol phosphate production in insulin-secreting cells (Gromada and Dissing, 1996). Therefore, the deterioration of the ACh Ca^{2+} effect in α-cells may reflect a reduction in muscarinic rather than nicotinic signalling.

Alternatively, the two pathways could act separately, rather than synergistically. Without nicotinic stimulation, oxotremorine M was still capable of potently increasing $[Ca^{2+}]_i$ and glucagon secretion. And, notably, a direct effect of nicotine on glucagon secretion existed in both the static secretion and pancreas perfusion experiments, suggesting the pathway can stimulate glucagon secretion directly, independent of the muscarinic pathway. Crucially, this increase in glucagon secretion is in contention with Ganic et al. (2016), who actually observed a slight 'dip' in insulin secretion upon application of nicotine alone. Although not disproving a potential 'priming' role for the nicotinic pathway, this at least suggests there are differences in the pathway in the two cell types. Notably, in the pancreas perfusion experiments, nicotine had minimal effect on insulin secretion (Figure A3.2 b). The nicotinic pathway, therefore, could instead function as a fine-tuning mechanism, providing a slight 'kick' in glucagon secretion (as observed in the pancreas perfusion experiments), which precedes the larger increases in $[Ca^{2+}]_i$ and glucagon secretion

associated with the muscarinic pathway. This could be explained by the nAChRs being more sensitive to ACh than the mAChRs, with progressive activation of the two pathways as glucose falls and intraislet ACh increases.

It must be noted that nAChR subunit expression in α-cells is low relative to the M3 mAChR (Benner et al., 2014). However, as P/Q-type channels are integral to glucagon secretion at low glucose (Zhang et al., 2013), even a small change initiated by influx via the nAChR may be enough to potentiate glucagon secretion.

4.4.5. Smoking-induced nicotine exposure and type 2 diabetes

The stimulatory effect of nicotine on the secretion of the body's principle hyperglycaemic hormone, glucagon, could explain some of the risk associated with smoking in the development of type 2 diabetes. Smoking's role in type 2 diabetes pathogenesis has generally been ascribed to nicotine-induced insulin resistance (Tweed et al., 2012). A direct stimulatory effect of nicotine on the α-cell would likely further compound these effects. Notably, diabetic patients who smoke also have poorer glycaemic control compared to non-smokers, reflected by high HbA1c levels (Nilsson et al., 2004), an observation that could, in part, be caused by nicotinic potentiation of glucagon secretion.

4.4.6. Extracellular Ca^{2+} plays a permissive role in acetylcholine-induced glucagon secretion

The effects of voltage-gated Ca^{2+} channel blockers on the ACh effect were dwarfed by the inhibitory effect of CPA, illustrating that the ER Ca^{2+} stores are largely responsible for the response. Notably, the L-type Ca^{2+} channel blocker isradipine had no effect on the ACh

$[Ca^{2+}]_i$ response, despite greatly reducing cholinergically-induced glucagon secretion. The contrast between the two can be explained by the long 1 h incubation in the static secretion assay. As argued in Chapter 3, L-type Ca^{2+} channels likely play a permissive role, providing the bulk of Ca^{2+} required for the ER stores. The longer application time thereby depletes the ER Ca^{2+} stores, reducing the potency of the ACh response. Reduced phospholipase C activity, which is Ca^{2+}-dependent, should also be considered (Gromada and Dissing, 1996). By contrast, α-cells were still responsive in $[Ca^{2+}]_i$ imaging experiments, where the application time was ~10 min.

Notably, this contrasts with the dramatic inhibitory effects of isradipine on the adrenaline $[Ca^{2+}]_i$ response. As the application time of isradipine was similar in both sets of $[Ca^{2+}]_i$ imaging experiments, this rules out ER store depletion as the reason for application of isradipine blocking the adrenaline $[Ca^{2+}]_i$ response as one would expect to observe the same phenomenon with ACh. Alternatively, the loss of the adrenaline response may result from reduced Ca^{2+}-dependent adenylyl cyclase function, depletion of the (endo)lysosomal Ca^{2+} stores or the shared pharmacology between TPC2 and the L-type Ca^{2+} channel.

P/Q-type Ca^{2+} channels appear to be critical to nicotinic signalling, this was also reflected in the overall ACh effect. P/Q-type channel blockade reduced both the $[Ca^{2+}]_i$ response and cholinergic glucagon secretion, presumably due to a reduction in nicotinic signalling. These effects were minimal however with most cells still responsive to the neurotransmitter, reaffirming that the bulk of the ACh $[Ca^{2+}]_i$ response is store-driven.

4.4.7. Somatostatin signalling plays no role in the α-cell cholinergic response

The observation that SSTR2 antagonism has no effect on the ACh response in α-cells rules out the possibility of a secondary cholinergic effect mediated through the δ-cell. If δ-cell stimulation occurred, one would expect a significantly larger $[Ca^{2+}]_i$ response in the presence of CYN 154806 due to it blocking any inhibitory effect of ACh-induced somatostatin secretion on α-cells. Cholinergic inhibition of the δ-cell at low glucose (measured by $[Ca^{2+}]_i$) was also not evident, with the ACh effect on α-cells remaining intact in CYN154806-treated islets. This is likely due to the lack of active δ-cells at low glucose, meaning any inhibitory effect of ACh on somatostatin secretion has little impact due to the already low somatostatin levels. Interestingly, however, basal Ca^{2+} increased in some cells after CYN 154806 application (presumably α-cells which neighboured δ-cells), suggesting some tonic inhibition of α-cells exists already at low glucose, which when relieved by CYN 154806 leads to an increase in $[Ca^{2+}]_i$. However, as inhibition of α-cell somatostatin signalling did not diminish the $\Delta[Ca^{2+}]_i$ response to ACh, it can be concluded that any change in somatostatin signalling has little effect on ACh-induced glucagon secretion.

4.4.8. The acetylcholine effect in β-cells

ACh consistently increased $[Ca^{2+}]_i$ in β-cells, though the effects were often small and transient. The increase seemed to be dependent on the muscarinic G_q pathway, with little effect of nicotine or tubocurarine on the β-cell response at low glucose. Whether the activation of β-cells would have a paracrine effect on the α-cell response appears unlikely. The effects of ACh on insulin secretion are known to be glucose-dependent, occurring at concentrations which are stimulatory for insulin release (>5 mM glucose) (Hermans et al.,

1987, Gilon and Henquin, 2001). Indeed, when 1 μM ACh was applied to mouse islets at low (3 mM) glucose, there was no effect on insulin secretion, despite an observed increase in $[Ca^{2+}]_i$, and although high concentrations of ACh (100 μM) generated an increase in insulin secretion, this was dramatically smaller than the effects at high glucose (Garcia et al., 1988). This can be put down to a diminished Ca^{2+} response (Garcia et al., 1988, Gilon and Henquin, 2001) due to decreased filling of ER stores (Gylfe, 1991), reduced efficacy of Ca^{2+} on insulin-containing granules (Henquin, 2000, Gilon and Henquin, 2001) and failure to initiate electrical activity (Hermans et al., 1987). Therefore, despite the initiation of a Ca^{2+} response at low glucose, this is unlikely to greatly influence insulin secretion and consequently glucagon secretion.

4.4.9. Hyperglycaemia does not decrease sensitivity to acetylcholine

The ACh effect remained intact after exposure to both hypo- and hyperglycaemic conditions, with the response actually increasing in islets cultured at 30 mM glucose. This suggests diabetes does not negatively influence cholinergic signalling in the α-cell and that any aberrations to the parasympathetic response to hypoglycaemia are more likely due to defects in the central (e.g. HAAF) and PNS. Previous work had suggested hyperglycaemic conditions lead to downregulation of the M3 mAChR in islets, with a 50% reduction in M3 mAChR mRNA levels after 72 h culture at 16 mM glucose compared to 72 h at 5.5 mM glucose. This was further shown to reduce insulin secretion to carbachol (a non-specific cholinergic agonist) but whether this also translated to glucagon secretion is unknown (Hauge-Evans et al., 2014). The data here suggest this is not the case, although, it must be noted that *in vivo* studies using mouse models of diabetes may yield different results, due

to the increased longevity of hyperglycaemia. Notably, streptozotocin-treated diabetic rats exhibited a reduced glucagon response to carbachol (Ahren et al., 1995).

4.4.10. Acetylcholine also stimulates human α-cells

The difference in the cholinergic response between rodent and human islets is intriguing. Whilst ACh did not initiate a robust response in human α-cells compared to the results in mice, a subset of cells were activated by the neurotransmitter. Additionally, the generation of a response by both nicotine and oxotremorine M further suggests that the mechanism of the effect is conserved between the two species.

Whether a significant counterregulatory role persists, however, remains ambiguous. Application of ACh to human islets, stimulates insulin and somatostatin secretion, yet has minimal effects on glucagon secretion despite, as observed here, a subset of α-cells being responsive to the neurotransmitter (Molina et al., 2014). The clear increase in islet parasympathetic activity after induction of hypoglycaemia and the reduction in the glucagon response when autonomic input is blocked (Schwartz et al., 1978, Havel and Ahren, 1997) are unlikely to be coincidental. Notably, the parasympathetic neuropeptides co-secreted with ACh, including VIP, GRP and PACAP, have all been demonstrated to stimulate glucagon secretion in various animal models (Ahren and Lundquist, 1982, Bloom et al., 1983, Fridolf et al., 1992, Filipsson et al., 1997, Havel et al., 1997). It could, therefore, be the case that ACh alone does not suffice in mounting a clear counterregulatory response but instead potentiates the effects of the neuropeptides co-secreted alongside it to increase glucagon secretion. In addition, ACh may also act via an autocrine feedback loop to increase glucagon secretion in α-cells (Rodriguez-Diaz et al., 2011).

Limitations of working with human islets should also be considered. Islet quality was often lower than that seen with mouse islets and, crucially, there were large differences in the ACh Ca^{2+} response between different islet donors. This suggests the absence of a large and consistent response may be reflective of external factors, which could affect gene expression (e.g. ischaemia time), and not necessarily a true reflection of the human islet cholinergic response. This is further underlined by the minimal effect of ACh in non-α-cells, despite evidence to the contrary (Rodriguez-Diaz et al., 2011, Molina et al., 2014).

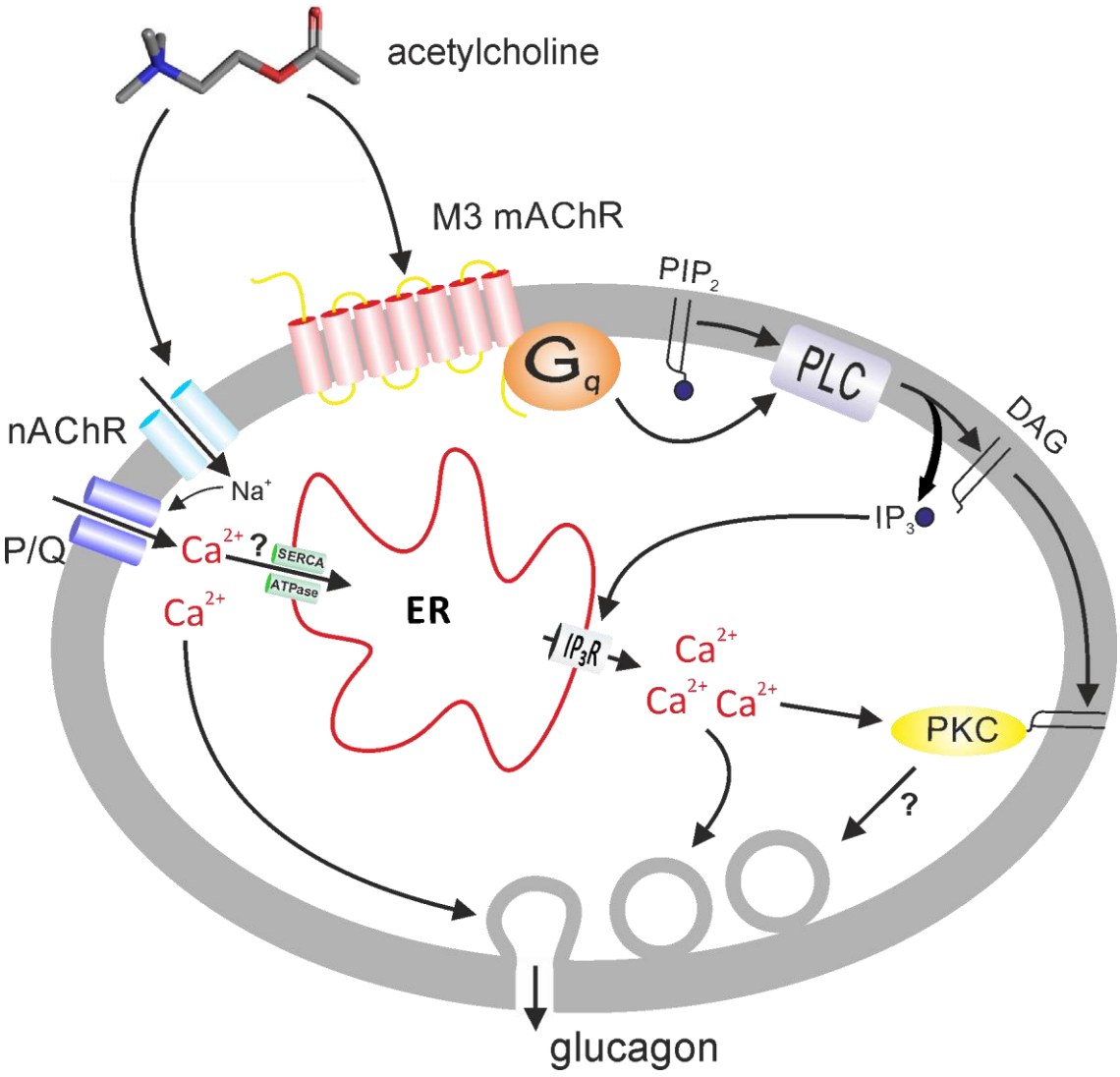


Figure 4.13 - Model

ACh targets both mAChRs and nAChRs in α-cells. The neurotransmitter predominantly functions via the muscarinic G_q pathway (likely by binding to the M3 mAChR), causing IP_3-mediated Ca^{2+} release, $[DAG]_i$ increase and subsequent PKC activation, resulting in an increase in glucagon secretion. PKC acts in a Ca^{2+}-independent manner, presumably targeting the secretory machinery. ACh also binds to nAChRs at the plasma membrane, leading to influx of Na^+ (and possibly Ca^{2+}), and subsequent activation of P/Q-type voltage-gated Ca^{2+} channels, directly causing glucagon secretion. It may also supplement the ER stores via the SERCA-ATPase, facilitating muscarinic-mediated ER-Ca^{2+} release.

4.5. Conclusion

Cholinergic signalling in α-cells encompasses both types of ACh receptors. The ACh effect appears to be largely the result of a muscarinic-driven mechanism, which targets the G_q pathway, initiating Ca^{2+}-release from the ER stores. Yet the existence of a nicotinic component is also shown, which can directly increase glucagon secretion independent of muscarinic stimulation. The mechanism appears to be conserved in human islets, although less widespread across the α-cell population and does not appear to be negatively influenced by hyperglycaemic conditions. Future work should focus on human islets, elucidating the role of neuropeptides and the nicotinic pathway.

Chapter 5: Cytoplasmic Acidification Drives Glucagon Secretory Defects in Diabetes

5.1. Introduction

This chapter will focus on how hyperglycaemia and diabetes affect intrinsic α-cell function. Dysfunctional glucagon secretion is a feature of both type 1 and type 2 diabetes (Cryer, 2012), yet the exact mechanisms underlying these changes are poorly understood. As the role of glucagon in diabetes is becoming clearer, understanding how hyperglycaemia targets the α-cell could be critical in our ability to manage the condition.

Glucagon secretion is 'inverted' in diabetes, it is reduced under hypoglycaemic conditions and stimulated rather than inhibited by hyperglycaemia (Cryer, 2012). As diabetes is characterised by β-cell failure, much of the effort to understand and explain these defects has focused on the resulting changes in β- to α-cell paracrine signalling (Kjems et al., 2001, Hope et al., 2004, Zhou et al., 2004, Zhou et al., 2007b, Cooperberg and Cryer, 2009, Cryer, 2012), with increased α-cell somatostatin signalling also implicated (Yue et al., 2012, Karimian et al., 2013).

However, loss of paracrine signalling is insufficient to fully explain all glucagon secretory defects, particularly the absent glucagon response to hypoglycaemia (see 1.4.1). The main limitation is that α-cell activity is viewed as merely a product of its paracrine environment, ignoring the intrinsic control the α-cell possesses, which has been convincingly demonstrated (Bode et al., 1999, Liu et al., 2004, Leclerc et al., 2011, Zhang et al., 2013). Intrinsic control must therefore also become defective for the glucagon response to

become absent. Notably, diabetic abnormalities can be recreated in non-diabetic human islets by increasing K_{ATP} channel activity and alleviated in type 2 diabetic islets by decreasing K_{ATP} channel activity, without disrupting α-cell paracrine input (Zhang et al., 2013). It has therefore been postulated that type 2 diabetes and the resulting hyperglycaemia increases α-cell K_{ATP} channel activity, driving dysregulation of glucagon secretion. The mechanism by which this occurs however remains unknown.

To investigate how hyperglycaemia interacts with the α-cell and disrupts glucagon secretion, mice lacking the citric acid enzyme fumarate hydratase (which converts fumarate into malate) in their β-cells were used (Fh1βKO). Crucially, these mice exhibit a progressive form of the disease, similar to type 2 diabetes, they are normoglycaemic until approximately 8 weeks of age but then undergo rapid and progressive deterioration of glucose homeostasis, with almost complete loss of glucose-stimulated insulin secretion at 15 weeks (Figure A4.1). A reduction in fumarate hydratase expression or activity causes intracellular fumarate levels to increase. Accumulation of fumarate can then cause the post-translational modification, succination, in which fumarate reacts with cysteine residues on proteins (Alderson et al., 2006). Notably, this is often regarded as a biomarker for impaired mitochondrial dysfunction and is deleterious for protein function (Merkley et al., 2014). As expected, succination was clearly evident in β-cells yet, notably, was also observed in α-cells[17] (Figure A4.2 a), despite Fh1 knockdown being β-cell-specific (Figure A4.2 b). Furthermore, glucagon secretion was also aberrant. While it remained normal in young, normoglycaemic Fh1βKO mice it became dysregulated once hyperglycaemia had developed. In such islets, glucagon secretion was attenuated at 1 mM glucose with no change in secretion at 6 mM glucose (Figure A4.3 a). Notably, similarly to

[17] Also observed in cardiomyocytes and renal tubular cells.

human type 2 diabetic islets (Zhang et al., 2013) these defects could be corrected by tolbutamide application (Figure A4.3 b). Suggesting that they result from increased K_{ATP} channel activity.

The progressive nature of disease onset and similar secretion profiles to type 2 diabetes in these mice, makes the Fh1βKO mouse a useful model to explore the dysregulation of glucagon secretion. Due to evidence of α-cell mitochondrial dysfunction (succination) and the finding that secretory defects were alleviated by tolbutamide application, it appeared likely that glucagon secretory defects were the result of reduced ATP production. The principle determinant of mitochondrial ATP production is pH, with the electron transport chain pumping protons into the mitochondrial intermembrane space before they re-enter the mitochondrial matrix via ATP synthase. Crucially, pH of the mitochondrial matrix is tightly linked to pH_i (Azarias et al., 2011), which can be affected by various acute metabolic processes including metabolic H^+ production[18] (Casey et al., 2010) and mitochondrial H^+ consumption (Shepherd and Henquin, 1995, Salgado et al., 1996). Furthermore, increases in $[Ca^{2+}]_i$ have been reported to acidify the cytoplasm (Shepherd and Henquin, 1995, Salgado et al., 1996, Stiernet et al., 2007). These processes are offset by plasmalemmal acid extruders and acid loaders, which are critical in maintaining pH_i at appropriate levels (Casey et al., 2010). How glucose affects α-cell pH_i however has yet to be shown. Hence pH_i in intact islets from control and Fh1βKO islets was measured using the pH-indicator dye SNARF-5F and confocal microscopy, to test the effects of acute

[18] Glycolysis in the cytosol produces pyruvate and 2 H^+. In *anaerobic* respiration pyruvate is subsequently converted to lactate in a reaction catalysed by lactate dehydrogenase. Under *aerobic* conditions, pyruvate enters the mitochondria (the tricarboxylic acid (TCA) cycle and oxidative phosphorylation) releasing CO_2 and H_2O back into the cytoplasm. These react to form carbonic acid (H_2CO_3), catalysed by carbonic anhydrase, which dissociates to H^+ and HCO_3^-.

hyperglycaemia and succination, and see whether the effects on glucagon secretion in Fh1βKO mice correlated with changes in α-cell pH_i. At the same time $[Ca^{2+}]_i$ was measured using Fluo-4.

5.2. Methods

For islet isolation, islet culture, data analysis, general reagents and solutions

Please refer to main methods section

5.2.1. Mice

The knockout mice were generated by crossing Fh1fl/flRip2-Cre+/-22 or Fh1tm1Pjpfl/fl23 with Ins-Cre+/-24 to generate Fh1fl/flIns-Cre+/-designated Fh1βKO. Fh1 was deleted specifically in β-cells in these strains and littermates were used as controls (designated as CTL). Young, normoglycaemic Fh1βKO were culled at 6-8 weeks of age. Older, hyperglycaemic Fh1βKO mice were culled at 13-20 weeks of age. The mice were of a C57BL/6J background. Remaining experiments were carried out in islets isolated from NMRI or C57BL/6J mice (designated as *wildtype*). *n* was taken as number of cells.

5.2.2. Simultaneous $[Ca^{2+}]_i$ and pH_i measurements

Intact mouse islets were loaded in the Ca^{2+} indicator dye Fluo-4-AM (6 μM; Thermo Fisher, UK) for 90 min, followed by the ratiometric pH indicator dye SNARF-5F (6 μM; Thermo Fisher, UK; Figure 5.1) for a further 50 min. Both dyes were dissolved in EC1 solution containing 6 mM glucose, with 1 μl of pluronic F-127 (Thermo Fisher, UK) added to aid with solubility. Islets were then transferred to an 'open' perifusion chamber (Figure 2.2) before being imaged using a Zeiss AxioVert 200 microscope equipped with Zeiss 510-META laser confocal scanning system, using 40x/1.3 objective. The EC1 bath solution was perifused at 200 μl/min (using a peristaltic pump) with various stimuli added,

temperature of the bath solution was maintained at 34 °C throughout each recording. A 488 nm argon laser (1.8% intensity) was used to excite Fluo-4 and emitted light was collected at 530 nm; a 543 nm helium neon laser (2.6% intensity) was used to excite SNARF-5F with emission collected at 600 nm (emission maxima at pH6, and 650 nm, emission maxima at pH9). Images were acquired every 30 s (0.03 Hz), using 512x512 frame scanning mode with a pixel dwell time of 13 μs and a bit depth of 8-bit.

α-Cells were distinguished based on spontaneous $[Ca^{2+}]_i$ activity at 3 mM glucose (neurone-like cells were considered to be δ-cells and omitted). Glutamate was not used in this study due to the considerable length of the recordings compared to those in the previous 2 chapters (approx. 90 min compared to approx. 40 min); any further additional time to wash out the glutamate effect would have increased the impact of photobleaching on Fluo-4 and SNARF-5F. Ammonium chloride (NH_4Cl), which increases pH_i (due to entry of NH_3 into the cytoplasm) and sodium acetate ($NaCOOCH_3$), which decreases pH_i (due to entry of CH_3COOH into the cytoplasm), were used to confirm functionality of the SNARF-5F probe.

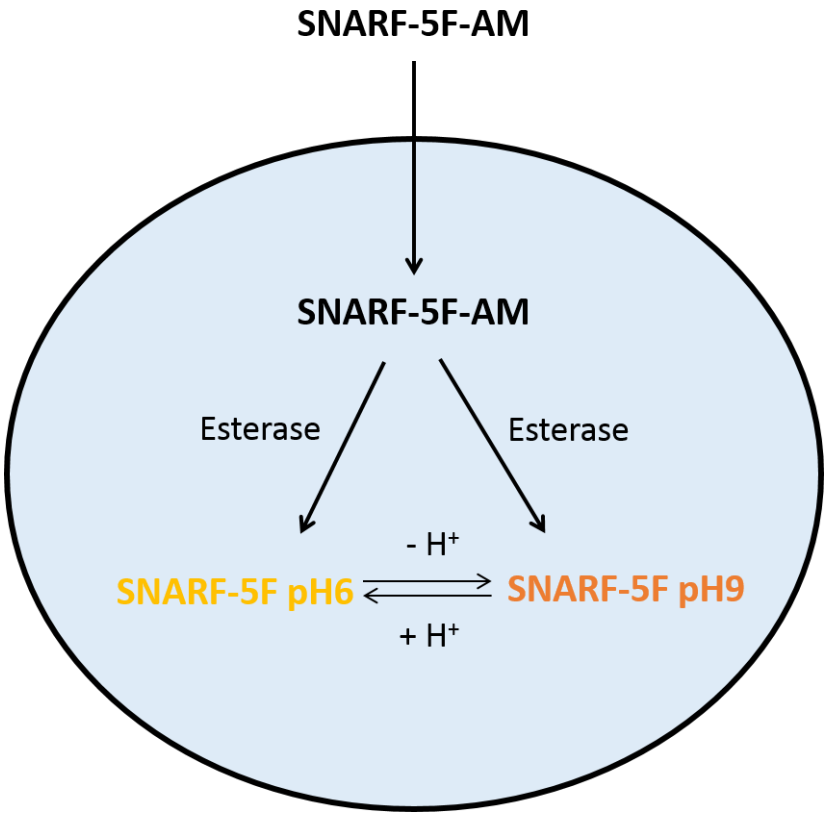


Figure 5.1 - SNARF-5F mechanism

SNARF-5F in its esterified form (SNARF-5F-AM) is able to cross the plasma membrane. Cellular esterases then break the ester bond. In its unesterified form SNARF-5F can bind H^+. The probe exists in an equilibrium between H^+-bound (SNARF-5F pH6) and H^+-unbound (SNARF-5F pH9) states, if pH_i falls the equilibrium is pushed towards the bound state, with a decrease in SNARF-5F pH9 fluorescence intensity and an increase in SNARF-5F pH6 florescence intensity, and *vice versa* if pH_i increases. Hence the SNARF-5F pH9:SNARF-5F pH6 ratio reports the pH_i of the cell.

5.2.3. Data analysis (simultaneous $[Ca^{2+}]_i$ and pH_i measurements)

Image sequences were analysed using open-source FIJI software (see 2.7). The numerical data produced was then analysed using Microsoft Excel, with corresponding traces produced using IgorPro. Basal pH_i was calculated by taking the mean of the first 15 SNARF-5F ratio values from each cell, while pH_i after glyceraldehyde and 20mM application was calculated by taking a mean of the values where the SNARF-5F ratio reached a nadir. These values were then averaged across the whole cell population. Statistical analysis was performed using SPSS. Kruskall-wallis ANOVA or Friedmann's ANOVA were used to compute the significance of difference between independent and dependent samples, respectively. Differences with $p < 0.05$ were considered significant.

5.2.4. Reagents

D-glyceraldehyde, NH_4Cl, $NaCOOCH_3$, the non-specific SGLT blocker phlorizin, the Na^+ substitute N-methyl-D-Glucamine and the SGLT2-specific blocker dapagliflozin were purchased from Sigma-Aldrich (UK)

5.3. Results

5.3.1. Effect of hyperglycaemia on cytoplasmic pH in pancreatic α-cells

To establish the acute effects of hyperglycaemia and succination on α-cell pH_i, islets from CTL mice were perifused in a bath solution containing 3 mM glucose before application of two stimuli: 10 mM D-glyceraldehyde and 20 mM glucose. D-glyceraldehyde was used to replicate the condition of succination, which is known to inhibit the enzyme D-glyceraldehyde-3-phosphate dehydrogenase (GAPDH) (Blatnik et al., 2008), reducing glycolytic flux and leading to the accumulation of upstream glycolytic 3- and 6- carbon intermediates, such as D-glyceraldehyde. The build-up of D-glyceraldehyde was expected to cause cytoplasmic acidification, as reported in β-cells (Best et al., 1988a, Best et al., 1988b, Arkhammar et al., 1986a), due to the accumulation of non-metabolisable acidic by-products with potentially toxic effects (MacDonald, 1989; Figure 5.2). 20 mM glucose was applied to ascertain whether acute hyperglycaemia affected α-cell pH_i. pH_i was quantified at the start of the recording, after D-glyceraldehyde application and after 20 mM glucose application. Effects in β-cells were also recorded.

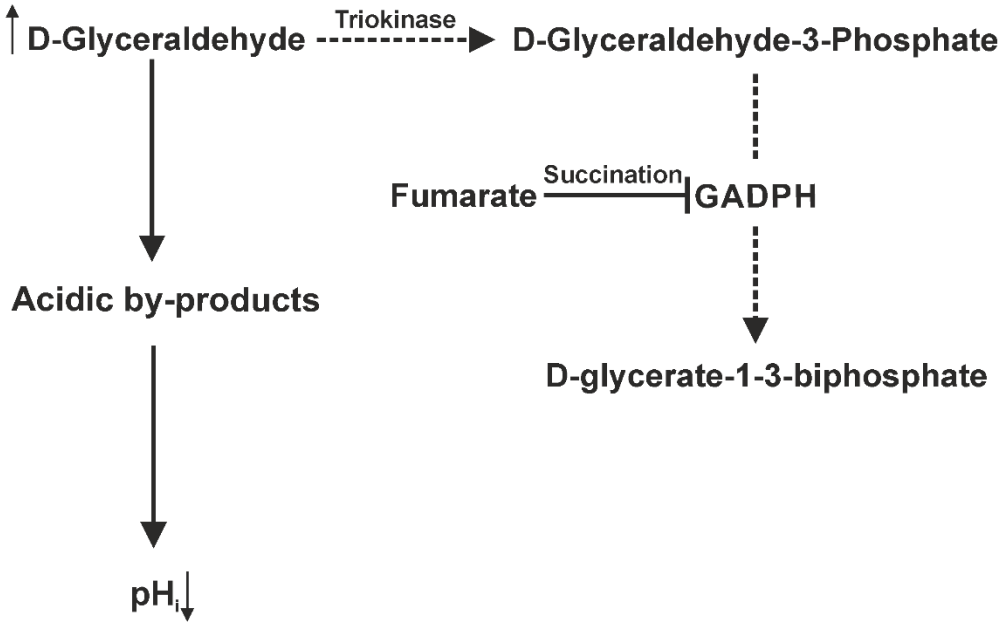


Figure 5.2 - Effect of glyceraldehyde on pH_i

GADPH is an enzyme involved in the 6th step of glycolysis. Succination of GADPH reduces glycolytic flux, this leads to accumulation of upstream D-glyceraldehyde, which is subsequently metabolised into non-metabolisable acidic by-products, lowering pH_i.

10 mM D-glyceraldehyde ($p < 0.001$ vs. basal) and 20 mM glucose ($p < 0.001$ vs. basal) both reversibly acidified the cytoplasm of CTL α-cells ($n = 66$; Figure 5.3 a, d, e, f). Notably, the drop in pH_i after D-glyceraldehyde application correlated with an increase in $[Ca^{2+}]_i$, with $[Ca^{2+}]_i$ oscillations increasing in frequency and/or amplitude in 61% (40/66) of cells. Remaining cells were either unaffected (29% -19/66 cells) or inhibited (11% - 7/66 cells). By contrast, the effect of 20 mM glucose on pH_i was $[Ca^{2+}]_i$-independent with minimal correlation between the two. Most cells were inhibited (48% - 32/66 cells) or unaffected by the change in glucose (47% - 31/66 cells), with only a small proportion stimulated (5% - 3/66 cells). In CTL β-cells, 10 mM D-glyceraldehyde ($p < 0.001$ vs. basal) and 20 mM glucose ($p < 0.001$ vs. basal) both sharply decreased pH_i, in both cases this correlated with a dramatic rise in $[Ca^{2+}]_i$ ($n = 163$; Figure 5.4 a, d).

After demonstrating that acute exposure to high glucose induced cytoplasmic acidification in α-cells, the difference in pH_i between CTL and Fh1βKO islets was investigated to establish the effects of prolonged hyperglycaemia on the α-cell (that remained genetically normal). 10 mM D-glyceraldehyde and 20 mM glucose were again added to test whether their effects on $[Ca^{2+}]_i$ and pH_i were altered in the diabetic α-cell. In hyperglycaemic Fh1βKO α-cells, the cytoplasm was acidified with basal pH_i significantly lower compared to CTL ($p < 0.001$ vs. CTL basal; $n = 57$; Figure 5.3 c, f). A minimal dip in pH_i persisted in response to 10 mM D-glyceraldehyde ($p < 0.001$ vs. Basal; Figure 5.3 f). However, there was no effect of 20 mM glucose on pH_i ($p = 0.354$ vs. Basal; Figure 5.3 d, e, f), presumably due to prolonged hyperglycaemia resulting in pH_i reaching a minimum. In terms of $[Ca^{2+}]_i$ activity, α-cells appeared to be less responsive to D-glyceraldehyde with only 37% (21/57 cells) stimulated by the metabolite, most unaffected (47% - 28/57 cells) and a small proportion inhibited (16% - 9/57 cells); correlating with the diminished pH_i

response. The $[Ca^{2+}]_i$ response to 20 mM glucose appeared to be largely unchanged with 56% (32/57 cells) of α-cells inhibited, 40% (23/57 cells) unaffected and 4% (2/57 cells) stimulated. In hyperglycaemic Fh1βKO β-cells, 10 mM D-glyceraldehyde ($p = 0.873$ vs. basal) and 20 mM glucose ($p = 0.631$ vs. basal) pH_i responses were absent, correlating with no effect on $[Ca^{2+}]_i$. There was also marked acidification at basal glucose ($p < 0.001$ vs. CTL basal; $p < 0.001$ vs. normoglycaemic Fh1βKO basal; $n = 39$; Figure 5.4 c, d).

Experiments were also performed on islets from younger, normoglycaemic Fh1βKO mice. In α-cells from these mice, cytoplasmic acidification was evident at basal glucose (3 mM) ($p < 0.001$ vs. CTL basal; $n = 26$; Figure 5.3 b, f). Crucially, however, application of 10 mM D-glyceraldehyde ($p = 0.003$ vs. basal) and 20 mM glucose ($p = 0.003$ vs. basal) (Figure 5.3 b, d, e, f) were still capable of acidifying the cytoplasm. In terms of $[Ca^{2+}]_i$ dynamics, normoglycaemic Fh1βKO α-cells were less responsive to D-glyceraldehyde than CTL α-cells but more so than hyperglycaemic Fh1βKO α-cells, with 54% (14/26 cells) stimulated by D-glyceraldehyde, 42% (11/26 cells) showing no change in $[Ca^{2+}]_i$ activity and 4% (1/26 cells) inhibited. Regarding the response to 20 mM glucose, its inhibitory effect was reduced compared to CTL, albeit only slightly, with 61% (16/26 cells) of α-cells unresponsive to 20 mM glucose, 31% (8/26 cells) inhibited and 8% (2/26 cells) stimulated. In normoglycaemic Fh1βKO β-cells, $[Ca^{2+}]_i$ and pH_i responses to D-glyceraldehyde and 20 mM glucose were similar to CTL, acidification at basal glucose was evident however ($p < 0.001$ vs. CTL basal; $n = 95$; Figure 5.4 b, d).

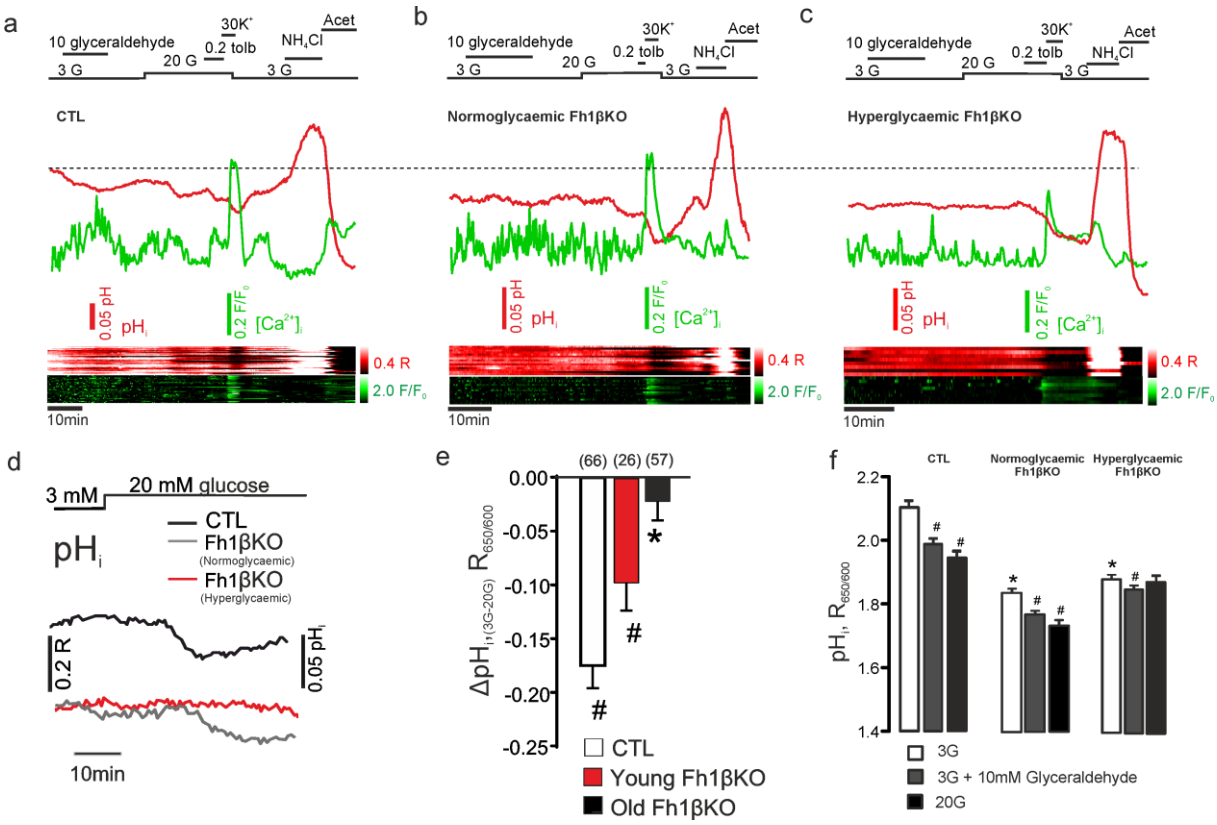


Figure 5.3 - α-Cells in islets from Fh1βKO mice display cytoplasmic acidification

(a-c) Top panel shows average pH_i (red) and average $[Ca^{2+}]_i$ (green) trace in α-cells from single recording of CTL islet (a), normoglycaemic Fh1βKO islet (b) and hyperglycaemic Fh1βKO islet (c). Bottom panel shows heatmaps depicting change in pH_i (red) and $[Ca^{2+}]_i$ (green) from corresponding recording. **(d)** Comparison of effect of 20 mM glucose on pH_i quantified as SNARF-5F ratio in CTL (black), normoglycaemic Fh1βKO (grey) and hyperglycaemic Fh1βKO (red) α-cells (n.b. difference in basal is also shown). **(e)** Change in pH_i after 20 mM glucose application quantified in CTL (open column), normoglycaemic (young) Fh1βKO (red column) and hyperglycaemic (old) Fh1βKO (black column) α-cells. **(f)** pH_i quantified as SNARF-5F ratio in α-cells from CTL, normoglycaemic Fh1βKO (red) and hyperglycaemic Fh1βKO islets at basal (open columns), after 10 mM D-glyceraldehyde application (grey columns) and 20 mM glucose application (black columns). # Effect of D-glyceraldehyde or 20 mM glucose is significant ($p < 0.05$) vs. basal * pH_i at basal is significantly different ($p < 0.05$) vs. CTL basal. Error bars represent ± SEM.

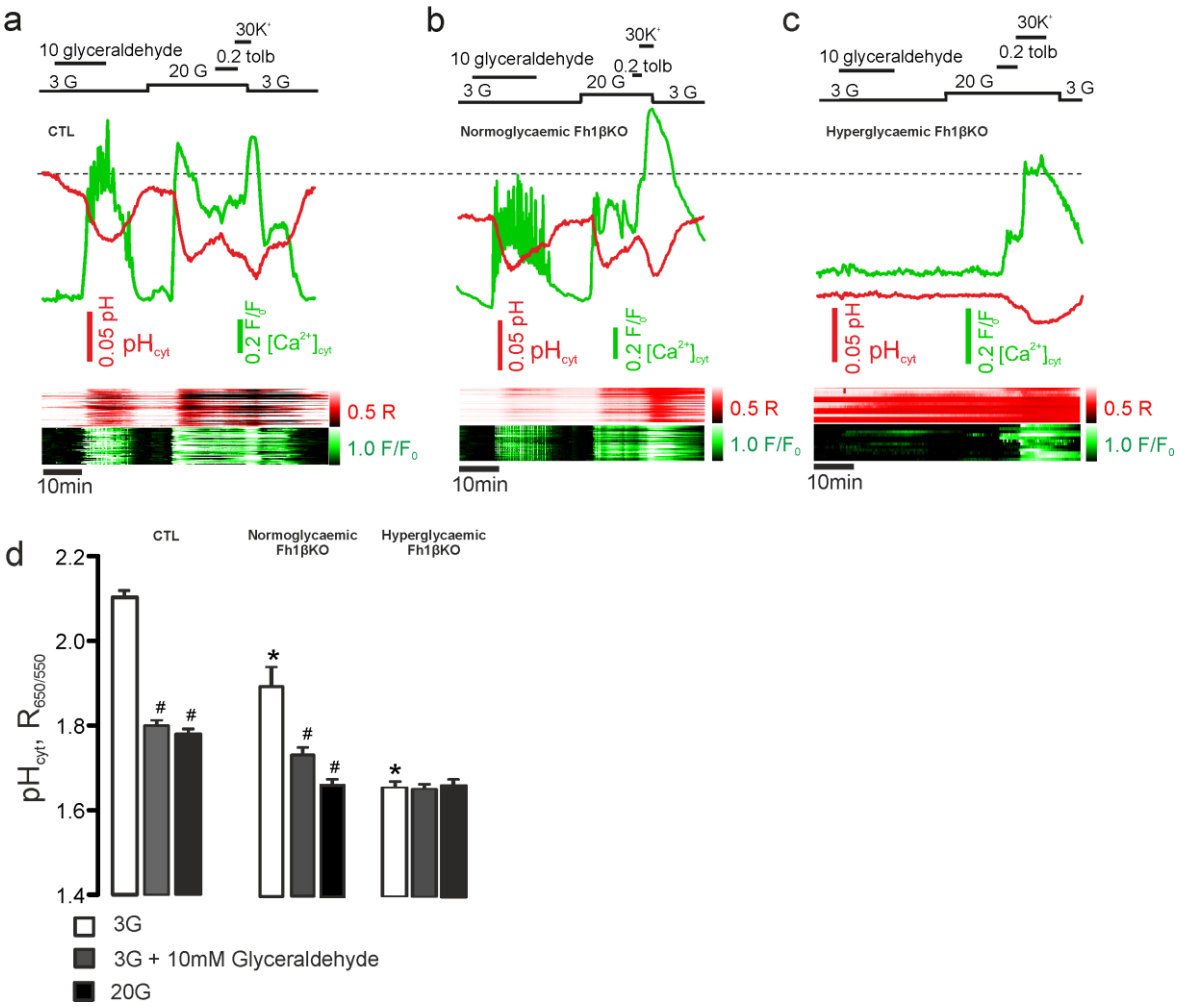


Figure 5.4 - β-Cells in islets from Fh1βKO mice display cytoplasmic acidification

(a-c) Top panel shows average pH_i (red) and average $[Ca^{2+}]_i$ (green) trace in β-cells from single recording of CTL islet (a), normoglycaemic Fh1βKO islet (b) and hyperglycaemic Fh1βKO islet (c) . Bottom panel shows heatmaps depicting change in pH_i (red) and $[Ca^{2+}]_i$ (green) from corresponding recording. **(d)** pH_i quantified as SNARF ratio in β-cells from CTL, normoglycaemic Fh1βKO (red) and hyperglycaemic Fh1βKO islets at basal (open columns), after 10 mM D-glyceraldehyde application (grey columns) and 20 mM glucose application (black columns). # Effect of D-glyceraldehyde or 20 mM glucose is significant ($p < 0.05$) vs. basal * pH_i at basal is significantly different ($p < 0.05$) vs. CTL basal. Error bars represent ± SEM.

5.3.2. Na^+-coupled glucose transport – a driver of α-cell dysfunction in diabetes?

The results from CTL and Fh1βKO islets demonstrated that both acute and prolonged hyperglycaemia acidified the cytoplasm in α-cells. What caused the acidification however was unclear. Na^+-dependent glucose transporters (SGLTs) co-transport Na^+ and glucose. They account for a small proportion of glucose-uptake in α-cells (Bonner et al., 2015); with evidence of expression of SGLT1 (*Slc5a1*) in mouse islets (Figure A4.4). Increased availability of glucose during hyperglycaemia would increase flux through SGLTs and could therefore also increase $[Na^+]_i$. As demonstrated by the non-metabolisable glucose analogue αMDG[19] increasing $[Na^+]_i$ in the α-cell, an effect abolished by the non-specific SGLT blocker phlorizin (Figure A4.5 b). Plasmalemmal Na^+/H^+ antiporters are critical in maintaining pH_i. By utilising the Na^+ gradient between the inside and outside of the cell they remove H^+ from the cytoplasm in exchange for Na^+ (Casey et al., 2010). Hence, it was hypothesised that the increase in $[Na^+]_i$ via hyperglycaemia-driven SGLT transport dissipates the Na^+ gradient, decreasing H^+ extrusion via Na^+/H^+ antiporters and thus acidifying the cytoplasm.

To test whether altering the Na^+ gradient could indeed influence α-cell pH_i, $[Na^+]_o$ was lowered from 140 mM to 10 mM[20] in *wildtype* islets (diazoxide was also applied to ensure effects were a result of changes in Na^+/H^+ exchange rather than changes in electrical activity). As expected, this significantly reduced pH_i in α-cells ($p < 0.001$ vs. basal; $n = 59$; Figure 5.5 a, b). The change was reversible, with pH_i returning to normal when $[Na^+]_o$ was increased back to 140 mM ($p = 0.896$ vs. basal).

[19] Used to avoid metabolic effects of glucose, which could affect the Na^+/K^+-ATPase and voltage gated Na^+ channels

[20] Na^+ was replaced in the extracellular solution with N-methyl-D-Glucamine

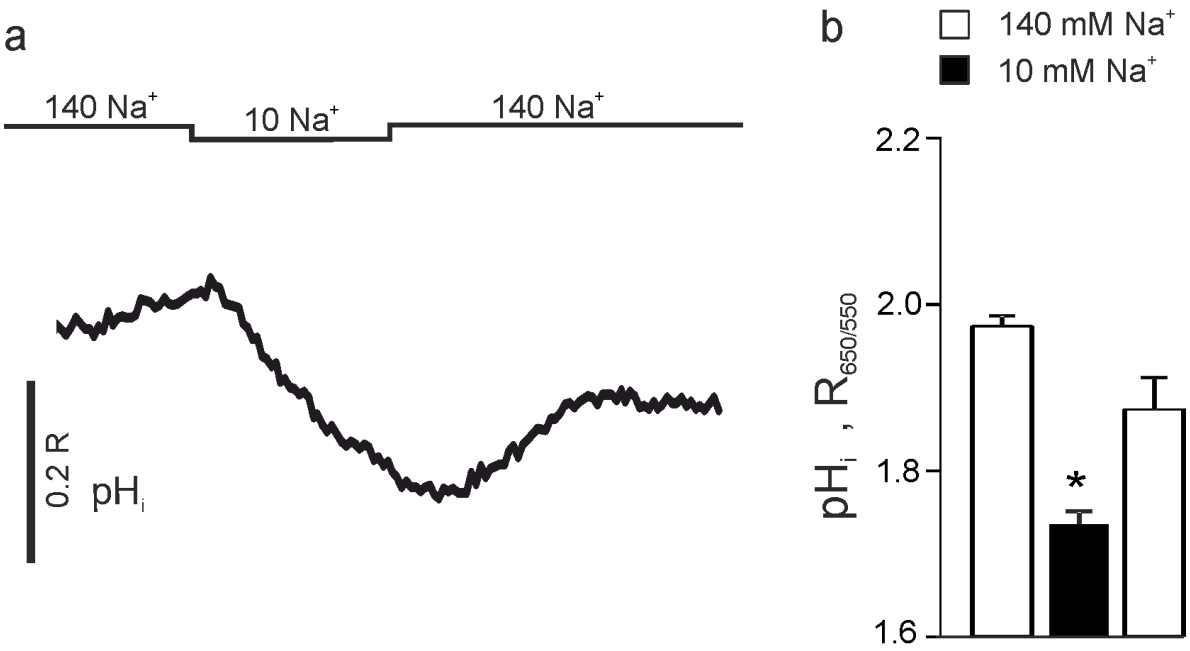


Figure 5.5 - Effect of $[Na^+]_o$ on cytoplasmic pH in α-cells

(a) Average pH_i trace of α-cells taken from a single recording of C57BL/6J islet, exposed to 10 mM $[Na^+]_o$ **(b)** pH_i quantified as SNARF-5F ratio for α-cells (from C57BL/6J islets) exposed to 140 mM Na^+ (open column *to left*), 10 mM Na^+ (black column) and after reapplication of 140 mM Na^+ (open column *to right*). Experiments done at 10 mM glucose. *Difference is significant vs. Initial pH_i at 140 mM $[Na^+]_o$. Error bars represent ± SEM.

After demonstrating the important relationship between Na^+ and pH_i in α-cells, the potential role of SGLT Na^+ import in the Fh1βKO α-cell phenotype was investigated. To test this, *wildtype* islets were exposed to 11 mM glucose, 20 mM glucose and 20 mM glucose + 50 μM phlorizin for 48 h and basal pH_i measured. As expected, α-cells exposed to 20 mM glucose presented with a significant reduction in pH_i compared to those incubated at 11 mM (p = 0.009 vs. 11 mM Basal; n = 67; Figure 5.6 a), similar to the acidification observed in α-cells from hyperglycaemic Fh1βKO mice. Interestingly, these effects were reversed in the 20 mM + 50 μM phlorizin group, with a significantly higher basal pH_i compared to the 20 mM group (p = 0.01 vs. 20 mM Basal; n = 33; Figure 5.6 a) and no significant difference in basal pH_i compared to the 11 mM group (p = 0.196 vs. 11 mM Basal).

Crucially, this correlated with effects on glucagon secretion, α-cells in islets cultured under normoglycaemic conditions behaved normally with high secretion at 1 mM glucose and reduced secretion at 20 mM. While in islets cultured at 20 mM glucose, glucagon secretion was inverted (low at 1 mM glucose and stimulated at 20 mM). However, when islets were incubated at 20 mM glucose in the presence of phlorizin, normal glucagon secretion was maintained (Figure A4.5 a). Notably, GSIS remained normal in the 20 mM group, thus ruling out altered insulin paracrine signalling as the cause of inverted glucagon secretion in these islets (Figure A4.5 f). The diminishment in glucagon secretion instead resulted from depleted ATP production, with the ATP response to 10 mM glucose greatly attenuated in the 20 mM group, this was also reversed by phlorizin application (Figure A4.5 d, e). Notably, the SGLT2-specific blocker dapagliflozin had no effect on pH_i (p = 0.188 vs. *wt* (20 mM glucose 48 h culture); n = 31; Figure 5.6 b), ATP production or glucagon secretion, suggesting increased transport through SGLT1 was responsible for the α-cell

phenotype, in keeping with the low islet expression of SGLT2 (*Slc5a2*) (Figure A4.4). In β-cells, chronic hyperglycaemia caused cytoplasmic alkalinisation ($p < 0.001$ vs. basal (11 mM); $n = 25$; Figure 5.7 a). Both phlorizin ($p = 0.057$ vs. basal (20 mM); $n = 63$; see Fig. 5.6 a) and dapagliflozin ($p = 0.086$ vs. basal (20 mM); $n = 31$; Figure 5.7 b) were without effect.

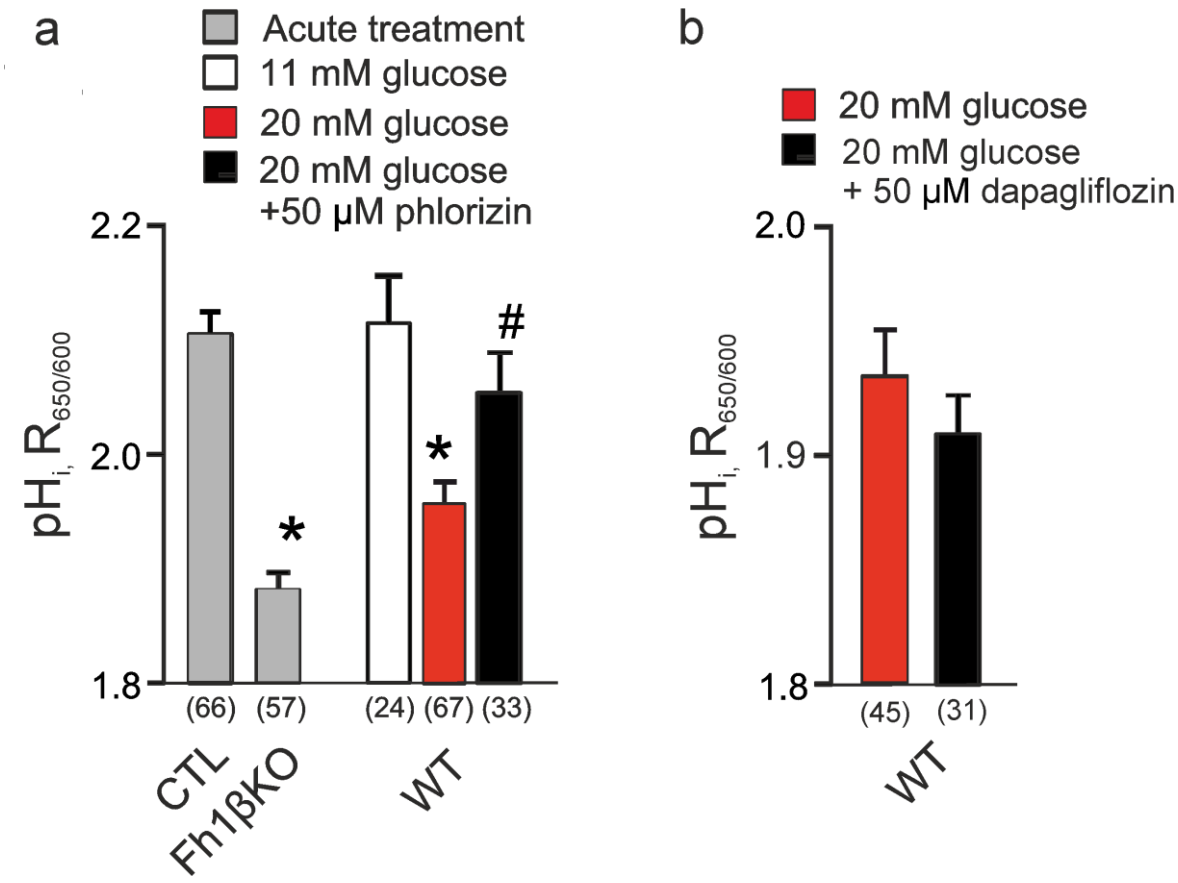


Figure 5.6 - Effect of chronic high glucose culture on cytoplasmic pH in α-cells is alleviated by phlorizin

(a) Basal pH_i quantified as SNARF-5F ratio for α-cells from CTL and hyperglycaemic Fh1βKO islets compared to α-cells from NMRI islets exposed to 11 mM glucose (open column), 20 mM glucose (red column) and 20 mM glucose + 50 µM phlorizin (black column) for 48 h. **(b)** pH_i quantified as SNARF-5F ratio for α-cells from NMRI islets exposed to 20 mM glucose (red column) and 20 mM glucose + 50 µM dapagliflozin (black column) for 48 h. *pH_i at basal is significant ($p < 0.05$) vs. CTL/11 mM glucose group. # pH_i at basal is significant ($p < 0.05$) vs. 20 mM glucose group. Error bars represent ± SEM.

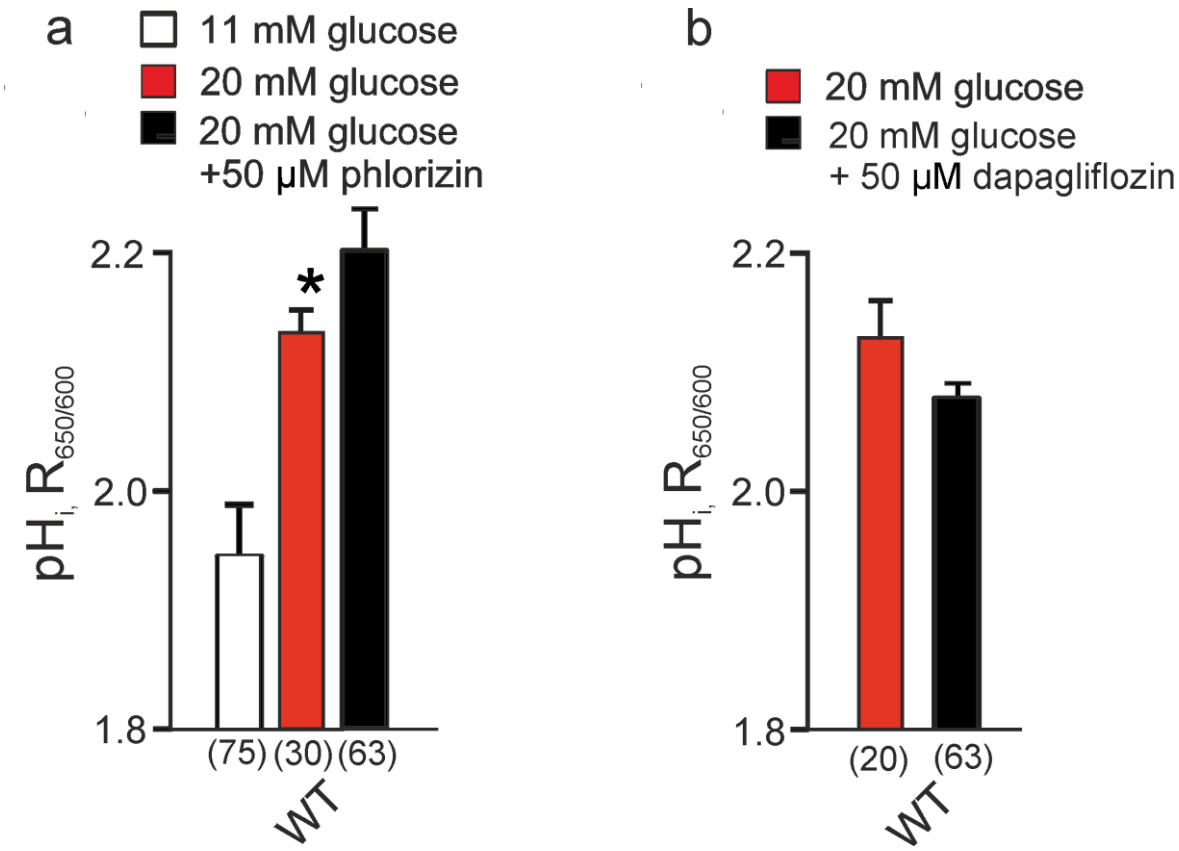


Figure 5.7 - Effect of chronic high glucose culture on cytoplasmic pH in β-cells with or without SGLT-blockers

(a) Basal pH_i quantified as SNARF ratio in β-cells from NMRI islets exposed to 11 mM glucose (open column), 20 mM glucose (red column) and 20 mM glucose + 50 µM phlorizin (black column) for 48 h. **(b)** pH_i quantified as SNARF ratio for β-cells from NMRI islets exposed to 20 mM glucose (red column) and 20 mM glucose + 50 µM dapagliflozin (black column) for 48 h. *pH_i at basal is significant ($p < 0.05$) vs. 11 mM glucose group. Error bars represent ± SEM.

5.4. Discussion

5.4.1. Hyperglycaemia disrupts α-cell glucose sensing via cytoplasmic acidification

These data provide a model that explains how glucagon secretion becomes dysregulated in diabetes. It is demonstrated that hyperglycaemia increases flux through SGLT1 in α-cells, thereby increasing $[Na^+]_i$ and reducing the Na^+ gradient, which, in turn, causes decreased H^+ export via Na^+/H^+ antiporters. It can be speculated that the fall in pH_i culminates in acidification of the mitochondrial matrix, disrupting fumarate hydratase activity and ATP production, and reducing glucagon secretion at low glucose.

5.4.2. Acute effect of 20 mM glucose in α-cells is $[Ca^{2+}]_i$ independent

Acute application of 10 mM D-glyceraldehyde and 20 mM glucose caused slight cytoplasmic acidification in α-cells from CTL or normoglycaemic Fh1βKO islets. The effect of D-glyceraldehyde on pH_i appeared to result from increased frequency of $[Ca^{2+}]_i$ oscillations (65% - 40/66 cells) rather than the production of acidic by-products by D-glyceraldehyde metabolism (Figure 5.8), whose build-up likely takes longer. To truly replicate succination chronic treatment with the triose may therefore be required. High K^+, which depolarises the plasma membrane and causes Ca^{2+} influx independently from metabolism, also reduced pH_i in α-cells, reaffirming a role for $[Ca^{2+}]_i$ in the regulation of α-cell pH_i. The acidifying effect of $[Ca^{2+}]_i$ is thought to result from displacement of H^+ from intracellular sites such as the lysosome (Patel and Docampo, 2010) and mitochondria (Jiang et al., 2009) by Ca^{2+}/H^+ exchange (via Na^+), as well as possible H^+ exchange at the plasma membrane via the Ca^{2+}-ATPase (Schwiening et al., 1993). Increased frequency of

action potentials (and therefore $[Ca^{2+}]_i$ oscillations) is observed in response to glucose concentrations that inhibit glucagon secretion (e.g. 6 mM glucose) (Zhang et al., 2013). As D-glyceraldehyde can enter glycolysis via conversion into D-glyceraldehyde-3-phosphate by triokinase (ExPASy, 2012), the same phenomenon is likely the case here. Of course, a proportion of the glyceraldehyde pH_i effect may be attributable to metabolic H^+ production that coincides with its effects on $[Ca^{2+}]_i$.

Notably, increases in $[Ca^{2+}]_i$ cannot explain the acute acidifying effects of 20 mM glucose as it generally inhibited or had no effect on $[Ca^{2+}]_i$ dynamics in α-cells (Figure 5.8). Based on my remaining data it can be assumed this phenomenon is at least in part the result of increased flux through SGLT1 (whilst acknowledging that H^+ production from metabolic pathways may also contribute). While the small dip in pH_i after acute elevation of glucose is unlikely to be deleterious to α-cell function, prolonged hyperglycaemia would chronically reduce pH_i affecting mitochondrial function as demonstrated by the effects of high glucose culture.

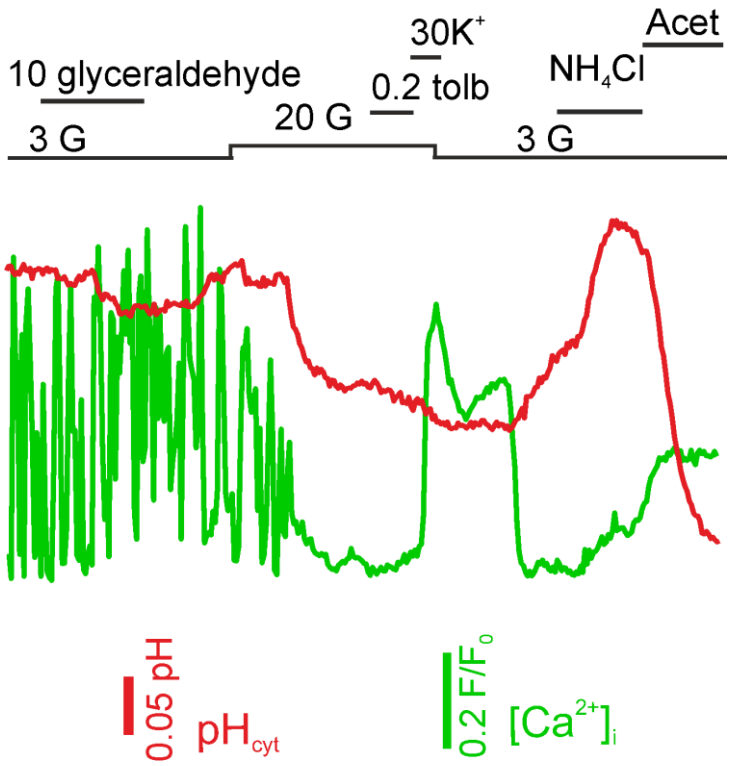


Figure 5.8 - Representation of $[Ca^{2+}]_i$ and pH_i relationship in CTL α-cell

Representative recording of $[Ca^{2+}]_i$ and pH_i in a single α-cell from a CTL islet. Note, cell shows increased frequency of oscillations after 10 mM D-glyceraldehyde application, which corresponds with a dip in pH_i; while, 20 mM silences $[Ca^{2+}]_i$ oscillations yet pH_i still falls sharply.

5.4.3. Acute effects of D-Glyceraldehyde and glucose in β-cells are dependent on $[Ca^{2+}]_i$

The effects of 10 mM glyceraldehyde and 20 mM glucose were much larger in β-cells than in α-cells. They appeared to be dependent on $[Ca^{2+}]_i$, which dramatically increased in response to 10 mM glyceraldehyde and 20 mM glucose. This was reinforced by the effect of high K^+, which caused a further reduction in pH_i. The acidifying effect of glyceraldehyde in β-cells is in agreement with previous literature (Best et al., 1988a, Best et al., 1988b, Arkhammar et al., 1986a). Although, as mentioned, this was thought to be via a metabolic effect (Figure 5.2). In my hands, it instead appeared to correlate with stimulation of $[Ca^{2+}]_i$ activity. Of course, metabolic H^+ production (via *aerobic/anaerobic* respiration) may explain some of the acute pH_i change. However, as alluded to in α-cells, one expects the damaging build-up of acidic metabolites to occur more slowly; notably, 24 h culture with D-glyceraldehyde (24 h) resulted in blunting of GSIS (Figure A4.6).

Unlike D-glyceraldehyde, previous studies have shown glucose to alkalinise rather than acidify pH_i in β-cells (Lindstrom and Sehlin, 1984, Deleers et al., 1985, Arkhammar et al., 1986a, Best et al., 1988a, Best et al., 1988b, Juntti-Berggren et al., 1991, Shepherd and Henquin, 1995, Salgado et al., 1996, Stiernet et al., 2007). This has been attributed to increased activity of the Na^+/H^+ antiporters (Deleers et al., 1985, Juntti-Berggren et al., 1991, Shepherd and Henquin, 1995), HCO_3^- uptake (Deleers et al., 1985, Shepherd and Henquin, 1995, Stiernet et al., 2007) and mitochondrial consumption of H^+ during ATP synthesis (Shepherd and Henquin, 1995, Salgado et al., 1996) overcoming the acidifying effects of Ca^{2+} and metabolic H^+ production. Contrastingly, in this study it instead appears the acidifying effect of $[Ca^{2+}]_i$ overcomes any alkalising effect of glucose on β-cell pH_i.

This disparity could be due to the use of different pH-indicator dyes, extracellular solutions, methodologies and the effects of islet dissociation. Importantly, under chronic hyperglycaemic conditions alkalisation was indeed observed, suggesting the acute acidifying effect of $[Ca^{2+}]_i$ is eventually overcome. Notably, a study in rat α-cells did also demonstrate a fall in pH_i in response to glucose applied acutely (Pace and Tarvin, 1986).

5.4.4. Acidification of α-cells in Fh1βKO islets results from increased Na^+ influx via SGLT1 due to hyperglycaemia

Hyperglycaemic Fh1βKO α-cells exhibited significantly lower basal pH_i compared to CTL α-cells, there was also no change in pH_i after application of 20 mM glucose (by contrast, 20 mM glucose reduced pH_i in normoglycaemic Fh1βKO α-cells). The latter may be the consequence of pH_i already being maximally reduced in hyperglycaemic Fh1βKO α-cells, glucose is therefore unable to produce a further reduction. Culture of islets under hyperglycaemic conditions mimicked these findings, with pH_i significantly lower after 48 h exposure to 20 mM glucose. In both cases, the glucagon response at low glucose was attenuated. One can therefore postulate that hyperglycaemia, whether in the hyperglycaemic Fh1βKO mouse or *wildtype* islets exposed to 20 mM glucose culture, results in decreased pH_i that causes the observed glucagon secretory defects.

The alleviation of the effects of high glucose culture by phlorizin, in terms of pH_i, ATP and glucagon secretion, suggests increased flux through SGLT1[21] is the cause of these effects. Notably, the ability of phlorizin to reverse the effects of high glucose culture on

[21] Due to the lack of effect with the SGLT2-specific inhibitor dapagliflozin

glucagon secretion cannot be due to it merely reducing glucose uptake into the α-cell. Glut1 and Glut3 are far more highly expressed than SGLT1 in mouse α-cells (Benner et al., 2014, Adriaenssens et al., 2016) and thus account for a far greater proportion of glucose uptake. Its effect on pH_i is therefore more likely to be a consequence of the associated Na^+ uptake, with the reduction in pH_i after lowering of $[Na^+]_o$ confirming the dependence of pH_i on the Na^+ gradient. This dependence likely stems from the plasmalemmal Na^+/H^+ antiporter (e.g. NHE1), whose activity is diminished when $[Na^+]_o$ decreases or $[Na^+]_i$ increases (due to SGLT1 Na^+ import). It should be noted, however, that pH_i is also under the regulation of Cl^-/HCO_3^- antiporters, Na^+/HCO_3^- cotransporters and Na^+-driven Cl^-/HCO_3^- antiporters (Bonar and Casey, 2008, Choi, 2012), with HCO_3^- uptake shown to play a critical role in neighbouring β-cells in both regulation of basal pH_i and prevention of the acidifying effects of Ca^{2+} influx (Deleers et al., 1983, Deleers et al., 1985, Shepherd and Henquin, 1995, Stiernet et al., 2007). While Cl^-/HCO_3^- antiporters usually act as acid loaders (although they can act in reverse) (Bonar and Casey, 2008) the Na^+/HCO_3^- cotransporters and Na^+-driven Cl^-/HCO_3^- antiporters are acid extruders, utilising the Na^+ gradient to facilitate entry of the alkaline HCO_3^- ion (Choi, 2012). They would, therefore, also be inhibited by an increase $[Na^+]_i$, meaning a proportion of the acidification may be due to reduced HCO_3^- import into the cytoplasm.

5.4.5. Cytoplasmic acidification as a marker for β-cell dysfunction in diabetes

Cytoplasmic acidification and glucagon secretory defects could be reproduced with 48 h high glucose culture. By contrast, β-cells underwent cytoplasmic alkalisation and were still functional under these conditions with GSIS remaining normal. This suggests the α-cell is more susceptible to the effects of hyperglycaemia and its dysregulation may manifest at

the early stages of type 2 diabetes or even prior to disease onset. Thus, the acidification seen in hyperglycaemic Fh1βKO β-cells must have a different cause. Fh1 ablation leads to the build-up of the acidic fumarate (and potentially other acidic metabolites via GADPH succination). This would overwhelm the acid extrusion machinery, with the build-up of these metabolites gradually reducing pH_i until mitochondrial function is compromised, disrupting ATP production (Figure A4.7) and removing the ability of the β-cell to respond to its environment.

In the normoglycaemic Fh1βKO β-cells, fumarate build-up and acidification are evident yet are minimised, presumably due to fumarate being shuttled out of the cytoplasm, metabolised and used in anaplerosis to maintain TCA cycle function and thus ATP production (Adam et al., 2013). When this process can no longer be sustained, cytoplasmic acidification occurs, mitochondrial ATP production falls and GSIS becomes suppressed, leading to hyperglycaemia. This initiates a vicious cycle by which β-cell function is further compromised, with the associated increase in mitochondrial metabolism further increasing fumarate levels and acidification, leading to rapidly worsening hyperglycaemia. Any alkalising effect of H^+ consumption by ATP synthase would also be lost. Interestingly, GSIS was restored when hyperglycaemic Fh1βKO islets were cultured for 72 h under normoglycaemic conditions (12 mM glucose) or at 20 mM glucose in the presence of the glucokinase inhibitor mannoheptulose (Figure A4.8), thereby confirming β-cell dysfunction during hyperglycaemia is driven by accelerated glucose metabolism. As succination is observed in human type 2 diabetic islets (Figure A4.2 c), the metabolic demand on the human β-cell resulting from hyperglycaemia (>48 h) appears to have similar consequences.

5.4.6. $[Ca^{2+}]_i$ dynamics in Fh1βKO α-cells

Ca^{2+} responsiveness in α-cells to D-glyceraldehyde decreased from CTL to normoglycaemic Fh1βKO to hyperglycaemic Fh1βKO, correlating with decreasing ΔpH_i after glyceraldehyde application across the three groups[22]. This could be perceived as a gradual loss of metabolic sensing with larger number of α-cells becoming unresponsive to the metabolite. However, there were no obvious trends in terms of the $[Ca^{2+}]_i$ response to 20 mM glucose between the three groups, disputing a loss of glucose sensing under hyperglycaemic conditions. One should note that due to the low sampling rate of 0.03 Hz, drawing accurate interpretations of the fast Ca^{2+} signal is difficult.

5.4.7. Reduced pH_i interferes with mitochondrial function

The observed decrease in α-cell pH_i in Fh1βKO and high glucose-cultured islets likely impacts negatively on mitochondrial function as evidenced by reduced ATP production (Figure A4.5 d, e). Protons in the cytoplasm can enter the outer mitochondrial membrane via porins (Blachly-Dyson and Forte, 2001) and the inner mitochondrial membrane via H^+ antiporters (Bernardi, 1999), UCP2 or due to the shuttling of metabolites across the inner mitochondrial membrane (Azarias et al., 2011). Crucially, a study in astrocytes illustrated that small changes in pH_i could have large effects on mitochondrial matrix pH (Azarias et al., 2011). Furthermore, glucose-induced alkalisation of the matrix is crucial for mitochondrial ATP production, as has been demonstrated in β-cells (Wiederkehr et al.,

[22] Although, this may also be caused by the lower basal pH_i meaning any further acidification due to D-glyceraldehyde has a limited effect on the overall H^+ concentration.

2009). Therefore, cytoplasmic (and mitochondrial) acidification can be expected to have detrimental effects on ATP production.

It is how this fall in ATP production affects the K_{ATP} channel that explains the absent glucagon response to low glucose in Fh1βKO and high glucose-cultured islets. Under physiological conditions, the increase in K_{ATP} channel activity caused by hypoglycaemia (low ATP/ADP ratio) increases glucagon secretion. However, by using a high dose of the K_{ATP} channel activator diazoxide to maximally activate K_{ATP} channels, it has been demonstrated that further K_{ATP} channel activation is inhibitory (MacDonald et al., 2007). This demonstrates that K_{ATP} channel activity and glucagon secretion in the α-cell follows a bell-shaped relationship. Similarly to diazoxide, the considerable diminution of ATP production would therefore increase K_{ATP} channel activity beyond physiological levels; meaning low glucose is no longer stimulatory and at high glucose glucagon secretion is not reduced, and even increased as observed in the islets cultured at 20 mM glucose for 48 h (Figure 5.9). Crucially, this model fits with the diazoxide and the mitochondrial inhibitor oligomycin inverting glucagon secretion in non-diabetic islets, and the glucagon secretory defects in type 2 diabetic donors (Zhang et al., 2013) and Fh1βKO (hyperglycaemic) mice being corrected by tolbutamide (Figure A4.3 b).

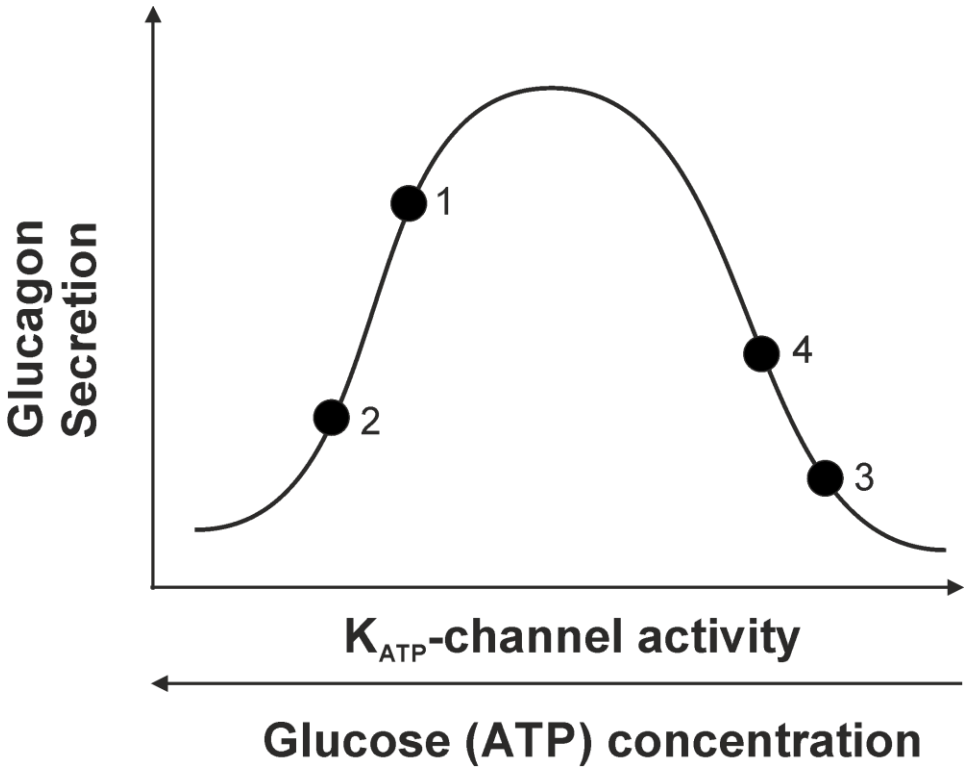


Figure 5.9 - K_{ATP} channel activity in α-cells and the effect of compromised ATP production

Under basal physiological conditions, ATP production is sufficient to maintain low K_{ATP} channel activity, to the left of the bell-shaped curve (1). This means when ATP production is increased by high glucose, K_{ATP} -channel activity is reduced thereby reducing glucagon secretion (2). Under hyperglycaemic conditions as seen in the Fh1βKO mouse, ATP production is compromised pushing K_{ATP} to the right hand-side of the bell-shaped curve (3). This means when ATP production is increased by high glucose K_{ATP}-channel activity is reduced but glucagon secretion is increased (4). Adapted from Walker et al. (2011)

The acidification of the mitochondria is yet to be demonstrated experimentally. It may not represent the only way cytoplasmic acidification compromises mitochondrial function. Cytoplasmic acidification, at least initially, would increase the proton-motive force across the inner mitochondrial membrane. An increase in the proton gradient may influence mitochondrial Ca^{2+}, which is critical for the function of TCA cycle dehydrogenases (Traaseth et al., 2004). Mitochondrial Ca^{2+} is regulated by the MCU, a Ca^{2+} uniporter responsible for Ca^{2+} influx into the mitochondrial matrix, and the NCLX, a Na^{+}/Ca^{2+} antiporter responsible for Ca^{2+} extrusion (Boyman et al., 2013). The increased proton-motive force can be expected to increase flux through the mitochondrial NHE (mNHE), leading to Na^{+} extrusion from the matrix and re-entry via the NCLX in exchange for Ca^{2+}, thus reducing mitochondrial matrix Ca^{2+} (Crompton and Heid, 1978; Figure 3.10 b). Indeed, a 0.1 unit decrease in pH was shown to result in Ca^{2+} release from rat insulinoma mitochondria (Prentki et al., 1983). In the same study, increasing Na^{+} also led to mitochondrial Ca^{2+} release (Prentki et al., 1983). Furthermore, in cardiomyocytes increasing $[Na^{+}]_i$ has been shown to compromise mitochondrial function reducing NADH production, a phenomenon attributed to the same mechanism (Maack et al., 2006). This suggests the increase in $[Na^{+}]_i$ due to SGLT1 import could also increase NCLX flux and thereby reduce ATP production, independently of its effect on pH (Figure 5.10 c).

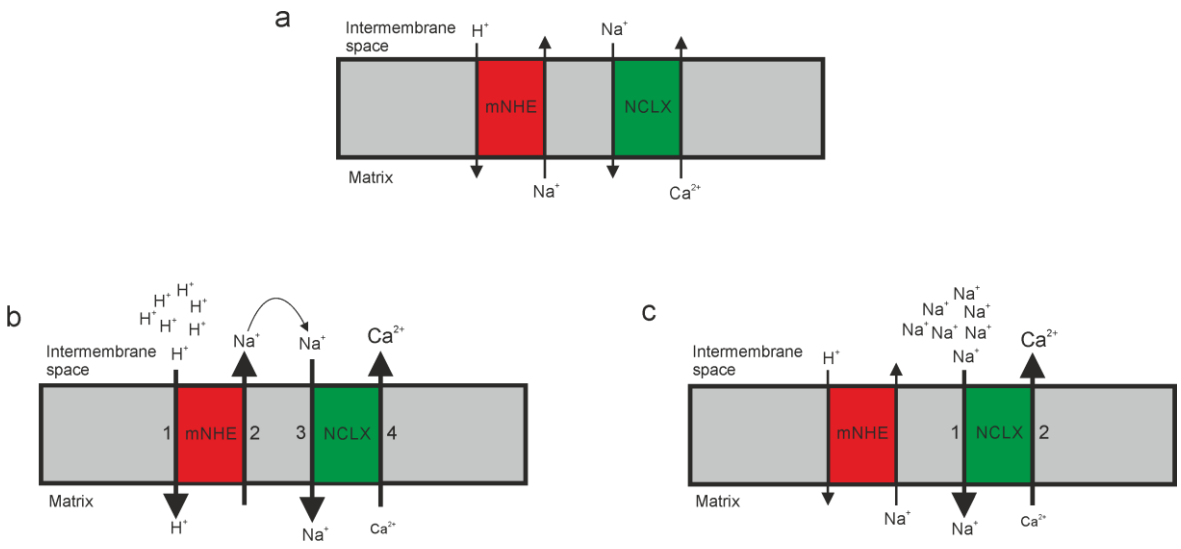


Figure 5.10 - Alternative Ca^{2+}-dependent mechanisms of mitochondrial acidification

(a) Transport proteins embedded in the inner mitochondrial membrane maintain mitochondrial ion concentrations under physiological conditions. Mitochondrial Ca^{2+} must be kept sufficiently high for the TCA cycle to function. **(b)** The increase in H^+ observed in Fh1βKO α-cells causes increased transport via the mNHE (1), leading to Na^+ extrusion from the mitochondrial matrix (2). Na^+ then renters via the NCLX (3) leading to Ca^{2+} extrusion from the matrix (4). **(c)** Increased flux via SGLT1 causes an increase in $[Na^+]_i$. This increases flux through the NCLX (1) resulting in Ca^{2+} extrusion from the mitochondrial matrix (2).

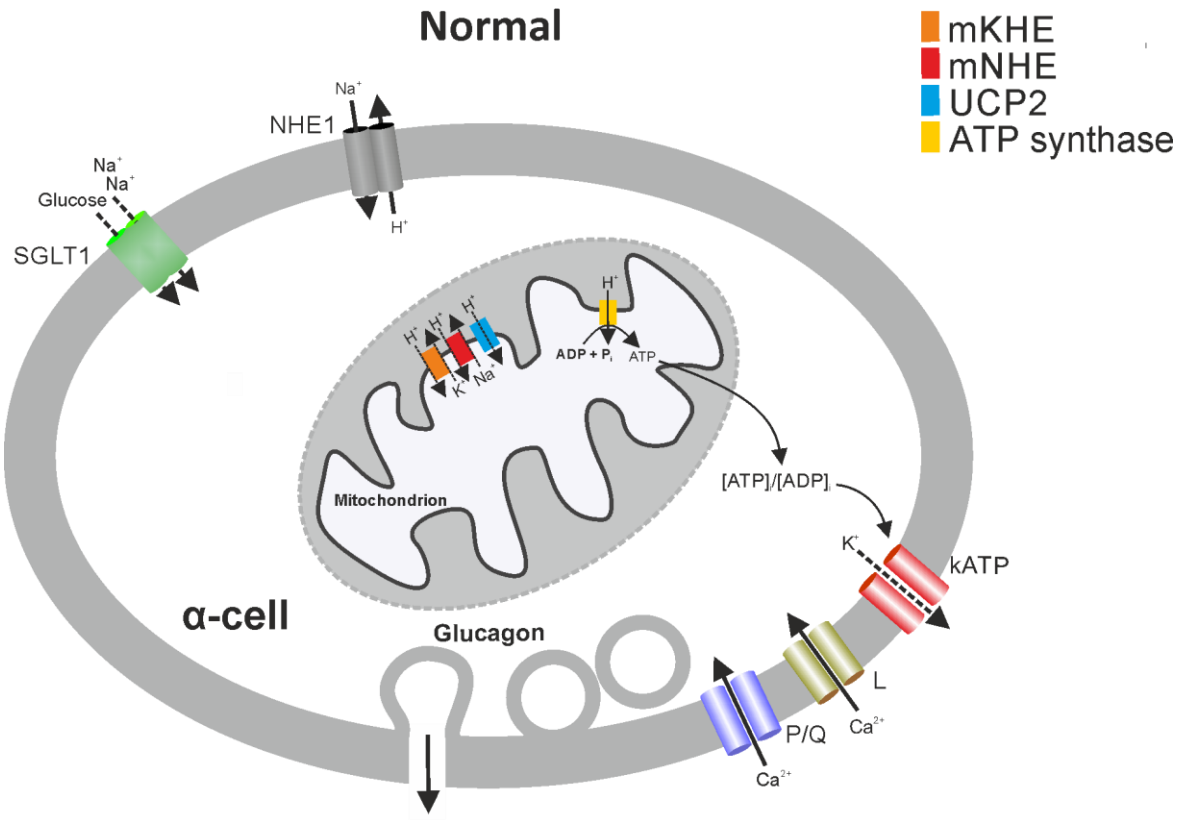
5.4.8. The pH-dependence of Fh1 results in increased succination in α-cells from Fh1βKO mice

While the differences in pH_i between CTL and Fh1βKO as well as islets exposed to 11 mM and 20 mM glucose were small, the relationship between Fh1 activity and pH is steep (Figure A4.9). Therefore, even a small change in mitochondrial matrix pH brought about by SGLT-mediated Na^+ influx could lead to a significant decrease in Fh1 activity, build-up of fumarate and increased appearance of succination, reducing mitochondrial matrix pH further and compromising ATP production. Notably, other TCA cycle enzymes, including malate dehydrogenase (Bernstein and Everse, 1978), α-ketoglutarate dehydrogenase (Lai and Cooper, 1986) and isocitrate dehydrogenase (Willson and Tipton, 1980), are pH dependent and would also respond unfavourably to the acidic conditions. As succination was also observed in cardiomyocytes and renal tubular cells, it is tempting to speculate that hyperglycaemia also affects these cells via a similar mechanism. Notably, these tissues express SGLT co-transporters (particularly high levels in the Kidney), which may explain why they are susceptible to the secondary complications of diabetes. Importantly, increased succination was also observed in α-cells in islets from type 2 diabetic patients (Figure A4.2 c).

5.4.9. An added benefit of SGLT-2 blockers?

For patients with type 2 diabetes, dapagliflozin and other SGLT-2 blockers are already commonly used anti-diabetic drugs that alleviate hyperglycaemia by preventing glucose reabsorption into the circulation from the kidney. Despite low expression in the mouse (Figure A4.4), there is evidence of SGLT2 expression in human α-cells (Bonner et al., 2015, Blodgett et al., 2015). Thus, these data suggest added beneficial effect of SGLT2

inhibitors on glucagon secretion and possibly secondary complications. Notably, type 2 diabetic patients who take SGLT2 inhibitors have increased rates of endogenous glucose production, driven by an increase in plasma glucagon (Ferrannini et al., 2014, Merovci et al., 2014). However, a consensus on the cause of this has not been reached, with a glucose-dependent (Bonner et al., 2015) and an electrogenic (Pedersen et al., 2016) effect of dapagliflozin on the α-cell both demonstrated. In consideration with the model in this study, the blocking of SGLT2 Na^+ import would (via cytoplasmic/matrix alkalisation) restore α-cell glucose sensing. This could lead to the observed increase in plasma glucagon. Notably, SGLT2 inhibition does not correct against postprandial hyperglucagonaemia (Ferrannini et al., 2014). This indicates that if the proposed correction of α-cell glucose sensing by SGLT2 inhibition is true, it does not alleviate hyperglucagonaemia. Instead loss of paracrine suppression rather than intrinsic α-cell dysfunction likely causes hyperglucagonaemia (see 1.4.1).



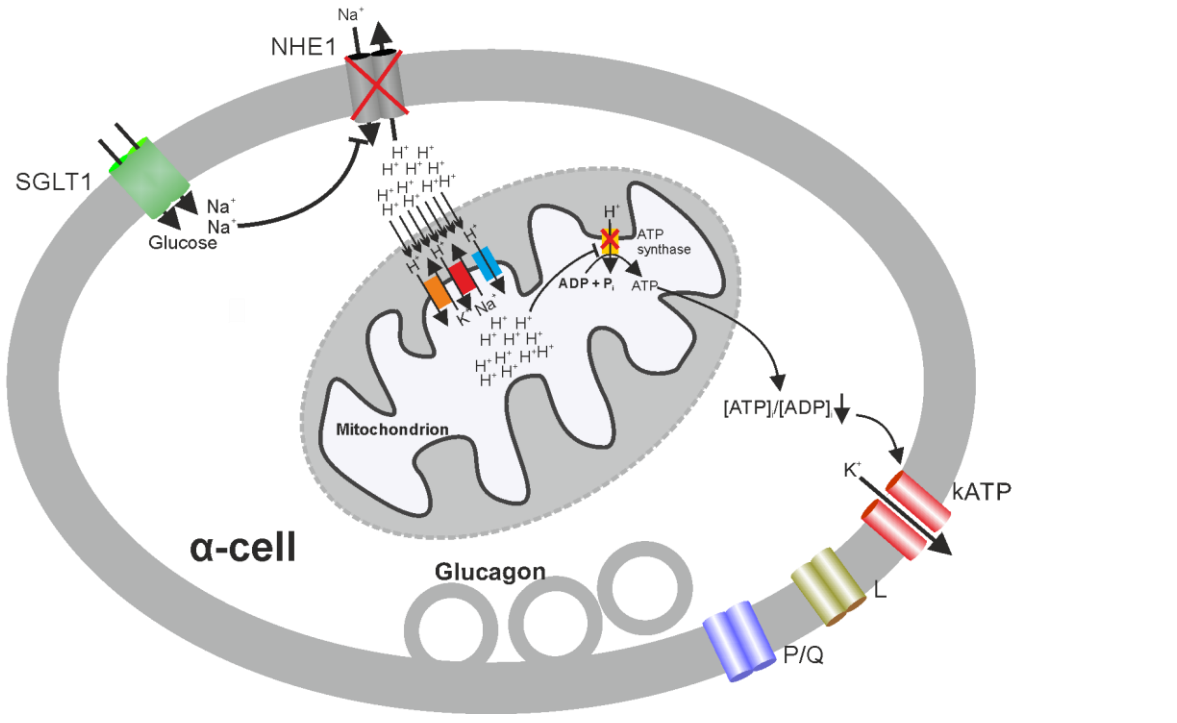

After Hyperglycaemia
Na+
NHE1
SGLT1
Na+
Na+
Glucose
H+ H+ H+

Figure 5.11 - Model

Under normoglycaemic conditions, glucose and 2 Na^+ ions are co-transported across the plasma membrane via SGLT1, while NHE1 utilises the Na^+ gradient to extrude 1 H^+ for 1 Na^+. Mitochondrial H^+ homeostasis is undisturbed and α-cell glucose sensing intact. However, when hyperglycaemia ensues, flux through SGLT1 is augmented due to the increased availability of the glucose substrate. This results in increased $[Na^+]_i$, which reduces the Na^+ gradient between the outside and inside of the α-cell reducing Na^+-dependent H^+ extrusion through NHE1 (and Na^+/HCO_3^- cotransporters). Without H^+ extrusion via NHE1, cytoplasmic H^+ concentration increases lowering pH_i. Protons can cross the outer mitochondrial membrane via porins, entering the mitochondrial intermembrane space before crossing the inner mitochondrial membrane and entering the mitochondrial matrix via mitochondrial transporters (and shuttling of metabolites). The acidification of the mitochondrial matrix dissipates the H^+ gradient disrupting ATP production. As Fh1 activity is highly pH-dependent, fumarate levels rise leading to increased succination and further matrix acidification (establishing a vicious cycle of progressive matrix acidification and reduced fumarate activity). Several other TCA cycle enzymes would also be affected by the acidic pH, meaning flux through the cycle would decrease. The lack of ATP production reduces the ATP/ADP ratio, increases K_{ATP} activity, thereby ablating glucagon secretion.

5.5. Conclusion

Using the Fh1βKO mouse model, hyperglycaemic-driven cytoplasmic acidification was identified as a potential cause for the absent glucagon response to hypoglycaemia in diabetes. Based on my data, acidification appears to occur as a result of chronic Na^+ influx via SGLT1 leading to abnormally high $[Na^+]_i$, thereby preventing H^+ extrusion via Na^+/H^+ antiporters. One can then speculate that H^+ entry into the intramitochondrial matrix causes the observed diminishment of ATP production, thus compromising proper glucose sensing in the α-cell leading to defective glucagon secretion. It was further found that the effects of chronic high glucose on pH_i in α-cells could be avoided using the SGLT-blocker phlorizin, which correlated with an improvement in ATP production and glucagon secretion. This suggests that defective glucagon secretion (and secondary complications) may be avoided or reduced by blocking SGLTs, thus warranting further mechanistic and clinical studies of SGLT2 inhibitors in humans.

Chapter 6: Insulin-induced Hypoglycaemia Suppresses Glucagon Secretion by SGLT2-dependent Stimulation of Somatostatin Secretion from Pancreatic δ-Cells

6.1. Introduction

Impaired glucose counterregulation is iatrogenic, it does not occur in diabetic patients who do not take insulin (or insulin secretagogues/sensitizers) (Cryer, 2002). Excessive or poorly-timed dosage of insulin is required to trigger hypoglycaemia with the absent glucagon response (and autonomic dysfunction) preventing its alleviation. These two processes are often viewed distinctly, with the excessive glucose-lowering effect of therapeutic insulin attributed to abnormally high levels of insulin in peripheral tissues, and a direct suppressive effect on the α-cell dismissed due to therapeutic concentrations of insulin falling considerably below intraislet levels (Davidson et al., 2016).

However, excessive insulin dosage has consistently been shown to suppress the glucagon response to hypoglycaemia in both type 1 diabetic patients (Liu et al., 1992, Cooperberg and Cryer, 2010) and in non-diabetic volunteers (Diamond et al., 1991, Liu et al., 1991). It was assumed that this effect was due to a direct inhibitory effect of insulin on the α-cell, which becomes hypersensitive due to endogenous insulin deprivation[23] (Liu et al., 1992). However, it may be better explained by an indirect effect via the δ-cell. Notably, δ-cells have been shown to exert a tonic inhibitory effect on glucagon secretion even at low

[23] Glucagon suppression in type 1 diabetic patients occurred upon the onset of hypoglycaemia. In non-diabetic volunteers, endogenous insulin had to have been 'persistently suppressed' before an effect of exogenous insulin on plasma glucagon levels was observed.

glucose concentrations (Vieira et al., 2007, de Heer et al., 2008, Hauge-Evans et al., 2009, Li et al., 2015). Further potentiation of somatostatin secretion under hypoglycaemic conditions could thus have adverse consequences on α-cell function. Notably (as mentioned in Chapter 1), increased intraislet somatostatin signalling has been proposed to explain the absent glucagon response to hypoglycaemia (Yue et al., 2012, Karimian et al., 2013). Yet the mechanism underlying this phenomenon is unknown. A stimulatory effect of therapeutic insulin on the pancreatic δ-cell may provide the answer and explain the suppression of glucagon secretion.

This possibility was examined in isolated *wildtype* mouse islets. Insulin was found to stimulate somatostatin secretion in a dose-dependent manner, correlating with concentration-dependent suppression of glucagon secretion (Figure A5.1 a). Crucially, insulin-induced inhibition of glucagon secretion was blocked by CYN 154806 (with no effect on the stimulatory effect on somatostatin secretion) (Figure A5.1 b, c), thus confirming the effect of insulin on glucagon secretion was mediated via an indirect effect on the δ-cell. Furthermore, genetic ablation of insulin receptors in δ-cells (SIRKO mice) abolished the effect of insulin on both somatostatin secretion and glucagon secretion (Figure 5.1 e, f). These mice were also less insulin-sensitive during insulin tolerance tests (Figure A5.1 g).

These data may appear to be in conflict with earlier work demonstrating little effect of insulin on somatostatin secretion (Hauge-Evans et al., 2012). Crucially, the effect of insulin on somatostatin secretion was shown to be glucose-dependent. At 1 mM glucose insulin (100 nM) had no effect on somatostatin secretion and at 10 mM it only increased somatostatin secretion by 50%, yet at 4 mM, insulin induced a 200% increase in

somatostatin secretion (Figure A5.1 d). This suggests a small window of activation, which may have been missed in previous studies[24].

The mechanism underlying the effect, however, was unclear. Interestingly, the effect of insulin was K_{ATP}-independent, with insulin having no additive effect on somatostatin secretion in the presence of tolbutamide (Figure A5.1 h), but was abolished by lowering extracellular Na^+ (Figure A5.1 j, k). As insulin has been shown to activate SGLT2 (Ghezzi and Wright, 2012) and the transporter is expressed in δ-cells (Adriaenssens et al., 2016), it was hypothesised that insulin increases somatostatin secretion via SGLT2-mediated Na^+ influx. Indeed, the SGLT2 blocker dapagliflozin was found to prevent insulin-induced somatostatin secretion and consequently prevent suppression of glucagon secretion (Figure A5.1 j, k). It also repolarized the δ-cell and reduced action potential firing in the presence of insulin (Figure A5.1 l), all at 4 mM glucose. To further define the precise mechanism underlying this effect, I performed $[Ca^{2+}]_i$ imaging experiments on islets isolated from mice expressing the Ca^{2+} sensor gCAMP3 specifically in their δ-cells (SST-gCAMP3 mice).

[24] In the previous study, 100 nM insulin was added at 1 mM glucose, 7 mM glucose and 20 mM glucose, and had no effect. Possibly due to a lack of effectiveness at these concentrations (e.g. Effective range = 3 mM – 5 mM glucose).

6.2. Methods

For islet isolation, islet culture, confocal $[Ca^{2+}]_i$ imaging and solutions

Please refer to main methods section

6.2.1. Mice

Mice expressing the Ca^{2+} sensitive probe gCAMP3 under the control of the somatostatin promoter, resulting in specific expression in pancreatic δ-cells, were used throughout. They were of a C57BL/6J background. *n* was taken as number of cells.

6.2.2. Reagents

The non-metabolisable glucose analogue Methyl-α-D-glucopyranoside (αMDG) was purchased from Sigma (UK).

6.3. Results

6.3.1. Effect of the non-metabolisable sugar methyl α-D-glucopyranoside (αMDG) on $[Ca^{2+}]_i$ activity in pancreatic δ-cells within intact mouse islets

To test the potentially stimulatory effect of SGLT2 transport on δ-cell $[Ca^{2+}]_i$ activity, the glucose derivative and SGLT2 substrate αMDG (19 mM) was applied at 1 mM glucose. As αMDG is a non-metabolisable sugar, any effect it has would be due to its transport via SGLT2 rather than due to ATP production. αMDG stimulated $[Ca^{2+}]_i$ activity in 29% (17/58) of sampled δ-cells (Figure 6.1 a). In these cells, subsequent lowering of $[Na^+]_o$ to 10 mM prevented oscillations in 83% (14/17). In 3 cells, a large transient increase in $[Ca^{2+}]_{i,}$, presumed to be due to the inhibitory effect of low $[Na^+]_o$ on the NCX, was followed by a reduction in $[Ca^{2+}]_i$ and suppression of $[Ca^{2+}]_i$ oscillations.

6.3.2. Effect of lowering the extracellular K^+ concentration on $[Ca^{2+}]_i$ activity in pancreatic δ-cells within intact mouse islets

It was hypothesised that the Na^+-dependence of the δ-cell may explain certain features of diabetes. Indeed, insulin-induced hypoglycaemia is associated with increased hypokalaemia (Caduff et al., 2011), which may disrupt Na^+ homeostasis in the δ-cell by inhibition of the Na^+/K^+-ATPase. Hypokalaemia occurs in diabetes as a direct consequence of high therapeutic insulin, but also due to release of adrenaline in response to insulin-induced hypoglycaemia. Both hormones stimulate potassium uptake via activation of Na^+/K^+-ATPase (in skeletal muscle and liver cells) (Heller and Robinson, 2000). To replicate these conditions $[K^+]_o$ was lowered from 3.6 mM to 1.7 mM at 1 mM

glucose. Low $[K^+]_o$ stimulated $[Ca^{2+}]_i$ activity in 23% (10/44) of δ-cells (Figure 6.1 b). It also caused build-up of $[Na^+]_i$, membrane depolarization, initiation of δ-cell electrical activity and somatostatin release with corresponding suppression of glucagon secretion (Figure A5.2 a, b, c, d, e). These effects on membrane potential were mimicked by the Na^+/K^+-ATPase antagonist oubain (Figure A5.2 f).

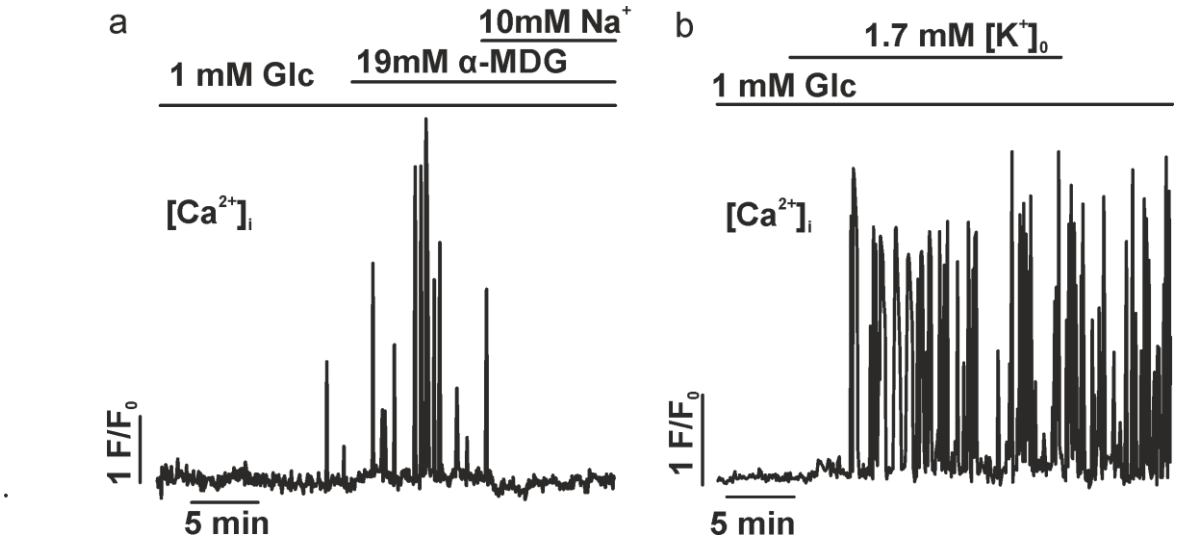


Figure 6.1 - Effect of α-MDG and low $[K^+]_o$ on $[Ca^{2+}]_i$ in mouse pancreatic δ-cells

(a) Representative recording of the effect of the non-metabolisable glucose derivative αMDG on $[Ca^{2+}]_i$ activity in 29% (17/58) of pancreatic δ-cells within islets from SST-gCAMP3. **(b)** Representative recording of the effect of low (1.7 mM) $[K^+]_o$ on $[Ca^{2+}]_i$ activity in 23% of (10/44) pancreatic δ-cells within islets from SST-gCAMP3 mice.

6.4. Discussion

6.4.1. Increasing flux through SGLT2 can activate the pancreatic δ-cell

These data suggest that glucose uptake via the SGLT2 Na^+/glucose transport stimulates the δ-cell by a direct non-metabolic effect. αMDG was shown to stimulate $[Ca^{2+}]_i$ dynamics in a subset of δ-cells, an effect which was stopped by lowering $[Na^+]_o$, indicating that increased Na^+ transport through SGLT2 is sufficient to initiate action potential generation and $[Ca^{2+}]_i$ influx, independent of glucose-mediated closure of the K_{ATP} channel. Notably, the concentration of αMDG used was high. Therefore, as it shares a similar affinity as glucose for SGLT2 (Wright et al., 2011), the experimental conditions were not reflective of hypoglycaemia (4 mM glucose), in terms of the rate of flux through SGLT2. However, as a lower concentration of αMDG (3 mM) was capable of stimulating electrical activity in the presence of insulin (Figure A5.2 g), one can assume at low glucose (4 mM), with the added stimulatory effect of high therapeutic insulin on SGLT2 transport, Na^+ uptake is at a sufficient level to initiate Ca^{2+} influx[25].

From this it appears that glucose-stimulated somatostatin secretion can occur via two distinct mechanisms - K_{ATP} channel closure (Gopel et al., 2000) and electrogenic Na^+/glucose uptake via SGLT2. This somewhat explains the glucose dependence of the insulin effect. At high glucose K_{ATP} channels would be fully closed and the δ-cell maximally stimulated, meaning any additional depolarization from insulin-induced SGLT2

[25] The influx of Ca^{2+} resulting from $[Na^+]_i$ build-up likely triggers CICR, with the SERCA-ATPase inhibitor thapsigargin reducing the effect of insulin on somatostatin secretion (Figure A5.1 i).

Na^+ uptake would have minimal effect. At 4 mM glucose, however, with a large proportion of K_{ATP} channels open and δ-cells relatively silent as a result, insulin-induced Na^+ uptake has a significant effect on membrane potential and is capable of stimulating electrical activity in some cells.

6.4.2. Hypokalaemia causes dysregulation of somatostatin secretion, dampening the glucagon response in type 2 diabetes

Similarly to αMDG, replication of hypokalaemia using low $[K^+]_o$ stimulated $[Ca^{2+}]_i$ activity in a subset of α-cells at 1 mM glucose. As the effect was mimicked by oubain (in terms of electrical activity) it may be assumed that suppression in the activity of the Na^+/K^+-ATPase is the cause of the effect. Lowering $[K^+]_o$ would acutely decrease Na^+/K^+-ATPase activity due to the drop in K^+ availability (Juel, 2009). Inhibition of the Na^+/K^+-ATPase then results in a build-up of $[Na^+]_i$ (Figure A5.2 c), subsequent membrane depolarization, Ca^{2+} influx and stimulation of somatostatin secretion. Importantly, prolonged hypokalaemia would also reduce the expression of the Na^+/K^+-ATPase subunits (Azuma et al., 1991), exerting a chronic oubain-like effect. This may explain the high levels of basal secretion and lack of stimulation by glucose in human type 2 diabetic islets (Vergari et al., In Press), with the δ-cell kept at maximal activity by hypokalaemia, even at low glucose, meaning any effect of high glucose is negligible. This increase in basal somatostatin would of course inhibit the α-cell at low glucose, resulting in impaired glucose counterregulation. As hypokalaemia is a feature of antecedent hypoglycaemia, its stimulatory effect on the δ-cell may explain the progressive deterioration of the glucose counterregulatory response after each episode of hypoglycaemia. Furthermore, improper activation of δ-cells at low glucose would counteract the adrenaline response by lowering

α-cell cAMP (Elliott et al., 2015). Moreover, as adrenaline is partly responsible for hypokalaemia (Heller and Robinson, 2000), it could indirectly increase basal somatostatin secretion[26], thus creating a negative feedback loop whereby adrenaline-induced hypokalaemia via δ-cell activation induces α-cell 'adrenaline resistance'. This suggests hypoglycaemia, like hyperglycaemia (see 3.4.8), may be deleterious for adrenergic signalling in the α-cell. Of course, aberrations in the CNS also occur but notably excitability of neurones would also be affected by hypokalaemia.

It must be conceded that both αMDG and low $[K^+]_o$ increased $[Ca^{2+}]_i$ activity in only a subset of δ-cells. However, due to the potency of somatostatin at inhibiting the α-cell, it is postulated that this is sufficient to blunt the glucagon response to hypoglycaemia - mediated by both inhibition of exocytosis (Gromada et al., 2001a) and membrane hyperpolarization via activation of α-cell GIRK channels (Gromada et al., 2001b).

6.4.3. Intrinsic α-cell dysfunction vs. Iatrogenic paracrine suppression

In relation to the previous chapter, which pointed towards hyperglycaemia and intrinsic α-cell dysfunction as the cause of the absent glucagon response to hypoglycaemia, the findings in this study may appear contradictory. However, *in vivo* the effects of insulin and hyperglycaemia on the glucagon response may instead represent two distinct causes, with the relative contribution of both mechanisms likely depending on the patient. For example, if a patient is prone to repeated episodes of insulin-induced hypoglycaemia this would induce hypokalaemia and SGLT2 Na^+ import resulting in δ-cell activation and suppression of glucagon secretion. Contrastingly, if a patient has a high HbA1c, the persistent

[26] Counteracting its direct inhibitory effect (Figure 3.9)

hyperglycaemia would result in α-cell dysfunction. Of course, many patients would fall between these two states and therefore both mechanisms may act alongside one and other in suppressing α-cell activity at low glucose. As increased SGLT transport is causal in both cases, the use of SGLT2 blockers could prove vital in maintaining α-cell function in type 2 diabetes.

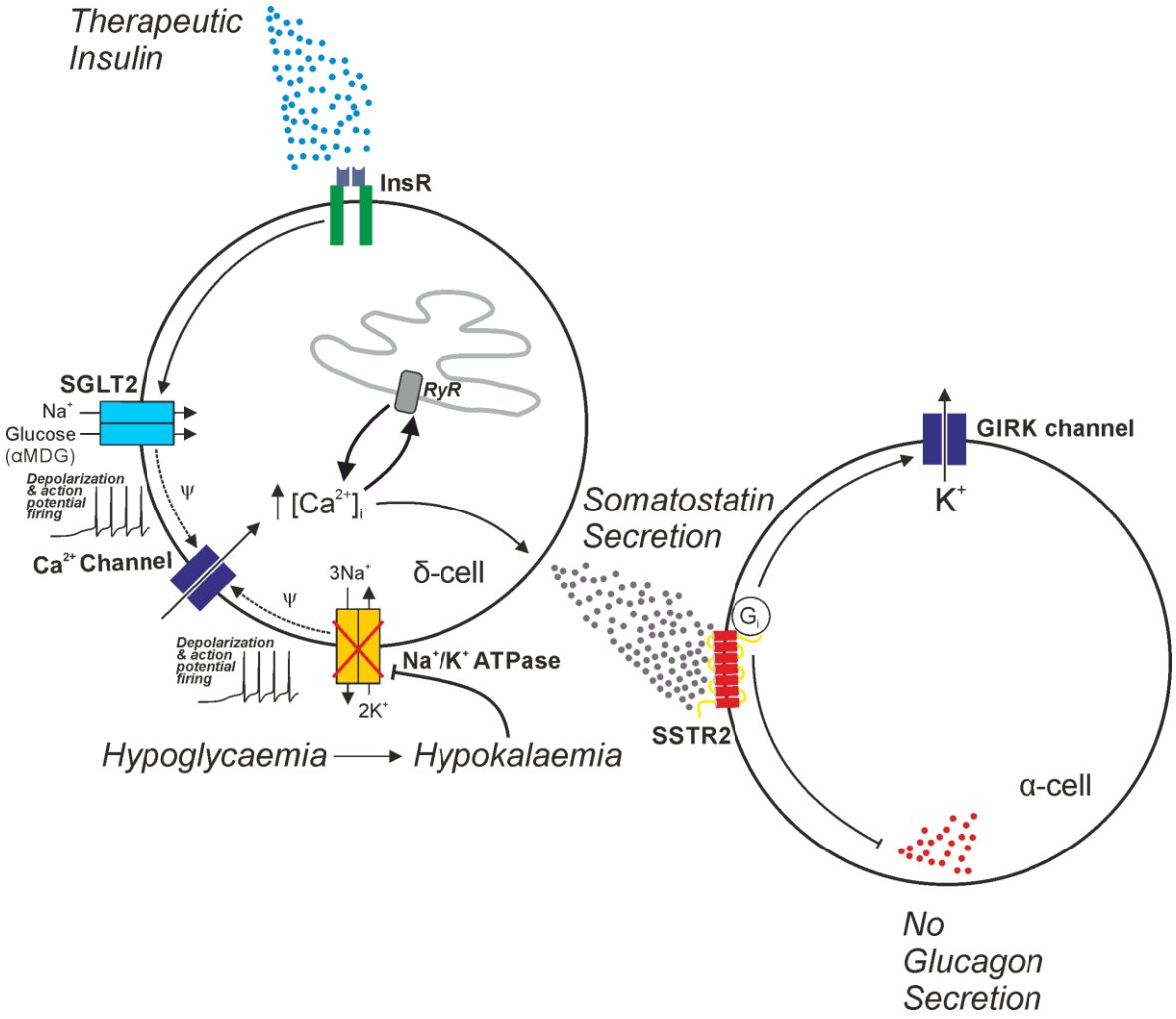


Figure 6.2 - Model

The electrogenic uptake of Na^+ ions through SGLT2 (promoted by high therapeutic insulin) and inhibition of the Na^+/K^+-ATPase by hypokalaemia (resulting from insulin-induced hypoglycaemia) results in a build-up of $[Na^+]_i$ in the δ-cell. This causes membrane depolarization, which triggers electrical activity in a subset of δ-cells, resulting in Ca^{2+} influx (and subsequent CICR) and stimulation of somatostatin secretion. Somatostatin subsequently binds to the SSTR2 on neighbouring α-cells, leading G_i activation, which both suppresses glucagon granule exocytosis and activates GIRK channels at the plasma membrane (leading to K^+ efflux and membrane hyperpolarization), inhibiting glucagon secretion.

6.5. Conclusion

The data presented in this chapter complements work demonstrating that high concentrations of insulin suppress glucagon secretion via stimulation of somatostatin secretion. It further highlights the importance of SGLTs in the function of islet cells and provides a new model for the loss of the glucagon response to hypoglycaemia, which likely acts alongside the intrinsic dysfunction described in Chapter 6. Clinically, the use of SSTR2 receptor antagonists or SGLT2 inhibitors in conjunction with insulin should now be considered to minimise any somatostatin-mediated inhibitory effects on glucagon secretion.

Chapter 7: General Discussion

7.1. Introduction

The research in this thesis has aimed to improve understanding of glucagon secretion in an effort to provide clues to the mechanisms underlying its dysregulation in diabetes. Specifically focusing on glucose counterregulation, Chapter 3 and Chapter 4 addressed autonomic regulation of glucagon secretion, aiming to define the mechanisms underlying the effects of adrenaline and ACh on the α-cell at low glucose, respectively. While Chapter 5 and Chapter 6 aimed to define the cause(s) of the absent glucagon response to hypoglycaemia, focusing on metabolic and paracrine dysregulation, respectively.

7.2. Key findings

In previous work, while it was clear that adrenaline stimulated glucagon secretion by elevating $[Ca^{2+}]_i$ in α-cells, a consensus on the source of the Ca^{2+} increase had not been reached, with the relative role of intracellular Ca^{2+} release or L-type Ca^{2+} channel influx disputed. In intact islets, intracellular Ca^{2+} release had not been demonstrated, while blockade of L-type Ca^{2+} channels with isradipine abolished adrenaline-induced glucagon secretion (De Marinis et al., 2010). However, paradoxically, membrane potential recordings did not support a role for L-type Ca^{2+} channel influx (Figure A2.1). This suggested at least part of the Ca^{2+} rise was due to intracellular Ca^{2+} release, as had been observed in single α-cells (Johansson et al., 1989, Liu et al., 2004, Vieira et al., 2004). Using intact islets, adrenaline was found to stimulate glucagon secretion via a store-operated mechanism. Most notably, the role of the lysosomal Ca^{2+} stores was revealed,

which acted in a hierarchal manner releasing Ca^{2+} via TPC2 and triggering CICR from ER stores. This explained the 'paradoxical' effect of adrenaline on membrane potential, with the inhibitory effect of isradipine deemed to be due to depletion of intracellular Ca^{2+} stores or shared pharmacology with TPC2. Additionally, adrenergic signalling was found to utilise PKA- and Epac2-dependent pathways, with both cAMP targets shaping the adrenaline-induced $[Ca^{2+}]_i$ response.

A crucial finding in relation to impaired glucose counterregulation is the smaller adrenaline response in islets cultured at high glucose. Currently, dysfunction of the autonomic response to hypoglycaemia has generally been attributed to HAAF in the CNS, and oxidation of nAChRs and eSIN in the PNS (Taborsky and Mundinger, 2012) . My data suggests the α-cell itself becomes resistant to sympathetic stimulation, after chronic hyperglycaemia. This is crucial as in type 1 diabetes and advanced type 2 diabetes the glucagon response to hypoglycaemia is lost before HAAF develops, and blunts autonomic responses. Furthermore, even when HAAF is reversed the glucagon response remains absent (Cryer, 2002). However, with the stimulatory effect of autonomic stimuli reported to account for 75-90% of the glucagon response to hypoglycaemia (Taborsky and Mundinger, 2012), autonomic dysfunction must also occur prior to HAAF. These findings together with early defects in the PNS (see 1.4.5) demonstrate exactly that. Furthermore, they show that hyperglycaemia contributes to autonomic dysfunction in diabetes, contesting the assumption that antecedent hypoglycaemia and the resulting HAAF are solely responsible.

Hypoglycaemia also results in an increase in islet parasympathetic activity and consequently release of ACh into the islet vicinity. Parasympathetic signalling acts in

conjunction with the sympathetic response to increase glucagon secretion and maintain normoglycaemia. Therefore, the mechanism underlying ACh-induced glucagon secretion was studied. Previous work had generally only explored the identity of surface receptors, confirming the role of the M3 muscarinic receptors (Verspohl et al., 1990, Karlsson and Ahren, 1993, Duttaroy et al., 2004). As a G_q-coupled receptor, it was assumed elevation in $[Ca^{2+}]_i$ and stimulation of glucagon secretion was due to IP_3-mediated ER Ca^{2+} release and PKC activation. As expected, ACh stimulated ER Ca^{2+} release (presumably IP_3-mediated) and increased $[DAG]_i$, reflective of G_q activation. Its effects were mimicked by the muscarinic agonist oxotremorine and attenuated by the antagonist atropine. However, evidence of nAChR involvement was also revealed. Nicotine increased $[Ca^{2+}]_i$ in 71% of α-cells. Its effects were specific to the α-cell (at least at low glucose) and somewhat mediated by activation P/Q-type Ca^{2+} channels, which are strongly linked to glucagon secretion (Zhang et al., 2013). Notably, hyperglycaemia did not blunt the ACh $[Ca^{2+}]_i$ response. This contrasts its effect on the adrenaline response and suggests any blunting of the parasympathetic response in diabetes likely results from HAAF. It also implies that defective α-cell cholinergic signalling does not contribute to the absent glucagon response to hypoglycaemia.

Chapter 5 explored the metabolic regulation of glucagon secretion specifically in relation to glucose counterregulation. It centred specifically on the diabetic state focusing on how hyperglycaemia drives glucagon secretory defects. Previous work had attributed glucagon secretory defects to β-cell loss (Cryer, 2012). However, there remained certain observations which contested this assumption and pointed towards intrinsic dysfunction in the α-cell itself. Namely, the inhibition of glucagon secretion at glucose concentrations not associated with stimulation of insulin secretion (Walker et al., 2011), which holds

particular relevance to impaired glucose counterregulation (see 1.4.1). Using the Fh1βKO mouse it was demonstrated that the diabetic α-cell had an absent glucagon response at low glucose and lower pH_i. Furthermore, these effects could be replicated by 48 h high glucose culture despite no change in insulin paracrine input, and were alleviated with the SGLT blocker phlorizin. In opposition to the 'switch-off hypothesis', this study proposes that hyperglycaemia increases SGLT flux, driving cytoplasmic acidification and subsequent mitochondrial acidification, thereby reducing ATP production and disrupting the glucagon response to hypoglycaemia.

As impaired counterregulation is iatrogenic, Chapter 6 explored the contribution of improper insulin dosage to the absent glucagon response. With previous work demonstrating suppression of glucagon secretion at low (4 mM) glucose as a result of insulin-induced somatostatin secretion (Figure A5.1), the data presented in Chapter 6 helped elucidate the mechanism of δ-cell stimulation. Inhibition of SGLT2 transporters had been shown to block the effect of insulin, and it was demonstrated that transport through SGLT2 was indeed capable of stimulating a subset of δ-cells; with low $[K^+]_o$, a feature of insulin-induced hypoglycaemia, having a similar effect. This complements the work of the previous chapter, highlighting the absent glucagon response in diabetes occurs largely due to increased SGLT transport, which can result in intrinsic α-cell dysfunction due to hyperglycaemia and improper paracrine signalling caused by insulin overdose.

7.3. Overall implications

Perhaps the most significant findings of this thesis are: (i) the involvement of the acidic Ca^{2+} stores in α-cell adrenergic signalling, (ii) evidence for a nicotinic pathway in α-cells,

a (iii) critical role of SGLTs in α-cell dysfunction (iv) and δ-cell stimulation in diabetes. Crucially, these findings open new avenues to explore and manipulate α-cell function.

The lysosomal (acidic) Ca^{2+} stores appear to be essential for adrenergic signalling: if their function is compromised, adrenaline does not increase $[Ca^{2+}]_i$ and therefore fails to induce glucagon secretion. This makes them an attractive drug target. Notably, they can be activated independently from adrenergic signalling, by agents elevating cytoplasmic cAMP such as phosphodiesterase inhibitors. Furthermore, they must also now be considered in the mechanisms of other α-cell secretagogues, particularly those driven via G_s signalling.

Secondly, the stimulation of α-cell $[Ca^{2+}]_i$ dynamics and glucagon secretion by nicotine has implications for health and disease, as it may explain some of the risk associated with smoking and the development of type 2 diabetes. It also further demonstrates the role of nicotinic receptors in non-neuronal tissues (Macklin et al., 1998, Maus et al., 1998, Andersson and Arner, 2001, Arredondo et al., 2001, Wang et al., 2001, Heeschen et al., 2002, Gahring et al., 2004, Arias et al., 2009, Ganic et al., 2016) contesting some of the early assumptions of cholinergic signalling (McCorry, 2007).

The observations with SGLTs in the maintenance of α-cell pH_i and δ-cell activity open potentially new ways to combat dysregulated glucagon secretion in diabetes, suggesting added advantages of SGLT2 inhibitors in diabetes, with potentially beneficial effects on the glucagon response to hypoglycaemia, and the development of renal and cardiac secondary complications.

7.4. Personal reflections

When looking at my work as a whole, some important features of α-cell regulation emerge. Parasympathetic and sympathetic branches are typically viewed as opposites, governing 'rest-and-digest' and 'flight-or-flight' responses, respectively. Despite this under hypoglycaemic stress both are activated and target the α-cell in a similar manner. The redundancy between the two pathways, suggests sympathetic activation acts as a failsafe if parasympathetic signalling is insufficient or compromised (e.g. due to receptor desensitisation). As the dangers of hypoglycaemia are life-threatening, one can speculate that evolution favoured this graded response with the activation of both sympathetic and parasympathetic branches protecting glucose-dependent organs (e.g. the brain) against the effects of prolonged fasting.

Additionally, the prominent role of intracellular Ca^{2+} stores in the enhancement of glucagon secretion at low glucose is underlined. It appears ER Ca^{2+} stores present a way for the α-cell to increase glucagon secretion dramatically in energetically unfavourable conditions. As reported by Johansson et al. (1989) and Liu et al. (2004), akin to a battery, Ca^{2+} is sequestered in the ER in response to glucose due to increased activity of the SERCA-ATPase, and then released at low glucose by ACh and adrenaline, to generate the increase in $[Ca^{2+}]_i$ required to increase glucagon secretion and maintain glucose homeostasis.

This contrasts with the finely-tuned response to glucose, evident in Chapter 5, which relies on small changes in action potential height dictating P/Q-type Ca^{2+} channel activation (Zhang et al., 2013). Crucially, the intrinsic response to glucose does not appear to be dictated by absolute levels of $[Ca^{2+}]_i$, with blockade of L-type Ca^{2+} channels having no

effect on glucagon secretion despite them accounting for a majority of the Ca^{2+} current (MacDonald et al., 2007). Therefore, it appears likely that under basal conditions, glucagon granule exocytosis is determined by the location of the Ca^{2+} signal, with only granules located near to P/Q-type Ca^{2+} channels being exocytosed. However, when adrenaline or ACh are applied, triggering ER Ca^{2+} release, the reliance on the P/Q-type channel is largely overcome. Evidenced by adrenaline- (Figure A2.2 c) and ACh (Figure A3.1 d) both substantially elevating glucagon secretion in the presence of the P/Q-type blocker ω-agatoxin. It appears that the large magnitude of the ER Ca^{2+} response allows additional granules further from the P/Q-type Ca^{2+} channel to be exocytosed. Of course, Ca^{2+}-independent effects will also play a role. Notably, the switch in reliance on P/Q-type Ca^{2+} channel influx to ER Ca^{2+} may also facilitate the stimulatory effects of amino acids and fatty acids on glucagon secretion, with any receptor-mediated effects that target ER stores overcoming the inhibitory metabolic effect of ATP, which would become negligible.

Regarding glucagon's dysregulation in diabetes, it is revealed that hyperglycaemia drives impaired glucose counterregulation, causing SGLT-driven cytoplasmic acidification, removing the ability of the α-cell to sense glucose, and disrupting α-cell adrenergic signalling, removing its ability to respond to external sympathetic stimuli. The α-cell has often been seen as a bystander in diabetes, with the dysregulation of glucagon secretion put down to external aberrations, whether these be β-cell loss (Cryer, 2012) or dysfunction in the CNS and PNS (Taborsky and Mundinger, 2012), affecting input to the α-cell. This thesis further highlights that the α-cell is not just a product of its environment but has intrinsic function, which can be affected by hyperglycaemia.

Additionally, insulin-induced hypoglycaemia is shown to augment intraislet somatostatin signalling, suppressing the α-cell. Together these processes cause the absent glucagon response to hypoglycaemia. Thus, highlighting that metabolic, autonomic and paracrine dysfunction can all contribute to α-cell dysregulation at low glucose, contesting previous assumptions (see 1.4.1).

7.5. Future work

As a whole, a key focus should be the confirmation of the mechanisms underlying the effects of adrenaline, ACh and hyperglycaemia in human islets. While in Chapters 3 and 4 human islet experiments were performed, these were not extensive and did not explore the intracellular mechanisms at play. Though similarities were found, there were some differences that need to be accounted for. In doing so, investigating the effects of neuropeptides should be prioritised.

Specifically, regarding α-cell adrenergic signalling, future research should firstly use noradrenaline as this appears the more likely candidate to stimulate glucagon secretion (see 3.4.2). Secondly, investigating what causes the resistance to (nor)adrenaline after hyperglycaemic culture and whether this can be prevented is crucial. If the effects of hyperglycaemia could be alleviated this would provide some hope in maintaining glucagon secretion in diabetes.

The central question regarding α-cell cholinergic signalling is the role of the nicotinic pathway. Specifically, whether it acts together with the muscarinic pathway, or whether the two pathways act in isolation, being activated sequentially as hypoglycaemia worsens. To ascertain the role of nicotine, a dose-dependence experiment with ACh may be useful.

As blood glucose falls, parasympathetic activity increases and intraislet ACh concentration rises (Taborsky and Mundinger, 2012). Therefore, if activation of the nicotinic pathway precedes activation of the muscarinic pathway, one would expect low ACh concentrations to initiate a nicotine-like effect. This method could be developed further by applying tubocurarine at low ACh concentrations to see if the nicotine-like effect is blocked. Increasing the number of patch clamp recordings of the effect of nicotine and ACh on α-cell electrical activity is also necessary.

Due to the stimulation of glucagon secretion by nicotine, it may be that smoking disrupts α-cell regulation. However, the acute application of nicotine used in the experiments may not be the best way to reproduce the conditions associated with smoking. Alternatively, one could expose mouse and human islets to chronic nicotine treatment (e.g. 48 h culture), before measuring any effects on α-cell $[Ca^{2+}]_i$ dynamics, electrophysiology and glucagon secretion.

In the Fh1βKO project, measuring mitochondrial pH is the obvious next step. This would confirm the fall in pH_i results in acidification of the mitochondria, thereby confirming the model. It is likewise a high priority to measure somatostatin secretion in islets from Fh1βKO mice and those exposed to high glucose, to ensure the dysregulated glucagon secretion is not the result of changes in somatostatin secretion.

In the project looking into insulin-induced somatostatin secretion, the findings with αMDG proved SGLT2 transport could trigger δ-cell activity independent of metabolism, however, adding αMDG at a lower concentration (e.g. 3 mM) but in the presence of insulin may provide a better recreation of hypoglycaemia in the diabetic state. Secondly, one should

confirm the stimulatory effects of insulin, αMDG and low $[K^+]_o$ on δ-cell $[Ca^{2+}]_i$ dynamics correlate both spatially and temporally with suppression of α-cell $[Ca^{2+}]_i$ dynamics. This would further reaffirm the critical role of the δ-cell in the suppressive effect of insulin on glucagon secretion. It could be achieved by performing confocal $[Ca^{2+}]$ imaging (using Fluo-4) on islets isolated from mice expressing RFP under control of the somatostatin promoter (facilitating identification of δ-cells). If insulin(/αMDG/low $[K^+]_o$) -induced suppression of α-cells correlated with an increase in activity from neighbouring δ-cells, this would confirm the model (Figure 6.2). While suppression independent of δ-cell activity would indicate a direct effect of insulin on α-cell $[Ca^{2+}]_i$ dynamics.

One limitation of the experimental design used throughout this thesis is that it replicates the *in vivo* conditions only partially. In my experiments, the α-cell is exposed to a maximum of two stimuli a time (e.g. low glucose and adrenaline), excluding autocrine and paracrine effects. *In vivo*, the α-cell will receive metabolic input from low glucose, amino acids and fatty acids, and autonomic input from ACh, adrenaline and noradrenaline. Therefore, rather than looking at adrenergic and cholinergic stimulation in isolation, one could look at both simultaneously to mirror *in vivo* conditions. For instance, apply ACh first, as parasympathetic activation precedes sympathoadrenal/sympathetic, and on top of this apply (nor)adrenaline. It may also be useful to add amino acids and fatty acids to the basal solution. Together, this would allow greater understanding of how the α-cell integrates these signals and thus increases its output as glucose falls. It is highly likely that there is redundancy between different stimuli, with overlap between the targets they act upon. Alternatively, there could also be subsets of α-cells more susceptible to parasympathetic or sympathetic stimulation.

Indeed, a clear feature of α-cells that I recognised throughout my work was the large heterogeneity in their responses to various stimuli, whether these be low and high glucose, glutamate, adrenaline, ACh or nicotine. Although not visited in great detail in the chapters, it was evident in my results, with certain α-cells being resistant to particular stimuli or treatment (e.g. 29% of α-cells were unaffected by nicotine). $[Ca^{2+}]_i$ activity at low and high glucose was also often varied. Despite the variability by studying many α-cells statistically significant effects have been obtained. However, defining what causes this heterogeneity would be a crucial step in our understanding of α-cell physiology. Whether the difference in response is due to distinct α-cell subsets, which express varying levels of surface receptors or metabolic enzymes; or whether it is simply a product of the environment the α-cell is located in and the paracrine input it receives.

Appendix 1: Methods performed by collaborators

A1.1. Methods performed by collaborators throughout thesis

A1.1.1. Hormone secretion assays

The method of hormone secretion assays differed between projects. In the secretion experiments done in conjunction with the work in Chapter 3, Chapter 4 and Chapter 6, groups of 12 size-matched islets from at least 3 mice were pooled together and preincubated for 30 min at 37ºC in a water bath in 1ml of KRB containing (mM) 120 NaCl, 4.7 KCl, 2.5 $CaCl_2$, 1.2 KH_2PO_4, 1.2 $MgSO_4$, 10 HEPES and 25 $NaHCO_3$ (pH 7.4 with NaOH) which was gassed with 95/5% O_2/CO_2 and supplemented with 0.1% fatty acid free BSA and 1mM glucose. After preincubation, the buffer was changed to a medium supplemented as indicated (e.g. glucose, receptor antagonist and ion channel blockers), and the islets were incubated for 60 min at 37ºC with gentle shaking - 30 cycles/min. Following incubation aliquots of the medium were immediately removed for assay of glucagon (and somatostatin). Radioimmunoassays were performed using a Eurodiagnostica kit (Sweden) and following the manufacturer's protocols. For the experiments on the *Tpcn1*, *Tpcn*$^{-/-}$ and *CD38*$^{-/-}$ mice and corresponding control mice in Chapter 3, an MSD Quickplex (USA) and MSD glucagon assay (USA) were used, following the manufacturer's protocols.

In secretion experiments linked to Chapter 5, 10-12 size-matched islets were pre-incubated for 1h in a water bath at 37ºC (5% CO_2/95% air) in 300 µl of KRB containing (mM) 140 NaCl, 3.6 KCl, 2.6 $CaCl_2$, 0.5 $MgSO_4.7H_2O$, 0.5 NaH_2PO_4, 2 $NaHCO_3$, 5 HEPES and 2

mg/ml BSA (pH adjusted to 7.4 with 1M NaOH) supplemented 1mM glucose. After preincubation, the buffer was changed to a medium supplemented as indicated for a further 1 h. After incubation, an aliquot of the supernatant was collected and stored at -20 ºC (any remaining supernatant was discarded) to be used for quantification of hormone secretion later. The remaining islet pellet was then lysed in 100 µl of ice-cold acid ethanol solution (containing ethanol, H_2O and HCl in a ratio of 52:47:1) to release hormone content with resulting lysates immediately frozen at -20ºC for later analysis. Radio-immunoassays for insulin and glucagon were performed using kits from Millipore (UK) and Eurodiagnostica (Sweden), respectively, following the manufacturer's protocols.

A1.1.2. Human islet isolation

Human pancreatic islets were isolated at the Diabetes Research & Wellness Foundation Human Islet Isolation (Oxford, UK), following adapted versions of the published protocols (Lake et al., 1989, Ricordi et al., 1988).

A1.1.3. Imaging of $[Na^+]_i$

For the $[Na^+]_i$ measurements performed in conjunction with Chapter 5 and Chapter 6, islets were dispersed into a single-cell suspension, which was plated on 0.17 mm thick glass coverslips in 10 µl droplets and left to attach for >2 h (for experiments relating to Chapter 5, cells were then cultured for 24 h with or without phlorizin). Cells were then pre-loaded with 6 µM of the $[Na^+]_i$-indicator dye Sodium Green (Molecular Probes) for 30 min and imaged on a Zeiss AxioZoom.V16 zoom microscope, using magnifications in the range 15x-20x. To enhance the statistical power of comparisons (e.g. with/without phlorizin),

cells were imaged at several locations throughout the coverslip simultaneously. Sodium Green was excited at 490 nm and emission was collected at 515 nm.

In Chapter 5, cells were loaded with the 'red downward cADDis cAMP recombinant sensor' (Montana Molecular, USA), α-cells were identified as those that increased cAMP (corresponding with a drop in probe fluorescence) in response to adrenaline (5 μM) (De Marinis et al., 2010). The probe was delivered using a BacMam vector, according to the manufacturer's guidelines. Red downward cADDis was excited at 572 nm and the emission was collected at 629 nm. In Chapter 6, mice expressing RFP under the control of the somatostatin promoter were used, δ-cells were thus identified based on the RFP fluorescence. Image sequences were analysed (registration, background subtraction, ROI intensity vs. time analysis) using open-source FIJI software.

A1.2. Methods performed by collaborators specifically for Chapter 3

A1.2.1. Electrophysiology

Membrane potential recordings were performed as in Chapter 4 (4.2.2). Capacitance measurements were performed as described by Gopel et al. (2004)

A1.3. Methods performed by collaborators specifically for Chapter 4

A1.3.1. Pancreas perfusion

Animals were culled by cervical dislocation. Using 0.25 mm nylon thread, the renal arteries were sutured, followed by the descending abdominal artery, just above the branching of the celiac artery. To further isolate the blood flow to the pancreas, both the gastric artery and the splenic artery was sutured off. A catheter was inserted in the ascending artery just below the branching of the mesenteric artery, and connected to a peristaltic pump, kept at a flow of 1.34 µl/min/mg pancreas (Carlsson et al., 1996) (pancreas weight was calculated as 8mg/g body weight (Bock et al., 2005)). The portal vein was then catheterised and connected to an outflow tube. Perfusion speed was estimated from the first 10 min flow though after which the experiment was initiated. The secretion rate pg/min was calculated using the estimated perfusion speed.

A1.4. Methods performed by collaborators specifically for Chapter 5

A1.4.1. Imaging of $[ATP/ADP]_i$

Time-lapse imaging of $[ATP/ADP]_i$ ratio was performed as described by Adam et al. (2017).

A1.4.2. Immunofluorescence

Mouse and human pancreata were fixed (in 10% neutral-buffered formalin) and dehydrated, before being embedded in paraffin wax and sectioned (3 µM). The following

primary antibodies were applied to the samples: FH (Autogen Bioclear, UK), insulin (MP Biomedicals, UK and Dr Anne Clark), glucagon (MP Biomedicals, UK and Sigma, UK) and 2SC ((Nagai et al., 2007), A gift from Dr. Norma Frizzell), with Alexa Fluor® secondary antibodies (Life technologies, UK) then added. Images were taken using a Zeiss LSM510 META confocal imaging system.

A1.4.3. SGLT expression analysis

Using a combination of TRIzol and PureLink RNA Mini Kit (Ambion, UK), total RNA was isolated from mouse tissues. To prevent against DNA contamination DNase treatment was also performed. RNA was then converted to cDNA using the High Capacity RNA-to-cDNA kit (Applied Biosystems, UK). To perform Real-time qPCR, SYBR Green detection and gene specific QuantiTect Primer Assays (Qiagen, UK) were used, with relative expression calculated as $2^{-\Delta\Delta CT}$. *Actb* and *PPIA* were used for normalisation.

A1.4.4. Plasma glucose measurements

Glucose levels (fed) were measured from a blood drop obtained from a nick made in the tail vein, using an Accuchek Aviva meter (Roche Diagnostic, UK) at 9 am.

A1.4.5. Fumarate hydratase activity measurements

Fumarate hydrate activity was measured as described previously (Massey, 1953), with pH dependent changes recorded by adjusting the pH of the assay buffer using KOH.

A1.5. Methods by collaborators specific for Chapter 6

A1.5.1. Electrophysiology

Membrane potential recordings were performed as in Chapter 4 (4.2.2).

A1.5.2. Plasma glucose determinations and insulin tolerance tests

Fed blood glucose levels were measured as in A1.4.4. Mice were then fasted for 3-4 h. At time zero, fast-acting human insulin (Actrapid, Novo Nordisk, Denmark) was injected intraperitoneally using a gauge needle. Blood glucose levels were measured from time zero at 15 min intervals using the same method as above.

Appendix 2 - Data collected by collaborators in Chapter 3

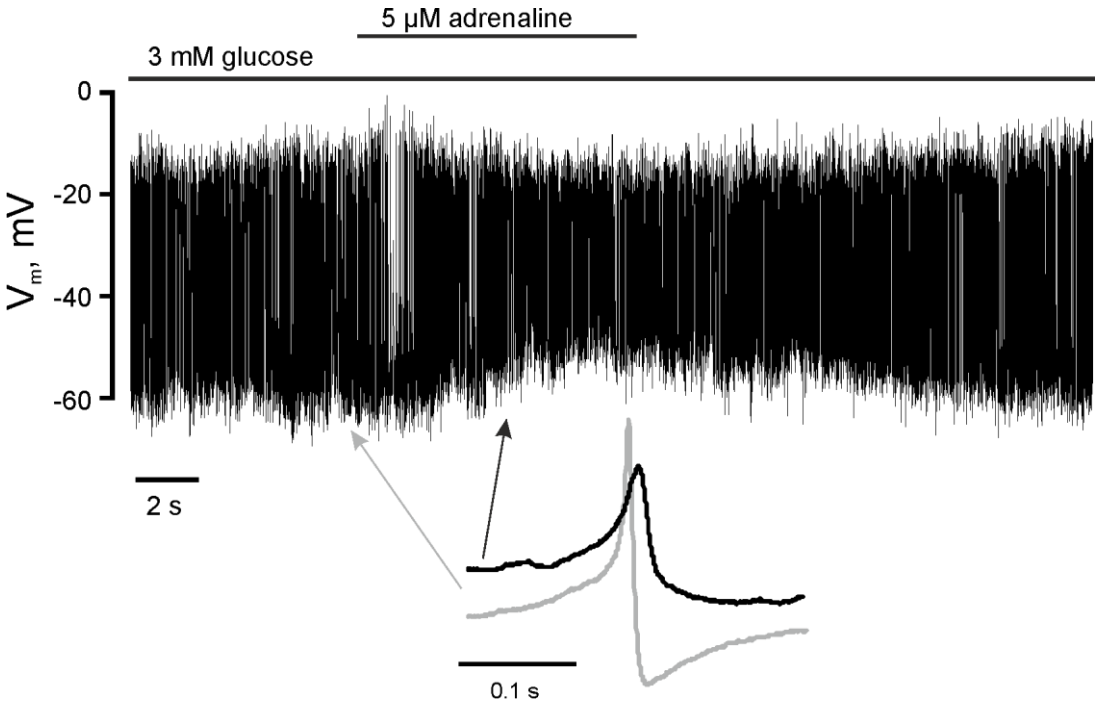


Figure A2.1 - Effect of adrenaline on electrical activity

Representative trace of the effect of adrenaline on membrane potential of α-cells within intact islets. (*n* = 11). Note the change in the spike duration and amplitude.

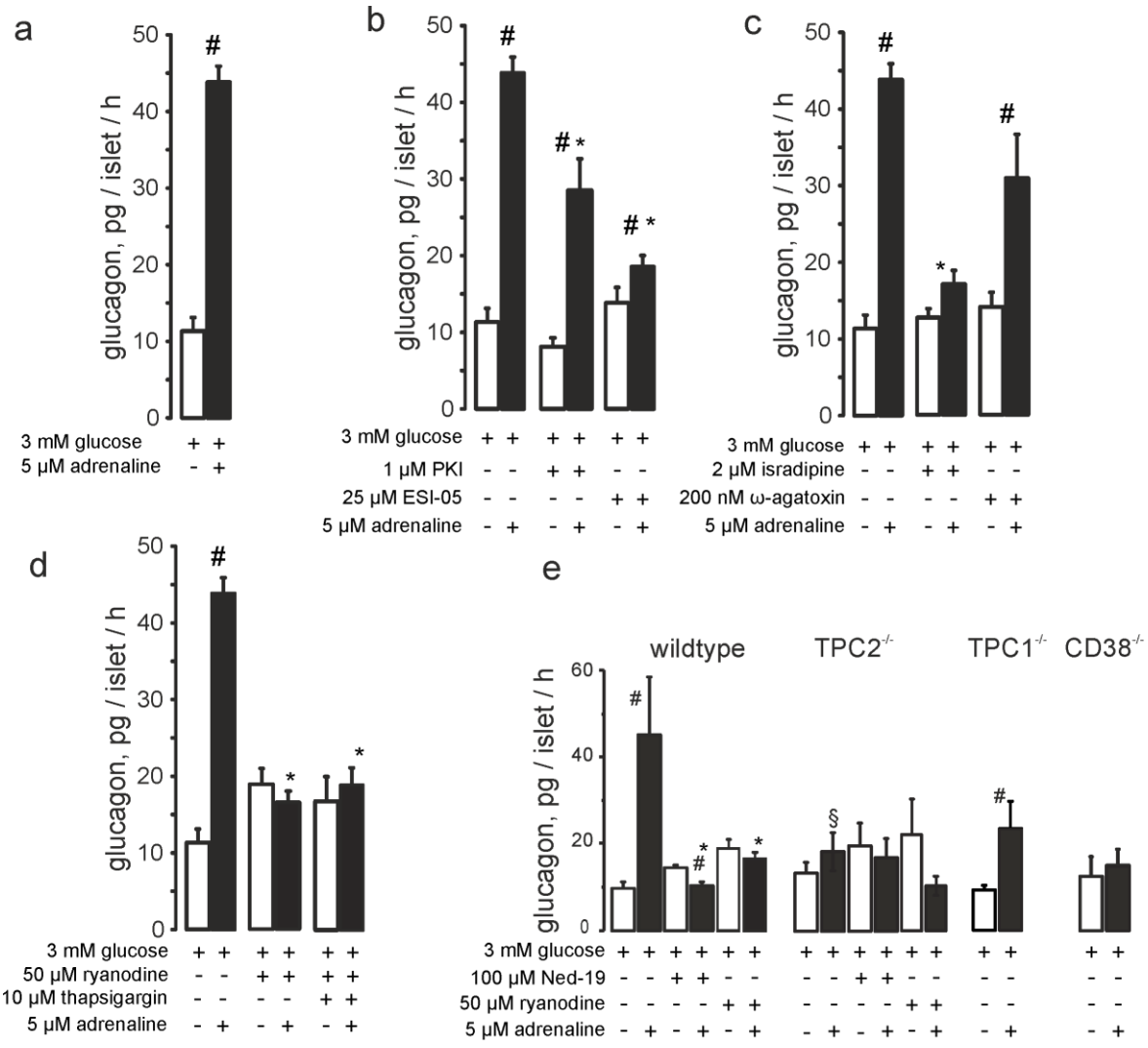


Figure A2.2 - Adrenaline and glucagon secretion

(a) Effect of adrenaline on glucagon secretion in islets from NMRI mice. **(b)** Effect of adrenaline alone or in the presence of PKI or ESI-05 on glucagon secretion in islets from NMRI mice. **(c)** Effect of adrenaline alone or in the presence of isradipine or ω-agatoxin on glucagon secretion in islets from NMRI mice. **(d)** Effect of adrenaline alone or in the presence of ryanodine or thapsigargin on glucagon secretion in islets from NMRI mice. **(e)** Effect of adrenaline alone or in the presence of Ned19 or ryanodine on glucagon secretion in islets from C57BL/6N mice (*wildtype*) and *Tpcn2*$^{-/-}$ mice. Effect of adrenaline alone on glucagon secretion in islets from *Tpcn1*$^{-/-}$ and *CD38*$^{-/-}$ mice. # Denotes significant ($p < 0.05$) vs. basal; * Denotes significant ($p < 0.05$) vs. control; § Denotes significant ($p < 0.05$) vs. *wildtype*

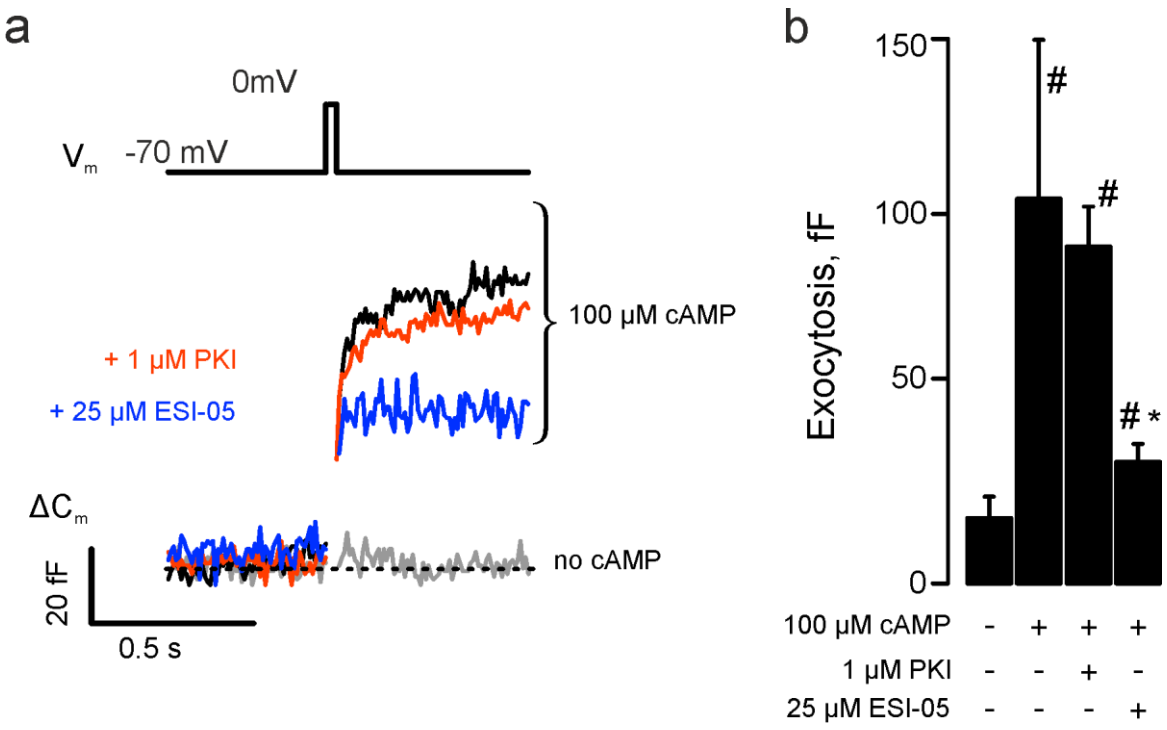


Figure A2.3 - cAMP effect on exocytosis

(a) Depolarization-induced effect on glucagon granule exocytosis, monitored using membrane capacitance ΔC_m, with no cAMP (grey), with 100 µM cAMP alone (black) or in the presence of PKI (red) and ESI-05 (blue). (**b**) Exocytosis quantified in fF in the presence of no cAMP, 100 µM cAMP alone or in the presence of PKI and ESI-05 (*left to right*). Pulse duration was 20ms. # Difference is significant vs. no cAMP *Difference is significant vs. 100 µM cAMP alone.

Appendix 3: Data collected by collaborators in Chapter 4

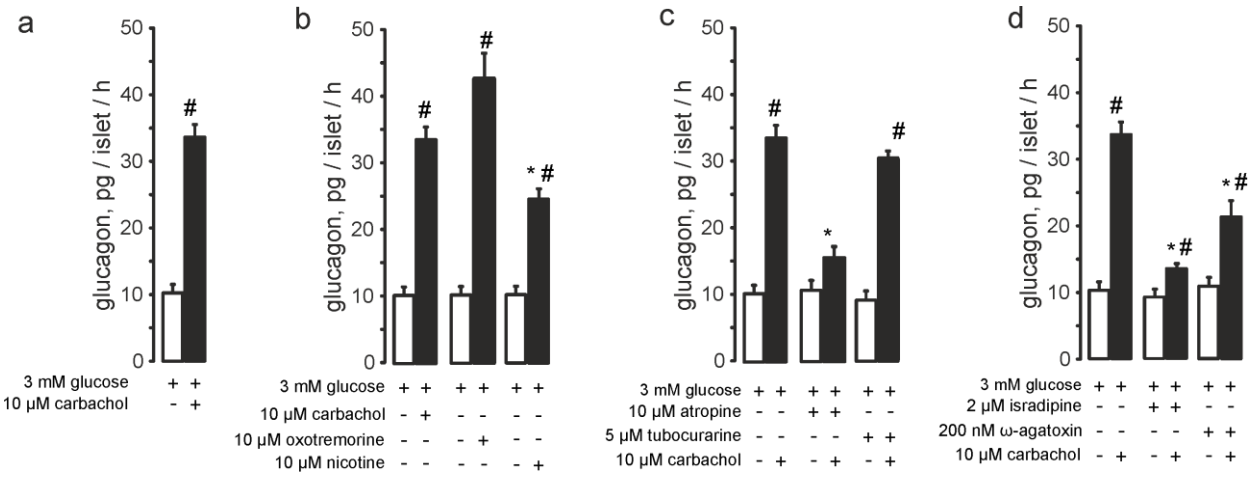


Figure A3.1 - Cholinergic signalling and glucagon secretion

(a) Effect of the cholinergic agonist carbachol on glucagon secretion **(b)** Effect of carbachol, oxotremorine and nicotine on glucagon secretion. **(c)** Effect of carbachol alone or in the presence of atropine or tubocurarine. **(d)** Effect of carbachol alone or in the presence of isradipine or ω-agatoxin on glucagon secretion. All experiments performed on islets from C57BL/6J mice # Denotes significant ($p < 0.05$) vs. basal; * Denotes significant ($p < 0.05$) vs. C57BL/6J control.

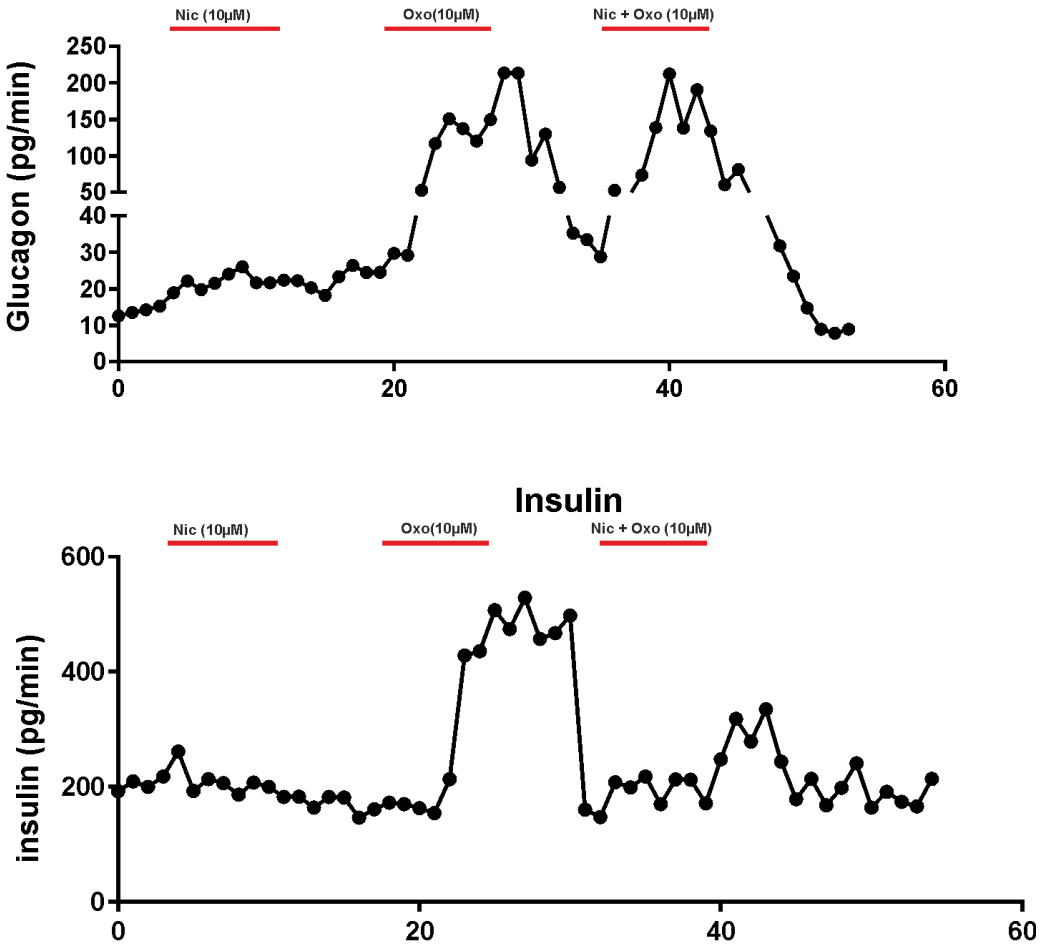


Figure A3.2 - Effect of nicotine and oxotremorine on glucagon and insulin secretion in pancreas perfusion experiments

(a) Effect of nicotine, oxotremorine and nicotine and oxotremorine together on glucagon secretion at 3 mM glucose. Note slight increase in glucagon secretion after nicotine application and lack of additive effect when nicotine and oxotremorine applied together. **(b)** As in (a) but measuring insulin.

Appendix 4: Data collected by collaborators in Chapter 5

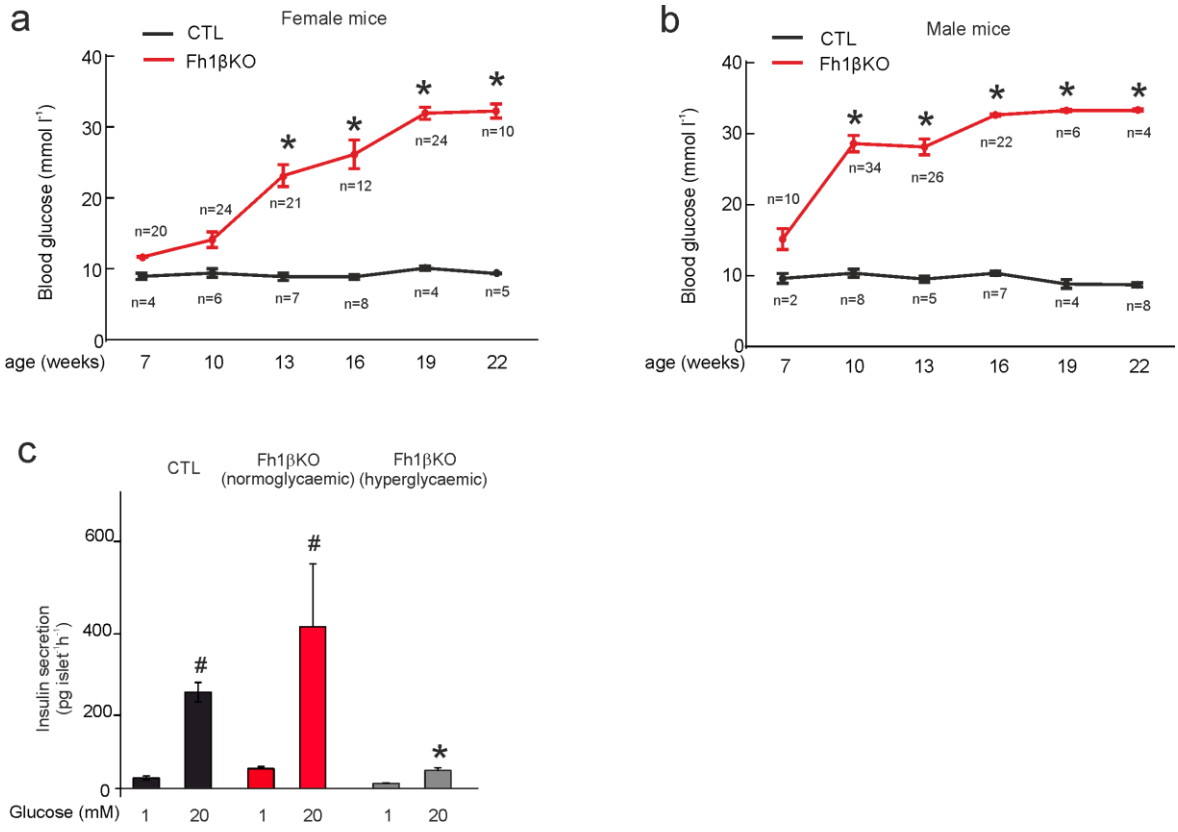


Figure A4.1 - Fh1βKO glucose profiles and insulin secretion

(a) Relationship between blood glucose and age in Fh1βKO mice compared to littermate control (CTL) in female mice. **(b)** Relationship between blood glucose and age in Fh1βKO mice compared to littermate control (CTL) in male mice. **(c)** Insulin secretion at 1 mM and 20 mM glucose in islets from CTL mice (black columns), normoglycaemic Fh1βKO mice (red columns) and hyperglycaemic Fh1βKO mice (grey columns). # Denotes significant ($p < 0.05$) vs. basal; * Denotes significant ($p < 0.05$) vs. control.

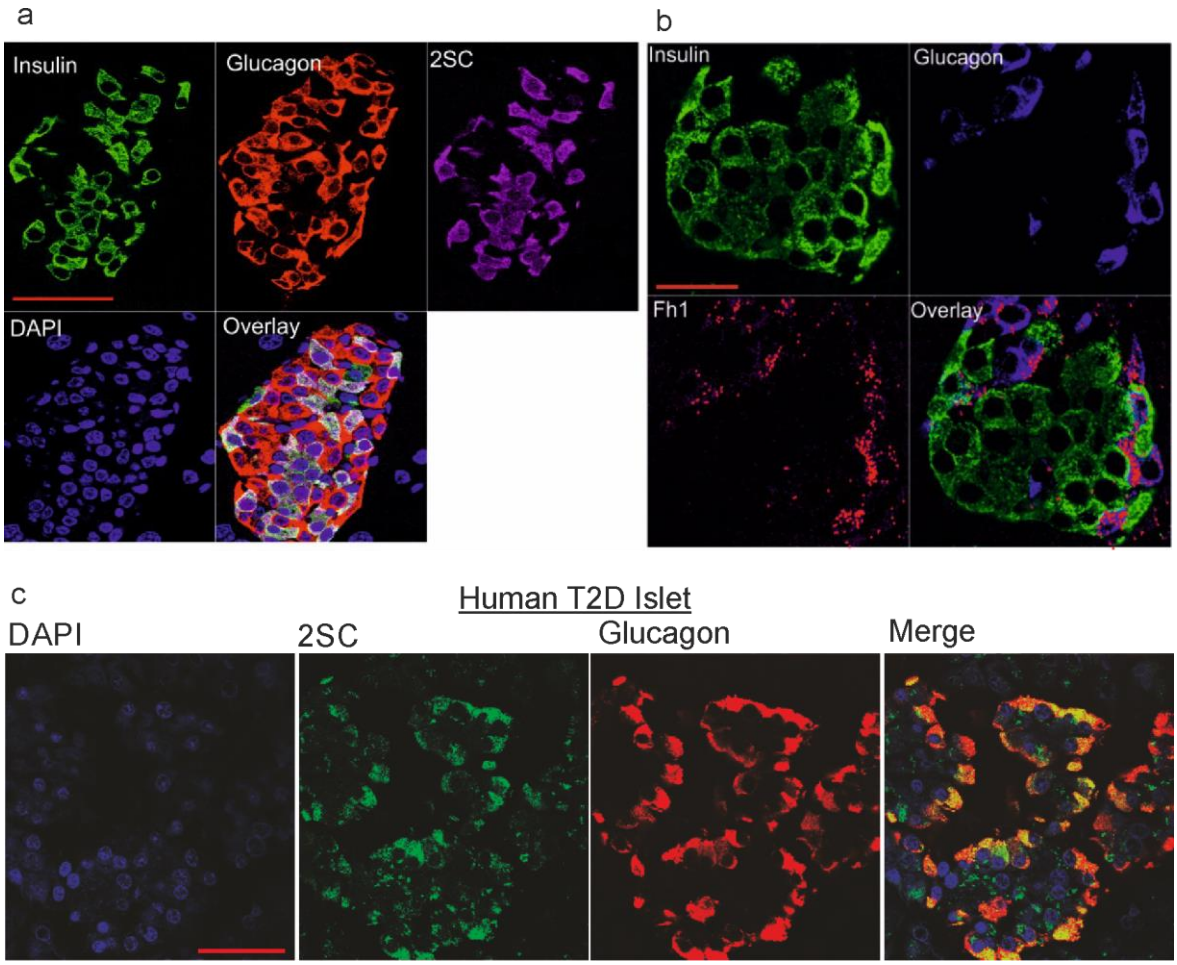


Figure A4.2 - 2SC staining in tissues from non-diabetic and diabetic mouse models and human donors

(a) From *left to right*, immunofluorescence of insulin (green), glucagon (red), 2SC (purple), DAPI nuclear stain (blue) and overlay of islet hormones insulin, glucagon and 2SC (white) in Fh1βKO islets. **(b)** From *left to right*, immunofluorescence of insulin (green), glucagon (blue), Fh1 (red) and overlay of all three channels in Fh1βKO islets. **(c)** From *left to right*, immunofluorescence of DAPI (blue), 2SC (green), glucagon (red) and merge (yellow) in type 2 diabetic islet. Note strong 2SC staining in α-cells.

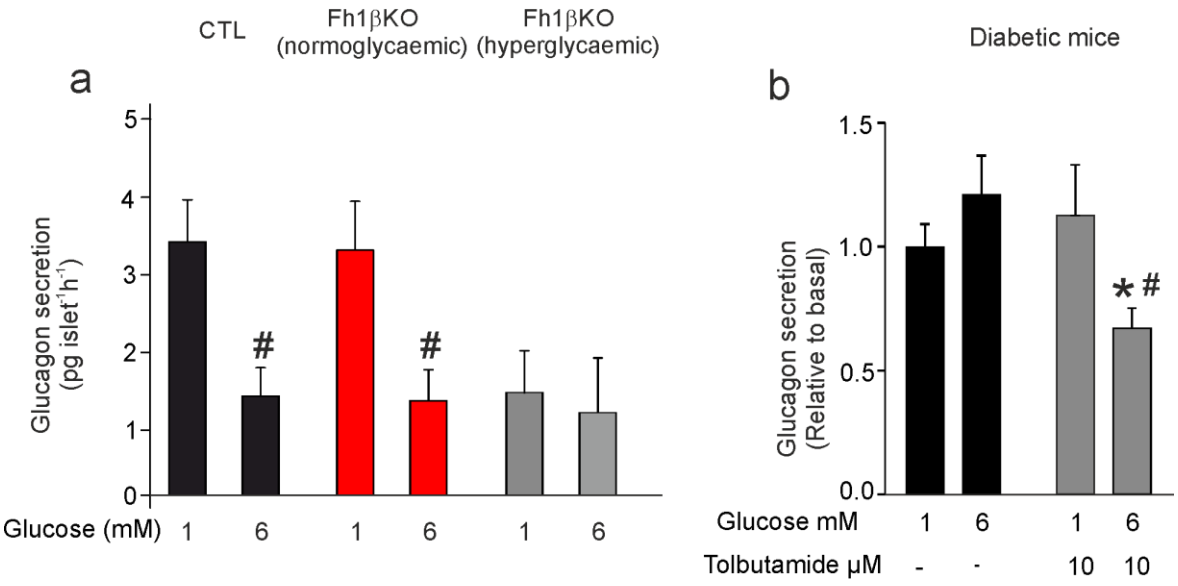


Figure A4.3 - Glucagon secretion in Fh1βKO mice

(a) Glucagon secretion at 1 mM and 20 mM glucose in islets from CTL mice (black columns), normoglycaemic Fh1βKO mice (red columns) and hyperglycaemic Fh1βKO mice (grey columns). *Difference is significant vs. 1 mM glucose. # Denotes significant (p < 0.05) vs. basal **(b)** Glucagon secretion at 1 mM and 6 mM glucose, with (black columns) or without (grey columns) tolbutamide in diabetic mice. *Denotes significant vs. 6 mM glucose without tolbutamide.

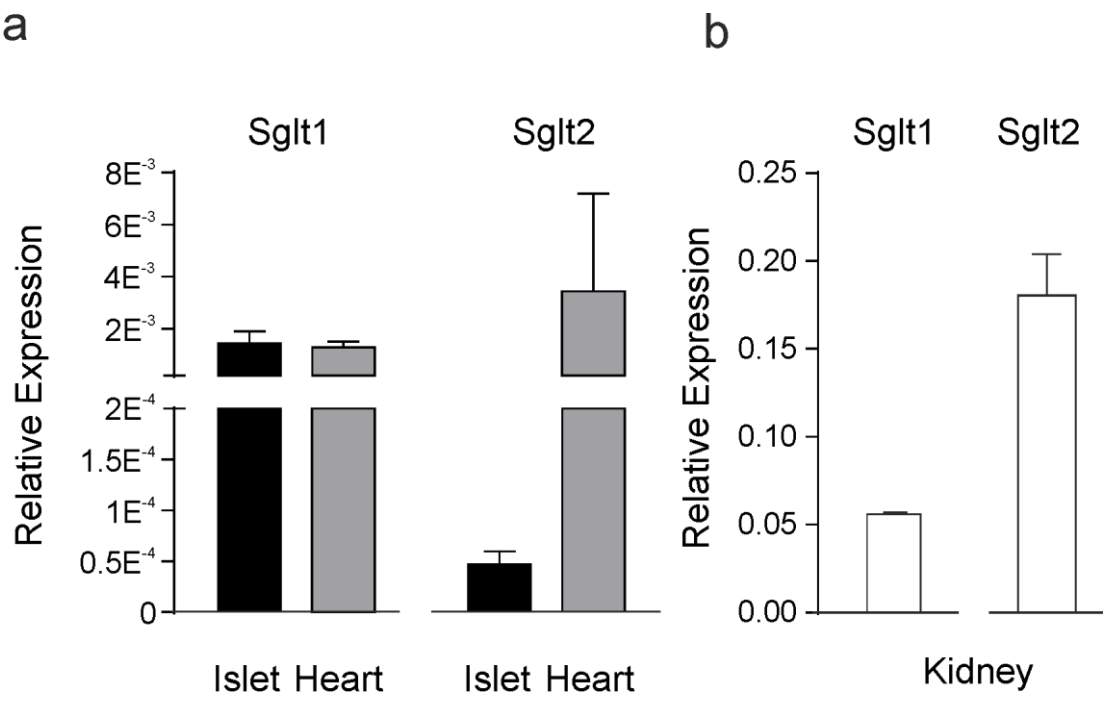


Figure A4.4 - SGLT 1 and SGLT 2 expression in islet, heart and kidney

(a) qPCR of mRNA expression of the genes encoding Slc5a1 and Slc5a2 in islet and heart from C57BL/6J mice. **(b)** qPCR of mRNA expression of the genes encoding SGLT1 and SGLT2 in kidney from C57BL/6J mice.

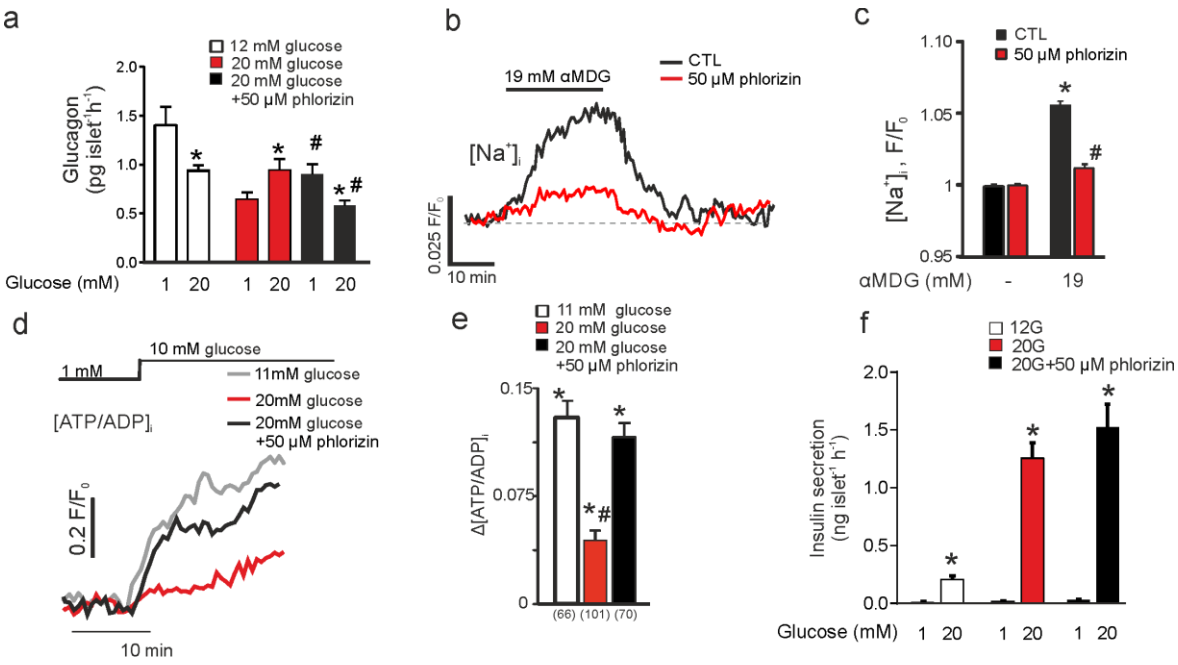


Figure A4.5 - Effect of phlorizin on glucagon secretion and $[ATP/ADP]_i$

(a) Glucagon secretion at 1 mM and 20 mM glucose in islets cultured for 48 h at 12 mM glucose (open columns), 20 mM glucose (red columns) and 20 mM glucose + 50 µM phlorizin (black columns) **(b)** Effect of the non-metabolisable sugar derivative αMDG on $[Na^+]_i$ with (red trace) or without (black trace) phlorizin in CTL mice. 1 mM glucose applied throughout **(c)** $[Na^+]_i$ quantified as F/F_0 with (red columns) or without (black columns) phlorizin. **(d)** $[ATP/ADP]_i$ in response to 10 mM glucose in islets cultured for 48 h at 11 mM glucose (grey trace), 20 mM glucose (red trace) and 20 mM glucose + 50 µM phlorizin (black trace). **(e)** $\Delta[ATP/ADP]_i$ upon 10 mM glucose application in islets cultured for 48 h at 11 mM glucose (open columns), 20 mM glucose (red columns) and 20 mM glucose + 50 µM phlorizin (black columns). **(f)** Insulin secretion at 1 mM and 20 mM glucose in islets cultured for 48 h at 12 mM glucose (open columns), 20 mM glucose (red columns) and 20 mM glucose + 50 µM phlorizin (black columns). All experiments performed on NMRI mice unless otherwise stated. *Denotes significant ($p < 0.05$) vs. basal. # Denotes significant ($p < 0.05$) vs. control.

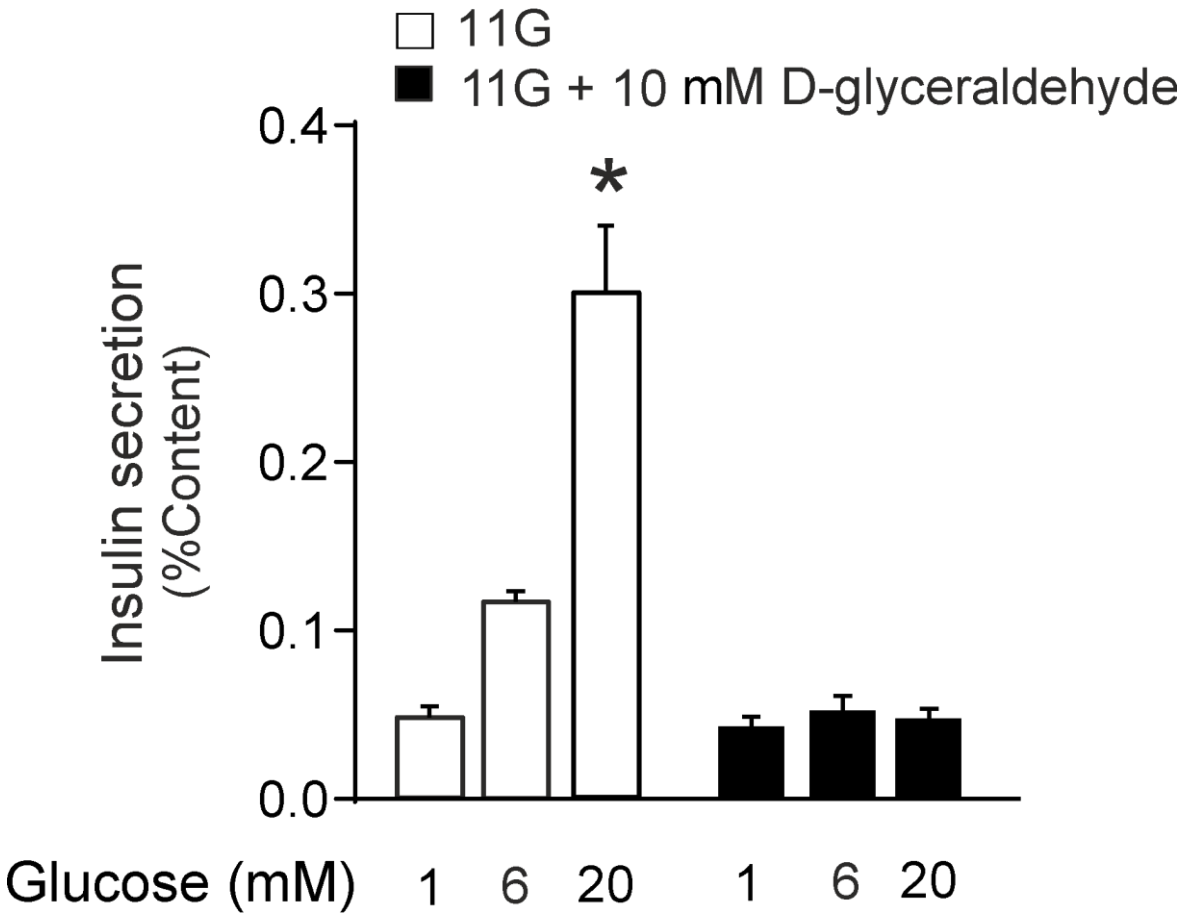


Figure A4.6 - Effect of chronic glyceraldehyde on insulin secretion

Insulin secretion (%Content) at 1 mM, 6 mM and 20 mM glucose in islets from C57BL/6J mice cultured for 24 h at 11 mM glucose (open columns) and 11 mM glucose + 10 mM D-glyceraldehyde. * Denotes significant vs. 6 mM glucose (without D-glyceraldehyde). Adapted from Adam et al. (2017) (for which I am an author).

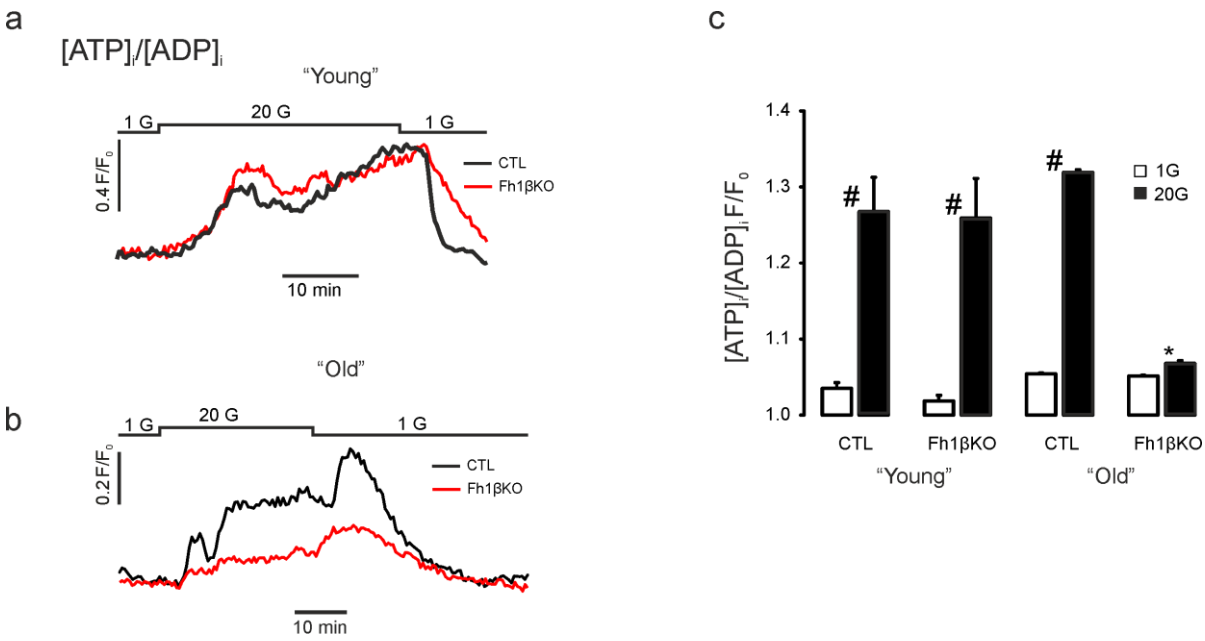


Figure A4.7 - Effect of high glucose on $[ATP/ADP]_i$ in islets from CTL, normoglycaemic Fh1βKO and hyperglycaemic Fh1βKO mice

(a) β-cell $[ATP/ADP]_i$ in response to 20 mM glucose in islets from 'Young' normoglycaemic Fh1βKO mice (red trace) and littermate controls (CTL) (black trace). **(b)** β-cell $[ATP/ADP]_i$ in response to 20 mM glucose in islets from 'Old' hyperglycaemic Fh1βKO mice (red trace) and littermate controls (CTL) (black trace). **(c)** β-cell $[ATP/ADP]_i$ at 1 mM glucose (open columns) and 20 mM glucose (grey columns) in young CTL mice, young Fh1βKO, old CTL and old Fh1βKO mice. # Denotes significant ($p < 0.05$) vs. basal *Denotes significant ($p < 0.05$) vs. control. Adapted from Adam et al. (2017) (for which I am an author)

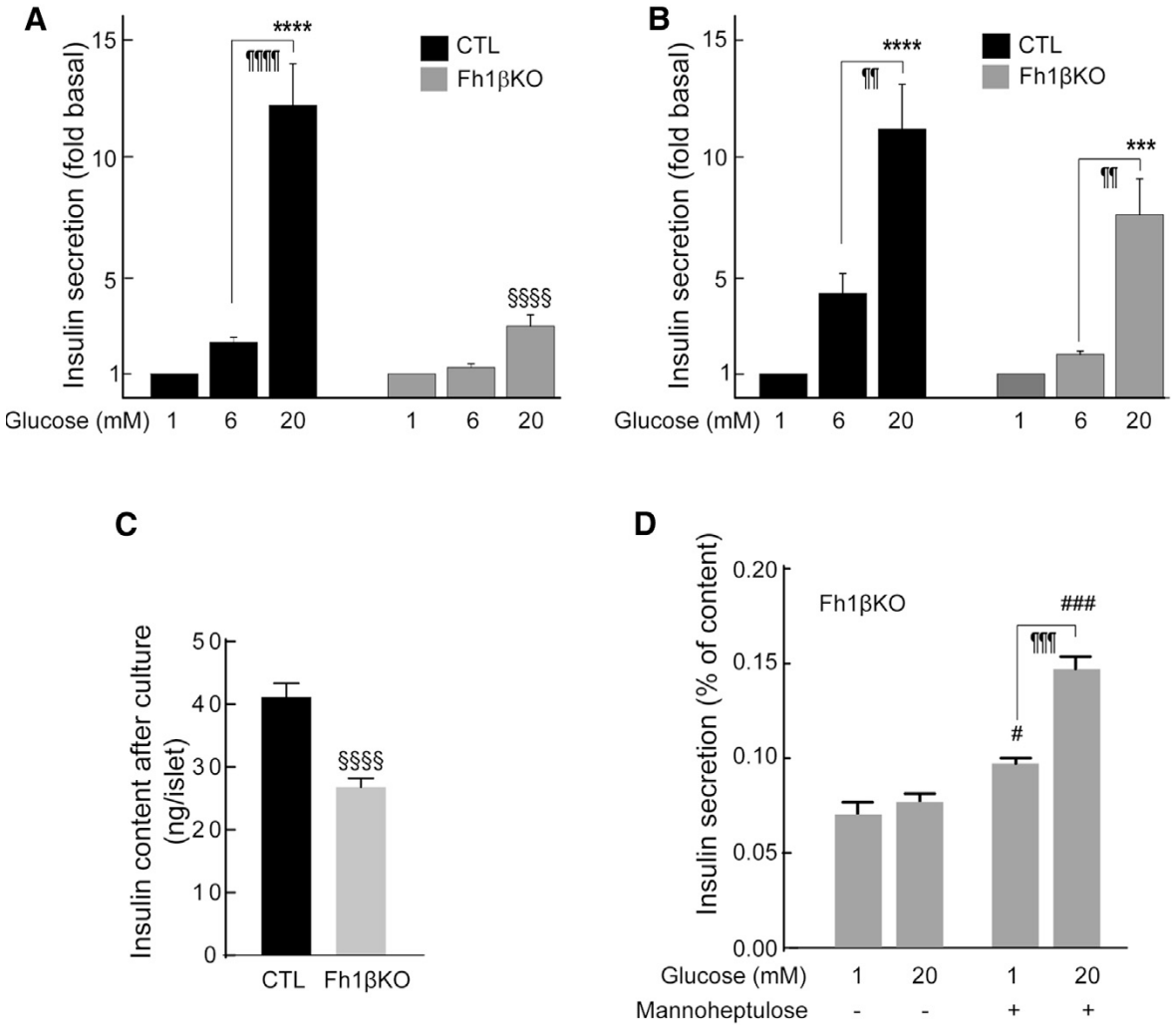


Figure A4.8 - Restoration of glucose-stimulated insulin secretion by normoglycaemic culture and culture with the glucokinase inhibitor mannoheptulose

(a) Insulin secretion from acutely isolated islets from hyperglycaemic Fh1βKO mice and littermate controls (CTL) at 1 mM, 6 mM and 20 mM glucose. ****$p < 0.0001$ vs. 1 mM glucose; ¶¶¶¶$p < 0.0001$ vs. 6 mM glucose §§§§p < 0.0001 versus 20 mM glucose in CTL. **(b)** Insulin secretion from same islets as in (a) cultured for 65 h at 12 mM glucose. ***$p < 0.001$ versus 1 mM glucose; ¶¶$p < 0.01$ versus 6 mM glucose; §§§§$p < 0.0001$ versus 20 mM glucose in CTL. **(c)** Difference in insulin content between Fh1βKO and CTL after 65 h culture at 12 mM glucose. §§§§$p < 0.0001$ vs. 1 mM glucose **(d)** Insulin secretion from islets from hyperglycaemic Fh1βKO mice after culture at 20 mM glucose with or without the GK inhibitor mannoheptulose. ¶¶¶$p < 0.001$ *vs.* 1 mM glucose; #$p < 0.05$, and ###$p < 0.001$ *vs.* corresponding condition (without mannoheptulose). Error Bars represent SEM. Figure is from Adam et al. (2017) (for which I am an author)

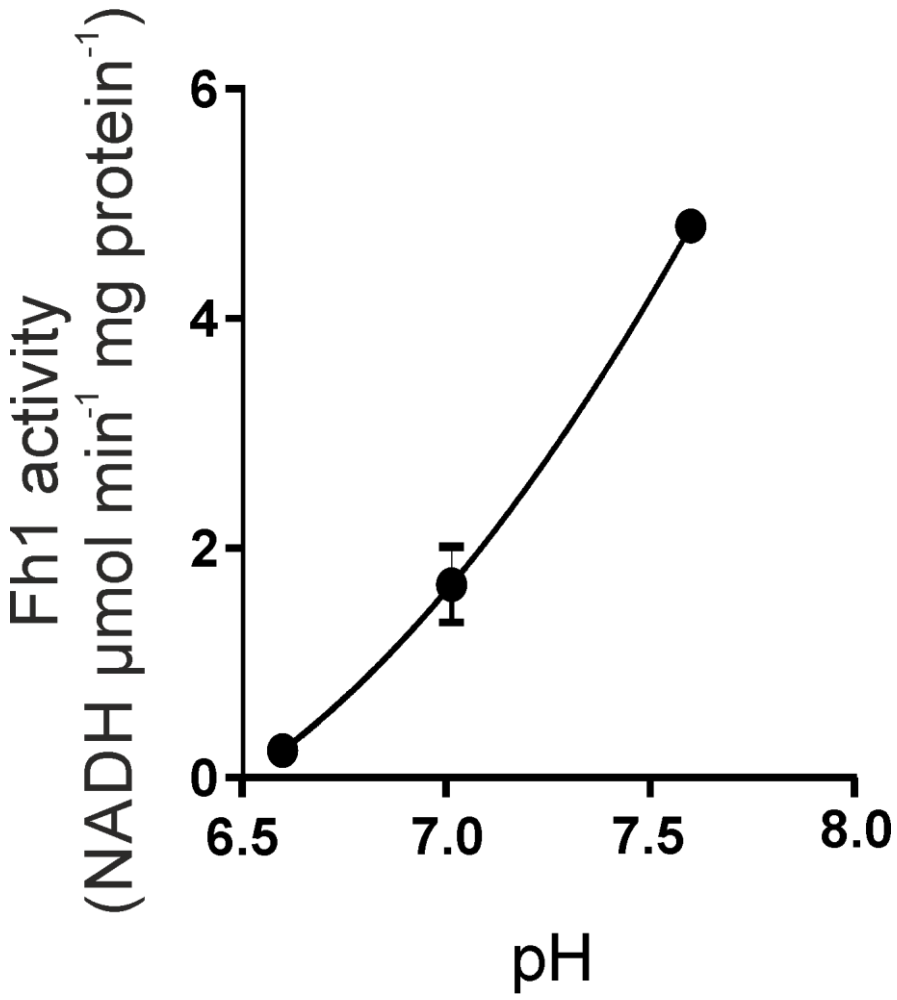


Figure A4.9 - pH dependence of fumarate hydratase activity

pH dependence of Fh1 activity, measured as NADH production. The curve is a least-squares fit to the data points.

Appendix 5: Data collected by collaborators in Chapter 6

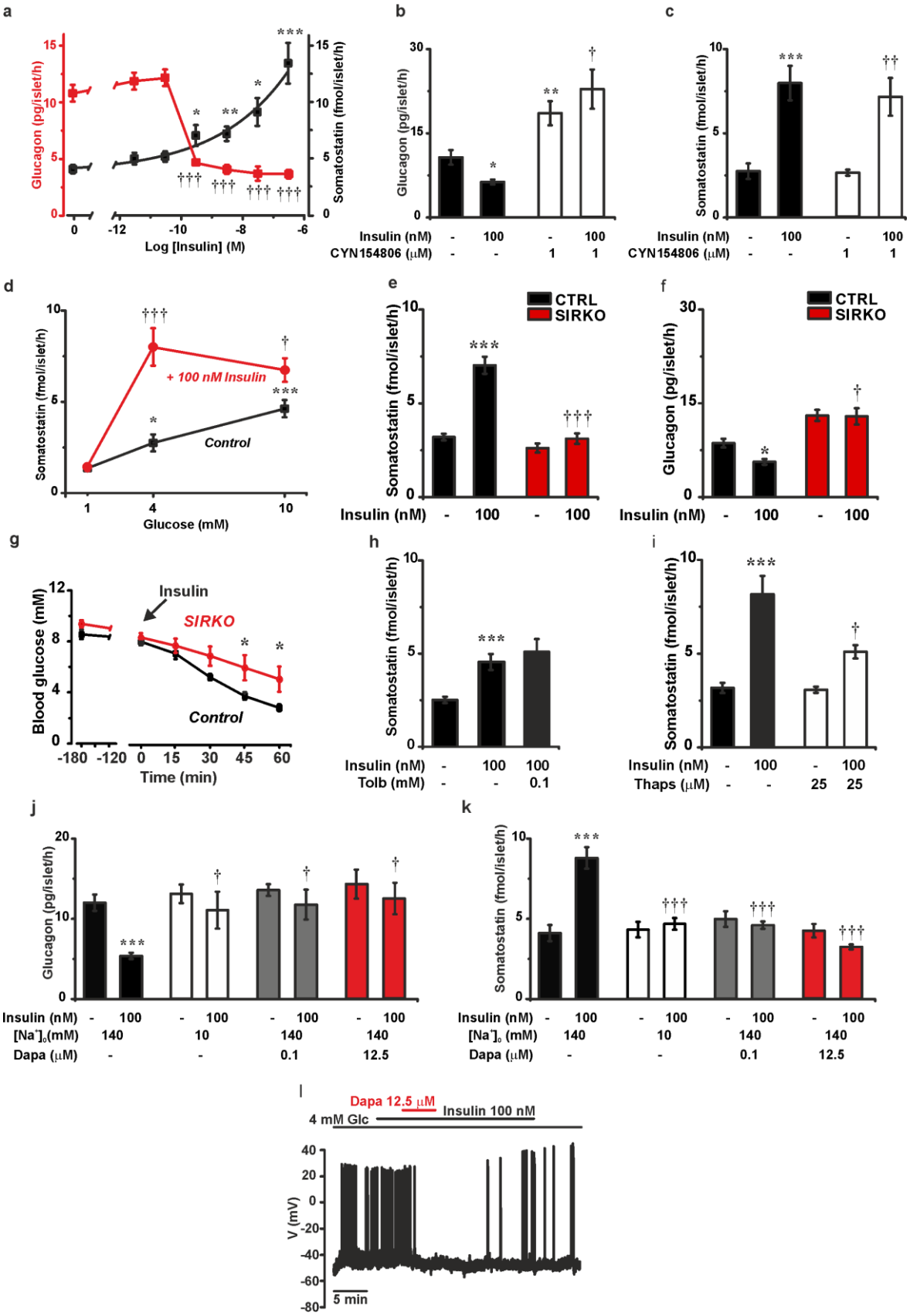


Figure A5.1 - Effects of insulin on somatostatin release in isolated mouse pancreatic islets.

(a) Effect of increasing concentrations of insulin (3 pM, 30 pM, 300 pM, 3 nM, 30 nM, 300 nM; ; logarithmic abscissa) on glucagon (red) and somatostatin (black) secretion. *p < 0.05, **p < 0.01 and ***p < 0.001 and †††p < 0.001 for the effects of insulin on somatostatin and glucagon secretion vs. 4 mM glucose alone, respectively. **(b)** Glucagon secretion in the absence or presence of insulin with or without the SSTR2 antagonist CYN 154806. *p < 0.05 and **p < 0.005 vs. 4 mM glucose; †p < 0.05 vs. 4 mM glucose and insulin. **(c)** Same as (b) but measuring somatostatin secretion. ***p < 0.001 vs. 4 mM glucose; ††p < 0.005 vs. 4 mM glucose and CYN 154806. **(d)** Somatostatin secretion at 1 mM, 4 mM and 10 mM glucose with or without insulin. *p < 0.05, ***p < 0.001 vs. 1 mM glucose in the absence of insulin; †p < 0.05, †††p < 0.005 vs. the same glucose concentration but in the absence of insulin. **(e)** Somatostatin secretion in the absence or presence of insulin in control (CTRL) and δ-cell-specific insulin receptor knockout (SIRKO) mice. **(f)** As in (e) but measuring glucagon secretion. *p < 0.05 and ***p < 0.001 vs. 4 mM glucose; †p < 0.05 and †††p < 0.001 vs. 4 mM glucose and 100 nM insulin. **(g)** Insulin tolerance test in control and SIRKO mice. *p < 0.05 vs. control. **(h)** Effect of insulin on somatostatin secretion in the presence or absence of tolbutamide **(i)** Somatostatin secretion in the absence or presence of insulin with or without the SERCA-ATPase inhibitor thapsigargin. ***p < 0.001 vs. 1 mM glucose alone. **(j)** The effect of insulin on glucagon secretion at normal $[Na^+]_o$ (140 mM), at low $[Na^+]_o$ (10 mM), and in the presence of 0.1 µM or 12.5 µM dapagliflozin. ***p < 0.001 vs. 4 mM glucose; †p < 0.05 vs. 4 mM glucose incl. insulin and 140 mM $[Na^+]_o$ **(k)** As with (j) but measuring somatostatin secretion. ***p < 0.001 vs. 4 mM glucose †††p < 0.001 vs. 4 mM glucose incl. insulin and 140 mM $[Na^+]_o$ **(i)** The effect of dapagliflozin on action potential firing in the presence of insulin. All secretion experiments done at 4 mM glucose unless stated otherwise.

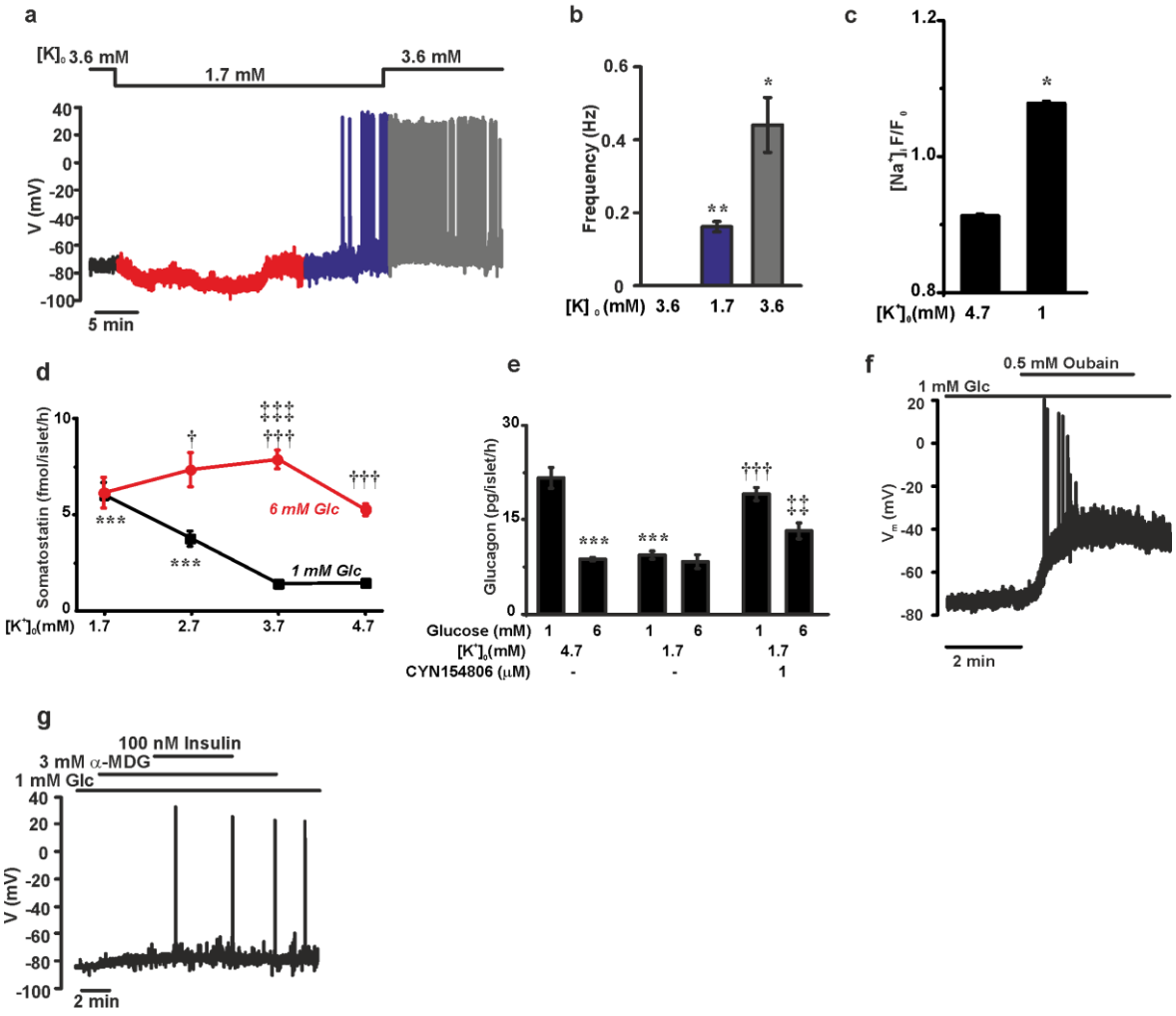


Figure A5.2 - Effects of low $[K^+]_o$ and αMDG on electrical activity, somatostatin and glucagon secretion

(a-b) Effect of low $[K^+]_o$ (1.7 mM) on δ-cell electrical activity (a) Action potential frequency (b) at 3.6 mM $[K^+]_o$, at 1.7 mM $[K^+]_o$ and returning to 3.6 mM $[K^+]_o$ (representative of 5 δ-cells from 5 different islets). Experiments done at 1 mM glucose * $p < 0.05$ and ** $p < 0.005$ vs. 3.6 mM $[K^+]_o$. **(c)** $[Na^+]_i$ measured with the fluorescent dye Sodium green at 4.7 mM $[K^+]_o$ and 1 mM $[K^+]_o$. * $p < 0.05$ vs. 4.7 mM $[K^+]_o$. **(d)** Effect of increasing concentrations of $[K^+]_o$ on somatostatin secretion at 1 mM (black) and 6 mM (red) glucose *** $p < 0.001$ vs. 1 mM glucose at 4.7 mM $[K^+]_o$; † $p < 0.05$ and ††† $p < 0.001$ vs. 1 mM glucose at the corresponding $[K^+]_o$; ‡‡‡ $p < 0.001$ vs. 6 mM glucose at 4.7 mM $[K^+]_o$. **(e)** Glucagon secretion at 1 mM and 6 mM glucose at normal $[K^+]_o$ (4.7 mM), at low $[K^+]_o$ (1.7 mM) in the absence or present of CYN 154806. *** $p < 0.001$ vs. 1 mM glucose at 4.7 mM $[K^+]_o$; ††† $p < 0.001$ *vs.* 1 mM glucose at 1.7 mM $[K^+]_o$; ‡‡ $p < 0.005$ vs. 1 mM glucose at 1.7 mM $[K^+]_o$ in the presence of CYN 154806. **(f)** Effect of the Na^+/K^+ ATPase inhibitor oubain on δ cell electrical activity. **(g)** Effect of insulin on δ-cell electrical activity at 1 mM glucose in the presence of the non-metabolisable glucose derivative αMDG. (Representative of 2 out of 3 δ-cells from 3 different islets).

References

ADAM, J., RAMRACHEYA, R., CHIBALINA, M. V., TERNETTE, N., HAMILTON, A., TARASOV, A. I., ZHANG, Q., REBELATO, E., RORSMAN, N. J. G., MARTIN-DEL-RIO, R., LEWIS, A., OZKAN, G., DO, H. W., SPEGEL, P., SAITOH, K., KATO, K., IGARASHI, K., KESSLER, B. M., PUGH, C. W., TAMARIT-RODRIGUEZ, J., MULDER, H., CLARK, A., FRIZZELL, N., SOGA, T., ASHCROFT, F. M., SILVER, A., POLLARD, P. J. & RORSMAN, P. 2017. Fumarate Hydratase Deletion in Pancreatic beta Cells Leads to Progressive Diabetes. *Cell Rep,* 20**,** 3135-3148.

ADAM, J., YANG, M., BAUERSCHMIDT, C., KITAGAWA, M., O'FLAHERTY, L., MAHESWARAN, P., OZKAN, G., SAHGAL, N., BABAN, D., KATO, K., SAITO, K., IINO, K., IGARASHI, K., STRATFORD, M., PUGH, C., TENNANT, D. A., LUDWIG, C., DAVIES, B., RATCLIFFE, P. J., EL-BAHRAWY, M., ASHRAFIAN, H., SOGA, T. & POLLARD, P. J. 2013. A role for cytosolic fumarate hydratase in urea cycle metabolism and renal neoplasia. *Cell Rep,* 3**,** 1440-8.

ADRIAENSSENS, A. E., SVENDSEN, B., LAM, B. Y., YEO, G. S., HOLST, J. J., REIMANN, F. & GRIBBLE, F. M. 2016. Transcriptomic profiling of pancreatic alpha, beta and delta cell populations identifies delta cells as a principal target for ghrelin in mouse islets. *Diabetologia,* 59**,** 2156-65.

AHREN, B. & LUNDQUIST, I. 1982. Interaction of vasoactive intestinal peptide (VIP) with cholinergic stimulation of glucagon secretion. *Experientia,* 38**,** 405-6.

AHREN, B., STERN, J. S., GINGERICH, R. L., CURRY, D. L. & HAVEL, P. J. 1995. Glucagon secretory response to hypoglycaemia, adrenaline and carbachol in streptozotocin-diabetic rats. *Acta Physiol Scand,* 155**,** 215-21.

AKATSUKA, A., SINGH, T. J., NAKABAYASHI, H., LIN, M. C. & HUANG, K. P. 1985. Glucagon-stimulated phosphorylation of rat liver glycogen synthase in isolated hepatocytes. *J Biol Chem,* 260**,** 3239-42.

ALBUQUERQUE, E. X., PEREIRA, E. F., ALKONDON, M. & ROGERS, S. W. 2009. Mammalian nicotinic acetylcholine receptors: from structure to function. *Physiol Rev,* 89**,** 73-120.

ALDERSON, N. L., WANG, Y., BLATNIK, M., FRIZZELL, N., WALLA, M. D., LYONS, T. J., ALT, N., CARSON, J. A., NAGAI, R., THORPE, S. R. & BAYNES, J. W. 2006. S-(2-Succinyl)cysteine: a novel chemical modification of tissue proteins by a Krebs cycle intermediate. *Arch Biochem Biophys,* 450**,** 1-8.

ALLEN, M. D. & ZHANG, J. 2006. Subcellular dynamics of protein kinase A activity visualized by FRET-based reporters. *Biochem Biophys Res Commun,* 348**,** 716-21.

ALMACA, J., MOLINA, J., MENEGAZ, D., PRONIN, A. N., TAMAYO, A., SLEPAK, V., BERGGREN, P. O. & CAICEDO, A. 2016. Human Beta Cells Produce and Release Serotonin to Inhibit Glucagon Secretion from Alpha Cells. *Cell Rep,* 17**,** 3281-3291.

ALQUIER, T., KAWASHIMA, J., TSUJI, Y. & KAHN, B. B. 2007. Role of hypothalamic adenosine 5'-monophosphate-activated protein kinase in the impaired counterregulatory response induced by repetitive neuroglucopenia. *Endocrinology,* 148**,** 1367-75.

AMMALA, C., ELIASSON, L., BOKVIST, K., BERGGREN, P. O., HONKANEN, R. E., SJOHOLM, A. & RORSMAN, P. 1994. Activation of protein kinases and

inhibition of protein phosphatases play a central role in the regulation of exocytosis in mouse pancreatic beta cells. *Proc Natl Acad Sci U S A,* 91**,** 4343-7.
ANDERSSON, K. & ARNER, P. 2001. Systemic nicotine stimulates human adipose tissue lipolysis through local cholinergic and catecholaminergic receptors. *Int J Obes Relat Metab Disord,* 25**,** 1225-32.
ARBELAEZ, A. M., POWERS, W. J., VIDEEN, T. O., PRICE, J. L. & CRYER, P. E. 2008. Attenuation of counterregulatory responses to recurrent hypoglycemia by active thalamic inhibition: a mechanism for hypoglycemia-associated autonomic failure. *Diabetes,* 57**,** 470-5.
ARIAS, H. R., RICHARDS, V. E., NG, D., GHAFOORI, M. E., LE, V. & MOUSA, S. A. 2009. Role of non-neuronal nicotinic acetylcholine receptors in angiogenesis. *Int J Biochem Cell Biol,* 41**,** 1441-51.
ARKHAMMAR, P., BERGGREN, P. O. & RORSMAN, P. 1986a. Direct evidence for opposite effects of D-glucose and D-glyceraldehyde on cytoplasmic pH of mouse pancreatic beta-cells. *Biosci Rep,* 6**,** 355-61.
ARKHAMMAR, P., NILSSON, T. & BERGGREN, P. O. 1986b. Stimulation of insulin release by the phorbol ester 12-O-tetradecanoylphorbol 13-acetate in the clonal cell line RINm5F despite a lowering of the free cytoplasmic Ca2+ concentration. *Biochim Biophys Acta,* 887**,** 236-41.
ARREDONDO, J., NGUYEN, V. T., CHERNYAVSKY, A. I., JOLKOVSKY, D. L., PINKERTON, K. E. & GRANDO, S. A. 2001. A receptor-mediated mechanism of nicotine toxicity in oral keratinocytes. *Lab Invest,* 81**,** 1653-68.
ARREDOUANI, A., RUAS, M., COLLINS, S. C., PARKESH, R., CLOUGH, F., PILLINGER, T., COLTART, G., RIETDORF, K., ROYLE, A., JOHNSON, P., BRAUN, M., ZHANG, Q., SONES, W., SHIMOMURA, K., MORGAN, A. J., LEWIS, A. M., CHUANG, K. T., TUNN, R., GADEA, J., TEBOUL, L., HEISTER, P. M., TYNAN, P. W., BELLOMO, E. A., RUTTER, G. A., RORSMAN, P., CHURCHILL, G. C., PARRINGTON, J. & GALIONE, A. 2015. Nicotinic Acid Adenine Dinucleotide Phosphate (NAADP) and Endolysosomal Two-pore Channels Modulate Membrane Excitability and Stimulus-Secretion Coupling in Mouse Pancreatic beta Cells. *J Biol Chem,* 290**,** 21376-92.
ASHCROFT, F. M. & RORSMAN, P. 2012. Diabetes mellitus and the beta cell: the last ten years. *Cell,* 148**,** 1160-71.
AUTHIER, F. & DESBUQUOIS, B. 2008. Glucagon receptors. *Cell Mol Life Sci,* 65**,** 1880-99.
AZARIAS, G., PERRETEN, H., LENGACHER, S., POBURKO, D., DEMAUREX, N., MAGISTRETTI, P. J. & CHATTON, J. Y. 2011. Glutamate transport decreases mitochondrial pH and modulates oxidative metabolism in astrocytes. *J Neurosci,* 31**,** 3550-9.
AZUMA, K. K., HENSLEY, C. B., PUTNAM, D. S. & MCDONOUGH, A. A. 1991. Hypokalemia decreases Na(+)-K(+)-ATPase alpha 2- but not alpha 1-isoform abundance in heart, muscle, and brain. *Am J Physiol,* 260**,** C958-64.
BAJORUNAS, D. R., FORTNER, J. G. & JASPAN, J. B. 1986. Glucagon immunoreactivity and chromatographic profiles in pancreatectomized humans. Paradoxical response to oral glucose. *Diabetes,* 35**,** 886-93.
BANKIR, L., ROUSSEL, R. & BOUBY, N. 2015. Protein- and diabetes-induced glomerular hyperfiltration: role of glucagon, vasopressin, and urea. *Am J Physiol Renal Physiol,* 309**,** F2-23.
BARNES, A. J. & BLOOM, S. R. 1976. Pancreatectomised man: A model for diabetes without glucagon. *Lancet,* 1**,** 219-21.

BARON, A. D., SCHAEFFER, L., SHRAGG, P. & KOLTERMAN, O. G. 1987. Role of hyperglucagonemia in maintenance of increased rates of hepatic glucose output in type II diabetics. *Diabetes,* 36**,** 274-83.
BATTEZZATI, A., SIMONSON, D. C., LUZI, L. & MATTHEWS, D. E. 1998. Glucagon increases glutamine uptake without affecting glutamine release in humans. *Metabolism,* 47**,** 713-23.
BEALL, C., ASHFORD, M. L. & MCCRIMMON, R. J. 2012. The physiology and pathophysiology of the neural control of the counterregulatory response. *Am J Physiol Regul Integr Comp Physiol,* 302**,** R215-23.
BEGUM, N. A. & DATTA, A. G. 1991. Effect of glucagon and some other alpha and beta adrenergic agonists and antagonists on alanine amino transferase of perfused rat liver. *Mol Cell Biochem,* 105**,** 7-13.
BENNER, C., VAN DER MEULEN, T., CACERES, E., TIGYI, K., DONALDSON, C. J. & HUISING, M. O. 2014. The transcriptional landscape of mouse beta cells compared to human beta cells reveals notable species differences in long non-coding RNA and protein-coding gene expression. *BMC Genomics,* 15**,** 620.
BERNARDI, P. 1999. Mitochondrial transport of cations: channels, exchangers, and permeability transition. *Physiol Rev,* 79**,** 1127-55.
BERNSTEIN, L. H. & EVERSE, J. 1978. Studies on the mechanism of the malate dehydrogenase reaction. *J Biol Chem,* 253**,** 8702-7.
BERTS, A., GYLFE, E. & HELLMAN, B. 1997. Cytoplasmic Ca2+ in glucagon-producing pancreatic alpha-cells exposed to carbachol and agents affecting Na+ fluxes. *Endocrine,* 6**,** 79-83.
BEST, L., BONE, E. A., MEATS, J. E. & TOMLINSON, S. 1988a. Is intracellular pH a coupling factor in nutrient-stimulated pancreatic islets? *J Mol Endocrinol,* 1**,** 33-8.
BEST, L., YATES, A. P., GORDON, C. & TOMLINSON, S. 1988b. Modulation by cytosolic pH of calcium and rubidium fluxes in rat pancreatic islets. *Biochem Pharmacol,* 37**,** 4611-5.
BJAALAND, T., HII, C. S., JONES, P. M. & HOWELL, S. L. 1988. Role of protein kinase C in arginine-induced glucagon secretion from isolated rat islets of Langerhans. *J Mol Endocrinol,* 1**,** 105-10.
BLACHLY-DYSON, E. & FORTE, M. 2001. VDAC channels. *IUBMB Life,* 52**,** 113-8.
BLATNIK, M., FRIZZELL, N., THORPE, S. R. & BAYNES, J. W. 2008. Inactivation of glyceraldehyde-3-phosphate dehydrogenase by fumarate in diabetes: formation of S-(2-succinyl)cysteine, a novel chemical modification of protein and possible biomarker of mitochondrial stress. *Diabetes,* 57**,** 41-9.
BLODGETT, D. M., NOWOSIELSKA, A., AFIK, S., PECHHOLD, S., CURA, A. J., KENNEDY, N. J., KIM, S., KUCUKURAL, A., DAVIS, R. J., KENT, S. C., GREINER, D. L., GARBER, M. G., HARLAN, D. M. & DIIORIO, P. 2015. Novel Observations From Next-Generation RNA Sequencing of Highly Purified Human Adult and Fetal Islet Cell Subsets. *Diabetes,* 64**,** 3172-81.
BLOOM, S. R., EDWARDS, A. V. & GHATEI, M. A. 1983. Endocrine responses to exogenous bombesin and gastrin releasing peptide in conscious calves. *J Physiol,* 344**,** 37-48.
BOCK, T., PAKKENBERG, B. & BUSCHARD, K. 2005. Genetic background determines the size and structure of the endocrine pancreas. *Diabetes,* 54**,** 133-7.
BODE, H. P., WEBER, S., FEHMANN, H. C. & GOKE, B. 1999. A nutrient-regulated cytosolic calcium oscillator in endocrine pancreatic glucagon-secreting cells. *Pflugers Arch,* 437**,** 324-34.

BOFFI, J. C., MARCOVICH, I., GILL-THIND, J. K., CORRADI, J., COLLINS, T., LIPOVSEK, M. M., MOGLIE, M., PLAZAS, P. V., CRAIG, P. O., MILLAR, N. S., BOUZAT, C. & ELGOYHEN, A. B. 2017. Differential Contribution of Subunit Interfaces to alpha9alpha10 Nicotinic Acetylcholine Receptor Function. *Mol Pharmacol,* 91**,** 250-262.

BOLLHEIMER, L. C., LANDAUER, H. C., TROLL, S., SCHWEIMER, J., WREDE, C. E., SCHOLMERICH, J. & BUETTNER, R. 2004. Stimulatory short-term effects of free fatty acids on glucagon secretion at low to normal glucose concentrations. *Metabolism,* 53**,** 1443-8.

BOLLI, G. B. & FANELLI, C. G. 1999. Physiology of glucose counterregulation to hypoglycemia. *Endocrinol Metab Clin North Am,* 28**,** 467-93, v.

BONAR, P. T. & CASEY, J. R. 2008. Plasma membrane Cl(-)/HCO(3)(-) exchangers: structure, mechanism and physiology. *Channels (Austin),* 2**,** 337-45.

BONNER, C., KERR-CONTE, J., GMYR, V., QUENIAT, G., MOERMAN, E., THEVENET, J., BEAUCAMPS, C., DELALLEAU, N., POPESCU, I., MALAISSE, W. J., SENER, A., DEPREZ, B., ABDERRAHMANI, A., STAELS, B. & PATTOU, F. 2015. Inhibition of the glucose transporter SGLT2 with dapagliflozin in pancreatic alpha cells triggers glucagon secretion. *Nat Med,* 21**,** 512-7.

BOYMAN, L., WILLIAMS, G. S., KHANANSHVILI, D., SEKLER, I. & LEDERER, W. J. 2013. NCLX: the mitochondrial sodium calcium exchanger. *J Mol Cell Cardiol,* 59**,** 205-13.

BOZEM, M., NENQUIN, M. & HENQUIN, J. C. 1987. The ionic, electrical, and secretory effects of protein kinase C activation in mouse pancreatic B-cells: studies with a phorbol ester. *Endocrinology,* 121**,** 1025-33.

BRAUN, M. 2014. The somatostatin receptor in human pancreatic beta-cells. *Vitam Horm,* 95**,** 165-93.

BRAUN, M., RAMRACHEYA, R., BENGTSSON, M., CLARK, A., WALKER, J. N., JOHNSON, P. R. & RORSMAN, P. 2010. Gamma-aminobutyric acid (GABA) is an autocrine excitatory transmitter in human pancreatic beta-cells. *Diabetes,* 59**,** 1694-701.

BRIANT, L. J. B., REINBOTHE, T. M., SPILIOTIS, I., MIRANDA, C., RODRIGUEZ, B. & RORSMAN, P. 2017. delta- and beta-cells are electrically coupled and regulate alpha-cell activity via somatostatin. *J Physiol*.

BRINGER, J., MIROUZE, J., MARCHAL, G., PHAM, T. C., LUYCKX, A., LEFEBVRE, P. & ORSETTI, A. 1981. Glucagon immunoreactivity and antidiabetic action of somatostatin in the totally duodeno-pancreatectomized and gastrectomized human. *Diabetes,* 30**,** 851-6.

BRISCOE, C. P., TADAYYON, M., ANDREWS, J. L., BENSON, W. G., CHAMBERS, J. K., EILERT, M. M., ELLIS, C., ELSHOURBAGY, N. A., GOETZ, A. S., MINNICK, D. T., MURDOCK, P. R., SAULS, H. R., JR., SHABON, U., SPINAGE, L. D., STRUM, J. C., SZEKERES, P. G., TAN, K. B., WAY, J. M., IGNAR, D. M., WILSON, S. & MUIR, A. I. 2003. The orphan G protein-coupled receptor GPR40 is activated by medium and long chain fatty acids. *J Biol Chem,* 278**,** 11303-11.

BROCKMAN, R. P. & BERGMAN, E. N. 1975. Effect of glucagon on plasma alanine and glutamine metabolism and hepatic gluconeogenesis in sheep. *Am J Physiol,* 228**,** 1628-33.

BURCELIN, R., LI, J. & CHARRON, M. J. 1995. Cloning and sequence analysis of the murine glucagon receptor-encoding gene. *Gene,* 164**,** 305-10.

CABRERA, O., BERMAN, D. M., KENYON, N. S., RICORDI, C., BERGGREN, P. O. & CAICEDO, A. 2006. The unique cytoarchitecture of human pancreatic islets has implications for islet cell function. *Proc Natl Acad Sci U S A,* 103**,** 2334-9.

CABRERA, O., JACQUES-SILVA, M. C., SPEIER, S., YANG, S. N., KOHLER, M., FACHADO, A., VIEIRA, E., ZIERATH, J. R., KIBBEY, R., BERMAN, D. M., KENYON, N. S., RICORDI, C., CAICEDO, A. & BERGGREN, P. O. 2008. Glutamate is a positive autocrine signal for glucagon release. *Cell Metab,* 7**,** 545-54.

CADUFF, A., LUTZ, H. U., HEINEMANN, L., DI BENEDETTO, G., TALARY, M. S. & THEANDER, S. 2011. Dynamics of blood electrolytes in repeated hyper- and/or hypoglycaemic events in patients with type 1 diabetes. *Diabetologia,* 54**,** 2678-89.

CALCRAFT, P. J., RUAS, M., PAN, Z., CHENG, X., ARREDOUANI, A., HAO, X., TANG, J., RIETDORF, K., TEBOUL, L., CHUANG, K. T., LIN, P., XIAO, R., WANG, C., ZHU, Y., LIN, Y., WYATT, C. N., PARRINGTON, J., MA, J., EVANS, A. M., GALIONE, A. & ZHU, M. X. 2009. NAADP mobilizes calcium from acidic organelles through two-pore channels. *Nature,* 459**,** 596-600.

CAMPANUCCI, V., KRISHNASWAMY, A. & COOPER, E. 2010. Diabetes depresses synaptic transmission in sympathetic ganglia by inactivating nAChRs through a conserved intracellular cysteine residue. *Neuron,* 66**,** 827-34.

CAPEL, R. A., BOLTON, E. L., LIN, W. K., ASTON, D., WANG, Y., LIU, W., WANG, X., BURTON, R. A., BLOOR-YOUNG, D., SHADE, K. T., RUAS, M., PARRINGTON, J., CHURCHILL, G. C., LEI, M., GALIONE, A. & TERRAR, D. A. 2015. Two-pore Channels (TPC2s) and Nicotinic Acid Adenine Dinucleotide Phosphate (NAADP) at Lysosomal-Sarcoplasmic Reticular Junctions Contribute to Acute and Chronic beta-Adrenoceptor Signaling in the Heart. *J Biol Chem,* 290**,** 30087-98.

CARAFOLI, E., SANTELLA, L., BRANCA, D. & BRINI, M. 2001. Generation, control, and processing of cellular calcium signals. *Crit Rev Biochem Mol Biol,* 36**,** 107-260.

CARLSSON, P. O., ANDERSSON, A. & JANSSON, L. 1996. Pancreatic islet blood flow in normal and obese-hyperglycemic (ob/ob) mice. *Am J Physiol,* 271**,** E990-5.

CASEY, J. R., GRINSTEIN, S. & ORLOWSKI, J. 2010. Sensors and regulators of intracellular pH. *Nat Rev Mol Cell Biol,* 11**,** 50-61.

CHAN, O., CHENG, H., HERZOG, R., CZYZYK, D., ZHU, W., WANG, A., MCCRIMMON, R. J., SEASHORE, M. R. & SHERWIN, R. S. 2008. Increased GABAergic tone in the ventromedial hypothalamus contributes to suppression of counterregulatory responses after antecedent hypoglycemia. *Diabetes,* 57**,** 1363-70.

CHAN, O., PARANJAPE, S., CZYZYK, D., HORBLITT, A., ZHU, W., DING, Y., FAN, X., SEASHORE, M. & SHERWIN, R. 2011. Increased GABAergic output in the ventromedial hypothalamus contributes to impaired hypoglycemic counterregulation in diabetic rats. *Diabetes,* 60**,** 1582-9.

CHAN, O., PARANJAPE, S. A., HORBLITT, A., ZHU, W. & SHERWIN, R. S. 2013. Lactate-induced release of GABA in the ventromedial hypothalamus contributes to counterregulatory failure in recurrent hypoglycemia and diabetes. *Diabetes,* 62**,** 4239-46.

CHAN, O., ZHU, W., DING, Y., MCCRIMMON, R. J. & SHERWIN, R. S. 2006. Blockade of GABA(A) receptors in the ventromedial hypothalamus further stimulates glucagon and sympathoadrenal but not the hypothalamo-pituitary-adrenal response to hypoglycemia. *Diabetes,* 55**,** 1080-7.

CHENG-XUE, R., GOMEZ-RUIZ, A., ANTOINE, N., NOEL, L. A., CHAE, H. Y., RAVIER, M. A., CHIMIENTI, F., SCHUIT, F. C. & GILON, P. 2013. Tolbutamide controls glucagon release from mouse islets differently than glucose: involvement of K(ATP) channels from both alpha-cells and delta-cells. *Diabetes,* 62**,** 1612-22.

CHERRINGTON, A. D. 1999. Banting Lecture 1997. Control of glucose uptake and release by the liver in vivo. *Diabetes,* 48**,** 1198-214.

CHERRINGTON, A. D., FUCHS, H., STEVENSON, R. W., WILLIAMS, P. E., ALBERTI, K. G. & STEINER, K. E. 1984. Effect of epinephrine on glycogenolysis and gluconeogenesis in conscious overnight-fasted dogs. *Am J Physiol,* 247**,** E137-44.

CHOI, I. 2012. SLC4A transporters. *Curr Top Membr,* 70**,** 77-103.

COLQUHOUN, D., UNWIN, N., SHELLEY, C., HATTON, C. & SIVILOTTI, L. 2003. Nicotinic acetylcholine receptors *In:* ABRAHAM, D. (ed.) *Burger's Medicinal Chemistry.* New York: J. Wiley.

COOPERBERG, B. A. & CRYER, P. E. 2009. Beta-cell-mediated signaling predominates over direct alpha-cell signaling in the regulation of glucagon secretion in humans. *Diabetes Care,* 32**,** 2275-80.

COOPERBERG, B. A. & CRYER, P. E. 2010. Insulin reciprocally regulates glucagon secretion in humans. *Diabetes,* 59**,** 2936-40.

CROMPTON, M. & HEID, I. 1978. The cycling of calcium, sodium, and protons across the inner membrane of cardiac mitochondria. *Eur J Biochem,* 91**,** 599-608.

CRYER, P. E. 1999. Symptoms of hypoglycemia, thresholds for their occurrence, and hypoglycemia unawareness. *Endocrinol Metab Clin North Am,* 28**,** 495-500, v-vi.

CRYER, P. E. 2002. Hypoglycaemia: the limiting factor in the glycaemic management of Type I and Type II diabetes. *Diabetologia,* 45**,** 937-48.

CRYER, P. E. 2007. Hypoglycemia, functional brain failure, and brain death. *J Clin Invest,* 117**,** 868-70.

CRYER, P. E. 2012. Minireview: Glucagon in the pathogenesis of hypoglycemia and hyperglycemia in diabetes. *Endocrinology,* 153**,** 1039-48.

CRYER, P. E. 2013. Mechanisms of hypoglycemia-associated autonomic failure in diabetes. *N Engl J Med,* 369**,** 362-72.

CULLEN, K. S., AL-OANZI, Z. H., O'HARTE, F. P., AGIUS, L. & ARDEN, C. 2014. Glucagon induces translocation of glucokinase from the cytoplasm to the nucleus of hepatocytes by transfer between 6-phosphofructo 2-kinase/fructose 2,6-bisphosphatase-2 and the glucokinase regulatory protein. *Biochim Biophys Acta,* 1843**,** 1123-34.

CUMMINGS, D. E., BRANDON, E. P., PLANAS, J. V., MOTAMED, K., IDZERDA, R. L. & MCKNIGHT, G. S. 1996. Genetically lean mice result from targeted disruption of the RII beta subunit of protein kinase A. *Nature,* 382**,** 622-6.

CZYZYK, A., LAWECKI, J. & STRYCEK-KAMINSKA, D. 1981. [Cholinergic regulation of insulin and glucagon secretion in healthy people and in patients with non-insulin dependent diabetes]. *Z Gesamte Inn Med,* 36**,** 43-7.

D'SOUZA A, M., NEUMANN, U. H., GLAVAS, M. M. & KIEFFER, T. J. 2017. The glucoregulatory actions of leptin. *Mol Metab,* 6**,** 1052-1065.

DAVIDSON, J. A., HOLLAND, W. L., ROTH, M. G., WANG, M. Y., LEE, Y., YU, X., MCCORKLE, S. K., SCHERER, P. E. & UNGER, R. H. 2016. Glucagon therapeutics: Dawn of a new era for diabetes care. *Diabetes Metab Res Rev,* 32**,** 660-665.

DAVIS, S. N., SHAVERS, C., COSTA, F. & MOSQUEDA-GARCIA, R. 1996. Role of cortisol in the pathogenesis of deficient counterregulation after antecedent hypoglycemia in normal humans. *J Clin Invest,* 98**,** 680-91.

DAVIS, S. N., SHAVERS, C., DAVIS, B. & COSTA, F. 1997. Prevention of an increase in plasma cortisol during hypoglycemia preserves subsequent counterregulatory responses. *J Clin Invest,* 100**,** 429-38.

DE HEER, J., RASMUSSEN, C., COY, D. H. & HOLST, J. J. 2008. Glucagon-like peptide-1, but not glucose-dependent insulinotropic peptide, inhibits glucagon secretion via somatostatin (receptor subtype 2) in the perfused rat pancreas. *Diabetologia,* 51**,** 2263-70.

DE MARINIS, Y. Z., SALEHI, A., WARD, C. E., ZHANG, Q., ABDULKADER, F., BENGTSSON, M., BRAHA, O., BRAUN, M., RAMRACHEYA, R., AMISTEN, S., HABIB, A. M., MORITOH, Y., ZHANG, E., REIMANN, F., ROSENGREN, A. H., SHIBASAKI, T., GRIBBLE, F., RENSTROM, E., SEINO, S., ELIASSON, L. & RORSMAN, P. 2010. GLP-1 inhibits and adrenaline stimulates glucagon release by differential modulation of N- and L-type Ca2+ channel-dependent exocytosis. *Cell Metab,* 11**,** 543-53.

DEL PRATO, S., RIVA, F., DEVIDE, A., NOSADINI, R., FEDELE, D. & TIENGO, A. 1980. Glucagon levels and ketogenesis in human diabetes following total or partial pancreatectomy and severe chronic pancreatitis. *Acta Diabetol Lat,* 17**,** 111-8.

DELEERS, M., LEBRUN, P. & MALAISSE, W. J. 1983. Increase in CO3H- influx and cellular pH in glucose-stimulated pancreatic islets. *FEBS Lett,* 154**,** 97-100.

DELEERS, M., LEBRUN, P. & MALAISSE, W. J. 1985. Nutrient-induced changes in the pH of pancreatic islet cells. *Horm Metab Res,* 17**,** 391-5.

DENROCHE, H. C., GLAVAS, M. M., TUDURI, E., KARUNAKARAN, S., QUONG, W. L., PHILIPPE, M., BRITTON, H. M., CLEE, S. M. & KIEFFER, T. J. 2016. Disrupted Leptin Signaling in the Lateral Hypothalamus and Ventral Premammillary Nucleus Alters Insulin and Glucagon Secretion and Protects Against Diet-Induced Obesity. *Endocrinology,* 157**,** 2671-85.

DIAMOND, M. P., HALLARMAN, L., STARICK-ZYCH, K., JONES, T. W., CONNOLLY-HOWARD, M., TAMBORLANE, W. V. & SHERWIN, R. S. 1991. Suppression of counterregulatory hormone response to hypoglycemia by insulin per se. *J Clin Endocrinol Metab,* 72**,** 1388-90.

DIGGS-ANDREWS, K. A., ZHANG, X., SONG, Z., DAPHNA-IKEN, D., ROUTH, V. H. & FISHER, S. J. 2010. Brain insulin action regulates hypothalamic glucose sensing and the counterregulatory response to hypoglycemia. *Diabetes,* 59**,** 2271-80.

DIGRUCCIO, M. R., MAWLA, A. M., DONALDSON, C. J., NOGUCHI, G. M., VAUGHAN, J., COWING-ZITRON, C., VAN DER MEULEN, T. & HUISING, M. O. 2016. Comprehensive alpha, beta and delta cell transcriptomes reveal that ghrelin selectively activates delta cells and promotes somatostatin release from pancreatic islets. *Mol Metab,* 5**,** 449-58.

DINNEEN, S., ALZAID, A., TURK, D. & RIZZA, R. 1995. Failure of glucagon suppression contributes to postprandial hyperglycaemia in IDDM. *Diabetologia,* 38**,** 337-43.

DOBBINS, R. L., CONNOLLY, C. C., NEAL, D. W., PALLADINO, L. J., PARLOW, A. F. & CHERRINGTON, A. D. 1991. Role of glucagon in countering hypoglycemia induced by insulin infusion in dogs. *Am J Physiol,* 261**,** E773-81.

DUMONTEIL, E., MAGNAN, C., RITZ-LASER, B., KTORZA, A., MEDA, P. & PHILIPPE, J. 2000. Glucose regulates proinsulin and prosomatostatin but not

proglucagon messenger ribonucleic acid levels in rat pancreatic islets. *Endocrinology,* 141**,** 174-80.
DUNN, J. T., CRANSTON, I., MARSDEN, P. K., AMIEL, S. A. & REED, L. J. 2007. Attenuation of amydgala and frontal cortical responses to low blood glucose concentration in asymptomatic hypoglycemia in type 1 diabetes: a new player in hypoglycemia unawareness? *Diabetes,* 56**,** 2766-73.
DUNNING, B. E. & GERICH, J. E. 2007. The role of alpha-cell dysregulation in fasting and postprandial hyperglycemia in type 2 diabetes and therapeutic implications. *Endocr Rev,* 28**,** 253-83.
DUTTAROY, A., ZIMLIKI, C. L., GAUTAM, D., CUI, Y., MEARS, D. & WESS, J. 2004. Muscarinic stimulation of pancreatic insulin and glucagon release is abolished in m3 muscarinic acetylcholine receptor-deficient mice. *Diabetes,* 53**,** 1714-20.
ELLIOTT, A. D., USTIONE, A. & PISTON, D. W. 2015. Somatostatin and insulin mediate glucose-inhibited glucagon secretion in the pancreatic alpha-cell by lowering cAMP. *Am J Physiol Endocrinol Metab,* 308**,** E130-43.
EXPASY. 2012. *ENZYME entry: EC 2.7.1.28* [Online]. Available: http://enzyme.expasy.org/EC/2.7.1.28 [Accessed 29th August 2017].
EXTON, J. H. 1987. Mechanisms of hormonal regulation of hepatic glucose metabolism. *Diabetes Metab Rev,* 3**,** 163-83.
FAN, X., DING, Y., BROWN, S., ZHOU, L., SHAW, M., VELLA, M. C., CHENG, H., MCNAY, E. C., SHERWIN, R. S. & MCCRIMMON, R. J. 2009. Hypothalamic AMP-activated protein kinase activation with AICAR amplifies counterregulatory responses to hypoglycemia in a rodent model of type 1 diabetes. *Am J Physiol Regul Integr Comp Physiol,* 296**,** R1702-8.
FERRANNINI, E., MUSCELLI, E., FRASCERRA, S., BALDI, S., MARI, A., HEISE, T., BROEDL, U. C. & WOERLE, H. J. 2014. Metabolic response to sodium-glucose cotransporter 2 inhibition in type 2 diabetic patients. *J Clin Invest,* 124**,** 499-508.
FERRERO, E., LO BUONO, N., HORENSTEIN, A. L., FUNARO, A. & MALAVASI, F. 2014. The ADP-ribosyl cyclases--the current evolutionary state of the ARCs. *Front Biosci (Landmark Ed),* 19**,** 986-1002.
FILIPPONI, P., GREGORIO, F., FERRANDINA, C., NICOLETTI, I., MANNARELLI, C., PIPPI, R. & SANTEUSANIO, F. 1986. Alpha-adrenergic system in the modulation of pancreatic A and B cell function in normal rats. *Diabetes Res Clin Pract,* 2**,** 325-36.
FILIPSSON, K., TORNOE, K., HOLST, J. & AHREN, B. 1997. Pituitary adenylate cyclase-activating polypeptide stimulates insulin and glucagon secretion in humans. *J Clin Endocrinol Metab,* 82**,** 3093-8.
FLODGREN, E., OLDE, B., MEIDUTE-ABARAVICIENE, S., WINZELL, M. S., AHREN, B. & SALEHI, A. 2007. GPR40 is expressed in glucagon producing cells and affects glucagon secretion. *Biochem Biophys Res Commun,* 354**,** 240-5.
FRANKLIN, I., GROMADA, J., GJINOVCI, A., THEANDER, S. & WOLLHEIM, C. B. 2005. Beta-cell secretory products activate alpha-cell ATP-dependent potassium channels to inhibit glucagon release. *Diabetes,* 54**,** 1808-15.
FRAYN, K. N. 2010. *Metabolic Regulation: a human perspective,* Chichester, UK, Wiley-Blackwell.
FRIDOLF, T., SUNDLER, F. & AHREN, B. 1992. Pituitary adenylate cyclase-activating polypeptide (PACAP): occurrence in rodent pancreas and effects on insulin and glucagon secretion in the mouse. *Cell Tissue Res,* 269**,** 275-9.

FRITSCHE, A., STUMVOLL, M., GRUB, M., SIESLACK, S., RENN, W., SCHMULLING, R. M., HARING, H. U. & GERICH, J. E. 1998. Effect of hypoglycemia on beta-adrenergic sensitivity in normal and type 1 diabetic subjects. *Diabetes Care,* 21**,** 1505-10.

FRIZZELL, R. T., HENDRICK, G. K., BIGGERS, D. W., LACY, D. B., DONAHUE, D. P., GREEN, D. R., CARR, R. K., WILLIAMS, P. E., STEVENSON, R. W. & CHERRINGTON, A. D. 1988. Role of gluconeogenesis in sustaining glucose production during hypoglycemia caused by continuous insulin infusion in conscious dogs. *Diabetes,* 37**,** 749-59.

FUJIKAWA, T., CHUANG, J. C., SAKATA, I., RAMADORI, G. & COPPARI, R. 2010. Leptin therapy improves insulin-deficient type 1 diabetes by CNS-dependent mechanisms in mice. *Proc Natl Acad Sci U S A,* 107**,** 17391-6.

GAHRING, L. C., PERSIYANOV, K., DUNN, D., WEISS, R., MEYER, E. L. & ROGERS, S. W. 2004. Mouse strain-specific nicotinic acetylcholine receptor expression by inhibitory interneurons and astrocytes in the dorsal hippocampus. *J Comp Neurol,* 468**,** 334-46.

GANIC, E., SINGH, T., LUAN, C., FADISTA, J., JOHANSSON, J. K., CYPHERT, H. A., BENNET, H., STORM, P., PROST, G., AHLENIUS, H., RENSTROM, E., STEIN, R., GROOP, L., FEX, M. & ARTNER, I. 2016. MafA-Controlled Nicotinic Receptor Expression Is Essential for Insulin Secretion and Is Impaired in Patients with Type 2 Diabetes. *Cell Rep,* 14**,** 1991-2002.

GANNON, M. C. & NUTTALL, F. Q. 2010. Amino acid ingestion and glucose metabolism--a review. *IUBMB Life,* 62**,** 660-8.

GARCIA, M. C., HERMANS, M. P. & HENQUIN, J. C. 1988. Glucose-, calcium- and concentration-dependence of acetylcholine stimulation of insulin release and ionic fluxes in mouse islets. *Biochem J,* 254**,** 211-8.

GARFIELD, A. S., SHAH, B. P., MADARA, J. C., BURKE, L. K., PATTERSON, C. M., FLAK, J., NEVE, R. L., EVANS, M. L., LOWELL, B. B., MYERS, M. G., JR. & HEISLER, L. K. 2014. A parabrachial-hypothalamic cholecystokinin neurocircuit controls counterregulatory responses to hypoglycemia. *Cell Metab,* 20**,** 1030-7.

GAUTAM, D., HAN, S. J., HAMDAN, F. F., JEON, J., LI, B., LI, J. H., CUI, Y., MEARS, D., LU, H., DENG, C., HEARD, T. & WESS, J. 2006. A critical role for beta cell M3 muscarinic acetylcholine receptors in regulating insulin release and blood glucose homeostasis in vivo. *Cell Metab,* 3**,** 449-61.

GEDULIN, B. R., JODKA, C. M., HERRMANN, K. & YOUNG, A. A. 2006. Role of endogenous amylin in glucagon secretion and gastric emptying in rats demonstrated with the selective antagonist, AC187. *Regul Pept,* 137**,** 121-7.

GEDULIN, B. R., RINK, T. J. & YOUNG, A. A. 1997. Dose-response for glucagonostatic effect of amylin in rats. *Metabolism,* 46**,** 67-70.

GENAZZANI, A. A., MEZNA, M., DICKEY, D. M., MICHELANGELI, F., WALSETH, T. F. & GALIONE, A. 1997. Pharmacological properties of the Ca2+-release mechanism sensitive to NAADP in the sea urchin egg. *Br J Pharmacol,* 121**,** 1489-95.

GERICH, J. E. 1988. Lilly lecture 1988. Glucose counterregulation and its impact on diabetes mellitus. *Diabetes,* 37**,** 1608-17.

GERICH, J. E., LORENZI, M., BIER, D. M., SCHNEIDER, V., TSALIKIAN, E., KARAM, J. H. & FORSHAM, P. H. 1975. Prevention of human diabetic ketoacidosis by somatostatin. Evidence for an essential role of glucagon. *N Engl J Med,* 292**,** 985-9.

GERZANICH, V., WANG, F., KURYATOV, A. & LINDSTROM, J. 1998. alpha 5 Subunit alters desensitization, pharmacology, Ca++ permeability and Ca++ modulation of human neuronal alpha 3 nicotinic receptors. *J Pharmacol Exp Ther,* 286**,** 311-20.

GHEZZI, C. & WRIGHT, E. M. 2012. Regulation of the human Na+-dependent glucose cotransporter hSGLT2. *Am J Physiol Cell Physiol,* 303**,** C348-54.

GIANANI, R., CAMPBELL-THOMPSON, M., SARKAR, S. A., WASSERFALL, C., PUGLIESE, A., SOLIS, J. M., KENT, S. C., HERING, B. J., WEST, E., STECK, A., BONNER-WEIR, S., ATKINSON, M. A., COPPIETERS, K., VON HERRATH, M. & EISENBARTH, G. S. 2010. Dimorphic histopathology of long-standing childhood-onset diabetes. *Diabetologia,* 53**,** 690-8.

GILON, P. & HENQUIN, J. C. 2001. Mechanisms and physiological significance of the cholinergic control of pancreatic beta-cell function. *Endocr Rev,* 22**,** 565-604.

GOLDBERG, P. A., WEISS, R., MCCRIMMON, R. J., HINTZ, E. V., DZIURA, J. D. & SHERWIN, R. S. 2006. Antecedent hypercortisolemia is not primarily responsible for generating hypoglycemia-associated autonomic failure. *Diabetes,* 55**,** 1121-6.

GOPEL, S., ZHANG, Q., ELIASSON, L., MA, X. S., GALVANOVSKIS, J., KANNO, T., SALEHI, A. & RORSMAN, P. 2004. Capacitance measurements of exocytosis in mouse pancreatic alpha-, beta- and delta-cells within intact islets of Langerhans. *J Physiol,* 556**,** 711-26.

GOPEL, S. O., KANNO, T., BARG, S. & RORSMAN, P. 2000. Patch-clamp characterisation of somatostatin-secreting -cells in intact mouse pancreatic islets. *J Physiol,* 528**,** 497-507.

GOSMANOV, N. R., SZOKE, E., ISRAELIAN, Z., SMITH, T., CRYER, P. E., GERICH, J. E. & MEYER, C. 2005. Role of the decrement in intraislet insulin for the glucagon response to hypoglycemia in humans. *Diabetes Care,* 28**,** 1124-31.

GRAVHOLT, C. H., MOLLER, N., JENSEN, M. D., CHRISTIANSEN, J. S. & SCHMITZ, O. 2001. Physiological levels of glucagon do not influence lipolysis in abdominal adipose tissue as assessed by microdialysis. *J Clin Endocrinol Metab,* 86**,** 2085-9.

GREENBAUM, C. J., PRIGEON, R. L. & D'ALESSIO, D. A. 2002. Impaired beta-cell function, incretin effect, and glucagon suppression in patients with type 1 diabetes who have normal fasting glucose. *Diabetes,* 51**,** 951-7.

GREMLICH, S., BONNY, C., WAEBER, G. & THORENS, B. 1997. Fatty acids decrease IDX-1 expression in rat pancreatic islets and reduce GLUT2, glucokinase, insulin, and somatostatin levels. *J Biol Chem,* 272**,** 30261-9.

GROMADA, J., BOKVIST, K., DING, W. G., BARG, S., BUSCHARD, K., RENSTROM, E. & RORSMAN, P. 1997. Adrenaline stimulates glucagon secretion in pancreatic A-cells by increasing the Ca2+ current and the number of granules close to the L-type Ca2+ channels. *J Gen Physiol,* 110**,** 217-28.

GROMADA, J. & DISSING, S. 1996. Membrane potential and cytosolic free calcium levels modulate acetylcholine-induced inositol phosphate production in insulin-secreting BTC3 cells. *Biochim Biophys Acta,* 1310**,** 145-8.

GROMADA, J., FRANKLIN, I. & WOLLHEIM, C. B. 2007. Alpha-cells of the endocrine pancreas: 35 years of research but the enigma remains. *Endocr Rev,* 28**,** 84-116.

GROMADA, J., HOY, M., BUSCHARD, K., SALEHI, A. & RORSMAN, P. 2001a. Somatostatin inhibits exocytosis in rat pancreatic alpha-cells by G(i2)-dependent activation of calcineurin and depriming of secretory granules. *J Physiol,* 535**,** 519-32.

GROMADA, J., HOY, M., OLSEN, H. L., GOTFREDSEN, C. F., BUSCHARD, K., RORSMAN, P. & BOKVIST, K. 2001b. Gi2 proteins couple somatostatin receptors to low-conductance K+ channels in rat pancreatic alpha-cells. *Pflugers Arch,* 442**,** 19-26.

GRUETTER, R. 2003. Glycogen: the forgotten cerebral energy store. *J Neurosci Res,* 74**,** 179-83.

GYLFE, E. 1991. Carbachol induces sustained glucose-dependent oscillations of cytoplasmic Ca2+ in hyperpolarized pancreatic beta cells. *Pflugers Arch,* 419**,** 639-43.

GYLFE, E. & GILON, P. 2014. Glucose regulation of glucagon secretion. *Diabetes Res Clin Pract,* 103**,** 1-10.

HAUGE-EVANS, A. C., ANDERSON, R. L., PERSAUD, S. J. & JONES, P. M. 2012. Delta cell secretory responses to insulin secretagogues are not mediated indirectly by insulin. *Diabetologia,* 55**,** 1995-2004.

HAUGE-EVANS, A. C., KING, A. J., CARMIGNAC, D., RICHARDSON, C. C., ROBINSON, I. C., LOW, M. J., CHRISTIE, M. R., PERSAUD, S. J. & JONES, P. M. 2009. Somatostatin secreted by islet delta-cells fulfills multiple roles as a paracrine regulator of islet function. *Diabetes,* 58**,** 403-11.

HAUGE-EVANS, A. C., KING, A. J., FAIRHALL, K., PERSAUD, S. J. & JONES, P. M. 2010. A role for islet somatostatin in mediating sympathetic regulation of glucagon secretion. *Islets,* 2**,** 341-4.

HAUGE-EVANS, A. C., REERS, C., KERBY, A., FRANKLIN, Z., AMISTEN, S., KING, A. J., HASSAN, Z., VILCHES-FLORES, A., TIPPU, Z., PERSAUD, S. J. & JONES, P. M. 2014. Effect of hyperglycaemia on muscarinic M3 receptor expression and secretory sensitivity to cholinergic receptor activation in islets. *Diabetes Obes Metab,* 16**,** 947-56.

HAVEL, P. J. & AHREN, B. 1997. Activation of autonomic nerves and the adrenal medulla contributes to increased glucagon secretion during moderate insulin-induced hypoglycemia in women. *Diabetes,* 46**,** 801-7.

HAVEL, P. J., DUNNING, B. E., VERCHERE, C. B., BASKIN, D. G., O'DORISIO, T. & TABORSKY, G. J., JR. 1997. Evidence that vasoactive intestinal polypeptide is a parasympathetic neurotransmitter in the endocrine pancreas in dogs. *Regul Pept,* 71**,** 163-70.

HAVEL, P. J., MUNDINGER, T. O. & TABORSKY, G. J., JR. 1996. Pancreatic sympathetic nerves contribute to increased glucagon secretion during severe hypoglycemia in dogs. *Am J Physiol,* 270**,** E20-6.

HECKEMEYER, C. M., BARKER, J., DUCKWORTH, W. C. & SOLOMON, S. S. 1983. Studies of the biological effect and degradation of glucagon in the rat perifused isolated adipose cell. *Endocrinology,* 113**,** 270-6.

HEDLUND, B., OWEN, D. G. & BARKER, J. L. 1985. Non-muscarinic effects of atropine on calcium conductances in cultured mouse spinal cord neurons. *Neurosci Lett,* 55**,** 355-9.

HEDO, J. A., VILLANUEVA, M. L. & MARCO, J. 1978. Stimulation of pancreatic polypeptide and glucagon secretion by 2-deoxy-D-glucose in man: evidence for cholinergic mediation. *J Clin Endocrinol Metab,* 47**,** 366-71.

HEESCHEN, C., WEIS, M., AICHER, A., DIMMELER, S. & COOKE, J. P. 2002. A novel angiogenic pathway mediated by non-neuronal nicotinic acetylcholine receptors. *J Clin Invest,* 110**,** 527-36.

HELLER, S. R. & CRYER, P. E. 1991. Reduced neuroendocrine and symptomatic responses to subsequent hypoglycemia after 1 episode of hypoglycemia in nondiabetic humans. *Diabetes,* 40**,** 223-6.
HELLER, S. R. & ROBINSON, R. T. 2000. Hypoglycaemia and associated hypokalaemia in diabetes: mechanisms, clinical implications and prevention. *Diabetes Obes Metab,* 2**,** 75-82.
HENQUIN, J. C. 2000. Triggering and amplifying pathways of regulation of insulin secretion by glucose. *Diabetes,* 49**,** 1751-60.
HERMANS, M. P., SCHMEER, W. & HENQUIN, J. C. 1987. Modulation of the effect of acetylcholine on insulin release by the membrane potential of B cells. *Endocrinology,* 120**,** 1765-73.
HERZOG, R. I., JIANG, L., HERMAN, P., ZHAO, C., SANGANAHALLI, B. G., MASON, G. F., HYDER, F., ROTHMAN, D. L., SHERWIN, R. S. & BEHAR, K. L. 2013. Lactate preserves neuronal metabolism and function following antecedent recurrent hypoglycemia. *J Clin Invest,* 123**,** 1988-98.
HILSTED, J., FRANDSEN, H., HOLST, J. J., CHRISTENSEN, N. J. & NIELSEN, S. L. 1991. Plasma glucagon and glucose recovery after hypoglycemia: the effect of total autonomic blockade. *Acta Endocrinol (Copenh),* 125**,** 466-9.
HOLST, J. J. 2007. The physiology of glucagon-like peptide 1. *Physiol Rev,* 87**,** 1409-39.
HOLST, J. J., WEWER ALBRECHTSEN, N. J., PEDERSEN, J. & KNOP, F. K. 2017. Glucagon and Amino Acids Are Linked in a Mutual Feedback Cycle: The Liver-alpha-Cell Axis. *Diabetes,* 66**,** 235-240.
HONG, J., ABUDULA, R., CHEN, J., JEPPESEN, P. B., DYRSKOG, S. E., XIAO, J., COLOMBO, M. & HERMANSEN, K. 2005. The short-term effect of fatty acids on glucagon secretion is influenced by their chain length, spatial configuration, and degree of unsaturation: studies in vitro. *Metabolism,* 54**,** 1329-36.
HONG, J., JEPPESEN, P. B., NORDENTOFT, I. & HERMANSEN, K. 2007. Fatty acid-induced effect on glucagon secretion is mediated via fatty acid oxidation. *Diabetes Metab Res Rev,* 23**,** 202-10.
HOPE, K. M., TRAN, P. O., ZHOU, H., OSEID, E., LEROY, E. & ROBERTSON, R. P. 2004. Regulation of alpha-cell function by the beta-cell in isolated human and rat islets deprived of glucose: the "switch-off" hypothesis. *Diabetes,* 53**,** 1488-95.
HUGHES, S. J., CHRISTIE, M. R. & ASHCROFT, S. J. 1987. Potentiators of insulin secretion modulate Ca2+ sensitivity in rat pancreatic islets. *Mol Cell Endocrinol,* 50**,** 231-6.
INOUYE, K., SHUM, K., CHAN, O., MATHOO, J., MATTHEWS, S. G. & VRANIC, M. 2002. Effects of recurrent hyperinsulinemia with and without hypoglycemia on counterregulation in diabetic rats. *Am J Physiol Endocrinol Metab,* 282**,** E1369-79.
ISHIHARA, H., MAECHLER, P., GJINOVCI, A., HERRERA, P. L. & WOLLHEIM, C. B. 2003. Islet beta-cell secretion determines glucagon release from neighbouring alpha-cells. *Nat Cell Biol,* 5**,** 330-5.
ISRAELIAN, Z., GOSMANOV, N. R., SZOKE, E., SCHORR, M., BOKHARI, S., CRYER, P. E., GERICH, J. E. & MEYER, C. 2005. Increasing the decrement in insulin secretion improves glucagon responses to hypoglycemia in advanced type 2 diabetes. *Diabetes Care,* 28**,** 2691-6.
IUPHAR/BPS. 2015. *(-)-adrenaline: Structure and Physico-chemical Properties* [Online]. Available: http://www.guidetopharmacology.org/GRAC/LigandDisplayForward?tab=biology&ligandId=479 [Accessed 27th June 2017].

IUPHAR/BPS. 2016. *(-)-noradrenaline: Structure and Physico-chemical Properties* [Online]. Available: http://www.guidetopharmacology.org/GRAC/LigandDisplayForward?tab=biology&ligandId=505 [Accessed 27th June 2017].
IVERSEN, J. 1973. Effect of acetyl choline on the secretion of glucagon and insulin from the isolated, perfused canine pancreas. *Diabetes,* 22**,** 381-7.
IWANIR, S. & REUVENY, E. 2008. Adrenaline-induced hyperpolarization of mouse pancreatic islet cells is mediated by G protein-gated inwardly rectifying potassium (GIRK) channels. *Pflugers Arch,* 456**,** 1097-108.
IYNEDJIAN, P. B., JOTTERAND, D., NOUSPIKEL, T., ASFARI, M. & PILOT, P. R. 1989. Transcriptional induction of glucokinase gene by insulin in cultured liver cells and its repression by the glucagon-cAMP system. *J Biol Chem,* 264**,** 21824-9.
JANSEN, A. S., HOFFMAN, J. L. & LOEWY, A. D. 1997. CNS sites involved in sympathetic and parasympathetic control of the pancreas: a viral tracing study. *Brain Res,* 766**,** 29-38.
JANSSON, L., BARBU, A., BODIN, B., DROTT, C. J., ESPES, D., GAO, X., GRAPENSPARR, L., KALLSKOG, O., LAU, J., LILJEBACK, H., PALM, F., QUACH, M., SANDBERG, M., STROMBERG, V., ULLSTEN, S. & CARLSSON, P. O. 2016. Pancreatic islet blood flow and its measurement. *Ups J Med Sci,* 121**,** 81-95.
JIANG, D., ZHAO, L. & CLAPHAM, D. E. 2009. Genome-wide RNAi screen identifies Letm1 as a mitochondrial Ca2+/H+ antiporter. *Science,* 326**,** 144-7.
JIANG, G. & ZHANG, B. B. 2003. Glucagon and regulation of glucose metabolism. *Am J Physiol Endocrinol Metab,* 284**,** E671-8.
JOHANSSON, H., GYLFE, E. & HELLMAN, B. 1989. Cyclic AMP raises cytoplasmic calcium in pancreatic alpha 2-cells by mobilizing calcium incorporated in response to glucose. *Cell Calcium,* 10**,** 205-11.
JONES, P. M., STUTCHFIELD, J. & HOWELL, S. L. 1985. Effects of Ca2+ and a phorbol ester on insulin secretion from islets of Langerhans permeabilised by high-voltage discharge. *FEBS Lett,* 191**,** 102-6.
JUEL, C. 2009. Na+-K+-ATPase in rat skeletal muscle: muscle fiber-specific differences in exercise-induced changes in ion affinity and maximal activity. *Am J Physiol Regul Integr Comp Physiol,* 296**,** R125-32.
JUNTTI-BERGGREN, L., ARKHAMMAR, P., NILSSON, T., RORSMAN, P. & BERGGREN, P. O. 1991. Glucose-induced increase in cytoplasmic pH in pancreatic beta-cells is mediated by Na+/H+ exchange, an effect not dependent on protein kinase C. *J Biol Chem,* 266**,** 23537-41.
KANG, L., SANDERS, N. M., DUNN-MEYNELL, A. A., GASPERS, L. D., ROUTH, V. H., THOMAS, A. P. & LEVIN, B. E. 2008. Prior hypoglycemia enhances glucose responsiveness in some ventromedial hypothalamic glucosensing neurons. *Am J Physiol Regul Integr Comp Physiol,* 294**,** R784-92.
KARIMIAN, N., QIN, T., LIANG, T., OSUNDIJI, M., HUANG, Y., TEICH, T., RIDDELL, M. C., CATTRAL, M. S., COY, D. H., VRANIC, M. & GAISANO, H. Y. 2013. Somatostatin receptor type 2 antagonism improves glucagon counterregulation in biobreeding diabetic rats. *Diabetes,* 62**,** 2968-77.
KARLSSON, S. & AHREN, B. 1991. Contribution of adrenergic nerves and the adrenals to 2-deoxy-D-glucose-induced insulin and glucagon secretion in the mouse. *Int J Pancreatol,* 10**,** 207-15.

KARLSSON, S. & AHREN, B. 1993. Muscarinic receptor subtypes in carbachol stimulated insulin and glucagon secretion in the mouse *J. Auton. Pharmacol,* 13**,** 439-46.

KARLSSON, S., MYRSEN, U., NIEUWENHUIZEN, A., SUNDLER, F. & AHREN, B. 1997. Presynaptic sympathetic mechanism in the insulinostatic effect of epinephrine in mouse pancreatic islets. *Am J Physiol,* 272**,** R1371-8.

KAWAMORI, D., KURPAD, A. J., HU, J., LIEW, C. W., SHIH, J. L., FORD, E. L., HERRERA, P. L., POLONSKY, K. S., MCGUINNESS, O. P. & KULKARNI, R. N. 2009. Insulin signaling in alpha cells modulates glucagon secretion in vivo. *Cell Metab,* 9**,** 350-61.

KEENAN, H. A., COSTACOU, T., SUN, J. K., DORIA, A., CAVELLERANO, J., CONEY, J., ORCHARD, T. J., AIELLO, L. P. & KING, G. L. 2007. Clinical factors associated with resistance to microvascular complications in diabetic patients of extreme disease duration: the 50-year medalist study. *Diabetes Care,* 30**,** 1995-7.

KEENAN, H. A., SUN, J. K., LEVINE, J., DORIA, A., AIELLO, L. P., EISENBARTH, G., BONNER-WEIR, S. & KING, G. L. 2010. Residual insulin production and pancreatic ss-cell turnover after 50 years of diabetes: Joslin Medalist Study. *Diabetes,* 59**,** 2846-53.

KIMURA, H., KATAGIRI, K., OHNO, T., HARADA, N., IMANISHI, H., IWASAKI, M., ITO, M. & TAKEUCHI, T. 1982. Effect of acetylcholine and new cholinergic derivative on amylase output, insulin, glucagon, and somatostatin secretions from perfused isolated rat pancreas. *Horm Metab Res,* 14**,** 356-60.

KJEMS, L. L., KIRBY, B. M., WELSH, E. M., VELDHUIS, J. D., STRAUME, M., MCINTYRE, S. S., YANG, D., LEFEBVRE, P. & BUTLER, P. C. 2001. Decrease in beta-cell mass leads to impaired pulsatile insulin secretion, reduced postprandial hepatic insulin clearance, and relative hyperglucagonemia in the minipig. *Diabetes,* 50**,** 2001-12.

KORYTKOWSKI, M. T., MOKAN, M., VENEMAN, T. F., MITRAKOU, A., CRYER, P. E. & GERICH, J. E. 1998. Reduced beta-adrenergic sensitivity in patients with type 1 diabetes and hypoglycemia unawareness. *Diabetes Care,* 21**,** 1939-43.

KRISTINSSON, H., SARGSYAN, E., MANELL, H., SMITH, D. M., GOPEL, S. O. & BERGSTEN, P. 2017. Basal hypersecretion of glucagon and insulin from palmitate-exposed human islets depends on FFAR1 but not decreased somatostatin secretion. *Sci Rep,* 7**,** 4657.

KUHARA, T., IKEDA, S., OHNEDA, A. & SASAKI, Y. 1991. Effects of intravenous infusion of 17 amino acids on the secretion of GH, glucagon, and insulin in sheep. *Am J Physiol,* 260**,** E21-6.

LACEY, R. J., CABLE, H. C., JAMES, R. F., LONDON, N. J., SCARPELLO, J. H. & MORGAN, N. G. 1993. Concentration-dependent effects of adrenaline on the profile of insulin secretion from isolated human islets of Langerhans. *J Endocrinol,* 138**,** 555-63.

LAI, J. C. & COOPER, A. J. 1986. Brain alpha-ketoglutarate dehydrogenase complex: kinetic properties, regional distribution, and effects of inhibitors. *J Neurochem,* 47**,** 1376-86.

LAKE, S. P., BASSETT, P. D., LARKINS, A., REVELL, J., WALCZAK, K., CHAMBERLAIN, J., RUMFORD, G. M., LONDON, N. J., VEITCH, P. S., BELL, P. R. & ET AL. 1989. Large-scale purification of human islets utilizing discontinuous albumin gradient on IBM 2991 cell separator. *Diabetes,* 38 Suppl 1**,** 143-5.

LAMY, C. M., SANNO, H., LABOUEBE, G., PICARD, A., MAGNAN, C., CHATTON, J. Y. & THORENS, B. 2014. Hypoglycemia-activated GLUT2 neurons of the nucleus tractus solitarius stimulate vagal activity and glucagon secretion. *Cell Metab,* 19**,** 527-38.

LANGER, P. 1987. Effects of alpha 1- and alpha 2-adrenoceptors on basal and adrenaline mediated insulin secretion in rats. *Endocrinol Exp,* 21**,** 285-90.

LAURENT, D., PETERSEN, K. F., RUSSELL, R. R., CLINE, G. W. & SHULMAN, G. I. 1998. Effect of epinephrine on muscle glycogenolysis and insulin-stimulated muscle glycogen synthesis in humans. *Am J Physiol,* 274**,** E130-8.

LECLERC, I., SUN, G., MORRIS, C., FERNANDEZ-MILLAN, E., NYIRENDA, M. & RUTTER, G. A. 2011. AMP-activated protein kinase regulates glucagon secretion from mouse pancreatic alpha cells. *Diabetologia,* 54**,** 125-34.

LECLERCQ-MEYER, V., MARCHAND, J., WOUSSEN-COLLE, M. C., GIROIX, M. H. & MALAISSE, W. J. 1985. Multiple effects of leucine on glucagon, insulin, and somatostatin secretion from the perfused rat pancreas. *Endocrinology,* 116**,** 1168-74.

LEE, C. S., TONG, B. C., CHENG, C. W., HUNG, H. C. & CHEUNG, K. H. 2016a. Characterization of Two-Pore Channel 2 by Nuclear Membrane Electrophysiology. *Sci Rep,* 6**,** 20282.

LEE, Y., BERGLUND, E. D., WANG, M. Y., FU, X., YU, X., CHARRON, M. J., BURGESS, S. C. & UNGER, R. H. 2012. Metabolic manifestations of insulin deficiency do not occur without glucagon action. *Proc Natl Acad Sci U S A,* 109**,** 14972-6.

LEE, Y., BERGLUND, E. D., YU, X., WANG, M. Y., EVANS, M. R., SCHERER, P. E., HOLLAND, W. L., CHARRON, M. J., ROTH, M. G. & UNGER, R. H. 2014. Hyperglycemia in rodent models of type 2 diabetes requires insulin-resistant alpha cells. *Proc Natl Acad Sci U S A,* 111**,** 13217-22.

LEE, Y., WANG, M. Y., DU, X. Q., CHARRON, M. J. & UNGER, R. H. 2011. Glucagon receptor knockout prevents insulin-deficient type 1 diabetes in mice. *Diabetes,* 60**,** 391-7.

LEE, Y. H., WANG, M. Y., YU, X. X. & UNGER, R. H. 2016b. Glucagon is the key factor in the development of diabetes. *Diabetologia,* 59**,** 1372-5.

LEIBIGER, B., MOEDE, T., MUHANDIRAMLAGE, T. P., KAISER, D., VACA SANCHEZ, P., LEIBIGER, I. B. & BERGGREN, P. O. 2012. Glucagon regulates its own synthesis by autocrine signaling. *Proc Natl Acad Sci U S A,* 109**,** 20925-30.

LEVIN, B. E., BECKER, T. C., EIKI, J., ZHANG, B. B. & DUNN-MEYNELL, A. A. 2008. Ventromedial hypothalamic glucokinase is an important mediator of the counterregulatory response to insulin-induced hypoglycemia. *Diabetes,* 57**,** 1371-9.

LEWIS, A. M., ALEY, P. K., ROOMI, A., THOMAS, J. M., MASGRAU, R., GARNHAM, C., SHIPMAN, K., PARAMORE, C., BLOOR-YOUNG, D., SANDERS, L. E., TERRAR, D. A., GALIONE, A. & CHURCHILL, G. C. 2012. beta-Adrenergic receptor signaling increases NAADP and cADPR levels in the heart. *Biochem Biophys Res Commun,* 427**,** 326-9.

LI, C., LIU, C., NISSIM, I., CHEN, J., CHEN, P., DOLIBA, N., ZHANG, T., NISSIM, I., DAIKHIN, Y., STOKES, D., YUDKOFF, M., BENNETT, M. J., STANLEY, C. A., MATSCHINSKY, F. M. & NAJI, A. 2013. Regulation of glucagon secretion in normal and diabetic human islets by gamma-hydroxybutyrate and glycine. *J Biol Chem,* 288**,** 3938-51.

LI, J., YU, Q., AHOOGHALANDARI, P., GRIBBLE, F. M., REIMANN, F., TENGHOLM, A. & GYLFE, E. 2015. Submembrane ATP and Ca2+ kinetics in alpha-cells: unexpected signaling for glucagon secretion. *FASEB J,* 29**,** 3379-88.

LIN, W. K., BOLTON, E. L., CORTOPASSI, W. A., WANG, Y., O'BRIEN, F., MACIEJEWSKA, M., JACOBSON, M. P., GARNHAM, C., RUAS, M., PARRINGTON, J., LEI, M., SITSAPESAN, R., GALIONE, A. & TERRAR, D. A. 2017. Synthesis of the Ca2+-mobilizing messengers, NAADP and cADPR, by intracellular CD38 enzyme in mouse heart: role in beta-adrenoceptor signaling. *J Biol Chem*.

LINDSTROM, P. & SEHLIN, J. 1984. Effect of glucose on the intracellular pH of pancreatic islet cells. *Biochem J,* 218**,** 887-92.

LIU, D., MOBERG, E., KOLLIND, M., LINS, P. E. & ADAMSON, U. 1991. A high concentration of circulating insulin suppresses the glucagon response to hypoglycemia in normal man. *J Clin Endocrinol Metab,* 73**,** 1123-8.

LIU, D. T., ADAMSON, U. C., LINS, P. E., KOLLIND, M. E., MOBERG, E. A. & ANDREASSON, K. 1992. Inhibitory effect of circulating insulin on glucagon secretion during hypoglycemia in type I diabetic patients. *Diabetes Care,* 15**,** 59-65.

LIU, E. H., DIGON, B. J., 3RD, HIRSHBERG, B., CHANG, R., WOOD, B. J., NEEMAN, Z., KAM, A., WESLEY, R. A., POLLY, S. M., HOFMANN, R. M., ROTHER, K. I. & HARLAN, D. M. 2009. Pancreatic beta cell function persists in many patients with chronic type 1 diabetes, but is not dramatically improved by prolonged immunosuppression and euglycaemia from a beta cell allograft. *Diabetologia,* 52**,** 1369-80.

LIU, Y. J., VIEIRA, E. & GYLFE, E. 2004. A store-operated mechanism determines the activity of the electrically excitable glucagon-secreting pancreatic alpha-cell. *Cell Calcium,* 35**,** 357-65.

LONGUET, C., SINCLAIR, E. M., MAIDA, A., BAGGIO, L. L., MAZIARZ, M., CHARRON, M. J. & DRUCKER, D. J. 2008. The glucagon receptor is required for the adaptive metabolic response to fasting. *Cell Metab,* 8**,** 359-71.

LUDWIG, J., GERLICH, M., HALBRUGGE, T. & GRAEFE, K. H. 1990. The synaptic noradrenaline concentration in humans as estimated from simultaneous measurements of plasma noradrenaline and dihydroxyphenylglycol (DOPEG). *J Neural Transm Suppl,* 32**,** 441-5.

LUND, A., VILSBOLL, T., BAGGER, J. I., HOLST, J. J. & KNOP, F. K. 2011. The separate and combined impact of the intestinal hormones, GIP, GLP-1, and GLP-2, on glucagon secretion in type 2 diabetes. *Am J Physiol Endocrinol Metab,* 300**,** E1038-46.

LUSCHER, C. & SLESINGER, P. A. 2010. Emerging roles for G protein-gated inwardly rectifying potassium (GIRK) channels in health and disease. *Nat Rev Neurosci,* 11**,** 301-15.

MA, X., ZHANG, Y., GROMADA, J., SEWING, S., BERGGREN, P. O., BUSCHARD, K., SALEHI, A., VIKMAN, J., RORSMAN, P. & ELIASSON, L. 2005. Glucagon stimulates exocytosis in mouse and rat pancreatic alpha-cells by binding to glucagon receptors. *Mol Endocrinol,* 19**,** 198-212.

MAACK, C., CORTASSA, S., AON, M. A., GANESAN, A. N., LIU, T. & O'ROURKE, B. 2006. Elevated cytosolic Na+ decreases mitochondrial Ca2+ uptake during excitation-contraction coupling and impairs energetic adaptation in cardiac myocytes. *Circ Res,* 99**,** 172-82.

MACDONALD, M. J. 1989. Does glyceraldehyde enter pancreatic islet metabolism via both the triokinase and the glyceraldehyde phosphate dehydrogenase reactions? A study of these enzymes in islets. *Arch Biochem Biophys,* 270**,** 15-22.

MACDONALD, P. E., DE MARINIS, Y. Z., RAMRACHEYA, R., SALEHI, A., MA, X., JOHNSON, P. R., COX, R., ELIASSON, L. & RORSMAN, P. 2007. A K ATP channel-dependent pathway within alpha cells regulates glucagon release from both rodent and human islets of Langerhans. *PLoS Biol,* 5**,** e143.

MACKLIN, K. D., MAUS, A. D., PEREIRA, E. F., ALBUQUERQUE, E. X. & CONTI-FINE, B. M. 1998. Human vascular endothelial cells express functional nicotinic acetylcholine receptors. *J Pharmacol Exp Ther,* 287**,** 435-9.

MALAISSE, W., MALAISSE-LAGAE, F., WRIGHT, P. H. & ASHMORE, J. 1967. Effects of adrenergic and cholinergic agents upon insulin secretion in vitro. *Endocrinology,* 80**,** 975-8.

MARAN, A., CREPALDI, C., TRUPIANI, S., LUCCA, T., JORI, E., MACDONALD, I. A., TIENGO, A., AVOGARO, A. & DEL PRATO, S. 2000. Brain function rescue effect of lactate following hypoglycaemia is not an adaptation process in both normal and type I diabetic subjects. *Diabetologia,* 43**,** 733-41.

MARTY, N., DALLAPORTA, M. & THORENS, B. 2007. Brain glucose sensing, counterregulation, and energy homeostasis. *Physiology (Bethesda),* 22**,** 241-51.

MASHITER, K., HARDING, P. E., CHOU, M., MASHITER, G. D., STOUT, J., DIAMOND, D. & FIELD, J. B. 1975. Persistent pancreatic glucagon but not insulin response to arginine in pancreatectomized dogs. *Endocrinology,* 96**,** 678-93.

MASSEY, V. 1953. Studies on fumarase. II. The effects of inorganic anions on fumarase activity. *Biochem J,* 53**,** 67-71.

MATSUYAMA, T., WIDER, M. D., TANAKA, R., SHIMA, K., TARUI, S., NISHIKAWA, M. & FOA, P. P. 1979. A-Cell and gut glucagon in normal and depancreatized dogs. Inhibition by somatostatin and insulin. *Diabete Metab,* 5**,** 141-7.

MAUS, A. D., PEREIRA, E. F., KARACHUNSKI, P. I., HORTON, R. M., NAVANEETHAM, D., MACKLIN, K., CORTES, W. S., ALBUQUERQUE, E. X. & CONTI-FINE, B. M. 1998. Human and rodent bronchial epithelial cells express functional nicotinic acetylcholine receptors. *Mol Pharmacol,* 54**,** 779-88.

MCCORRY, L. K. 2007. Physiology of the autonomic nervous system. *Am J Pharm Educ,* 71**,** 78.

MCCRIMMON, R. J., SHAW, M., FAN, X., CHENG, H., DING, Y., VELLA, M. C., ZHOU, L., MCNAY, E. C. & SHERWIN, R. S. 2008. Key role for AMP-activated protein kinase in the ventromedial hypothalamus in regulating counterregulatory hormone responses to acute hypoglycemia. *Diabetes,* 57**,** 444-50.

MEI, Q., MUNDINGER, T. O., LERNMARK, A. & TABORSKY, G. J., JR. 2002. Early, selective, and marked loss of sympathetic nerves from the islets of BioBreeder diabetic rats. *Diabetes,* 51**,** 2997-3002.

MEIER, J. J., BHUSHAN, A., BUTLER, A. E., RIZZA, R. A. & BUTLER, P. C. 2005. Sustained beta cell apoptosis in patients with long-standing type 1 diabetes: indirect evidence for islet regeneration? *Diabetologia,* 48**,** 2221-8.

MEIER, J. J., KJEMS, L. L., VELDHUIS, J. D., LEFEBVRE, P. & BUTLER, P. C. 2006. Postprandial suppression of glucagon secretion depends on intact pulsatile insulin secretion: further evidence for the intraislet insulin hypothesis. *Diabetes,* 55**,** 1051-6.

MEISSNER, G. 1986. Ryanodine activation and inhibition of the Ca2+ release channel of sarcoplasmic reticulum. *J Biol Chem,* 261**,** 6300-6.

MERKLEY, E. D., METZ, T. O., SMITH, R. D., BAYNES, J. W. & FRIZZELL, N. 2014. The succinated proteome. *Mass Spectrom Rev,* 33**,** 98-109.
MEROVCI, A., SOLIS-HERRERA, C., DANIELE, G., ELDOR, R., FIORENTINO, T. V., TRIPATHY, D., XIONG, J., PEREZ, Z., NORTON, L., ABDUL-GHANI, M. A. & DEFRONZO, R. A. 2014. Dapagliflozin improves muscle insulin sensitivity but enhances endogenous glucose production. *J Clin Invest,* 124**,** 509-14.
MILLAR, N. S. & GOTTI, C. 2009. Diversity of vertebrate nicotinic acetylcholine receptors. *Neuropharmacology,* 56**,** 237-46.
MOENS, K., HEIMBERG, H., FLAMEZ, D., HUYPENS, P., QUARTIER, E., LING, Z., PIPELEERS, D., GREMLICH, S., THORENS, B. & SCHUIT, F. 1996. Expression and functional activity of glucagon, glucagon-like peptide I, and glucose-dependent insulinotropic peptide receptors in rat pancreatic islet cells. *Diabetes,* 45**,** 257-61.
MOLINA, J., RODRIGUEZ-DIAZ, R., FACHADO, A., JACQUES-SILVA, M. C., BERGGREN, P. O. & CAICEDO, A. 2014. Control of insulin secretion by cholinergic signaling in the human pancreatic islet. *Diabetes,* 63**,** 2714-26.
MOULE, S. K. & MCGIVAN, J. D. 1987. Epidermal growth factor, like glucagon, exerts a short-term stimulation of alanine transport in rat hepatocytes. *Biochem J,* 247**,** 233-5.
MUNDINGER, T. O., MEI, Q., FIGLEWICZ, D. P., LERNMARK, A. & TABORSKY, G. J., JR. 2003. Impaired glucagon response to sympathetic nerve stimulation in the BB diabetic rat: effect of early sympathetic islet neuropathy. *Am J Physiol Endocrinol Metab,* 285**,** E1047-54.
MUNDINGER, T. O. & TABORSKY, G. J., JR. 2016. Early sympathetic islet neuropathy in autoimmune diabetes: lessons learned and opportunities for investigation. *Diabetologia,* 59**,** 2058-67.
MUNDINGER, T. O., VERCHERE, C. B., BASKIN, D. G., BOYLE, M. R., KOWALYK, S. & TABORSKY, G. J., JR. 1997. Galanin is localized in sympathetic neurons of the dog liver. *Am J Physiol,* 273**,** E1194-202.
NAGAI, R., BROCK, J. W., BLATNIK, M., BAATZ, J. E., BETHARD, J., WALLA, M. D., THORPE, S. R., BAYNES, J. W. & FRIZZELL, N. 2007. Succination of protein thiols during adipocyte maturation: a biomarker of mitochondrial stress. *J Biol Chem,* 282**,** 34219-28.
NAKAKI, T., NAKADATE, T. & KATO, R. 1980. Alpha 2-adrenoceptors modulating insulin release from isolated pancreatic islets. *Naunyn Schmiedebergs Arch Pharmacol,* 313**,** 151-3.
NEUMANN, U. H., HO, J. S., MOJIBIAN, M., COVEY, S. D., CHARRON, M. J. & KIEFFER, T. J. 2016. Glucagon receptor gene deletion in insulin knockout mice modestly reduces blood glucose and ketones but does not promote survival. *Mol Metab,* 5**,** 731-6.
NILSSON, P. M., GUDBJORNSDOTTIR, S., ELIASSON, B., CEDERHOLM, J. & STEERING COMMITTEE OF THE SWEDISH NATIONAL DIABETES, R. 2004. Smoking is associated with increased HbA1c values and microalbuminuria in patients with diabetes--data from the National Diabetes Register in Sweden. *Diabetes Metab,* 30**,** 261-8.
OLOFSSON, C. S., SALEHI, A., GOPEL, S. O., HOLM, C. & RORSMAN, P. 2004. Palmitate stimulation of glucagon secretion in mouse pancreatic alpha-cells results from activation of L-type calcium channels and elevation of cytoplasmic calcium. *Diabetes,* 53**,** 2836-43.

OLSEN, H. L., THEANDER, S., BOKVIST, K., BUSCHARD, K., WOLLHEIM, C. B. & GROMADA, J. 2005. Glucose stimulates glucagon release in single rat alpha-cells by mechanisms that mirror the stimulus-secretion coupling in beta-cells. *Endocrinology,* 146**,** 4861-70.

ORCI, L., BAETENS, D., RUFENER, C., AMHERDT, M., RAVAZZOLA, M., STUDER, P., MALAISSE-LAGAE, F. & UNGER, R. H. 1976. Hypertrophy and hyperplasia of somatostatin-containing D-cells in diabetes. *Proc Natl Acad Sci U S A,* 73**,** 1338-42.

ORGAARD, A. & HOLST, J. J. 2017. The role of somatostatin in GLP-1-induced inhibition of glucagon secretion in mice. *Diabetologia*.

OWEN, O. E., REICHARD, G. A., JR., PATEL, M. S. & BODEN, G. 1979. Energy metabolism in feasting and fasting. *Adv Exp Med Biol,* 111**,** 169-88.

OZ, G., TESFAYE, N., KUMAR, A., DEELCHAND, D. K., EBERLY, L. E. & SEAQUIST, E. R. 2012. Brain glycogen content and metabolism in subjects with type 1 diabetes and hypoglycemia unawareness. *J Cereb Blood Flow Metab,* 32**,** 256-63.

PACE, C. S. & TARVIN, J. T. 1986. Amiloride-sensitive regulation of intracellular pH in B-cells: activation by glucose. *Metabolism,* 35**,** 176-81.

PAPKE, R. L. 2014. Merging old and new perspectives on nicotinic acetylcholine receptors. *Biochem Pharmacol,* 89**,** 1-11.

PARKER, H. E., ADRIAENSSENS, A., ROGERS, G., RICHARDS, P., KOEPSELL, H., REIMANN, F. & GRIBBLE, F. M. 2012. Predominant role of active versus facilitative glucose transport for glucagon-like peptide-1 secretion. *Diabetologia,* 55**,** 2445-55.

PARKER, S. M., MOORE, P. C., JOHNSON, L. M. & POITOUT, V. 2003. Palmitate potentiation of glucose-induced insulin release: a study using 2-bromopalmitate. *Metabolism,* 52**,** 1367-71.

PATEL, D. G. 1984. Role of parasympathetic nervous system in glucagon response to insulin-induced hypoglycemia in normal and diabetic rats. *Metabolism,* 33**,** 1123-7.

PATEL, S. & DOCAMPO, R. 2010. Acidic calcium stores open for business: expanding the potential for intracellular Ca2+ signaling. *Trends Cell Biol,* 20**,** 277-86.

PEDERSEN, M. G., AHLSTEDT, I., EL HACHMANE, M. F. & GOPEL, S. O. 2016. Dapagliflozin stimulates glucagon secretion at high glucose: experiments and mathematical simulations of human A-cells. *Sci Rep,* 6**,** 31214.

PEGORIER, J. P., GARCIA-GARCIA, M. V., PRIP-BUUS, C., DUEE, P. H., KOHL, C. & GIRARD, J. 1989. Induction of ketogenesis and fatty acid oxidation by glucagon and cyclic AMP in cultured hepatocytes from rabbit fetuses. Evidence for a decreased sensitivity of carnitine palmitoyltransferase I to malonyl-CoA inhibition after glucagon or cyclic AMP treatment. *Biochem J,* 264**,** 93-100.

PEREA, A., CLEMENTE, F., MARTINELL, J., VILLANUEVA-PENACARRILLO, M. L. & VALVERDE, I. 1995. Physiological effect of glucagon in human isolated adipocytes. *Horm Metab Res,* 27**,** 372-5.

PETERSEN, M. C., VATNER, D. F. & SHULMAN, G. I. 2017. Regulation of hepatic glucose metabolism in health and disease. *Nat Rev Endocrinol,* 13**,** 572-587.

PILKIS, S. J. & CLAUS, T. H. 1991. Hepatic gluconeogenesis/glycolysis: regulation and structure/function relationships of substrate cycle enzymes. *Annu Rev Nutr,* 11**,** 465-515.

PIPELEERS, D., IN'T VELD, P., PIPELEERS-MARICHAL, M. & GORUS, F. 2008. The beta cell population in type 1 diabetes. *Novartis Found Symp,* 292**,** 19-24; discussion 24-31, 122-9, 202-3.

PIPELEERS, D. G., SCHUIT, F. C., VAN SCHRAVENDIJK, C. F. & VAN DE WINKEL, M. 1985. Interplay of nutrients and hormones in the regulation of glucagon release. *Endocrinology,* 117**,** 817-23.

PRENTKI, M., JANJIC, D. & WOLLHEIM, C. B. 1983. The regulation of extramitochondrial steady state free Ca2+ concentration by rat insulinoma mitochondria. *J Biol Chem,* 258**,** 7597-602.

QUOIX, N., CHENG-XUE, R., MATTART, L., ZEINOUN, Z., GUIOT, Y., BEAUVOIS, M. C., HENQUIN, J. C. & GILON, P. 2009. Glucose and pharmacological modulators of ATP-sensitive K+ channels control [Ca2+]c by different mechanisms in isolated mouse alpha-cells. *Diabetes,* 58**,** 412-21.

RAH, S. Y., MUSHTAQ, M., NAM, T. S., KIM, S. H. & KIM, U. H. 2010. Generation of cyclic ADP-ribose and nicotinic acid adenine dinucleotide phosphate by CD38 for Ca2+ signaling in interleukin-8-treated lymphokine-activated killer cells. *J Biol Chem,* 285**,** 21877-87.

RAJU, B. & CRYER, P. E. 2005. Loss of the decrement in intraislet insulin plausibly explains loss of the glucagon response to hypoglycemia in insulin-deficient diabetes: documentation of the intraislet insulin hypothesis in humans. *Diabetes,* 54**,** 757-64.

RAJU, B., MCGREGOR, V. P. & CRYER, P. E. 2003. Cortisol elevations comparable to those that occur during hypoglycemia do not cause hypoglycemia-associated autonomic failure. *Diabetes,* 52**,** 2083-9.

RAMRACHEYA, R., WARD, C., SHIGETO, M., WALKER, J. N., AMISTEN, S., ZHANG, Q., JOHNSON, P. R., RORSMAN, P. & BRAUN, M. 2010. Membrane potential-dependent inactivation of voltage-gated ion channels in alpha-cells inhibits glucagon secretion from human islets. *Diabetes,* 59**,** 2198-208.

RASKIN, P. & UNGER, R. H. 1978. Hyperglucagonemia and its suppression. Importance in the metabolic control of diabetes. *N Engl J Med,* 299**,** 433-6.

RASTOGI, K. S., LICKLEY, L., JOKAY, M., EFENDIC, S. & VRANIC, M. 1990. Paradoxical reduction in pancreatic glucagon with normalization of somatostatin and decrease in insulin in normoglycemic alloxan-diabetic dogs: a putative mechanism of glucagon irresponsiveness to hypoglycemia. *Endocrinology,* 126**,** 1096-104.

RAVIER, M. A. & RUTTER, G. A. 2005. Glucose or insulin, but not zinc ions, inhibit glucagon secretion from mouse pancreatic alpha-cells. *Diabetes,* 54**,** 1789-97.

RENO, C. M., PUENTE, E. C., SHENG, Z., DAPHNA-IKEN, D., BREE, A. J., ROUTH, V. H., KAHN, B. B. & FISHER, S. J. 2017. Brain GLUT4 Knockout Mice Have Impaired Glucose Tolerance, Decreased Insulin Sensitivity, and Impaired Hypoglycemic Counterregulation. *Diabetes,* 66**,** 587-597.

RICORDI, C., LACY, P. E., FINKE, E. H., OLACK, B. J. & SCHARP, D. W. 1988. Automated method for isolation of human pancreatic islets. *Diabetes,* 37**,** 413-20.

RIDER, M. H., BERTRAND, L., VERTOMMEN, D., MICHELS, P. A., ROUSSEAU, G. G. & HUE, L. 2004. 6-phosphofructo-2-kinase/fructose-2,6-bisphosphatase: head-to-head with a bifunctional enzyme that controls glycolysis. *Biochem J,* 381**,** 561-79.

ROACH, P. J. 1990. Control of glycogen synthase by hierarchal protein phosphorylation. *FASEB J,* 4**,** 2961-8.

RODRIGUEZ-DIAZ, R., DANDO, R., JACQUES-SILVA, M. C., FACHADO, A., MOLINA, J., ABDULREDA, M. H., RICORDI, C., ROPER, S. D., BERGGREN, P. O. & CAICEDO, A. 2011. Alpha cells secrete acetylcholine as a non-neuronal paracrine signal priming beta cell function in humans. *Nat Med,* 17**,** 888-92.

RORSMAN, P., BERGGREN, P. O., BOKVIST, K., ERICSON, H., MOHLER, H., OSTENSON, C. G. & SMITH, P. A. 1989. Glucose-inhibition of glucagon secretion involves activation of GABAA-receptor chloride channels. *Nature,* 341**,** 233-6.

RORSMAN, P., BOKVIST, K., AMMALA, C., ARKHAMMAR, P., BERGGREN, P. O., LARSSON, O. & WAHLANDER, K. 1991. Activation by adrenaline of a low-conductance G protein-dependent K+ channel in mouse pancreatic B cells. *Nature,* 349**,** 77-9.

ROSS, G., LICKLEY, L. & VRANIC, M. 1978. Extrapancreatic glucagon in control of glucose turnover in depancreatized dogs. *Am J Physiol,* 234**,** E213-19.

ROTHER, K. I., SPAIN, L. M., WESLEY, R. A., DIGON, B. J., 3RD, BARON, A., CHEN, K., NELSON, P., DOSCH, H. M., PALMER, J. P., BROOKS-WORRELL, B., RING, M. & HARLAN, D. M. 2009. Effects of exenatide alone and in combination with daclizumab on beta-cell function in long-standing type 1 diabetes. *Diabetes Care,* 32**,** 2251-7.

RUDCHENKO, A., AKUDE, E. & COOPER, E. 2014. Synapses on sympathetic neurons and parasympathetic neurons differ in their vulnerability to diabetes. *J Neurosci,* 34**,** 8865-74.

RUI, L. 2014. Energy metabolism in the liver. *Compr Physiol,* 4**,** 177-97.

SACCA, L., VIGORITO, C., CICALA, M., CORSO, G. & SHERWIN, R. S. 1983. Role of gluconeogenesis in epinephrine-stimulated hepatic glucose production in humans. *Am J Physiol,* 245**,** E294-302.

SALEHI, A., PARANDEH, F. & LUNDQUIST, I. 1998. The nitric oxide synthase inhibitor NG-nitro-L-arginine methyl ester potentiates insulin secretion stimulated by glucose and L-arginine independently of its action on ATP-sensitive K+ channels. *Biosci Rep,* 18**,** 19-28.

SALEHI, A., VIEIRA, E. & GYLFE, E. 2006. Paradoxical stimulation of glucagon secretion by high glucose concentrations. *Diabetes,* 55**,** 2318-23.

SALGADO, A., SILVA, A. M., SANTOS, R. M. & ROSARIO, L. M. 1996. Multiphasic action of glucose and alpha-ketoisocaproic acid on the cytosolic pH of pancreatic beta-cells. Evidence for an acidification pathway linked to the stimulation of Ca2+ influx. *J Biol Chem,* 271**,** 8738-46.

SAMOLS, E., WEIR, G. C., RAMSEUR, R., DAY, J. A. & PATEL, Y. C. 1978. Modulation of pancreatic somatostatin by adrenergic and cholinergic agonism and by hyper- and hypoglycemic sulfonamides. *Metabolism,* 27**,** 1219-21.

SCHEURINK, A. J., STEFFENS, A. B., BOURITIUS, H., DRETELER, G. H., BRUNTINK, R., REMIE, R. & ZAAGSMA, J. 1989. Adrenal and sympathetic catecholamines in exercising rats. *Am J Physiol,* 256**,** R155-60.

SCHUIT, F. C. & PIPELEERS, D. G. 1986. Differences in adrenergic recognition by pancreatic A and B cells. *Science,* 232**,** 875-7.

SCHWARTZ, T. W., HOLST, J. J., FAHRENKRUG, J., JENSEN, S. L., NIELSEN, O. V., REHFELD, J. F., DE MUCKADELL, O. B. & STADIL, F. 1978. Vagal, cholinergic regulation of pancreatic polypeptide secretion. *J Clin Invest,* 61**,** 781-9.

SCHWIENING, C. J., KENNEDY, H. J. & THOMAS, R. C. 1993. Calcium-hydrogen exchange by the plasma membrane Ca-ATPase of voltage-clamped snail neurons. *Proc Biol Sci,* 253**,** 285-9.

SHAH, P., VELLA, A., BASU, A., BASU, R., SCHWENK, W. F. & RIZZA, R. A. 2000. Lack of suppression of glucagon contributes to postprandial hyperglycemia in subjects with type 2 diabetes mellitus. *J Clin Endocrinol Metab,* 85**,** 4053-9.

SHEPHERD, R. M. & HENQUIN, J. C. 1995. The role of metabolism, cytoplasmic Ca2+, and pH-regulating exchangers in glucose-induced rise of cytoplasmic pH in normal mouse pancreatic islets. *J Biol Chem,* 270**,** 7915-21.

SHERCK, S. M., SHIOTA, M., SACCOMANDO, J., CARDIN, S., ALLEN, E. J., HASTINGS, J. R., NEAL, D. W., WILLIAMS, P. E. & CHERRINGTON, A. D. 2001. Pancreatic response to mild non-insulin-induced hypoglycemia does not involve extrinsic neural input. *Diabetes,* 50**,** 2487-96.

SHERR, J., XING, D., RUEDY, K. J., BECK, R. W., KOLLMAN, C., BUCKINGHAM, B., WHITE, N. H., FOX, L., TSALIKIAN, E., WEINZIMER, S., ARBELAEZ, A. M., TAMBORLANE, W. V. & DIABETES IN CHILDREN, N. 2013. Lack of association between residual insulin production and glucagon response to hypoglycemia in youth with short duration of type 1 diabetes. *Diabetes Care,* 36**,** 1470-6.

SHERWIN, R. S., FISHER, M., HENDLER, R. & FELIG, P. 1976. Hyperglucagonemia and blood glucose regulation in normal, obese and diabetic subjects. *N Engl J Med,* 294**,** 455-61.

SHI, Z. Q., RASTOGI, K. S., LEKAS, M., EFENDIC, S., DRUCKER, D. J. & VRANIC, M. 1996. Glucagon response to hypoglycemia is improved by insulin-independent restoration of normoglycemia in diabetic rats. *Endocrinology,* 137**,** 3193-9.

SJOBERG, S., AHREN, B. & BOLINDER, J. 2002. Residual insulin secretion is not coupled to a maintained glucagon response to hypoglycaemia in long-term type 1 diabetes. *J Intern Med,* 252**,** 342-51.

SPRAGUE, J. E. & ARBELAEZ, A. M. 2011. Glucose counterregulatory responses to hypoglycemia. *Pediatr Endocrinol Rev,* 9**,** 463-73; quiz 474-5.

STEINBUSCH, L., LABOUEBE, G. & THORENS, B. 2015. Brain glucose sensing in homeostatic and hedonic regulation. *Trends Endocrinol Metab,* 26**,** 455-66.

STEINER, D. J., KIM, A., MILLER, K. & HARA, M. 2010. Pancreatic islet plasticity: interspecies comparison of islet architecture and composition. *Islets,* 2**,** 135-45.

STICH, V., DE GLISEZINSKI, I., CRAMPES, F., SULJKOVICOVA, H., GALITZKY, J., RIVIERE, D., HEJNOVA, J., LAFONTAN, M. & BERLAN, M. 1999. Activation of antilipolytic alpha(2)-adrenergic receptors by epinephrine during exercise in human adipose tissue. *Am J Physiol,* 277**,** R1076-83.

STIERNET, P., NENQUIN, M., MOULIN, P., JONAS, J. C. & HENQUIN, J. C. 2007. Glucose-induced cytosolic pH changes in beta-cells and insulin secretion are not causally related: studies in islets lacking the Na+/H+ exchangeR NHE1. *J Biol Chem,* 282**,** 24538-46.

STROWSKI, M. Z., PARMAR, R. M., BLAKE, A. D. & SCHAEFFER, J. M. 2000. Somatostatin inhibits insulin and glucagon secretion via two receptors subtypes: an in vitro study of pancreatic islets from somatostatin receptor 2 knockout mice. *Endocrinology,* 141**,** 111-7.

SUDO, T., SUZUKI, T. & TOBE, T. 1980. Changes in plasma glucagon after total pancreatectomy in man. *Gastroenterol Jpn,* 15**,** 464-8.

SURINA, D. M., LANGHANS, W., PAULI, R. & WENK, C. 1993. Meal composition affects postprandial fatty acid oxidation. *Am J Physiol,* 264**,** R1065-70.

SURPRENANT, A., HORSTMAN, D. A., AKBARALI, H. & LIMBIRD, L. E. 1992. A point mutation of the alpha 2-adrenoceptor that blocks coupling to potassium but not calcium currents. *Science,* 257**,** 977-80.

TABORSKY, G. J., JR., MEI, Q., BORNFELDT, K. E., HACKNEY, D. J. & MUNDINGER, T. O. 2014. The p75 neurotrophin receptor is required for the

major loss of sympathetic nerves from islets under autoimmune attack. *Diabetes,* 63**,** 2369-79.
TABORSKY, G. J., JR., MEI, Q., HACKNEY, D. J., FIGLEWICZ, D. P., LEBOEUF, R. & MUNDINGER, T. O. 2009. Loss of islet sympathetic nerves and impairment of glucagon secretion in the NOD mouse: relationship to invasive insulitis. *Diabetologia,* 52**,** 2602-11.
TABORSKY, G. J., JR. & MUNDINGER, T. O. 2012. Minireview: The role of the autonomic nervous system in mediating the glucagon response to hypoglycemia. *Endocrinology,* 153**,** 1055-62.
TAMAGAWA, T., NIKI, H. & NIKI, A. 1985. Insulin release independent of a rise in cytosolic free Ca2+ by forskolin and phorbol ester. *FEBS Lett,* 183**,** 430-2.
TANJOH, K., TOMITA, R., FUKUZAWA, M. & HAYASHI, N. 2003. Peculiar glucagon processing in the intestine is the genesis of the paradoxical rise of serum pancreatic glucagon in patients after total pancreatectomy. *Hepatogastroenterology,* 50**,** 535-40.
TEVES, D., VIDEEN, T. O., CRYER, P. E. & POWERS, W. J. 2004. Activation of human medial prefrontal cortex during autonomic responses to hypoglycemia. *Proc Natl Acad Sci U S A,* 101**,** 6217-21.
THIBODEAU, G. A. & PATTON, K. T. 2003. *Anatomy and Physiology,* Mosby.
THOMSEN, M. S., ZWART, R., URSU, D., JENSEN, M. M., PINBORG, L. H., GILMOUR, G., WU, J., SHER, E. & MIKKELSEN, J. D. 2015. alpha7 and beta2 Nicotinic Acetylcholine Receptor Subunits Form Heteromeric Receptor Complexes that Are Expressed in the Human Cortex and Display Distinct Pharmacological Properties. *PLoS One,* 10**,** e0130572.
THORENS, B. 2012. Sensing of glucose in the brain. *Handb Exp Pharmacol***,** 277-94.
TOWLER, D. A., HAVLIN, C. E., CRAFT, S. & CRYER, P. 1993. Mechanism of awareness of hypoglycemia. Perception of neurogenic (predominantly cholinergic) rather than neuroglycopenic symptoms. *Diabetes,* 42**,** 1791-8.
TRAASETH, N., ELFERING, S., SOLIEN, J., HAYNES, V. & GIULIVI, C. 2004. Role of calcium signaling in the activation of mitochondrial nitric oxide synthase and citric acid cycle. *Biochim Biophys Acta,* 1658**,** 64-71.
TREVINO, L. A. U., M.L.; LIEGEY DOUGALL, A.J. 2012. Adrenal Glands. *Encyclopedia of Human Behavior.* Second ed.
TUDURI, E., FILIPUTTI, E., CARNEIRO, E. M. & QUESADA, I. 2008. Inhibition of Ca2+ signaling and glucagon secretion in mouse pancreatic alpha-cells by extracellular ATP and purinergic receptors. *Am J Physiol Endocrinol Metab,* 294**,** E952-60.
TUDURI, E., MARROQUI, L., SORIANO, S., ROPERO, A. B., BATISTA, T. M., PIQUER, S., LOPEZ-BOADO, M. A., CARNEIRO, E. M., GOMIS, R., NADAL, A. & QUESADA, I. 2009. Inhibitory effects of leptin on pancreatic alpha-cell function. *Diabetes,* 58**,** 1616-24.
TWEED, J. O., HSIA, S. H., LUTFY, K. & FRIEDMAN, T. C. 2012. The endocrine effects of nicotine and cigarette smoke. *Trends Endocrinol Metab,* 23**,** 334-42.
UNGER, R. H. & CHERRINGTON, A. D. 2012. Glucagonocentric restructuring of diabetes: a pathophysiologic and therapeutic makeover. *J Clin Invest,* 122**,** 4-12.
UNGER, R. H. & ORCI, L. 1975. The essential role of glucagon in the pathogenesis of diabetes mellitus. *Lancet,* 1**,** 14-6.
VERBERNE, A. J., KORIM, W. S., SABETGHADAM, A. & LLEWELLYN-SMITH, I. J. 2016. Adrenaline: insights into its metabolic roles in hypoglycaemia and diabetes. *Br J Pharmacol,* 173**,** 1425-37.

VERBERNE, A. J., SABETGHADAM, A. & KORIM, W. S. 2014. Neural pathways that control the glucose counterregulatory response. *Front Neurosci,* 8**,** 38.
VERBERNE, A. J. & SARTOR, D. M. 2010. Rostroventrolateral medullary neurons modulate glucose homeostasis in the rat. *Am J Physiol Endocrinol Metab,* 299**,** E802-7.
VERGARI, E., SALEHI, A., RAMRACHEYA, R., ZHANG, Q., ADAM, J., BRIANT, L. J. B., BRERETON, M., CHIBALINA, M. V., HAMILTON, A., HASTOY, B., GRIBBLE, F., JOHNSON, P. R. V., REIMANN, F., SPILOTIS, I. I., TARASOV, A., ASHCROFT, F. M. & RORSMAN, P. In Press. Insulin-induced hypoglycemia and suppression of glucagon secretion by SGLT2-dependent stimulation of somatostatin secretion from pancreatic delta cells.
VERSPOHL, E. J., TACKE, R., MUTSCHLER, E. & LAMBRECHT, G. 1990. Muscarinic receptor subtypes in rat pancreatic islets: binding and functional studies. *Eur J Pharmacol,* 178**,** 303-11.
VIEIRA, E., LIU, Y. J. & GYLFE, E. 2004. Involvement of alpha1 and beta-adrenoceptors in adrenaline stimulation of the glucagon-secreting mouse alpha-cell. *Naunyn Schmiedebergs Arch Pharmacol,* 369**,** 179-83.
VIEIRA, E., SALEHI, A. & GYLFE, E. 2007. Glucose inhibits glucagon secretion by a direct effect on mouse pancreatic alpha cells. *Diabetologia,* 50**,** 370-9.
VONEN, B., FLORHOLMEN, J., GIAEVER, A. K. & BURHOL, P. 1989. Somatostatin secretion from isolated rat pancreatic islets. *Scand J Clin Lab Invest,* 49**,** 139-43.
VONS, C., PEGORIER, J. P., GIRARD, J., KOHL, C., IVANOV, M. A. & FRANCO, D. 1991. Regulation of fatty-acid metabolism by pancreatic hormones in cultured human hepatocytes. *Hepatology,* 13**,** 1126-30.
WALKER, J. N., RAMRACHEYA, R., ZHANG, Q., JOHNSON, P. R., BRAUN, M. & RORSMAN, P. 2011. Regulation of glucagon secretion by glucose: paracrine, intrinsic or both? *Diabetes Obes Metab,* 13 Suppl 1**,** 95-105.
WANG, L., ZHAO, Y., GUI, B., FU, R., MA, F., YU, J., QU, P., DONG, L. & CHEN, C. 2011. Acute stimulation of glucagon secretion by linoleic acid results from GPR40 activation and [Ca2+]i increase in pancreatic islet {alpha}-cells. *J Endocrinol,* 210**,** 173-9.
WANG, Y., PEREIRA, E. F., MAUS, A. D., OSTLIE, N. S., NAVANEETHAM, D., LEI, S., ALBUQUERQUE, E. X. & CONTI-FINE, B. M. 2001. Human bronchial epithelial and endothelial cells express alpha7 nicotinic acetylcholine receptors. *Mol Pharmacol,* 60**,** 1201-9.
WENDT, A., BIRNIR, B., BUSCHARD, K., GROMADA, J., SALEHI, A., SEWING, S., RORSMAN, P. & BRAUN, M. 2004. Glucose inhibition of glucagon secretion from rat alpha-cells is mediated by GABA released from neighboring beta-cells. *Diabetes,* 53**,** 1038-45.
WESS, J., EGLEN, R. M. & GAUTAM, D. 2007. Muscarinic acetylcholine receptors: mutant mice provide new insights for drug development. *Nat Rev Drug Discov,* 6**,** 721-33.
WIEDERKEHR, A., PARK, K. S., DUPONT, O., DEMAUREX, N., POZZAN, T., CLINE, G. W. & WOLLHEIM, C. B. 2009. Matrix alkalinization: a novel mitochondrial signal for sustained pancreatic beta-cell activation. *EMBO J,* 28**,** 417-28.
WILLSON, V. J. & TIPTON, K. F. 1980. The effect of pH on the allosteric behaviour of ox-brain NAD+-dependent isocitrate dehydrogenase. *Eur J Biochem,* 109**,** 411-6.

WILSON, H. L. & GALIONE, A. 1998. Differential regulation of nicotinic acid-adenine dinucleotide phosphate and cADP-ribose production by cAMP and cGMP. *Biochem J,* 331 (Pt 3)**,** 837-43.

WRIGHT, E. M., LOO, D. D. & HIRAYAMA, B. A. 2011. Biology of human sodium glucose transporters. *Physiol Rev,* 91**,** 733-94.

XU, E., KUMAR, M., ZHANG, Y., JU, W., OBATA, T., ZHANG, N., LIU, S., WENDT, A., DENG, S., EBINA, Y., WHEELER, M. B., BRAUN, M. & WANG, Q. 2006. Intra-islet insulin suppresses glucagon release via GABA-GABAA receptor system. *Cell Metab,* 3**,** 47-58.

YUE, J. T., BURDETT, E., COY, D. H., GIACCA, A., EFENDIC, S. & VRANIC, M. 2012. Somatostatin receptor type 2 antagonism improves glucagon and corticosterone counterregulatory responses to hypoglycemia in streptozotocin-induced diabetic rats. *Diabetes,* 61**,** 197-207.

ZAIKA, O. L., POCHYNYUK, O. M., KOSTYUK, P. G., YAVORSKAYA, E. N. & LUKYANETZ, E. A. 2004. Acetylcholine-induced calcium signalling in adrenaline- and noradrenaline-containing adrenal chromaffin cells. *Arch Biochem Biophys,* 424**,** 23-32.

ZHANG, Q., RAMRACHEYA, R., LAHMANN, C., TARASOV, A., BENGTSSON, M., BRAHA, O., BRAUN, M., BRERETON, M., COLLINS, S., GALVANOVSKIS, J., GONZALEZ, A., GROSCHNER, L. N., RORSMAN, N. J., SALEHI, A., TRAVERS, M. E., WALKER, J. N., GLOYN, A. L., GRIBBLE, F., JOHNSON, P. R., REIMANN, F., ASHCROFT, F. M. & RORSMAN, P. 2013. Role of KATP channels in glucose-regulated glucagon secretion and impaired counterregulation in type 2 diabetes. *Cell Metab,* 18**,** 871-82.

ZHOU, H., TRAN, P. O., YANG, S., ZHANG, T., LEROY, E., OSEID, E. & ROBERTSON, R. P. 2004. Regulation of alpha-cell function by the beta-cell during hypoglycemia in Wistar rats: the "switch-off" hypothesis. *Diabetes,* 53**,** 1482-7.

ZHOU, H., ZHANG, T., HARMON, J. S., BRYAN, J. & ROBERTSON, R. P. 2007a. Zinc, not insulin, regulates the rat alpha-cell response to hypoglycemia in vivo. *Diabetes,* 56**,** 1107-12.

ZHOU, H., ZHANG, T., OSEID, E., HARMON, J., TONOOKA, N. & ROBERTSON, R. P. 2007b. Reversal of defective glucagon responses to hypoglycemia in insulin-dependent autoimmune diabetic BB rats. *Endocrinology,* 148**,** 2863-9.